University of Nottingham
UK | CHINA | MALAYSIA

Influence of Tunneling on Behavior of Adjacent Pile Structures

By

Low Wuu Shin
B.Eng

Thesis submitted to the University of Nottimgham for the degree of Master of Philosophy

July 2017

Table of Contents

CHAPTER ONE

INTRODUCTION

1.1 Research Background

Urban development has been increasing rapidly throughout the globe due to rapid increase of population especially in densely populated metropolitan cities. Within years of construction technology breakthrough, engineers have made high-rise and mega structures possible to realize. In addition, due to space constraint on the ground surface and due to the fact that some structures need to be built under the ground surface, underground constructions such as tunnels and deep excavations have become among major construction projects in many metropolitan cities where infrastructure development serves a vital role for today's civilization survival. Recently, the advancement in tunnel construction technology has enabled human beings to travel faster and easier through mountains or even under the sea. However, because tunnels are constructed below the ground surface, it may potentially have negative impacts on the adjacent structures especially on pile supporting building foundation which are situated close to the tunnel. Therefore, proper assessment and monitoring of stress changes and displacement of the ground must be taken into careful consideration for construction of tunnels in urban areas.

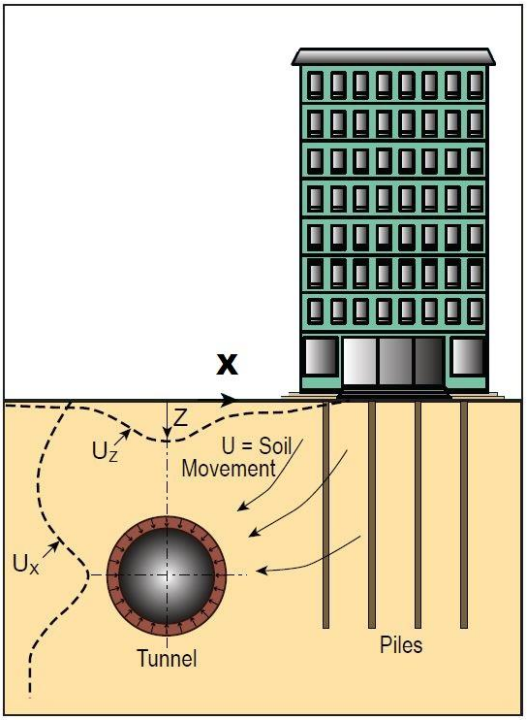

Figure 1.1 Influence of tunneling on behavior of adjacent pile structures

Problems and challenges of tunneling in urban areas are inevitable and challenges that are often encountered can be seen as follows.

Despites possible three-dimensional planning, many constraints limit the choices of design alignment of the tunnel which results in frequent and often unavoidable interferences with buildings at the surfaces and other existing underground structures.

Accessibility to do site investigation can be limited due to structures occupying the surface.

In some particular area, specific underground level of sub-surface is reserved exclusively for the installation of necessary underground utilities that must be assessed in

advanced for potential damages caused by tunneling-induced settlements.

Despites its known characteristic that tunnel is done underground, a high level of interaction with the city residents everyday lives are inevitable. Therefore, proper management must be done so that public disturbance can be reduced. Those works may include temporary traffic diversion, work site plan, air and noise pollution, as well as general safety issues.

To understand how much influence a tunnel has on the adjacent buildings, careful assessment must properly be performed. According to Korff (2012), this consists of four steps: first is to determine green field displacement, second is to impose displacement onto buildings, third is to assess potential damage and finally design protective measures if required.

Underground tunneling will inevitably induce ground movement and thus will result in both vertical and lateral movement of the soil above and nearby (See Figure 1.1). A better building response to the tunneling-induced ground movement must be performed to find appropriate protection to minimize problems such as cracks, excessive displacements or, in some worst case, the complete failure of the structures.

The magnitude of the settlements is the function of many interrelated factors including ground property, behavior of ground in response to tunneling, the existing condition of underground water and hydrogeological conditions etc. In Building Risk Assessment presented in a work co-edited by Vittorio et al. (2007), there are 3 types of damages induced by tunneling. Each represents certain degree of damages.

The first damage is aesthetic damages which basically refer to architectural

damages of slight cracks which can mostly be found on the building walls or other non-structural elements. It is usually easy to repair and redecoration is enough to cover those light cracks. The second is functional damages which refer to the loss of functionality or serviceability of non-structural elements that serves for services such as doors, windows and pipelines. Above all, the focus falls on the last category which is structural damage. It is the main problem of concern since this type of damage is the excessive deformation of the foundations of the structures which can eventually lead to partial or complete failure of the structures and thus can cause fatal consequences to human lives and properties.

Ground settlements are inevitable once a construction of a tunnel takes place. It is not possible to create an underground space immediately and maintain stiff lining without any ground changes and movement. Therefore, there exists a certain amount of deformation from the tunnel depth and makes its way to the top surface which result in visible ground surface settlement and other side effect on adjacent buildings. In order to be able to minimize the deformation of the nearby structures, one must understand the idea of ground loss mechanism which always comes after in every tunnel excavation. According to Nagen (2011), ground loss can be caused by three main components during tunneling which include face loss, shield loss and tail loss. Settlement induced by tunneling can be categorized into two types namely short and long term settlement.

Short-term or immediate settlement which refers to the ones directly caused by tunnel depends on various factors including stability of tunnel face, rate of advance, and tunnel lining installation time etc. Settlement due to deformation of tunnel lining which happens after the finish of lining and often found in shallow large tunnel construction where the excavation is huge and is done near to the ground surface.

Long-term settlements is primarily caused by ground consolidation of cohesive or compressible soil during dissipation of excess pore pressure.

The purpose of current research is to investigate the behavior of ground and pile foundation due to tunneling activities. Especially, progressive responses of ground settlement and axial force, bending moment, and shear force of pile foundation during tunnelling process should be investigated. Since the risk of failure of the nearby buildings is what matters the most, having clear and accurate predictions of the behavior of pile foundation and soil in response to the construction of tunnel is very important for engineers.

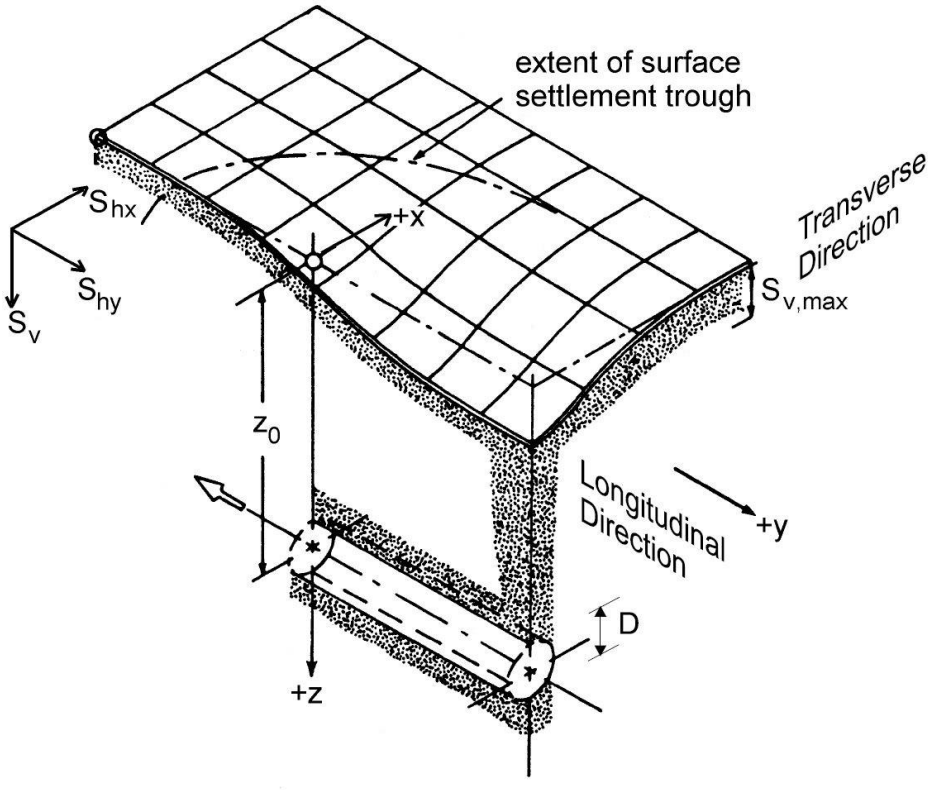

Figure 1.2 Ground settlements due to tunneling

1.2 Scope of Research

This study will focus mainly on the effect of tunneling on the behavior of pile foundation situated within the proximity of the deformation effect induced by the excavation of tunnel. The objective is to gain in-depth understanding of the mechanism of pile foundations behavior when exposed to the domain of soil movement induced by tunnel excavation by using numerical modeling approach. Analysis will be carried out to find out how to simulate the shield TBM tunneling properly, how shield TBM tunneling will affect on the axial force, bending moment, and shear force of pile foundation with respect to its relative position.

In the following chapter, important literature reviews will be conducted by looking at the previous works on geotechnical centrifuge testing which has increasingly become very important in simulating the actual behavior of soil by using the idea of model-prototype relation. Next, the soil-structure interaction which, as the name implies and according to Tuladhar et al. (2008), refers to the process in which the response of the soil influences the motion of the structures and the motion of the structure influences the response of the soil.

Numerical analysis will be conducted in Finite Different Method software, FLAC3D developed by Itasca Consulting Group, to investigate the effect of tunneling on the adjacent pile foundation. This study proposes suitable structural elements for a shield TBM tunneling model using 3D FDM and provides its modeling procedure. More

specifically, plate-type structural elements of skin plates and segment linings were simulated and by separating structural and ground elements, the behavior of ground and the stability of the shield TBM tunnel were examined simultaneously. In addition, the difference between liner and shell elements simulating structural components was analyzed using the FDM. An appropriate structure element was determined based on the analysis results, and the ground settlement observations obtained from a numerical analysis were validated using field monitoring data.

It should be noticed that soil-pile interaction is an extremely complex analysis since the behavior of soil itself is non-linear and anisotropic. Thus, the attempt to find an exact closed form solution for the problem is apparently impossible for such a complex and tedious soil-pile interaction analysis and that is why numerical analysis is adopted in this study.

1.3 Objectives of study

- Simulation process of shield TBM tunneling in soft ground
  - To study and simplify the structural component of shield TBM and installation process according to construction procedure considering face pressure in the numerical modeling,
  - To stimulate the soils arching effect and select reasonable simulation method between FEM and FDM which can mobilize the arching effect,
  - To simulate and monitor ground settlement profile, longitudinal profile, tangential

stress, radial stress and axial stress variation during shield TBM tunneling using numerical method,

- To simulate and monitor the bending stress resultant, shear stress resultant, and membrane stress resultant acting on the segment lining using numerical method.

- Pile-tunnel interaction
  - To derive proper material properties of pile element of numerical model
  - To study the pile condition with respect to relative position: Short pile condition and long pile condition
  - To stimulate and understand the progressive variation of axial force, bending moment, and shear force distribution along the pile foundation during shield TBM tunneling
  - To stimulate the mobilization of negative skin friction depending on the relative pile position

1.4 Organization

The content in this report is divided into six chapters. Chapter one will be the introduction and the overview of the research and scope of the project. In Chapter two, literature reviews of previous works will be done which are related to geotechnical centrifuge, soil-structure interaction and pile movement due to tunneling. Later, computer aided numerical analysis performed by using Finite Different Method software FLAC3D will be presented in Chapter three. Chapter four is devoted for a deeper analysis of soil-pile structural interaction such as model development, frictional resistance, evolution of negative skin friction and result verification. Then, Chapter five illustrates the possible

effects which contribute to the behavior of pile due to tunneling which includes the effect of pile, tunnel and ground characteristic. Finally, in Chapter six, overall conclusion of the study will be given along with other possible recommendation for further research opportunities in the related topic.

CHAPTER TWO

LITERATURE REVIEW

2.1 Geo-centrifuge

So far the study of pile and soil movement associated with tunneling has been done by using three approaches namely empirical or experimental approach, numerical approach and analytical approach. These different methods have their own advantages and weaknesses as shown in Table 2.1 below (Abdullah & Taha, 2013). Among these approaches, simulation of geotechnical centrifuge has been used for solving many geotechnical engineering problems which include settlement and stability of slopes and embankments, stability of tunnels as well as soil-structure interaction.

The history of centrifuge dates back to 1869 when Phillips suggested that it can be used to simulate self-weight stress in structural beams. It was not further pursued until Bucky (1931) used the centrifuge to study mining problems. The principle of this method, according to Joseph et al. (1988), in order to produce at corresponding points in a small scale model, the same unit stresses that exist in a full scale structure, the weight of the material of the model must be increased in the same ratio that the scale of the model is decreased with respect to the full scale structure. The effect of an increase in weight may be obtained by the use of centrifugal force, the model being placed in a suitable revolving apparatus. Based on this basic principle that stresses at geometrically similar points in

prototype and model should be the same, centrifuge modeling was developed. If the model and prototype are made of materials with identical mechanical properties, then, when a soil sample model is subjected to N times the acceleration due to earth's gravity by centrifugation, it results in identical self-weight stress at homologous points in the model and prototype as shown in figure 2.1. In a simpler way, if a $\frac{1}{N}$ scale model of a prototype is exposed to Ng on the centrifuge, then the model behavior is thought to be the same as that of the prototype.

In order to make the principle to be true, three assumption criteria must be satisfied. First, the model that represents the prototype is correctly scaled. Second, the $\frac{1}{N}$ scaled model when subjected to Ng gravity behaves like the prototype at 1g. Finally, the centrifuge must be able to produce ideal gravitational field.

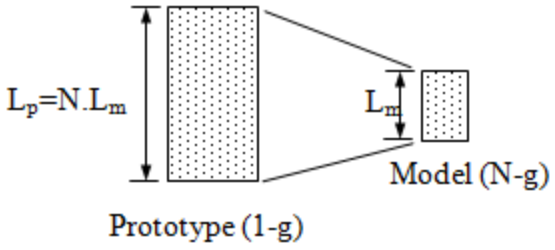

Figure 2.1 Model-prototype scaling

Table 2.1 Advantages and disadvantages of various approaches

Method	Advantages	Disadvantages
Analytical Methods		
Mindlin's Model	Describe both vertical and horizontal ground deformation within few steps of calculation	Their results are not accurate as those for numerical
Numerical Methods		
Mohr-Coulomb Model	Simple and applicable to three-dimensional stress space model	Doesn't include the influence of rotation of principal stress axes which has the effect in tunnel analysis where liquefaction is possible
Elastic Model	Gives reasonable results for small loading cases	Doesn't predict realistic results for unloading effects
Elasto-plastic Model	Helps to understand the stress strain behavior of soil during loading and unloading by distinguishes between the recoverable and irrecoverable deformations	has large numbers of parameters may reach 15, and some of them need special lab tests to get them
Displacement Control Model	Predicts realistic subsurface movements	Producing surface settlement troughs wider than the field observations
Experimental Methods		
Photo-Elasticity Technique	Gives a roughly indication about stresses transfer from tunnel to piles	Lack to deformation and creep observations
Photogrammetric Technique	Analyze the tunnel center movements with respect to volume loss	Does not simulate 2D models
Small Scale Testing Model	Well simulations of the tunnel advance operations	Good results have been taken when piles are symmetrically arranged around the tunnel
Centrifuge Model Test	Conducts the simulation in semi-ideal environment and gives real results for both short and long terms	Does not support the creep effects of the soil

Successful centrifuge testing requires that the scaling relations between the model and prototype be understood and satisfied. Assuming the correct use of prototype modeling and centrifuge procedure along with the satisfaction to the three assumptions, this method offers significant advantages. First, the analysis provides good approximation of the behavior of the problem which is close to that of the prototype. For these reasons, geotechnical centrifuge has been used extensively for the verification of theories, for the studies of problems involving the flow of water, as well as for various dynamic problems such as pile driving and earthquake effects (Joseph et al., 1988).

Application of the centrifuge has been seen in various disciplines in geotechnical engineering and soil mechanics such as flow of water through soils, soil-structure interaction, and underground construction and dynamics problems. A number of researchers have been using centrifuge in a considerable amount of tests.

The centrifuge at the Peter W. Rowe Laboratory at the University of Manchester has been used to investigate the problems related to coastal and offshore gravity structures. Barton (1984) used centrifuge to study the response of pile group to lateral loading while Oveson (1975) at the Danish Engineering Academy used it to run model footing tests as cohesionless soils.

Lyndon and Pearson (1984) studied pressure distribution on a rigid wall in cohesionless material and the result they obtained agreed well with the theory. Kimura et al. (1985) could obtain load-deformation curves and ultimate bearing capacity of footing on cohesionless soil through the aid of this centrifuge testing. Plus, retaining structures also have been studied in the centrifuge.

Scott (1979a, 1979b, 1981) investigated the behavior of piles subjected to cyclic loading using centrifuge. Similarly, Sabagh (1994) ran cyclic load axial load tests in piles in sand and found that the magnitude of cyclic load at failure was controlled by the existing static load, the size of the load increment and the number of cycles. Oldham (1984) investigated the lateral loading of single pile in sand and the results agreed with published field values.

Chen et al. (1999) did a parametric study of pile response caused by tunneling which shows that influence of tunneling on pile response depends considerably on a number of factors including tunnel geometry, ground loss ratio, soil strength, pile diameter and ratio of pile length to tunnel cove depth.

A study done by Jacobsz et al. (2004) demonstrates a centrifuge modeling of tunneling near driven piles. The test measures surface settlement profiles during tunneling induced volume loss and settlement of piles situated at different distances from the tunnel. The study concludes that there exists a certain zone of influence where large pile settlement could potentially develop due to tunneling. The volume loss induced by tunneling will result in a transfer of load from pile base to the pile shaft for piles with their bases located within the zone of influence.

Another study was done to determine responses of single piles to tunneling-induced soil movement in sandy ground by Lee & Chiang (2007). A series of centrifuge tests were carried out to access ground movement and their detrimental effects on neighboring single plies. The results show that only the depth ratio has a significant influence on the distribution of the bending moment along the piles, but both the depth ratio and the working load on the pile determine the profile of the axial force along the pile.

Through these literatures, it is clear that centrifuge can be very useful and can be applied to a wide range of problems in areas associated with geotechnical engineering. Modeling of soil-structure interaction problem is one of the major advantages of the centrifuge technique. If a theoretical model exists, then possible comparison can be made among theoretical and experimental results through which theoretical model can be validated or improved. If the theoretical model does not exist, through centrifuge modeling, an even further understanding is obtained which eventually leads to the development and verification of a theoretical model.

2.2 Soil-structure interaction

In every construction of structures on the ground, interactive reaction between the ground and the structures does exist. The progress begins with the balance of stress and strain from the start of construction phase until the end of the construction when all stress and strain have come to a balanced state influenced by ground and structures to one another. High-rise building structures, storage tanks, bridge adjacent to high embankment, buried pipes and culverts, tunnels all experience this interaction. According to ISE and ICE & IABSE (1989), soil-structure interaction is categorized into two types of interaction namely structures supported by ground and ground supported by structures. The first category includes conventional building structures, bridge structures, storage-tank structures, and offshore structures. On the other hand, earth-retaining structures, tunnels, and other buried structures fall into the second category.

In the case of this study which focuses mainly on soil-pile interaction, the analysis can be carried out using two methods by either modeling the structure or soil together

with appropriate interface behavior or by using principle of superposition. Soil pile interface modeling greatly contributes to the behavior of the soil-pile system. Soil-pile interface are usually modelled either as a perfectly bonded interface or as a frictional interface where soil-pile slipping and gapping can take place. Considering reality, the modeling of interface should allow slipping and gapping between soil and pile; however, due to high computational time and modeling difficulties, the interaction is usually considered to be a perfect bonding (Peiris, 2014). If the interface surface is in contact, full transfer of shear stress can be guaranteed. Soil-pile interaction behavior also depends greatly on the constitutive model of soil. Thus, selection of constitutive model in numerical analysis would affect the result of the modeling (Balendra, 2005).

The aspects of buildings that might affect the degree of influence are stiffness, weight and interface between the structure and soil. According to Franzius et al. (2006), for smooth interface, the horizontal strain in the building reduces dramatically.

Farrell et al. (2012) conducted a centrifuge modeling of the response of building to tunneling. The study investigates soil-structure interaction effects by observing the response of aluminum beams of varying stiffness to tunneling using 8m diameter beam centrifuge at Cambridge University. Some significant conclusions were drawn. Both the structure rigidity (EI) and the soil stiffness (Es) should be carefully considered when determining the relative structure-soil stiffness. Contact between the structure and the soil is not always maintained as volume losses occur. The separation of the soil depends on the relative structure-soil stiffness.

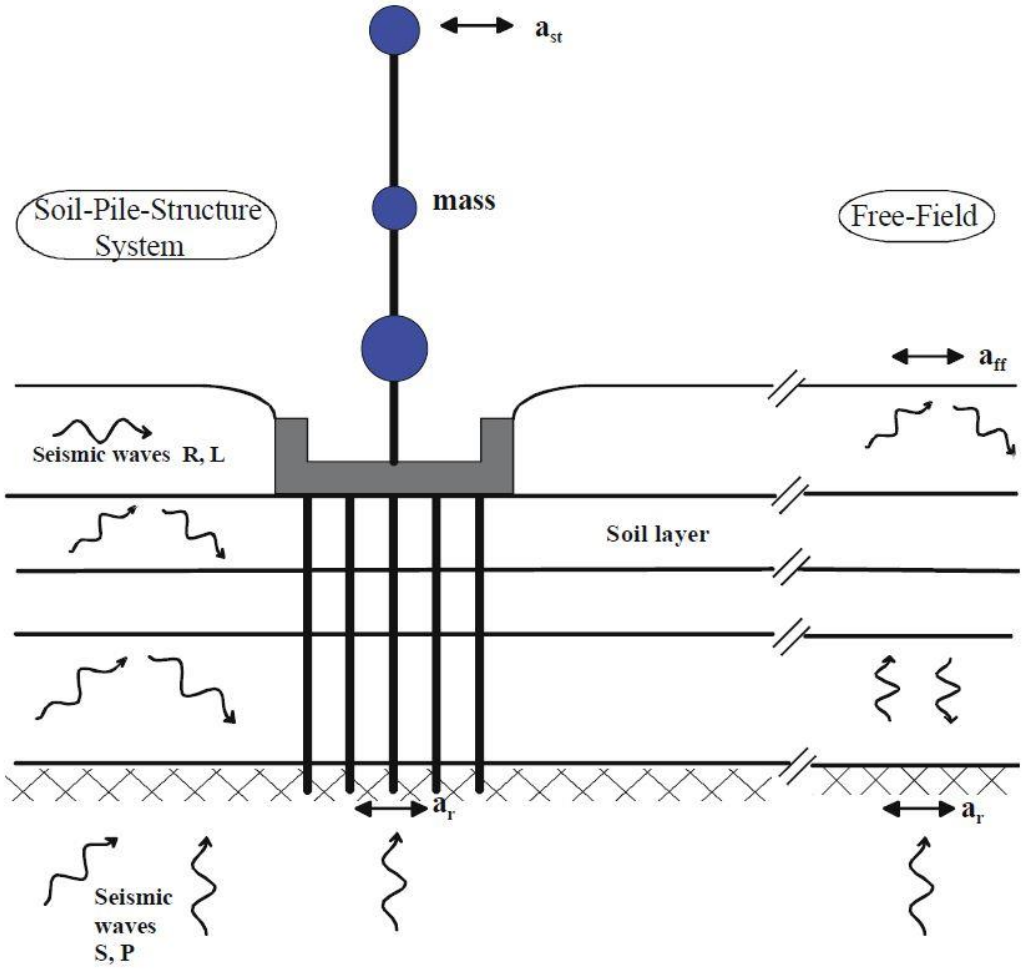

Figure 2.2 Sketch of Soil-Pile-Structure Interaction problems (Gazetas & Mylonakis, 1998)

Soil-pile test conducted by Jacobsz (2002) found out that piles located directly above the tunnel excavation are more likely to settle than the surface. In contrast, piles which are located next to the tunnel settle at about the same rate as the surface. Finally, piles outside the line of 45 degrees from mid tunnel are found to have a very small settlement or not to have any settlement at all.

2.3 Numerical analysis on Shield TBM

The construction of tunnels driven by the shield TBM has increased in urban areas for various purposes. The construction of tunnels in urban areas can cause ground settlement, which can affect the stability of existing structures over the tunnel. However, the behavior of ground and pile structure induced by tunnel construction using shield TBM has not been comprehensively examined. In addition, the simulation process of shield TBM tunneling is yet to be fully established.

Studies in the early 1980s employed numerical analysis methods to examine the mechanized tunneling method (Lambrughi et al., 2012). Rowe et al. (1983) numerically analyzed the behavior of soft ground from the tunnel advance. Previous studies have introduced a number of factors causing subsidence from mechanized tunneling.

The simulation of shield TBM tunneling with 3D FEM (finite-element method) has been examined since the early 1990s (Kasper and Meschke, 2004). Lee and Rowe (1990) examined the behavior of subsidence from tunneling in soft cohesive soil. Based on their study, other numerical studies have considered soil from the Thunder Bay sewer tunnel site based on the 3D FEM (Lee and Rowe, 1991). In addition, Lee et al. (1992) examined various causes of subsidence from tunneling by implementing the gap parameter concept.

Swoboda and Abu-Krisha (1999) examined the distribution of excess pore water pressure from shield TBM tunneling in consolidated clay by considering the structure of the shield TBM as a distinct component. In other words, the skin plate, the segment lining, and backfill grout were simulated using a thin shell element. However, this model did not take into account the friction and slip between the ground and structural elements composing the shield TBM in the simulation. Komiya et al. (1999) assumed the shield

TBM to be an undeformable, rigid body, and to simulate ground supported by backfill grout, they applied time-dependent pressure to the excavated ground boundary from the end of the skin plate. Here they took into account the friction and displacement between the ground and the shield TBM, but the mechanical behavior of the segment lining and backfill grout and that of backfill grout and ground were not considered. Kasper and Meschke (2004) also assumed the skin plate of the shield TBM as an undeformable, rigid body and simulated hydraulic jacks, backfill grout, and segment linings by using the finite-element method. Although they considered various structural elements to simulate the shield TBM, they provided insufficient information on structural elements regardless of the analysis method (Maynar & Rodriguez 2005; Hasanpour et al., 2014). No study has validated the arching effect of tunneling. As discussed earlier, 3D modeling has become a mainstream technique, and structural components have been modeled individually in detail to simulate shield TBM tunneling. Further, few studies have examined modeling methods based on structural components such as skin plates and segment linings, and the use of plate-type structural elements that can be used to simulate skin plates and segment linings in the FDM (Do et al. 2013, Mollon 2013). For this reason, it is important to select suitable structural elements for simulating the mechanical behavior of the shield TBM tunnel and the ground.

2.4 Pile movement due to tunneling

The behavior and capacity of piles under loading is governed by a complex mechanism which can be such as installation effects, positive and negative skin friction as well as base capacity and pile toe. The load displacement behavior of the piles depends on its bearing capacity and the displacement transferred from the piles or the soil beneath the piles.

The settlement of pile head is determined by the combined effects of the followings (Korff, 2012):

$$S = S_b + S_{el} + S_2$$

where

S is the settlement of the top of the pile

S_b is the settlement of the pile tip due to the load on the pile

S_{el} is the settlement of the top of the pile due to elastic compression of the pile

S_2 is the settlement due to compression of the soil under the pile tip owing to other effects than the load on the pile

The analysis of pile response due to tunneling falls into two aspects namely lateral and axial response. According to Chen et al. (1999), lateral displacement of each element of pile can be related to pile bending stiffness and horizontal pile-soil interaction stresses.

The response behavior of piles to tunneling was explained by Loganathan et al. (2010) to be involved in function of pile length and tunnel depth. Short-pile and long-pile cases were studied to access the effects of pile length with respect to tunnel depth. Short

piles are defined as those with ratio of pile length to tunnel depth is less than 1 $\left(\frac{L_p}{H} < 1\right)$, and in the case of long pile, this ratio is greater than 1 $\left(\frac{L_p}{H} > 1\right)$. In short pile cases, analysis shows that significant pile settlement is induced along with additional bending moment, lateral displacement and pile rotation. However, in the case of long pile, significant bending moment changes is observed while the pile head settlements are less than that of the ground.

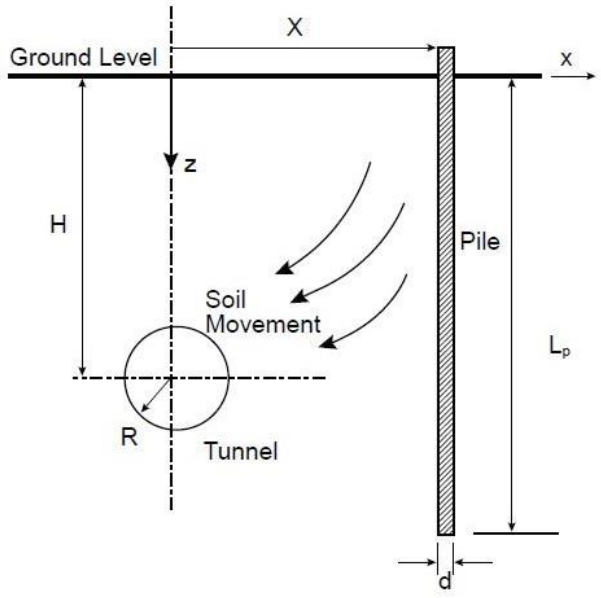

Figure 2.3 Single pile adjacent to tunneling (Loganathan et al., 2011)

According to another study done by Bezuijen et al. (1994) which focuses on the influence of bored tunnel on an existing pile foundation, three different types of tests were carried out. One preliminary test was done with limited instrumentation for a tunnel in saturated sand and the other two were with a soil model of sand with clay layers on top. The test shows that horizontal distance from the pile to the model tunnel as well as the soil materials that surround the model tunnel do have an influence on the load-settlement

behavior.

In a study on the response of full-scale piles to tunneling done by Selemetas et al. (2005), ground surface settlement, pile settlement and pile base load changes were monitored. With regard of pile position to tunnel, important conclusion was drawn as follows. Piles with toe founded in zone A (Figure 2.2) settle more than the ground surface settlement. In zone B, the settlement of pile is generally equal to that on the surface. For piles founded in zone C, pile settlement is relatively smaller than the corresponding deformation on the ground level. Furthermore, piles in zone A experience a marked reduction in their base loads during passage of TBM. For piles with their bases located in zone B and C, they experience small changes in their base loads.

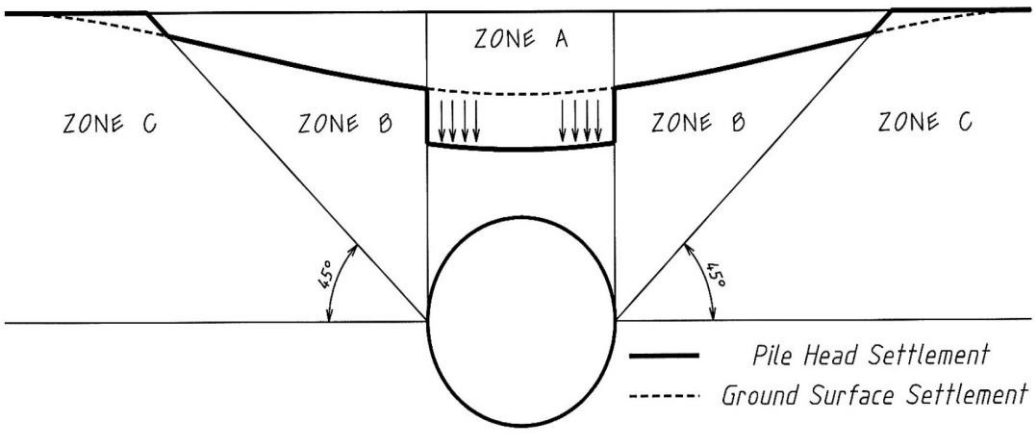

Figure 2.4 Zones of influence of pile settlement in London Clay (Selemetas et al., 2005)

Through a number of researches which have been reviewed, a study from the National University of Singapore, Pang (2006) investigates the effects of tunnel construction on nearby pile foundation which has a number of common objectives to this study. The NUS study was done on the Mass Rapid Transit (MRT) tunnel construction in Singapore with in-pile instrument pre-installed into piles which provide the information on the axial force and bending moment development in piles.

2.5 Gap analysis

This chapter will summarize the knowledge and conclusions which were drawn from the research done previously along with the proposed objectives and more important point this study aims to achieve.

To investigate the behavior of pile foundation due to adjacent tunneling, tunneling simulation process should be established. 3D modeling has become a main stream technique, and structural components should be considered individually in detail to simulate shield TBM tunneling. However, simulation process of shield TBM tunneling in soft ground has not been established. Moreover, modeling method of structural components such as skin plates and segment linings has not been established. For this reason, simulation process of shield TBM tunneling in soft ground should be set up. Moreover, simplification of structural component of shield TBM and installation process according to construction procedure considering face pressure should be performed. Reasonable simulation method should be selected among FEM and FDM which can mobilize the arching effect. To validate the simulation result, ground settlement profile, longitudinal profile, tangential stress, radial stress and axial stress should be monitored

during shield TBM tunneling. Moreover, bending stress resultant, shear stress resultant, and membrane stress resultant acting on the segment lining should be monitored.

The main objectives of previous studies includes understanding of single pile-single tunnel interaction, observing bending moment/axial forces developed during tunneling and 3D FEM numerical analysis. However, shear stress mobilized along the pile-soil interface has not been concerned.

From these previous studies, it is found that pile base resistance can be reduced due to soil settlement which in turn induces settlement of pile when tunnel is constructed under pile foundation. Because pile bearing capacity at the pile tip is reduced, base resistance is then transferred to pile shaft. It is presumed that pile skin friction is responsible for maintaining the applied load. However, the development of skin friction along the pile foundation due to tunneling has not been clearly presented yet. Thus, in this study, material properties of pile element should be derived properly to be used as reference. Depending on the relative position of pile with respect to tunnel, two representative classes should be defined: Short pile condition and long pile condition. Moreover, progressive variation of axial force, bending moment, and shear force distribution along the pile foundation during shield TBM tunneling should be obtained. Finally, the mobilization of negative skin friction depending on the relative pile position should be clearly presented.

CHAPTER THREE

NUMERICAL ANALYSIS OF SHIELD TBM TUNNELLING

3.1 Background

To investigate the effect on pile nearby due to tunneling, simulation of shield TBM tunneling should be well established. However, the modelling procedure to simulate the shield TBM tunneling has not been defined. Also, type of element for simulation of shield TBM components (such as skin plate, segment lining, backfill grouting, face pressure) has not been determined. Thus, in this chapter, simulation procedure for EPB shield TBM tunnelling is suggested. Numerical study is carried out by using commercial FDM software, FLAC3D and FEM software, MIDAS GTX NX. Based on the model validated in this chapter, single pile-tunnel interaction model can be established and examined considering various factors.

The type of shield TBM considered in this study is Earth Pressure Balance (EPB) shield TBM. EPB shield TBM is TBM used for the excavation of soil and rock where the pressure at the tunnel face is obtained by means of geo-materials excavated by cutterhead, which acts as a support medium. The cutterhead serves as the means of excavation whereas face support can be obtained by the excavated debris which is kept under pressure inside the excavation chamber by the thrust jacks on the shield. These jacks transfer the pressure to the separation bulkhead between the shield and the excavation chamber, and

hence to the excavated earth. Excavated debris is removed from the excavation chamber by a screw conveyor which allows the gradual reduction of pressure (ITA-AITES). The face pressure can be controlled with the RPM of screw conveyor: the higher the RPM of screw conveyor, the lower the face pressure and vise versa. RPM of cutterhead, face pressure, thrust force, torque and settlements at various positions should be regularly recorded during the excavation process.

3.2 3D Modeling with FDM and FEM

3.2.1 Geometry of 3D model

The outer diameter (D) of the EPB shield TBM is 6 m, inner diameter is 5.8 m and thickness of the backfill grout is 0.2 m. To avoid the effect of model boundary on the displacement and stress around the tunnel and ground during the EPB shield TBM tunneling, the distance from the tunnel center to the both side of the model is 5 times of the tunnel diameter which is 30 m (5D). The center of tunnel is assumed to be located at 26 m below the ground surface. Fig. 3.1(a) shows the components of the numerical model implemented in the simulation and Fig. 3.1(b) shows the 3D view of the model.

The geometry of model is initially modeled in Midas GTX NX. Each component (ground, tunnel, backfill grout, skin plate, etc) of EPB shield TBM is created and meshed separately. These elements can be used to model and analysis the behavior of EPB shield TBM in FEM. Also, the meshed geometry is then imported to FLAC3D in the form of tetrahedron solid zone. The mechanical behavior of the ground is assumed to follow elastic and perfectly plastic model, Mohr-Coulomb which is suitable for soil and weathered rock. Table 3.1 presents the mechanical properties of ground used in the

numerical modelling.

Previous researches use solid element to simulate the skin plate and segment lining. However, if the skin plate and segment lining are modelled with solid element, moment and force acting on the structural components cannot be obtained. Therefore, for the design of segment lining, plat-type structural element should be introduced. In this study, to obtain the stress resultant acting on structural components, skin plates and segment linings are simulated with built-in plate-type liner structural element in FLAC3D and shell element in MIDAS GTS NX. Shell element and liner element were assumed as elastic material.

In case of backfill grouting layer, solid element is adopted in this study. The backfill grouting layer is crucial for the control of ground settlement. If the backfill grouting is being delayed, the gap between the ground and segment lining is converging and it finally causes the settlement of ground. In recent years, therefore, backfill grouting is simultaneously injected right after the installation of segment lining. The backfill grouting is not a structural component which should be taken attention on the stress and force. It fills the space between ground and segment lining and transfer the ground load onto the segment lining. Thus, it can be considered as elastic mass which has thickness amount of gap parameter. The mechanical parameter of backfill grout is also tabulated in Table 3.1.

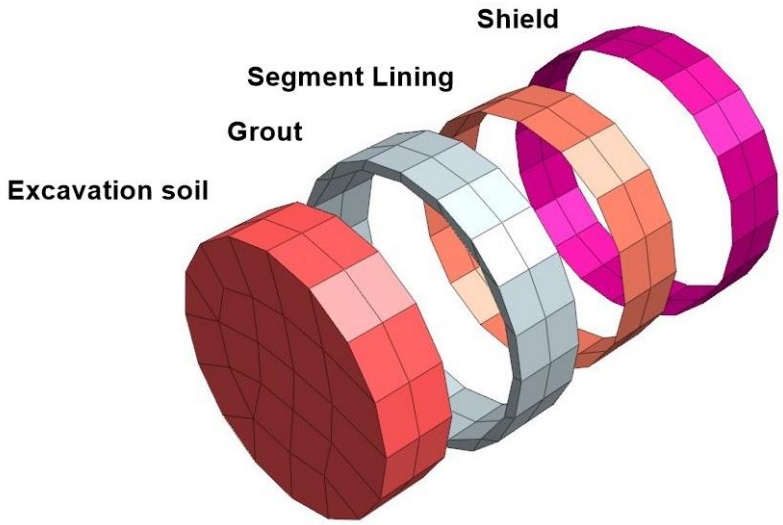

(a)

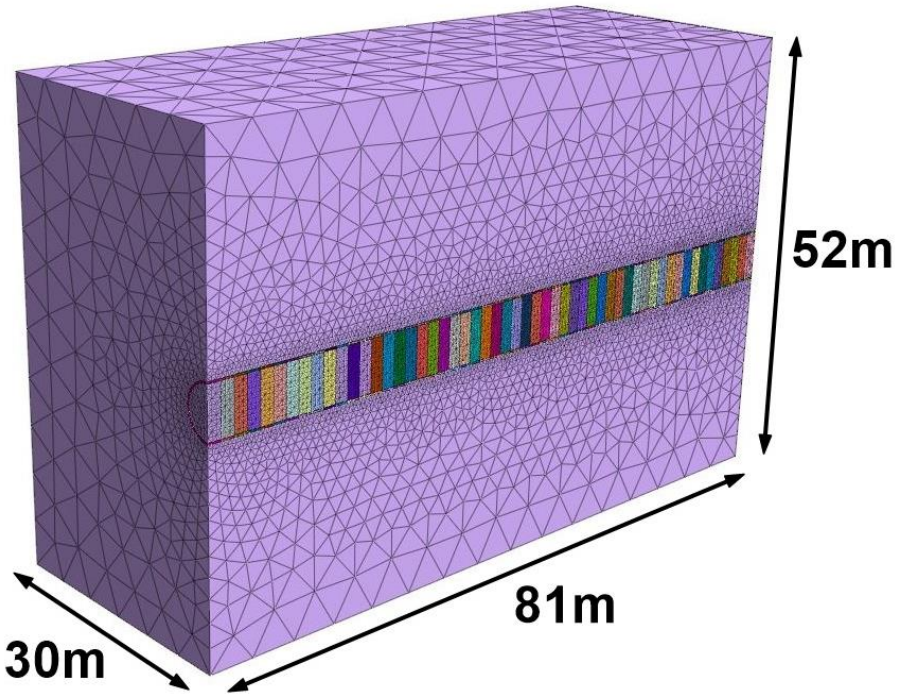

(b)

Figure 3.1 Geometric condition of the shield TBM tunnel simulation in Midas GTS NX. (a) Components of EPB shield TBM (b) 3D model

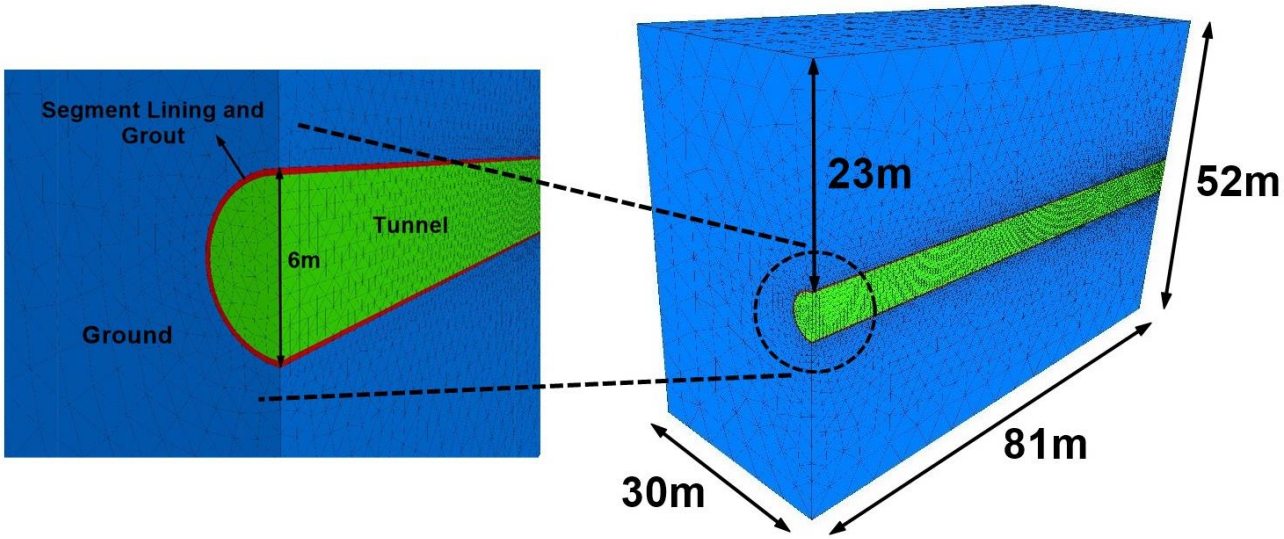

Figure 3.2 Geometric condition of the shield TBM tunnel in FLAC3D

3.2.2 Boundary condition and simulation process

By considering symmetrical geometry of the problem, only a half of the whole model is simulated to reduce calculation time. Also, the ground and tunnel in this numerical model are simplified by setting a symmetric boundary condition.

Figure 3.3 and 3.4 show respectively the boundary conditions of the numerial model simulated with FEM and FDM.

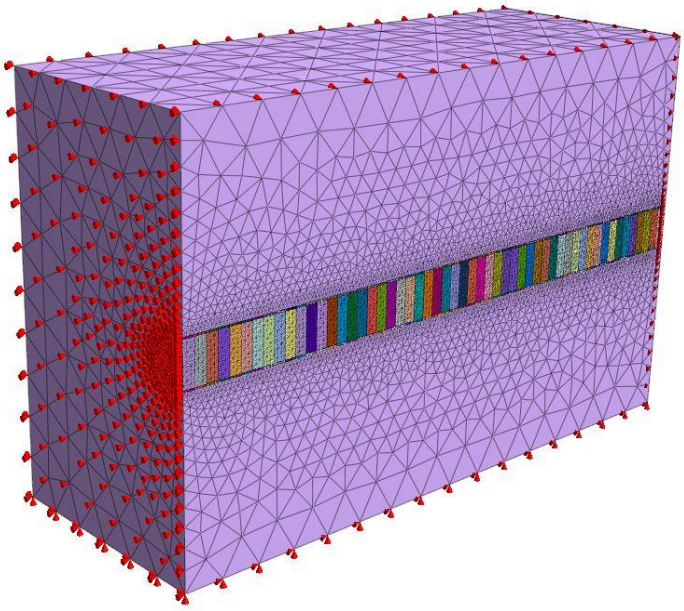

Figure 3.3 Boundary condition in Midas GTS NX

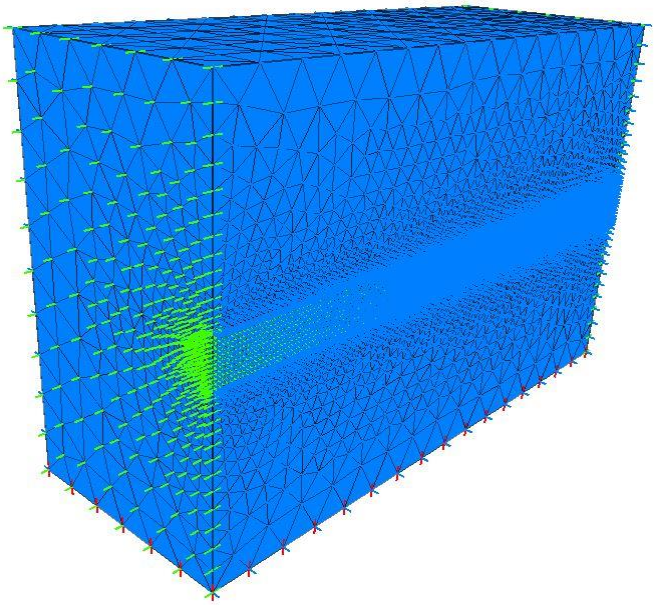

Figure 3.4 Boundary condition in FLAC3D

3.2.3 Face Pressure

Application of face pressure is important for the simulation of shield TBM. Face pressure works as a counter force at the face of the tunnel to stabilize the face of the tunnel and prevent the soil from falling during the operation. When face pressure is less than that exerted by the soil, there can be soil collapse at the face and area surrounding the excavation. However, when the pressure is greater than that of the soil at the face, it can lead to upward displacement at the ground surface. In this model, the face pressure of 150 kPa is uniformly applied to stabilize the ground at tunnel face as shown in figure 3.5 below.

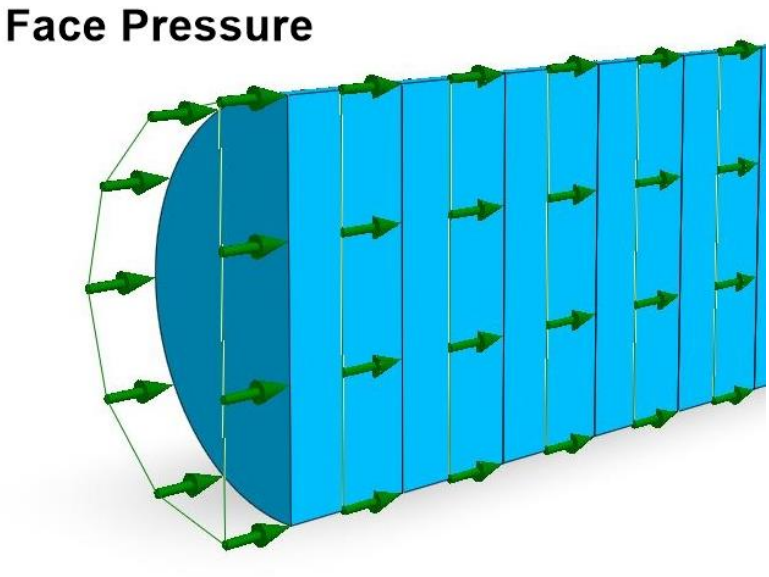

(a)

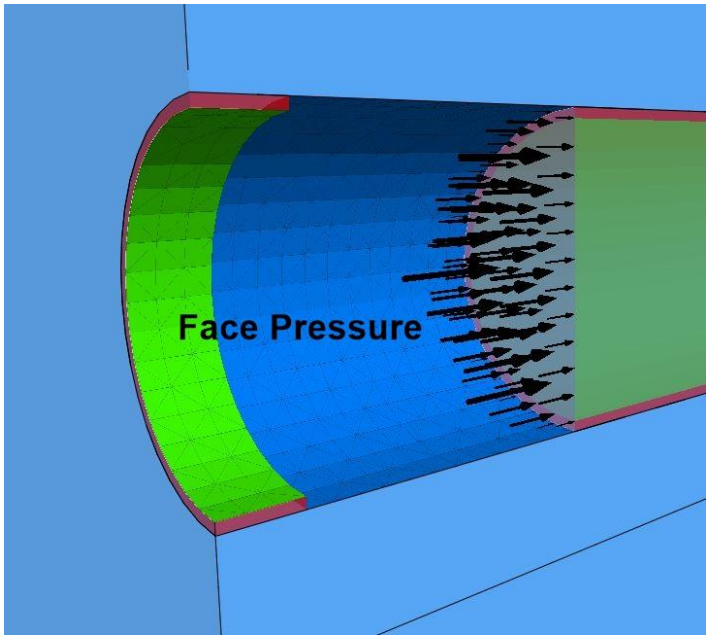

(b)

Figure 3.5 Face pressure applied on the tunnel face (a) In FEM (b) In FDM

3.2.4 Advance of EPB shield TBM tunnellling

The skin plate which is simulated with liner structural elements is then removed as the stage proceeds. Then, 0.2 m thick liner element is attached onto the inner perimeter of tunnel excavation to simulate the installation of segment lining.

And 0.2 m thick solid element between inner and outer diameter of tunnel is activated to simulate the backfill grout. Actually, the tail void which is the sum of tail clearance and thickness of skin plate should be filled with backfill grout after the installation of segment lining. In this study, backfill grout is assumed to be injected right after the installation of segment lining to minimize the ground settlement.

Normally, as the installation of backfill grout delays, the ground settlement increases and the sectional force acting on the segment lining decreases since backfill grout transfers the loads from the ground to the segment lining. In this study, backfill grout is assumed as elastic material showing maximum strength right after the injection.

Vertical displacement along the tunnel advance direction, transversal displacement at the center of model is monitored during the excavation and stress distribution around the tunnel is measured. Shear stress and moment acting on the segment lining is monitored at the middle of model as well.

3.3 Material properties and selection of structural element

Material properties are important for the simulation and it can affect the results of the analysis. In this study, a hard soil is considered for the ground. Segment linings are made of concrete while skin plate or shield takes the properties of steel. The behavior of the

ground is set to follow Mohr Coulomb while the remaining components namely skin plate, segment lining and grout are set to behave as an elastic material.

In FLAC3D, built-in liner structural element is used as the representation of segment lining and skin plate as stress resultant acting on structural components can be easily extracted. Table 3.1 and 3.2 below show respectively material properties being used in Midas GTS NX and FLAC3D.

Table 3.2 Material properties

	Ground	Segment lining	Skin plate	Grout
Model type	Solid	Plane	Plane	Solid
Constitutive model	MC	Elastic	Elastic	Elastic
Young's Modulus (Pa)	6.00E+07	2.10E+10	2.50E+11	1.00E+10
Poisson ratio	0.3	0.25	0.2	0.3
Shear Modulus (Pa)	2.31E+07	9.62E+09	1.04E+11	3.85E+09
Bulk Modulus (Pa)	5.00E+07	2.08E+10	1.39E+11	8.33E+09
Density (kg/m^3)	1900	2400	7850	2200
Cohesion (kPa)	20	-	-	-
Friction angle (degree)	30	-	-	-

In FLAC3D, there are a number of structural element choices available to be used for simulating actual structures. In this study, liner structural element is used by being attached to the surface of the grid to simulate the skin plate and segment lining of EPB shield TBM.

Liner structural elements are the three nodes, flat finite elements that are used to

model thin structures for which both normal-directed compressive/tensile interaction and shear-directed frictional interaction with the host medium occurs. In FLAC3D, plate-type structural elements include Constant Strain Triangle plane-stress element (CST, 6 degrees of freedom), Hybrid plane-stress element (CST, 9 degrees of freedom), Discrete Kirchhoff Triangle plate-bending element (DKT, 9 degrees of freedom), and the Hybrid shell element (DKT-CST, 18 degrees of freedom).

The plane-stress element considers only membrane actions, while the plate-bending element provides only the bending actions. However, the stress acting on skin plates and segment lining like the ones in this study are affected by both membrane and bending actions. Therefore, the DKT-CST hybrid formulation was adopted to obtain membrane and bending stress resultants acting on structural element of the shield TBM. Plate-type structural elements are assumed to behave as isotropic condition, thus Young's modulus (E), Poisson's ratio (v), and thickness (t) should be specified.

Table 3.2 Typical input parameters of Liner structural element

Element type	Notation	Description
Liner	K_n	Normal coupling spring stiffness per unit area (F/L^3)
	K_s	Shear coupling spring stiffness per unit area (F/L^3)
	c	Shear coupling spring cohesion (F/L^2)

Table 3.2 shows the input parameters of plate-type structural element used in this numerical model. Liner structural element is used in this study and, in order to simulate the behavior of the interaction between the ground and all the structural components,

normal coupling spring stiffness (Kn), shear coupling spring stiffness (Ks), and shear coupling spring cohesion (c) are defined. Table 3.3 below shows the parameters needed for the simulation and properties of Liner element used in the study.

Table 3.3 Input parameters of liner structural element used in the simulation

Material	Type	Model	Density (kg/m^3)	Isotropic		Thickness (m)	Kn, Ks (N/m^3)	c (Pa)
				Elastic Modulus (Pa)	Poisson's ratio			
Skin Plate	Liner	Elastic	7850	2.5e11	0.2	0.1	2.24e9	0
Segment Lining	Liner	Elastic	2400	2.1e10	0.25	0.2	8e8	0

3.4 Modelling procedures

The procedure for the simulation of EPB shield TBM tunneling is as follows. First of all, after the mesh of model is imported into FLAC3D from Midas GTX NX, the entire model is brought into equilibrium state under gravitational force in the elastic state. At each step, calculation is carried out until the unbalanced forces ratio reduced to 10e-6 which is pre-assumed by FLAC3D that the model is in equilibrium.

Next, the modification of horizontal stress is then set to equal half of the vertical stress by undergoing a built-in FISH code (i.e., K_0=0.5). After all the initialization of ground displacement and velocities are set to zero, the excavation starts by advancing at 1.5 m in each stage.

The excavation is simulated by changing the mechanical property of the ground located at the tunnel section to null. The installation of structural support and the application of face pressure are also imposed simultaneously at every stage. After each block of the ground is excavated, liner structural element with thickness of 0.1 m is installed accordingly to support the ground as the simulation the presence of skin plate of the TBM as presented in the Fig 3.1(b). The skin plate which is simulated with liner structural elements is then removed as the stage proceeds. 0.2m thick solid element between inner and outer diameter of tunnel is activated to simulate the backfill grout supported by another new liner element which represents segment linings. And 6 m of skin plate is installed along the tunnel advance direction in the first 4 stages of the excavation.

Actually, the tail void which is the sum of tail clearance and thickness of skin plate should be filled with backfill grout after the installation of segment lining. In this study, backfill grout is assumed to be injected right after the installation of segment lining.

3.5 Comparison between FEM and FDM

EPB shield TBM is simulated with FEM and FDM respectively and the result such as transversal deformation profile, longitudinal deformation profile, and vertical displacement at tunnel crown, and various stress components are compared. Monitoring data obtained from MRT project in Singapore (Pang, 2006) is included as a reference.

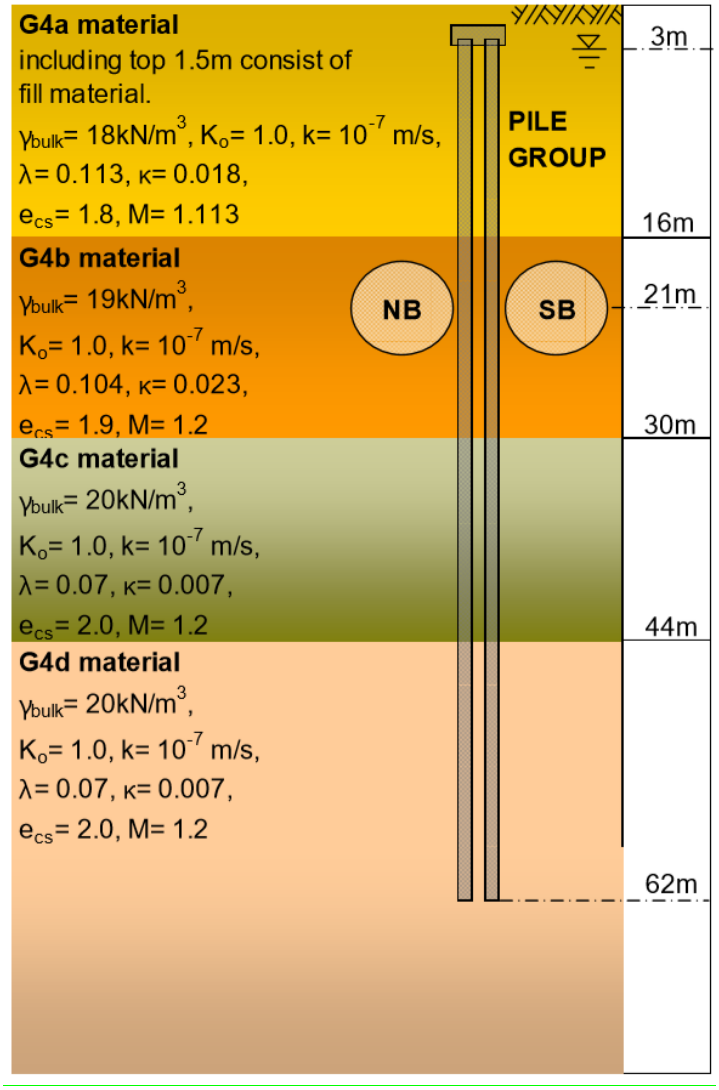

Fig. 3.6 Typical soil profile of C704 MRT project in Singapore (Pang, 2006)

The typical soil profile of C704 project is presented in Figure 3.6. At this section, main geological formation is Bukit Timah Granite residual soil (G4). The G4 material is predominantly reddish brown, sandy silty clay. Within the G4 material, further layering is classified according to the SPT-N value (Wang, 2003). G4a, G4b, G4c, G4d and G4e represent the residual soil with SPT-N < 15, 15 to 30, 30 to 50, 50 to 100 and >100,

respectively. In this representative section, the top 16m consists of G4a material. This was followed by 14m of G4b, 14m of G4c and finally G4d which was encountered all the way without encountering G4e material. The twin tunnels were located at a depth of 21m below ground surface. The diameter of MRT tunnel is 6.5m.

Extensive instrumentation was installed along the C704 tunnel route to monitor the surrounding ground during tunnel advancement. Over 800 settlement and building markers, 48 inclinometers, 12 deep level extensometers, 10 tiltmeters, 26 tape extensometers and 55 piezometers/standpipes were installed along the tunnel route (Knight-Hassell & Tan, 2000). Especially, 12 settlement markers were installed along the tunnel route as presented in Figure 3.7.

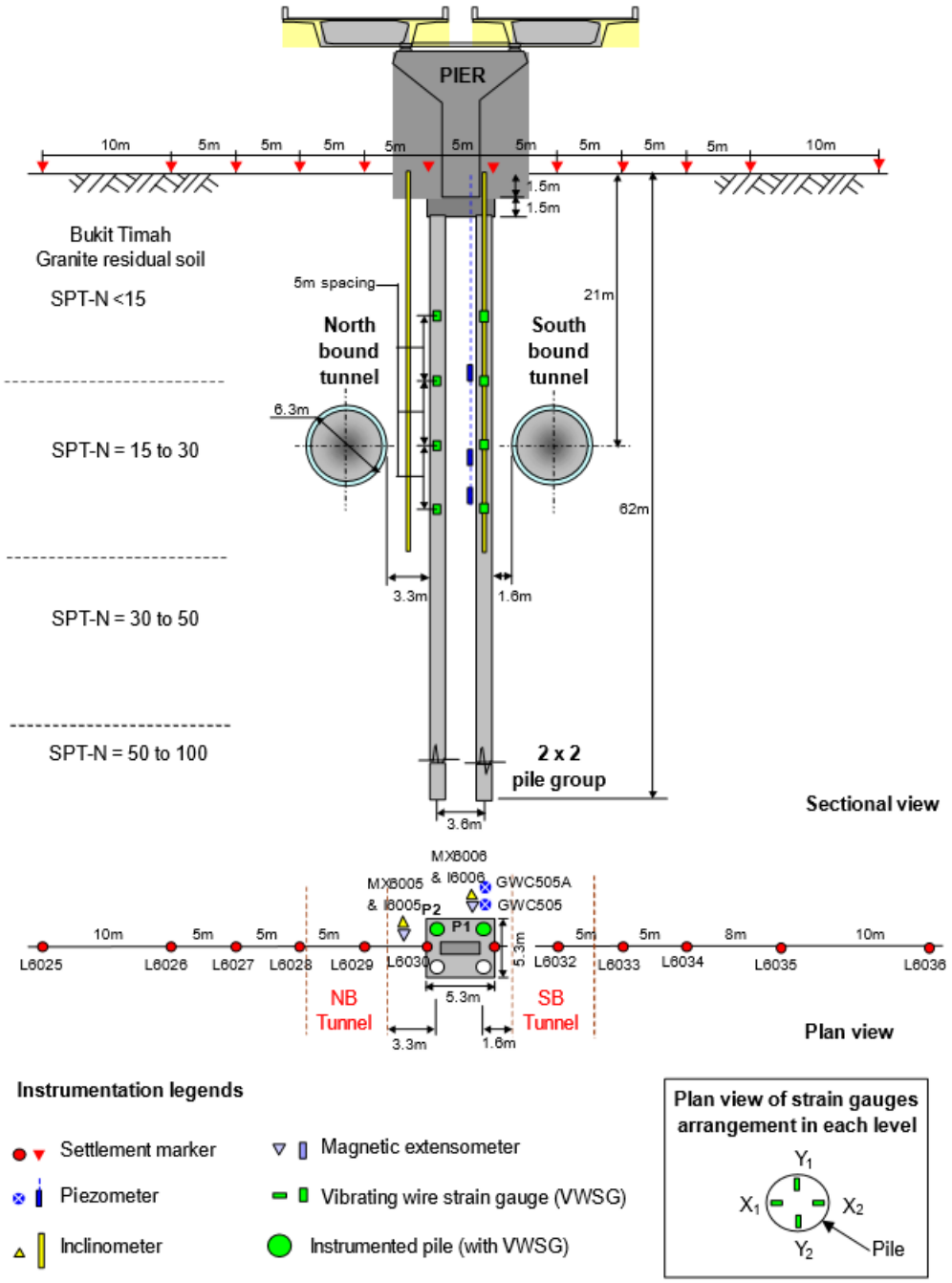

Fig. 3.7 Layout of monitoring instrumentation in C704

Since the ground property and the depth of monitoring data obtained from C704 are not identical to the numerical model simulated in this study, the results were

normalized with the maximum value. The normalized trend represents the behavior of ground and can be used as reference for the simulation result.

Transversal ground settlement

Transversal ground settlement shows Gaussian curve for both cases. The maximum transverse settlement of ground surface is approximately 3.3 mm in Flac3D and 1.1 mm in Midas GTS NX. Despite the difference in magnitude, both software show similar trend of soil settlement when investigated through normalized curves shown in Fig. 3.8 below. However, the transversal ground settlement from FDM shows wider shape than that obtained from FEM even though both uses same material properties, geometry and boundary condition. And the transversal ground settlement obtained from FDM shows good agreement with the monitoring data.

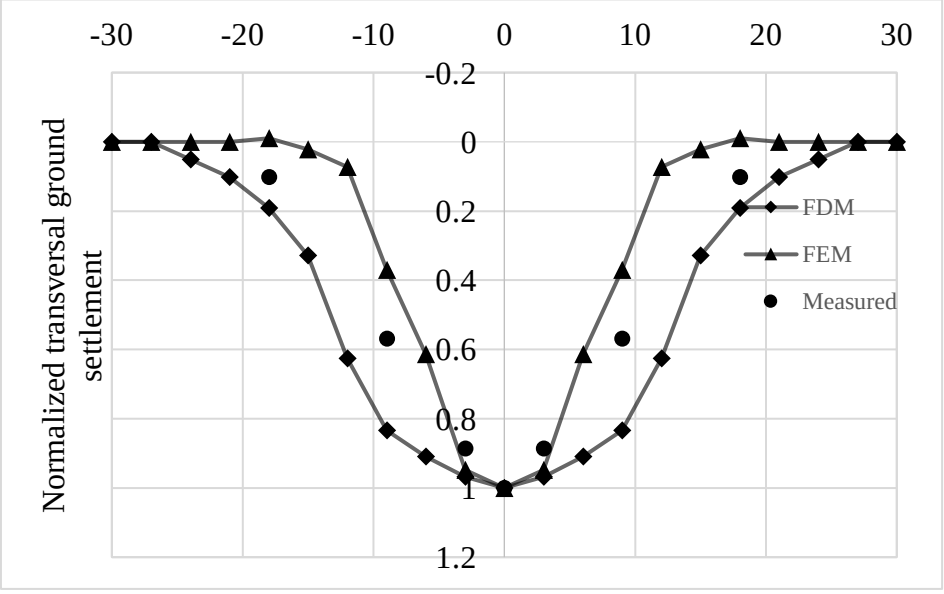

Figure 3.8 Normalized transversal ground settlement

Longitudinal deformation profile

Longitudinal deformation profile obtained from FEM and FDM is presented in Fig. 3.9. Although they show similar shape, the shape obtained from FDM shows better agreement with the monitored data than the curve obtained from FEM. Moreover, small amount of heave is found in the curve obtained from FEM as the advance length increase which is different from conventional understanding of ground behavior.

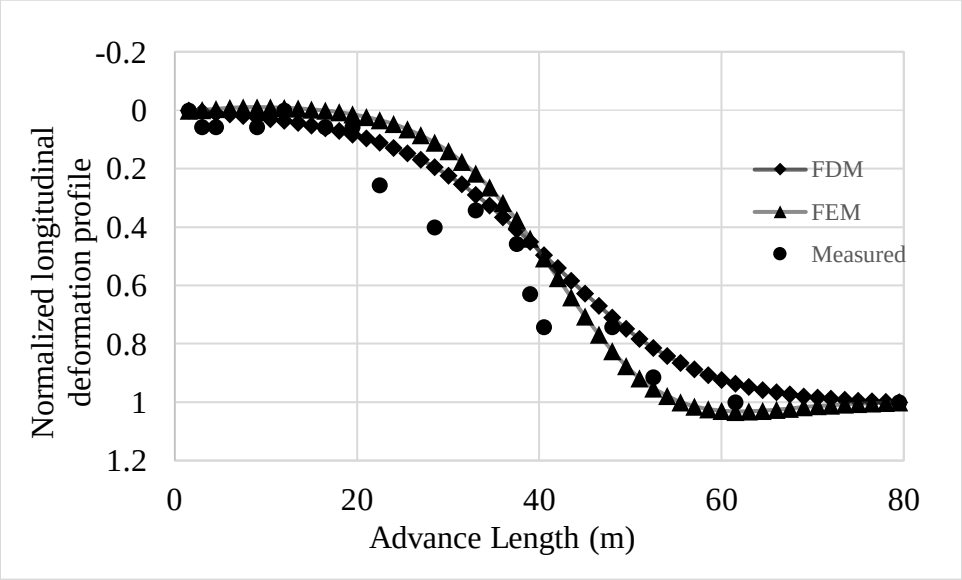

Figure 3.9 Normalized longitudinal deformation profile

Vertical displacement at tunnel crown

The maximum vertical displacement at tunnel crown is approximately 12.4 mm in Flac3D and 8.4 mm in Midas GTS NX. Although vertical displacement at tunnel crown shows radical reduction due to excavation for both cases, however, the displacement obtained from FEM shows a small amount of heave after the excavation. Vertical

displacement at tunnel crown obtained from FDM shows S-shape which is very similar with the longitudinal deformation profile. From the theoretical solution and empirical solution suggested by Panet & Guenot (1982), Corbetta (1991), Panet (1995), Chern (1998), Hoek (1999) and Unlu & Gercek (2003), the vertical displacement at tunnel crown and longitudinal deformation profile should be S-shaped. Therefore, the vertical displacement and longitudinal deformation profile obtained from FDM is reliable than that from FEM.

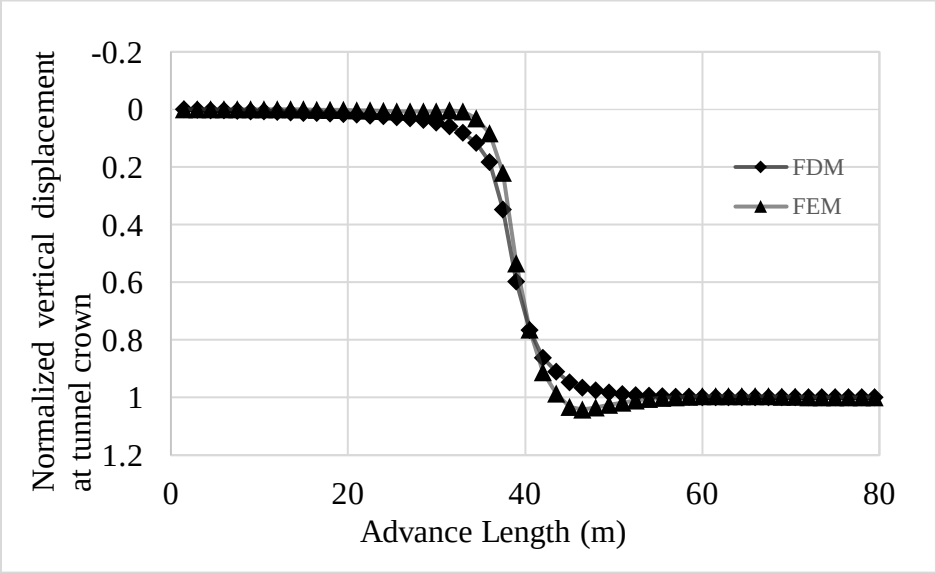

Figure 3.10 Normalized vertical displacement at tunnel crown

Stress distribution at spring line

The change of stress around the tunnel due to excavation should be monitored. In this section, the stress distribution due to shield TBM tunneling was obtained under isostatic pressure condition (K_0=0.5). As shown in Fig. 3.11, tangential, radial and axial stresses were measured slightly above the springline of the tunnel.

The shield TBM advance direction is along the y-axis. Therefore, the z-axis and x-

axis represent tangential and radial stress direction, respectively. Figure 3.11 shows the stress distribution along with the advance length. Figure 3.11 (a) shows the change of tangential stress: Tangential stress increases rapidly as the tunnel face approaches. However, after the installation of skin plate it suddenly decreases and again it increases due to advancing. After the installation of segment lining, it slightly decreases and approaches to convergence. The variation of tangential stress is sensitive to the tunnelling process and it can be used as good indicator of stress change around the tunnel springline.

Figure 3.11 (b) illustrates the radial stress change due to excavation. Radial stress decreases rapidly due to excavation and slightly increases after the installation of skin plate. It increases slightly due to advancing and it drops after the installation of segment lining. As the tunnel face move away from the monitoring point, it converges. It is found that the tangential stress increases due to tunnel excavation meanwhile radial stress decreases due to tunnel excavation.

Trend of axial stress at tunnel springline due to tunnelling is shown in Fig. 3.11 (c). Axial stress shows 260kPa before excavation and it gradually increases as the tunnel face approaching. After the excavation, it suddenly drops. As the tunnel face move away from the monitoring point, axial stress recovers its original stress level. The arching effect due to tunnel excavation can be found in axial stress change.

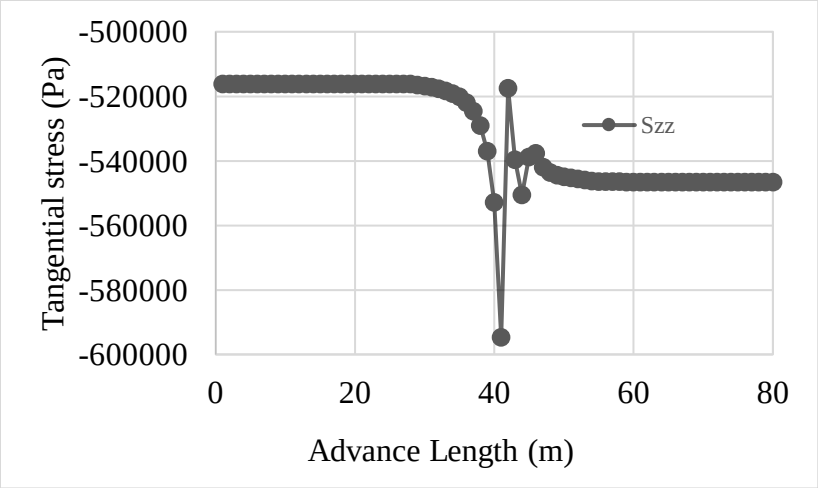
-500000
-520000
-540000
-560000
-580000
-600000
Tangential stress (Pa)
Szz
0
20
40
60
80
Advance Length (m)

(a)

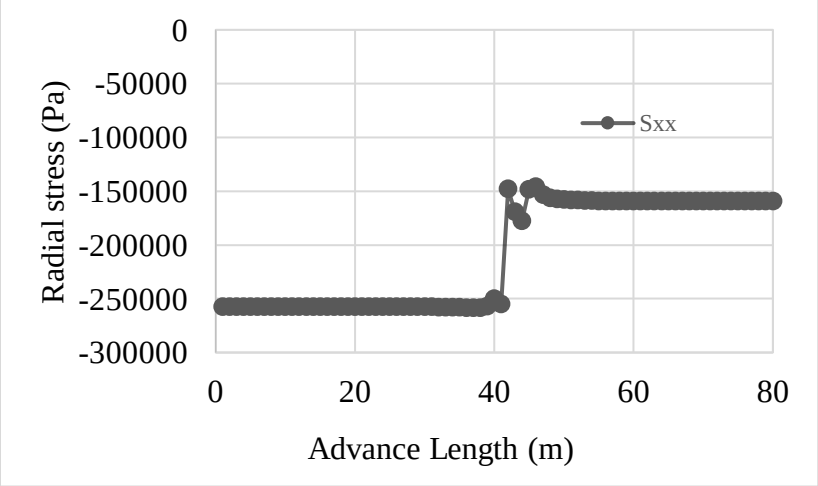
0
-50000
-100000
-150000
-200000
-250000
-300000
Radial stress (Pa)
Sxx
0
20
40
60
80
Advance Length (m)

(b)

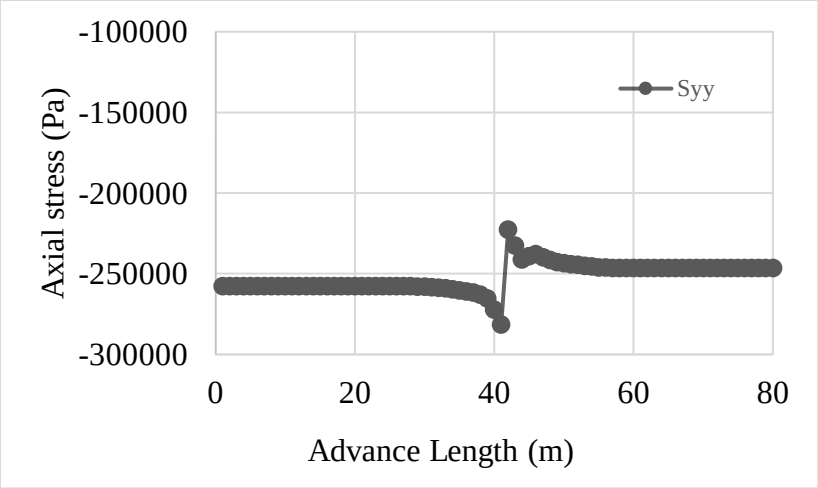

(c)

Figure 3.11 Variation of stress due to excavation at the tunnel springline. (a) Variation of tangential stress (b) Variation of radial stress (c) Variation of axial stress

Stress resultant acting on the segment lining

As mentioned above, both bending and membrane stresses can be obtained by using structural element for segment lining. Stress resultant acting on a plate-type structural element represent a combination of bending and membrane actions. Bending stresses produce bending and twisting moments and transverse shear forces while membrane stresses act in tangent to the mid-surface and produce mid-surface tangent forces. These moments and forces per unit area are referred to as stress resultants. The following are the eight stress resultants that can be obtained as for bending (Mx, My, Mxy), transverse shear (Qx, Qy), membrane (Nx, Ny, Nxy). In this study, stress resultants are measured at the side of the tunnel wall particularly at the wall of the segment lining located in the middle of the model.

$$M_x = \int_{-t/2}^{t/2} \sigma_{xx} z dz$$

$$M_y = \int_{-t/2}^{t/2} \sigma_{yy} z dz$$

$$M_{xy} = \int_{-t/2}^{t/2} \sigma_{xy} z dz$$

$$N_x = \int_{-t/2}^{t/2} \sigma_{xx} dz$$

$$N_y = \int_{-t/2}^{t/2} \sigma_{yy} dz$$

$$N_{xy} = \int_{-t/2}^{t/2} \sigma_{xy} dz$$

$$Q_x = \int_{-t/2}^{t/2} \sigma_{zx} dz$$

$$Q_y = \int_{-t/2}^{t/2} \sigma_{zy} dz$$

The stress distribution through the plate-type structural element follows particular theory. For both Kirchhoff (thin shell) theory and Reissner (thick shell) theory, stress distributions correspond to a supposition below:

$$\sigma_{xx} = \frac{N_x}{t} + \frac{12 M_x z}{t^3}$$

$$\sigma_{yy} = \frac{N_y}{t} + \frac{12 M_y z}{t^3}$$

$$\sigma_{xy} = \frac{N_{xy}}{t} + \frac{12 M_{xy} z}{t^3}$$

$$\sigma_{zz} = 0$$

$$\sigma_{zx} = \frac{3Q_x}{2t}\left(1-\left(\frac{2z}{t}\right)^2\right)$$

$$\sigma_{zy} = \frac{3Q_y}{2t}\left(1-\left(\frac{2z}{t}\right)^2\right)$$

Stress resultants were measured at the side wall of the segment lining at the center of the model. Figure 3.12 (a), (b) and (c) shows respectively the bending, shear and membrane stress resultants acting on the segment lining. In Fig. 3.12 (a), the bending stress resultant started to increase sharply and gradually reached a converged level. According to the Figs. 3.12 (b) and (c), when structural elements of the shield TBM were installed, the stress resultants quickly increase and reached their converged certain level.

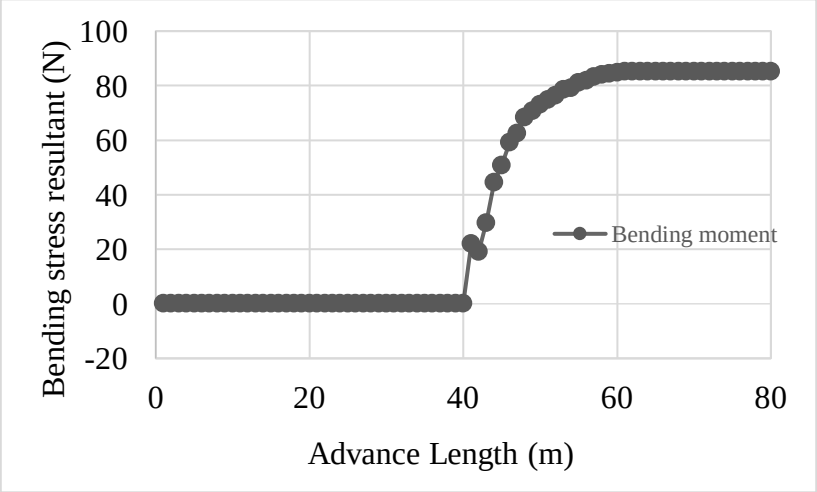

(a)

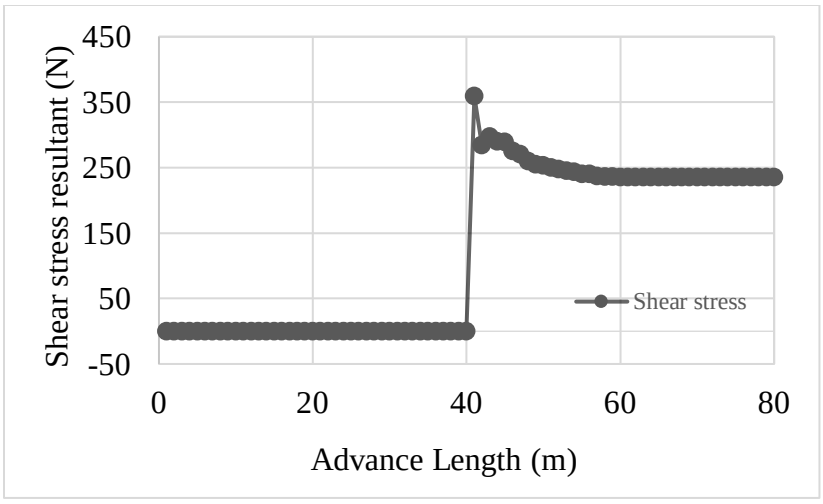

(b)

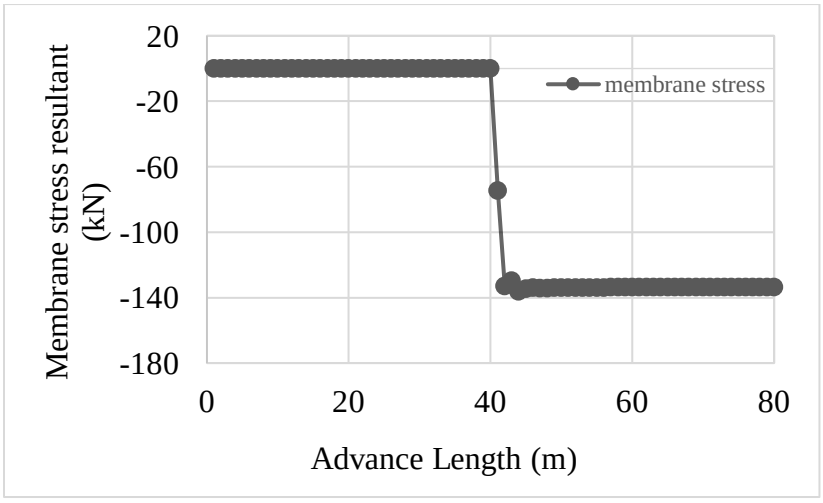

(c)

Figure 3.12 Variation of stress resultant acting on segment lining (a) Bending stress resultant (b) Shear stress resultant (c) Membrane stress resultant.

Summary

In this section, numerical analysis result is validated with monitoring data obtained

from C704 MRT project in Singapore. Despite the difference in magnitude, FEM and FDM show similar trend of soil settlement when investigated through normalized curves: Transversal ground settlement shows Gaussian curve. However, the transversal ground settlement from FDM shows wider shape than that obtained from FEM. Although they show similar shape, the transversal ground settlement and longitudinal deformation profile obtained from FDM shows better agreement with the monitoring data than the curve obtained from FEM.

Moreover, comprehensive stresses around the tunnel can be obtained with FDM analysis: Radial, tangential stress around the tunnel and bending stress resultant, shear stress resultant, and membrane stress resultant can be obtained from FDM analysis. From the axial stress variation during tunnelling, arching effect can be found: After the excavation, axial stress suddenly drops. As the tunnel face move away from the monitoring point, axial stress recovers its original stress level.

Therefore, FDM analysis is adopted in this study to investigate the progressive behavior of pile foundation during tunneling process.

CHAPTER FOUR

PILE-TUNNEL STRUCTURAL INTERACTION

4.1 Background

According to Lee et al. (2006), three-dimensional numerical simulation of tunneling effects on an existing pile was carried out for the case of pile tip located at the same as the tunnel axis and 5.5 m away from the tunnel center. The results showed that at initial stage, axial force in the pile increases only very slightly. As the tunnel face advances to y/D = - 1, the axial force increases to its maximum at the lower half of the pile. When the tunnel face is right below the pile axis, the axial force is reduced at the upper part of the pile, while it is increased near the pile toe. When the tunnel face moves pass the pile axis, the axial force in the pile increases again. When the tunnel moves away at about y/D = 3, axial force reduces slightly at the top and increases significantly at the lower part of the pile.

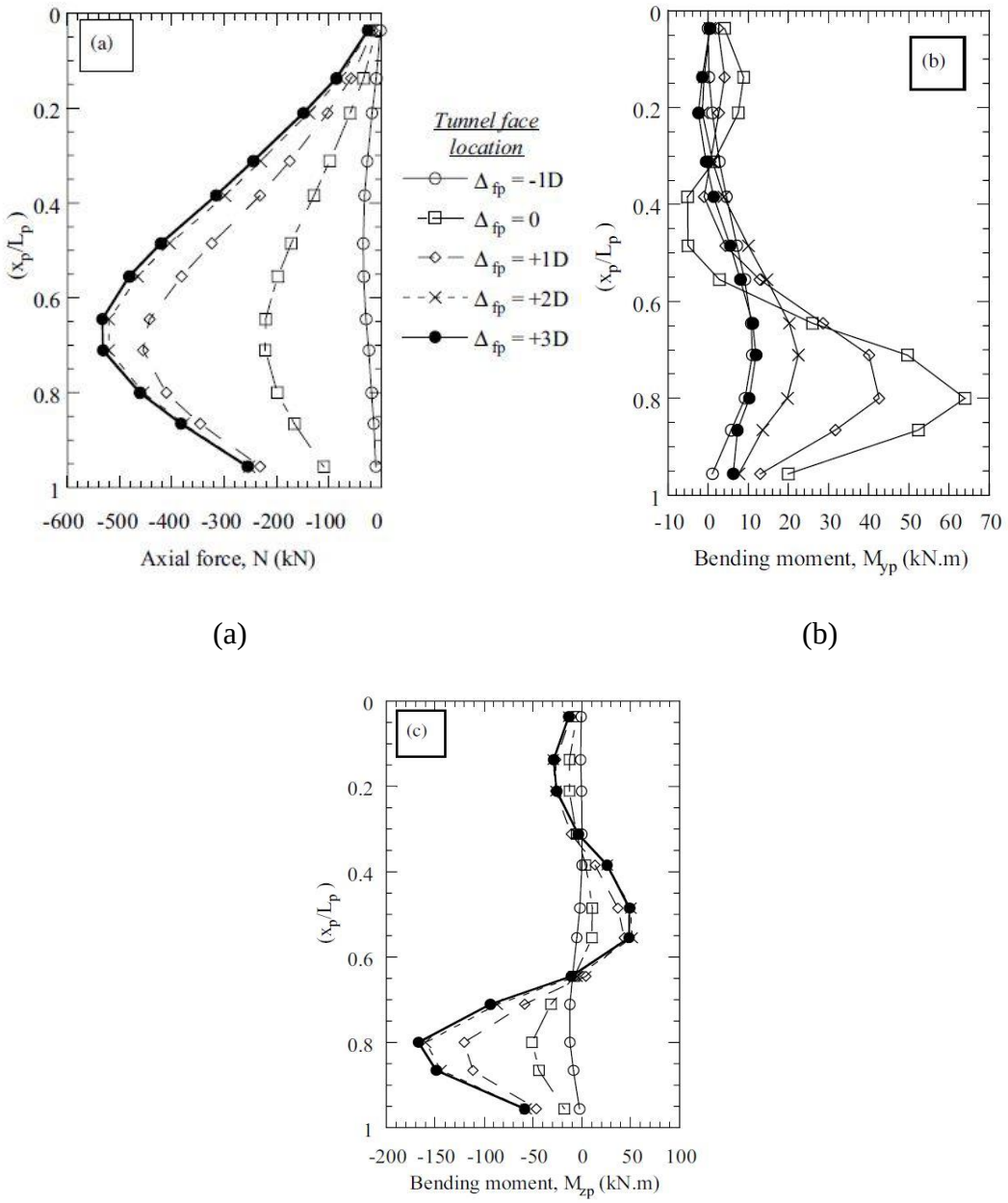

Figure 4.1 Axial force and bending moment variations (Lee et al., 2006)

According to Mroueh & Shahrour (2002), in the case of a shallow tunnel where the pile tip is below the tunnel horizontal axis, tunneling induces compressive axial force in the upper part of the pile which results from the downward movement of soil. In the lower

part of the pile, there is a decrease of the axial force.

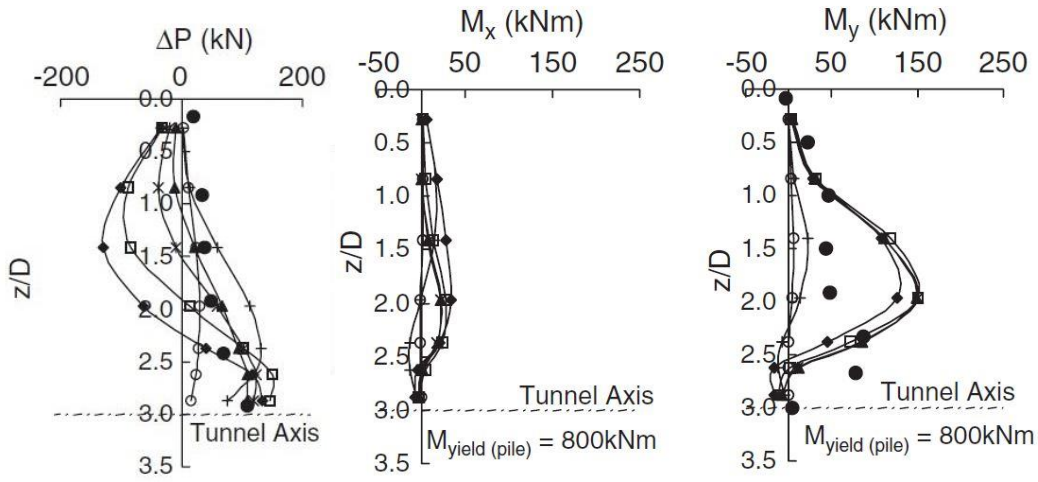

Figure 4.2 Axial force and bending moment variations (Mroueh & Shahrour, 2002)

However, the behavior of pile due to tunneling should be classified considering the relative location of tunnel with respect to pile. Short piles are defined as those with ratio of pile length (Lp) to tunnel depth (Lt) is less than 1 (Lp/Lt<1), and in the case of long pile, this ratio is greater than 1 (Lp/Lt>1).

In order to investigate the behavior of pile in response to tunneling, numerical analyses have been carried out for short pile condition and long pile condition. FLAC3D is used for numerical analysis and built-in pile structural element is adopted to model the pile structure in this study.

4.2 Parametric study

In order to further analyze the behavior of pile in response to tunneling, a series of

numerical simulations are to be carried out. The purpose of parametric study is to understand the behavior of pile subjected to ground modification induced by tunneling.

The most important focus is placed on the positions of tunnel with respect to the pile which can vary vertically and horizontally as the distance and depth change. As shown in the Figure 4.3, position of the pile is set to be fixed and only the tunnel is moved in vertical and horizontal direction. To simplify the variation of position of the tunnel, horizontal (X direction) and vertical (Z direction) changes of the tunnel are set to be in function of the tunnel diameter starting from 0.5D to 3D with 0.5 increment. The total number of cases to be carried is then 36 cases for short pile (tunnel located below the pile tip) and the other 36 cases for long pile (tunnel located above pile tip). Short-pile and long-pile cases were studied to access the effects of pile length with respect to tunnel depth.

As described above, short pile case shows significant pile settlement, with additional bending moment, lateral displacement and pile rotation. However, for long pile case, significant bending moment changes is observed while the pile head settlements are less than that of the ground.

As the position of the tunnel changes, boundary condition of the whole model needs to be adjusted so that the effects of tunneling can always be obtained. As mention above, the boundary condition are taken as 5 times the diameter of the tunnel. Therefore, for the furthest distance of the boundary condition to be modeled is set as shown in figure below.

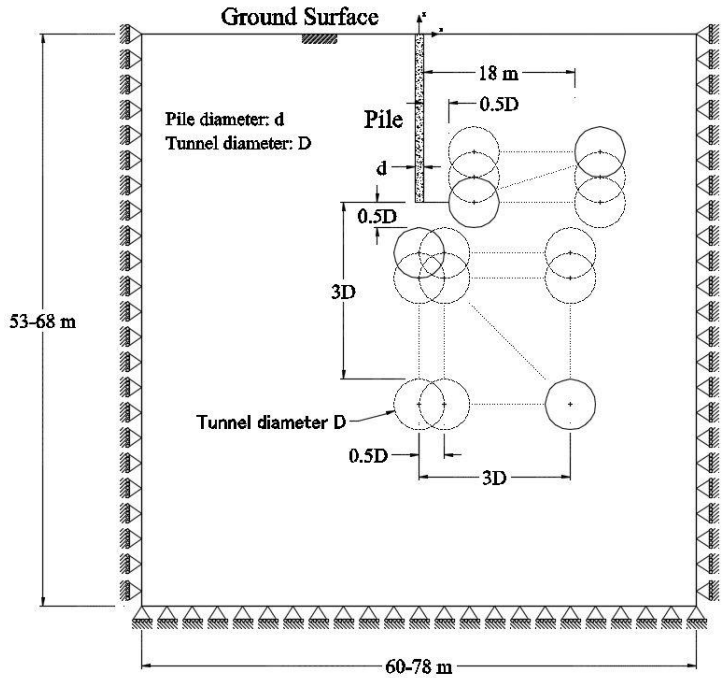

Figure 4.3 Parametric study and boundary condition

To evaluate the stability of pile structure, axial force, bending moment both in longitudinal and transverse direction, shear stress along the pile shaft and pile structural element nodal displacement are monitored for the investigations.

Based on the result of the series of simulations on different cases of parameters, the following conclusion are expected to be drawn: zone of influences, general phenomenon of pile dragloads and downdrag and ground settlement zone induced by tunnel in different positions.

4.3 Model construction

Numerical analysis of pile foundation is rarely carried out in routine design process. Axis-symmetric model is usually adopted in the numerical analysis of single pile foundation (Potts & Zdravkovic, 2001). To investigate the soil-structure interaction, 3D modelling is required to simulate the complicate geometry, construction processes and boundary conditions and so on (Ottaviani, 1975; Comodromos et al., 2003; Wakai et al., 1999; Yang and Jeremic, 2003; Jeong et al., 1997).

The most challenging problem that has been encountered is the selection of pile modeling methods. Pile foundation is usually assumed to be placed based on construction plan. The installation effect has been considered depending on the pile construction method. In case of bored pile, lateral stress and pressure acting on the borehole change during curing process (Zhu, 1999). Localized area around the pile structure could have affect on the behavior of pile. Powrie & Li (1991) and Wakai et al. (1999) tried to consider the effect of pile installation with finite element analysis.

So far, the study has been using two main different approaches to model the pile element. One approach was to conventionally use the zone generation and pile properties and apply interface between the soil and pile zones which has been found to be more difficult and time consuming. Another method was to take advantage of FLAC3D built-in structural pile element to model the pile element. It is found that the second approach is more reliable, less time consuming and easier management of results extraction as all the parameters to be monitored can be obtained easily than the first case by just using the FISH functions to extract the data.

In FLAC3D, pile structural element is two-noded, straight, finite element with six degrees of freedom per node. One single pile modeled in this study is composed of other

small pile component elements that make up the whole pile. Each pile element component consists of 2 nodes at its beginning and end part. Since the pile set to be composed of 30 pile element components, there are in total 31 nodes from top to bottom of the pile structure. Behavior of pile such as forces and bending moment can be obtained by extracting the information from these nodes. Both normal-directed and shear-directed frictional interaction occurs between the pile element and the grid generated. By default, pile structural element already includes skin-friction effects without the need of modification. However, the end-bearing effect is not taken into consideration by default unless modifications to the link of the pile tip are made. However, as described earlier, due to the condition that the whole ground to be simulated is soft soil, the bearing capacity of the pile contributed by the end-bearing effects is not considered. The load can be applied in a few ways including the initialization of velocity or applying either point or distributed loads. In this study, the 30 m-pile is constantly loaded by applying vertical nodal force at the top of the pile.

In addition to the selection of method to model the pile element, the choices of suitable properties to match with the simulation is also challenging and requires trial and error analysis before being able to officially adopt certain properties of the pile structural element. Pile structural element used in FLAC3D can deliver different pile monitoring response which includes coupling stress, coupling displacement, forces and bending moments depending on the input parameters. For example, in the case where pile is subjected to only the axial loading and only the axial force is to be monitored, certain parameters such as polar and second moment of inertia are optional. In contrast, if bending moments about certain axes are among the monitoring parameters, the above-mentioned

input properties must be given. Some important properties that make significant contribution to the changes in behavior of the pile include normal and shear coupling spring cohesion (cs_ncoh and cs_scoh), normal and shear coupling spring friction angle (cs_nfric and cs_sfric), normal coupling spring gap-use flag (cs_ngap), normal and shear coupling spring stiffness (cs_nk and cs_sk).

Normal and shear coupling spring cohesion are taken the same as the cohesion of soil and multiply by the exposed parameter of the pile. For normal and shear coupling spring friction angle, both are the same as that of soil. By default, normal coupling spring gap-use flag is set to off, however, it is set to on in this simulation for monitoring. Finally, normal and shear coupling spring stiffness are taken as 10 times the shear modulus of the soil and multiply by the exposed parameter of the pile. Properties of pile structural element used in the simulation are shown in Table 4.1.

Table 4.1 Properties of pile structural element

Pile Diameter [mm]	1000	Shear coupling spring cohesive strength [kN/m]	62831.85
Density (kg/m^3)	2400	Shear coupling spring friction angles [degrees]	30
Young's Modulus (N/m^2)	8.00E+10	Shear coupling spring stiffness [N/m^2]	7.26E+08
Poisson Ratio,	0.2	Normal coupling spring cohesive strength [N/m]	62831.85
Cross Section Area (m^2)	0.7854	Normal coupling spring friction angle [degrees]	30
Polar moment of inertia [m^4]	0.0982	Normal coupling spring gap-use flag [on/off]	on

Second moment w.r.t. local y-axis [m^4]	0.0491	Normal coupling spring stiffness [kN/m^2]	6.00E+07
Second moment w.r.t. local z-axis [m^4]	0.0491	Exposed perimeter [m]	3.1416

The coordinate axes are taken at the bottom corner of the whole zones and the z-axis is oriented upward. The model grid is shown in Figure below. Boundary condition at the top of the pile is set to be a free surface. The base of the model, at z = 0, is fixed in z-direction, and the boundaries of all the sides of the model are rollers. There are in total 72 cases of simulations which are then divided further into 2 categories. In both categories, all the tunnels and pile structural element are basically the same but the difference is the location of the tunnel with respect to the pile. In the first category which is assumed to be the case for short pile, the tunnel is situated below the end of the pile tip. In the second category, the tunnel is situated above the pile tip. The position of the tunnel with respect to the pile is varied by the following parameters:

- Δv is the vertical distance between the pile tip and the tunnel axis
- Δhl is the horizontal tunnel longitudinal direction distance between the pile axis and the tunnel advance face which is denoted by minus (-) sign when the tunnel is the front or has not passed the pile axis and plus (+) sign when tunnel is at the back or passes the pile axis
- Δhv is the horizontal tunnel transverse direction distance between the pile axis and the tunnel axis

It should be noticed that to make it easier for the simulation the x, y and z

coordinates of the center of the tunnel is fixed in all models and only the positions of the pile is varied. The reason is due to the fact the pile element can be placed at any locations by just specifying the coordinates of the first and second ending of the pile. Alternatively, if the pile element were to be fixed, and tunnel zone grid is to be changed, it would take much longer time since the each new tunnel zones generation requires new input of zone points which are too many compared to that of pile element.

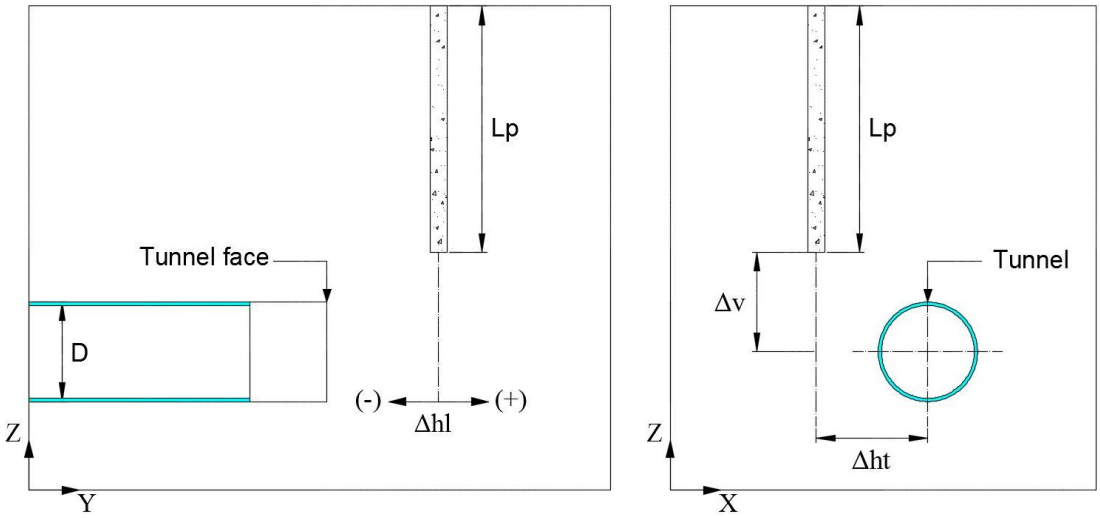

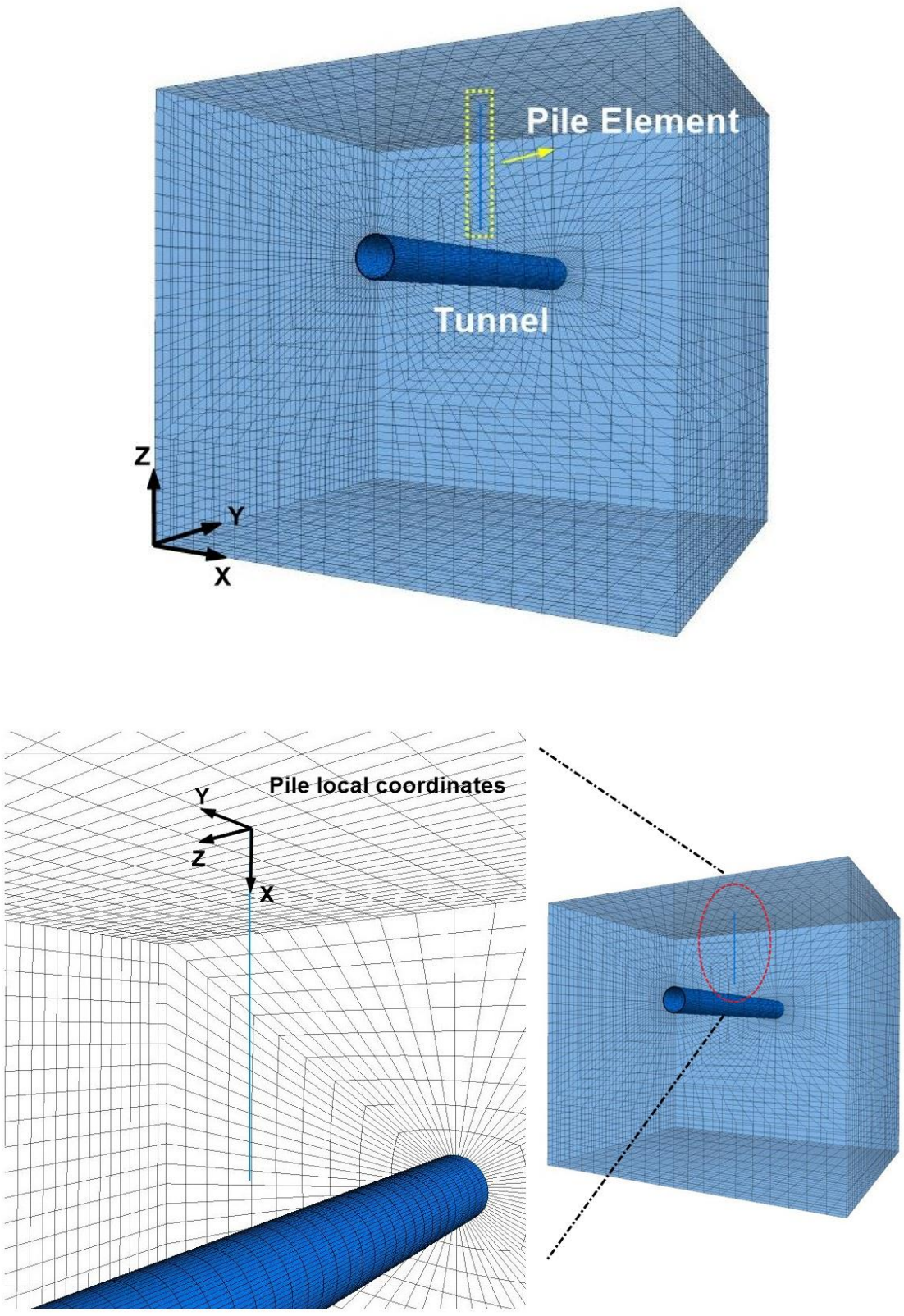

Figure 4.4 Model geometry using pile structural element for pile

4.4 Results of parametric study

All the parameters to be monitored are recorded and plotted at various locations of tunnel face with respect to the tunnel axis which include 4 positions from the front of the pile axis (Δhl: -3D, -2D, -1D, and -0.5D, 1 at the pile axis (Δhl: 0) and 4 at the back of the pile axis (Δhl: +0.5D, +1D, +2D, and +3D). The results of the progressive behavior pile is monitored and extracted from second node of the individual pile element component from top to bottom by 2 m interval. Thus, there are in total 16 monitoring points.

Axial force

From the results of the analysis, it can be seen in the case of short pile that the axial force of the pile is in compression and increases only slightly when the tunnel faces are at the front of the pile axis. However, when the tunnel face reaches the pile axis, the axial force starts to increase gradually from the pile top downwards and was at maximum 5 m from the pile end. When the tunnel position horizontally moves away from the pile tip, the position of the maximum axial force gradually increases until the middle of the pile when the tunnel is located about 3.5D from the pile axis.

In case of long pile condition, the compressive axial force increase due to tunnel excavation. Mostly, axial force shows maximum value when the pile axis located 3.5D behind the tunnel face. The axial force distribution is affected by vertical and horizontal position of tunnel center. However, when the horizontal distance between tunnel center and the pile axis is 1D, the vertical position of tunnel center influences the shape of axial force distribution.

The allowable compressive axial force was found to be about 450 kN as shown in the load-displacement in figure below. Maximum axial forces are derived from the all cases and plotted in Fig. 4.6. It can be found that the tensile axial force is developed when the tunnel center is located below the pile tip in short pile condition. Maximum axial force is decreases as the horizontal distance between tunnel center and pile increases. And, the vertical distance from the tunnel center to pile tip increases, the compressive axial force decrease. For long pile condition, compressive axial forces are developed when the tunnel center is close to pile axis regardless the vertical position. And it gradually decreases as the horizontal distance between tunnel center and pile axis increases. Considering the allowable force, it can be found that the allowable position of tunnel center around the pile.

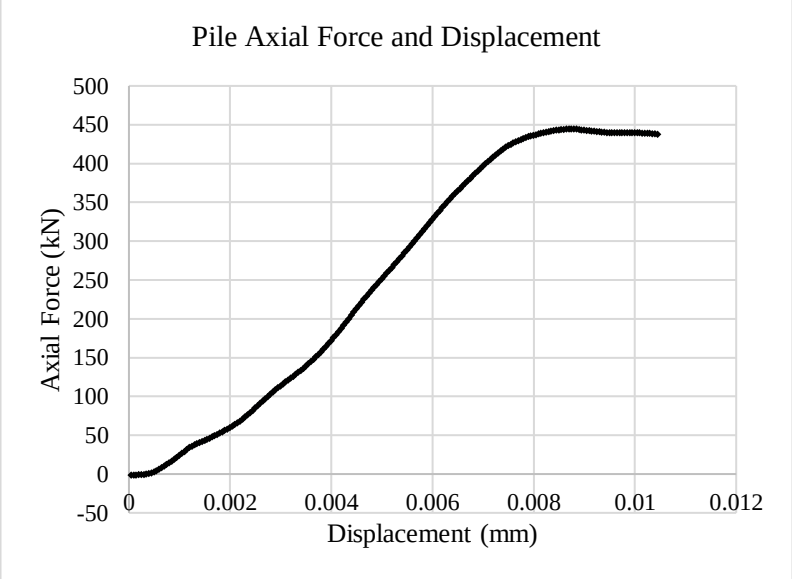

Figure 4.5 Pile load-displacement curve

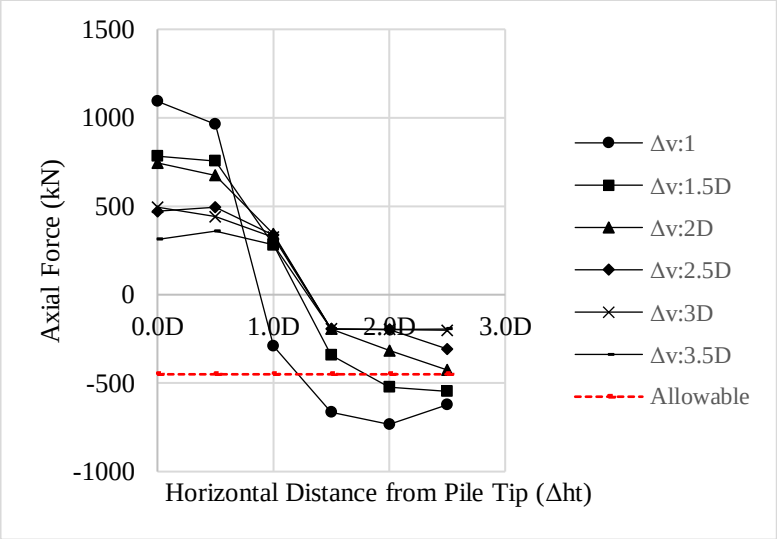

(a)

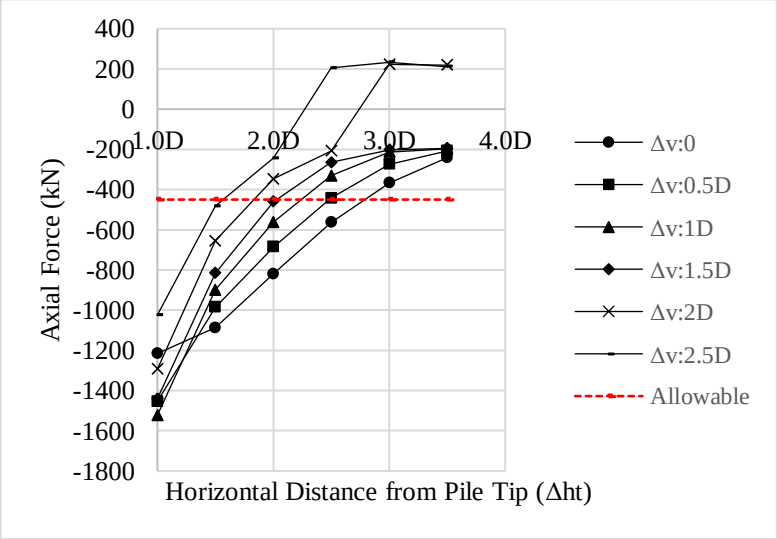

(b)

Figure 4.6 Axial forces (a) Short pile (b) Long pile

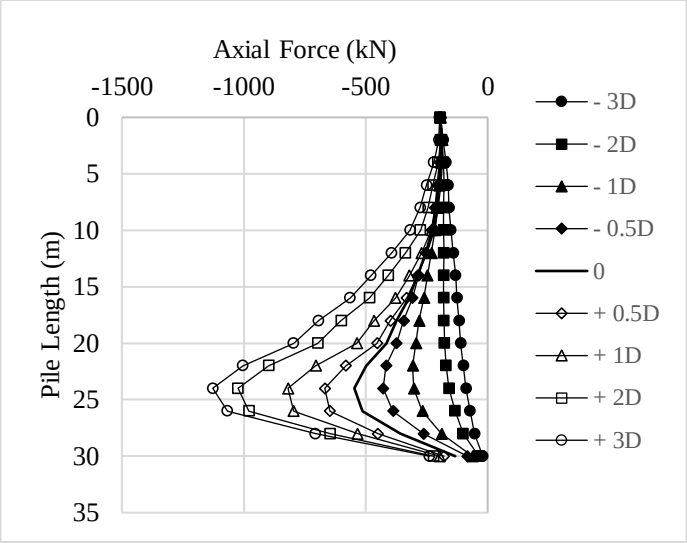

Figure 4.7 Maximum axial force when the horizontal distance from pile and depth of tunnel center are 1D and 27m

Bending Moment

Tunneling induced bending moments are monitored in two directions, one is the bending moment of pile about the axis perpendicular to the tunnel axis (Mz) and the other one is about the axis parallel to the tunnel axis (My). It should be noticed that the notations for the bending parameters are based on the pile local coordinate system as shown in Figure 4.4.

As the tunnel advances, the bending moments of the pile is developed due to the movement of soil induced by tunneling. The bending moment in both direction induced by tunneling on the pile in case of short pile condition is relatively low and insignificant compared to the bending moments in the case of long pile condition. In case of short pile condition, Bending moment, Mz, decreases as the vertical distance from the pile tip to

tunnel center increases and it decreases as the horizontal distance from the pile tip increases.

In cases of long pile condition, bending moment, Mz, is maximum when the horizontal distance of the tunnel center from the pile tip is 1D regardless of vertical position of tunnel center. As the horizontal distance of tunnel center from the pile tip increases, bending moment decreases significantly. As the vertical distance of tunnel center from the pile tip increases, bending moment decreases and maximum bending moment is found when the vertical position of tunnel center is 1D from the pile tip which implies that pile end is fully affected by the tunnel excavation.

As the horizontal distance of tunnel center from the pile tip increases, bending moment, My, increases. As the vertical distance of tunnel center from the pile tip increases, mobilized bending moment decreases and it is deeper than 2.5D from the pile tip, bending moment, My, is insignificant.

The allowable bending stress can be obtained as 9.6 MPa when the allowable bending stress is 40% of compressive strength of concrete (24 MPa for standard concrete). The maximum bending stress is around 6.11 MPa which is lower than the allowable bending stress.

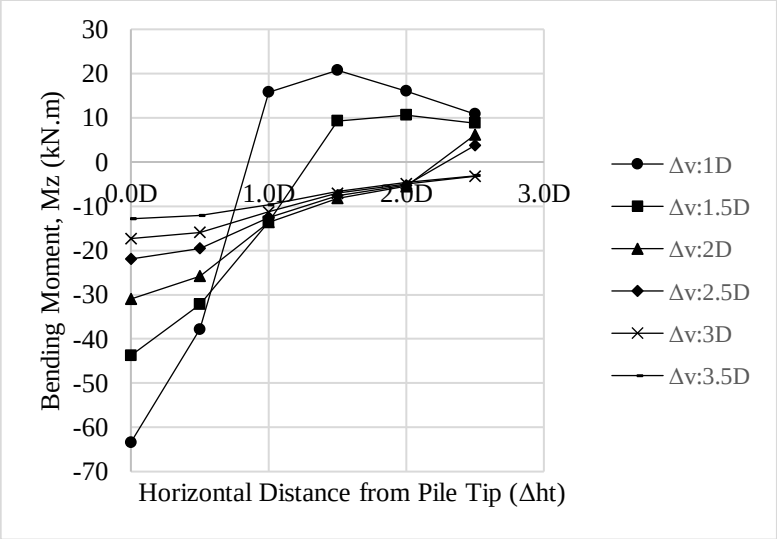

(a)

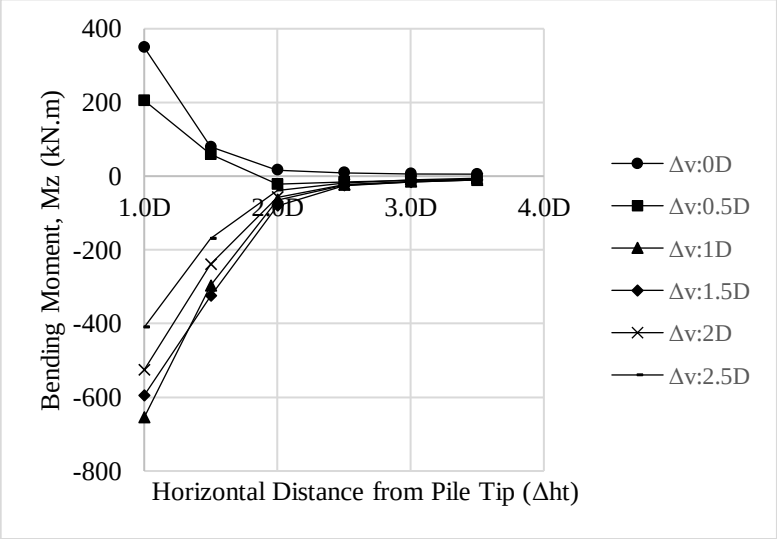

(b)

Figure 4.8 Bending moment Mz (a) Short pile (b) Long pile

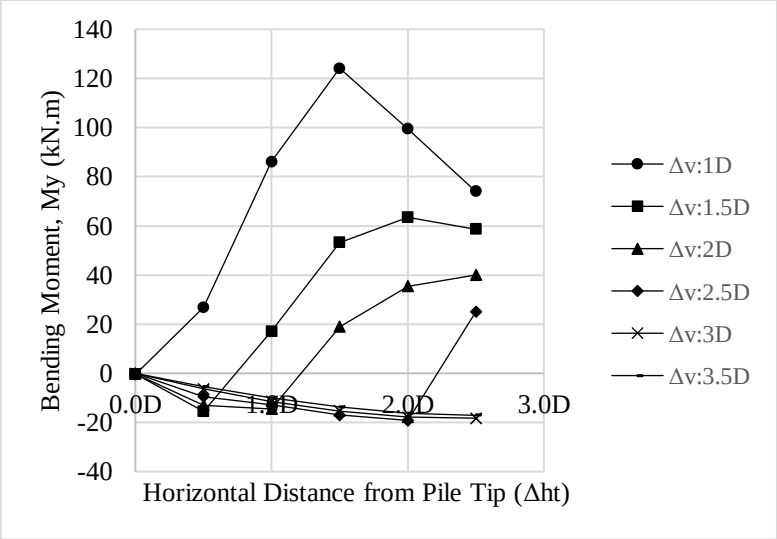

(a)

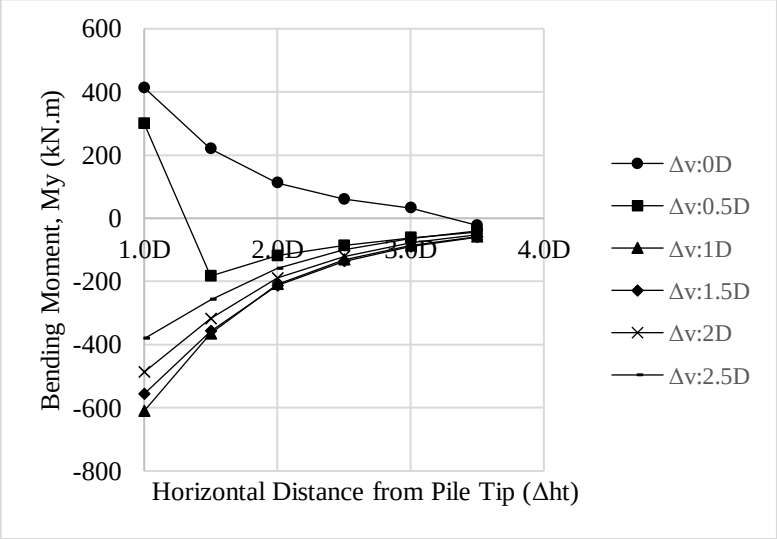

(b)

Figure 4.9 Bending moment My (a) Short pile (b) Long pile

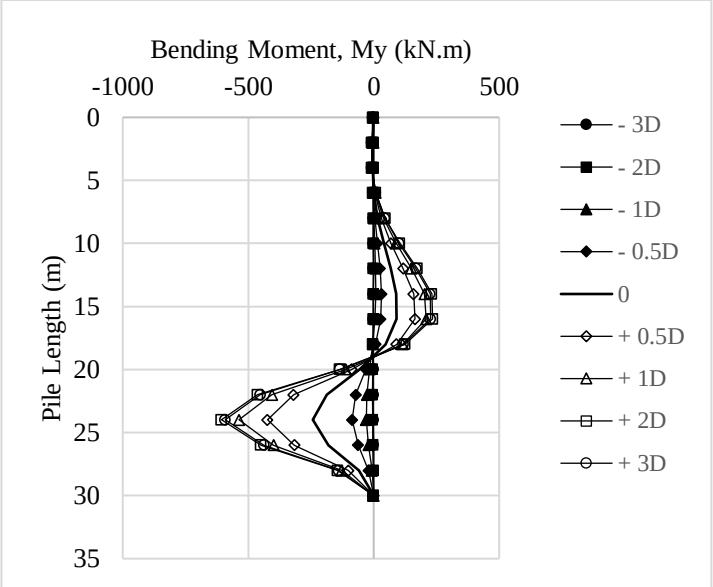

Figure 4.10 Maximum bending moment

Shear Stress

Pile element shear behavior is governed by the interaction with zone grid through shear coupling springs (i.e. the mechanical behavior of pile in shear direction is directly related to shear coupling spring properties of stiffness, cohesive strength, friction angle and exposed perimeter).

Shear stress along the pile was developed significant when the tunnel center is close to pile structure for short pile and long pile condition. And as the horizontal distance of tunnel center from the pile increases, mobilized shear stress decreases.

For short pile condition, mobilized maximum shear stress decreases as the vertical distance of tunnel center from the pile tip increases. When the tunnel center is very close to pile tip, shear stress and shear displacement is concentrated at pile tip (within 5m from the pile tip). However, when the vertical distance of tunnel center from the pile tip is

1.5D~2.0D, shear stress and shear displacement is distributed along the pile ranging 5~10 from the pile tip.

The allowable shear stress is computed as $0.08\sqrt{f_{ck}}$ which equals to 392 kPa larger than the maximum shear stress of 182 kPa.

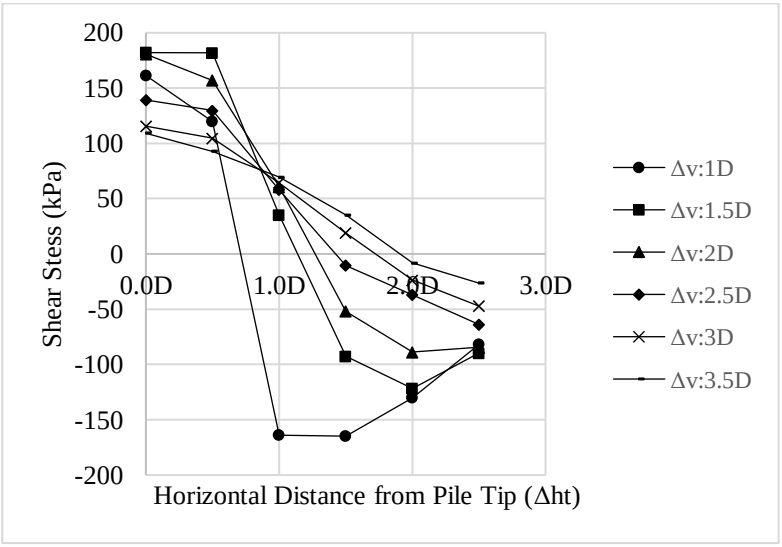

(a)

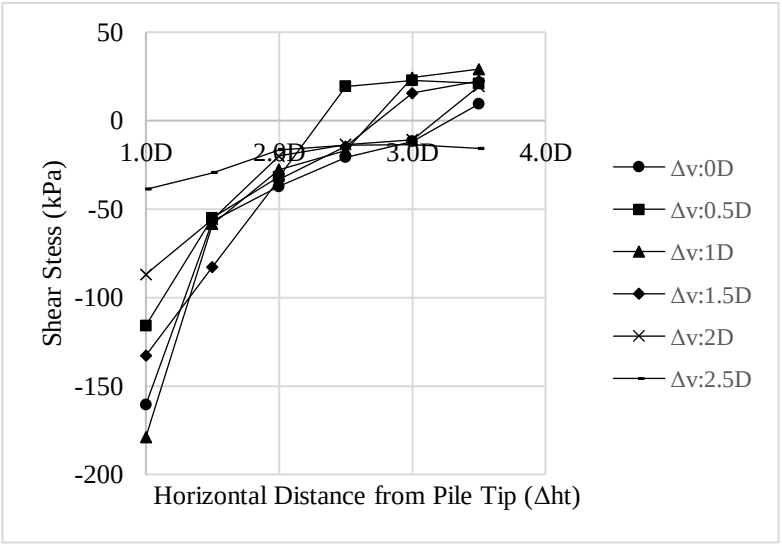

(b)

Figure 4.11 Shear Stress (a) Short pile (b) Long pile

Negative skin friction

When the tunnel is constructed below pile, pile base resistance is reduced due to soil settlement which in turn induces settlement of pile. Because pile bearing capacity at the pile tip is reduced, base resistance is then transferred to pile shaft i.e. pile skin friction is responsible for maintaining the applied load. As it is discussed earlier, when the tunnel center is very close to pile tip, shear stress and shear displacement is concentrated at pile shaft within 5m from the pile tip for short pile condition which implies the base resistance is transferred to pile shaft. Also, from the Figure 4.12, vertical displacement is significantly reduced due to the pile and positive(downward) shear stress is developed at the bottom of pile. Large vertical pile settlement is anticipated for short pile condition as it is found at Figure 4.15.

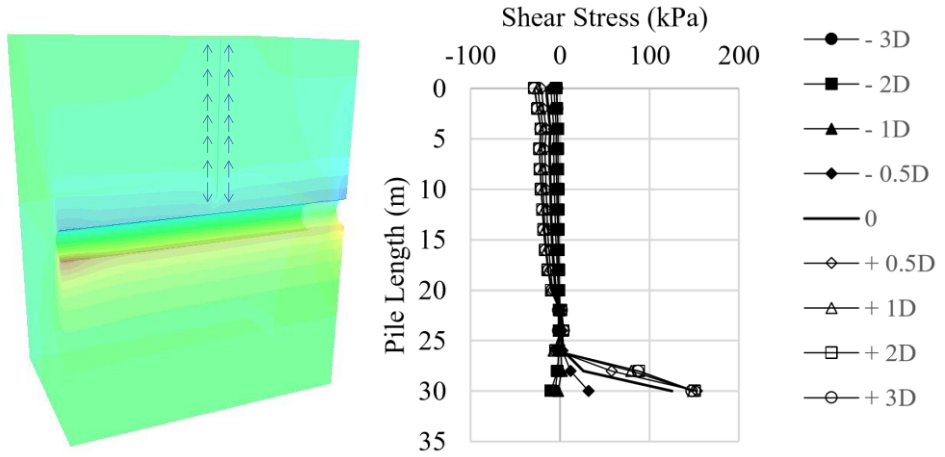

Figure 4.12 Shear stress and negative skin friction

In the case where tunnel is constructed adjacent to pile, tunneling will cause settlement above the tunnel, thus induce negative skin friction around the tunnel level. Pile shaft below the tunnel would then support dragload from negative skin friction above

the tunnel level. Unlike the above case, lateral pile response is significant due to large horizontal soil movement in long pile condition. As it is shown in Figure 4.13, positive(downward) shear stress induced by negative skin friction is developed above the tunnel center and negative(upward) shear stress is developed below the tunnel center which should support the dragload from negative skin friction above the tunnel level.

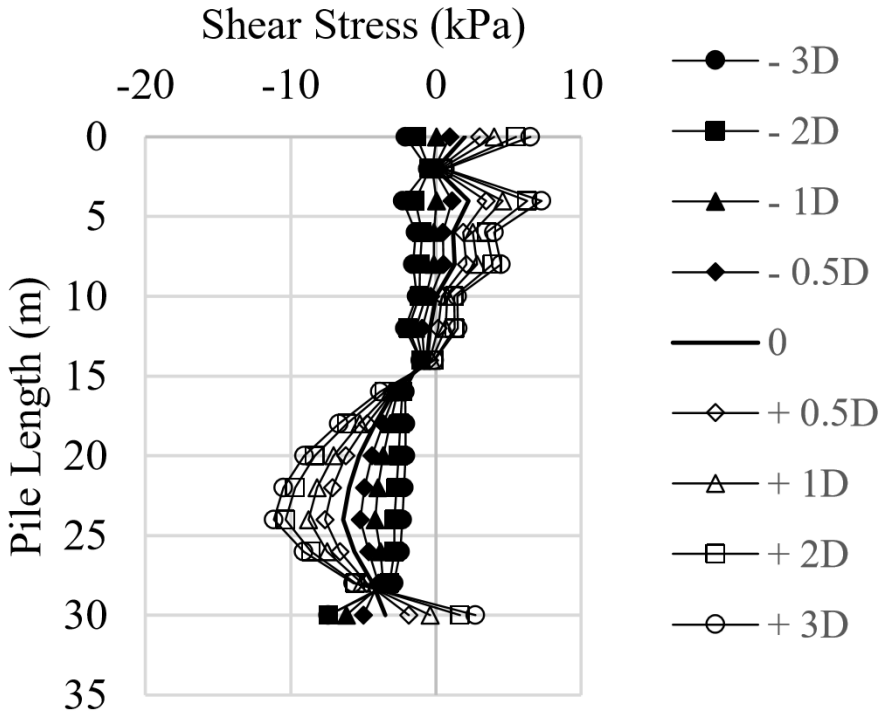

Figure 4.13 Shear stress distribution when the when the horizontal distance from pile and depth of tunnel center are 1D and 15m

In summary, as it is illustrated in Figure 4.14, downward shear stress is developed at the bottom of pile due to negative skin friction for short pile condition because the base resistance is transferred to pile shaft. In long pile condition, downward shear stress induced by negative skin friction is developed above the tunnel center and upward shear stress is developed below the tunnel center which should support the dragload from negative skin friction above the tunnel level.

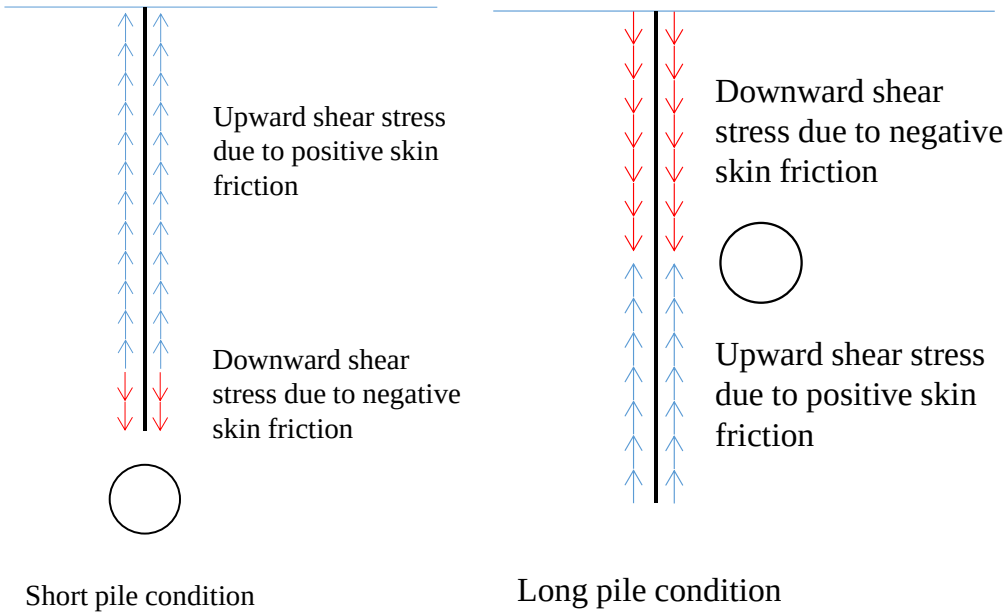

Figure 4.14 Shear stress and skin friction for long pile and short pile condition

Surface Settlement

Surface displacement is recorded and plotted when the tunnel reaches its final excavation stage. The maximum ground settlement in the short pile condition is 3.74 mm when the tunnel is right below the pile axis and decreases gradually as the tunnel moves

away from the pile. In short pile condition, especially, when the tunnel is below the pile tip, ground settlement is contributed by tunnel excavation as well as loaded pile movement.

In the long pile condition, maximum ground settlement is only about 1.92 mm. In long pile condition, the maximum ground settlement is less than that of short pile condition because ground settlement is mainly contributed by tunnel excavation only.

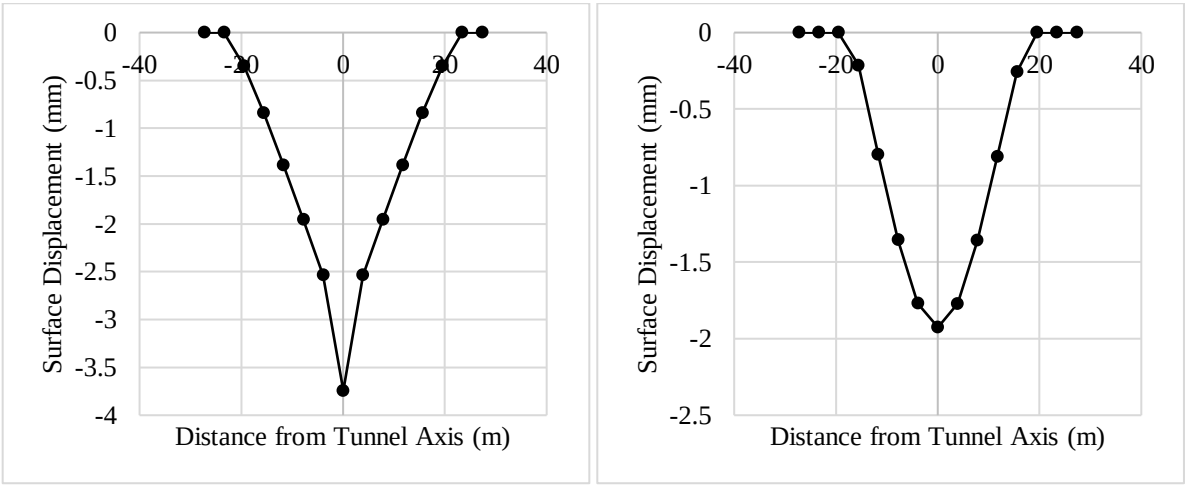

Figure 4.15 Maximum and minimum surface displacement in short pile cases

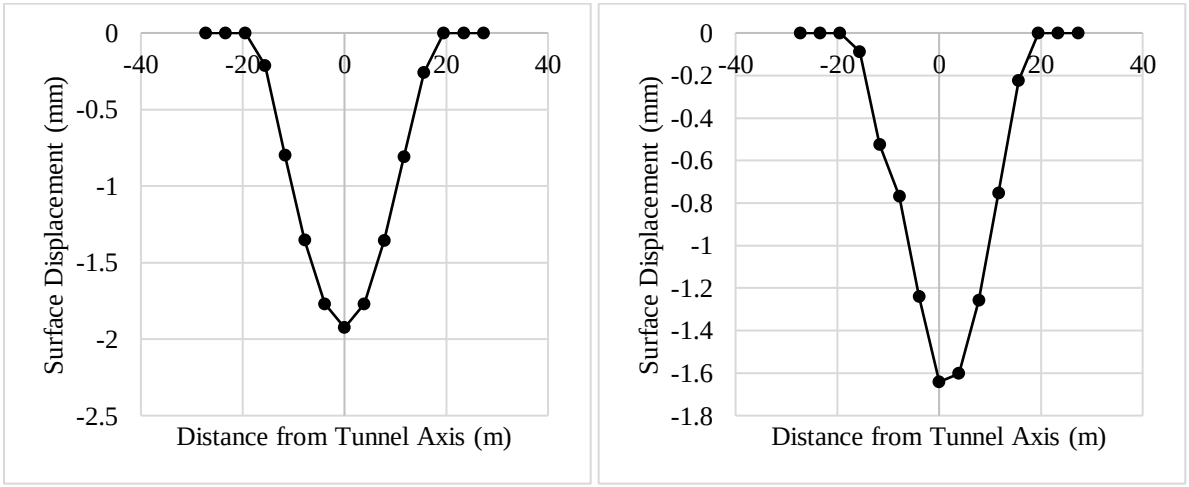

Figure 4.16 Maximum and minimum surface displacement in long pile cases

CHAPTER Five

Conclusion and Future research

5.1 Conclusion

It has become important to be able to determine the behavior of pile due to tunneling with reasonable accuracy. Relative movements of ground due to tunneling induce bending moments and down-drag forces on piles. In current practice, the effects of tunneling on pile are investigated using numerical analysis. Thus, a comprehensive picture of ground movements throughout the soil around the tunnel and the adjacent structures can be obtained.

Shield TBM Tunneling

In this study, the behavior of pile is investigated with numerical analysis. To investigate the behavior of ground and pile structure induced by tunnel construction using shield TBM, the simulation process of shield TBM tunneling is established. In this study, the mechanical behavior of the segment lining and backfill grout and that of backfill grout and ground were properly considered. No study has validated the arching effect of tunneling. Numerical studies were performed to examine FEM and FDM modeling

methods based on structural components such as skin plates and segment linings, and the use of plate-type structural elements that can be used to simulate skin plates and segment linings. 3D FDM analysis is adopted in this study by using finite different method software FLAC3D since the method can be more reliable specifically in favor to 3D FEM in terms of the effect of arching.

The transversal ground settlement from FDM shows wider shape than that obtained from FEM even though both use same material properties, geometry and boundary condition. And the transversal ground settlement obtained from FDM shows good agreement with the monitoring data.

As the tunnel face move away from the monitoring point, axial stress recovers its original stress level. The arching effect due to tunnel excavation can be found in axial stress change.

Liner structural element is adopted for segment lining and bending, shear and membrane stress resultants acting on the segment lining can be obtained. The bending stress resultant started to increase sharply and gradually reached a converged level. When structural elements of the shield TBM were installed, the stress resultants quickly increased and reached their converged certain level.

Behavior of pile due to tunneling

Type of pile is divided into short pile condition and long pile condition considering the position of pile with respect to tunnel. The behavior of pile during tunneling is monitored and examined.

It is found that the tensile axial force is developed when the tunnel center is located below the pile tip in short pile condition. Maximum axial force is decreases as the horizontal distance between tunnel center and pile increases. And, as the vertical distance from the tunnel center to pile tip increases, the compressive axial force decrease.

For long pile condition, compressive axial forces are developed when the tunnel center is close to pile axis regardless the vertical position. And it gradually decreases as the horizontal distance between tunnel center and pile axis increases.

As the tunnel advances, the bending moments of the pile is developed due to the movement of soil induced by tunneling. The bending moment induced by tunneling on the pile in case of short pile condition is relatively low and insignificant compared to the bending moments in the case of long pile condition.

In case of short pile condition, bending moment decreases as the vertical distance from the pile tip to tunnel center increases and it decreases as the horizontal distance from the pile tip increases.

In cases of long pile condition, bending moment is maximum when the horizontal distance of the tunnel center from the pile tip is 1D regardless of vertical position of tunnel center. As the horizontal distance of tunnel center from the pile tip increases, bending moment decreases significantly. As the vertical distance of tunnel center from the pile tip increases, bending moment decreases and maximum bending moment is found when the vertical position of tunnel center is 1D from the pile tip which implies that pile end is fully affected by the tunnel excavation.

Downward shear stress is developed at the bottom of pile due to negative skin

friction for short pile condition because the base resistance is transferred to pile shaft. In long pile condition, downward shear stress induced by negative skin friction is developed above the tunnel center and upward shear stress is developed below the tunnel center which should support the dragload from negative skin friction above the tunnel level.

5.2 Future research

The numerical analysis framework which is developed for the investigation of pile due to tunneling can be applied for various progressive behavior of pile. It is recommended to extend this study to gain a better understanding of structural behavior of pile and to develop new applications in geotechnical engineering. This requires diverse approaches, as follows:

Shield TBM tunneling

- Change of ground property due to shield TBM tunneling in soft soil
- Wave propagation in soft soil due to shield TBM tunneling and its effect on the surface structures
- Development of numerical approaches for simulation of advance rate of shield TBM

Behavior of pile due to tunneling

- Progressive behavior of end-bearing pile during tunneling

- The behavior of group pile due to single tunnel and the behavior of group pile due to twin tunnel
- Experimental study to monitor the behavior of pile and the development of negative skin friction in soft soil

References

Korff, M 2012, Response of Piled Buildings to the Construction of Deep Excavation, Ph.D. thesis, University of Cambridge, UK.

Guglielmetti, V, Grasso, P, Mahtab, A & Xu, S 2007, Mechanized Tunnelling in Urban Areas: Design methodology and construction control, Taylor & Francis, London.

Loganathan, N 2011, An Innovative Method For Assessing Tunnelling-Induced Risks To Adjacent Structures, PB 2009 William Barclay Parsons Fellowship Monograph 25.

Tuladhar, R, Maki, T & Mutsuyoshi, H 2008, 'Cyclic behavior of laterally loaded concrete piles embedded into cohesive soil', Earthquake Engng. Struct. Dyn.,Vol. 37, pp. 43-59.

Abdullah, MH & Taha, MR 2013, 'A review of the effects of tunneling on adjacent piles' Electronic Journal of Geotechnical Engineering, Vol. 18, pp. 2739-2762.

Phillips E 1869a, 'De l'equilibre des solides elastiques semblables', C.R. Acad. Sci., Paris 68: 75-79.

Phillips E 1869b. 'Du movement des corps solides elastiques semblables'. C.R. Acad. Sci., Paris 69: 911-012.

Bucky, PB 1931, The use of models for the study of mining problems, Technical Publication 425, New York: Am. Inst. of Min. & Met. Engng.

Joseph, PJ, Einstein, HH & Whitman, RV 1988, A literature review of geotechnical centrifuge modelling with particular emphasis on rock mechanics. Massachusetts: MIT.

Barton, YO 1984, 'Response of pile groups to lateral loading in the centrifuge', Proc., Symp. on the Application of Centrifuge Modeling to Geotechnical Design, Editor: Craig, WH., Balkema, Rotterdam, Netherlands, pp. 457-473.

Ovesen, NK 1975, 'Centrifugal Testing Applied to Bearing Capacity Problems of Footings on Sand', Geotechnique, Vol. 25, No. 2, pp. 394-401.

Lyndon, A & Pearson, R 1984, 'Pressure Distribution on a Rigid Retaining Wall in Cohesionless Material', Proceedings of the Application of Centrifugal Modelling to Geotechnical Design, Editor: Craig, WH, University of Manchester.

Kimura, T, Kusakabe, U & Saitoh, K 1985, 'Geotechnical Model Tests of Bearing Capacity Problems in a Centrifuge', Geotechnique, Vol. 35, No. 1, pp. 33-45.

Scott, RF 1979a, 'Cyclic Lateral Loading of Piles, Analysis of Centrifuge Tests', Research Program for API-OASAPR, Project 13. Calif. Inst. Tech.

Scott, RF 1979b, 'Cyclic Static Model Pile Tests in a Centrifuge', Proc. 11th Offshore Technology Conference, pp. 1159-1168, Paper OTC 3492.

Scott, RF 1981, 'Pile Testing in a Centrifuge', Proc. 10th Int. Conf. on S.M.F.E., Stockhold, Vol. 2, pp. 839-842.

Sabagh, SK 1984, 'Cyclic Axial Load Tests on Piles in Sand', Proceedings of the Application of Centrifugal Modelling in Geotechnical Design, Editor: Craig, WH, University of Manchester.

Oldham, DCE 1984, 'Experiments with Lateral Loading on Single Piles in Sand', Proceedings of the Application of Centrifugal Modelling to Geotechnical Design, Editor: Craig, WH, University of Manchester.

Chen, LT, Poulos, HG & Loganathan, N 1999, 'Pile responses caused by tunneling', Journal of Geotechnical and Geoenvironmental Engineering, ASCE, Vol. 125, No. 3, pp. 207-215.

Jacobsz, SW, Standing, JR, Mair, RJ, Hagiwara, T & Sugiyama, T 2004, 'Centrifuge modeling of tunneling near driven piles'. Soils Found., Vol. 44, No. 1, pp. 49-56.

Lee, CJ & Chiang, KH 2007, 'Responses of single piles to tunnelling-induced soil movements in sandy Ground', Canadian Geotechnical Journal, Vol. 44, No. 10, pp. 1224-1241.

INSTITUTION OF STRUCTURAL ENGINEERS (GREAT BRITAIN), INSTITUTION OF CIVIL ENGINEERS (GREAT BRITAIN), & INTERNATIONAL ASSOCIATION FOR BRIDGE AND STRUCTURAL ENGINEERING 1989, Soil-structure interaction: the real behaviour of structures. London, Institution of Structural Engineers.

Peiris, T, Thambiratnam, D, Perera, N & Gallage, C 2014, 'Soil–Pile Interaction of Pile Embedded in Deep-Layered Marine Sediment under Seismic Excitation', Structural Engineering International, Vol. 24, No. 4, pp. 521-531.

Balendra, S 2005, Numerical modeling of dynamic soil-pile-structure interaction, M.S. thesis in civil engineering, Washington State University, Washington, http://hdl.handle.net/2376/414.

Franzius, JN, Potts, DM & Burland, JB 2006, 'The response of surface structures to tunnel construction', Proc. Inst. Civ. Eng. Geotech. Eng., Vol. 159, No. 1, pp. 3-17.

Farrell, RP, Mair, RJ, Sciotti, A, Pigorini, A & Ricci. M 2012, 'The response of buildings to tunnelling: A case study', Geotechnical Aspects of Underground Construction in Soft Ground, pp. 877-885.

Gazetas, G & Mylonakis, G 1998, 'Seismic Soil-Structure Interaction: New Evidence and Emerging Issues', Geotechnical Special Publication 75, Geotechnical Earthquake Engineering and Soil Dynamics III, American Society of Civil Engineers, Reston, Virginia, pp. 1119-1174.

Jacobsz, SW 2002, 'The effects of tunnelling on piled foundations', Ph.D. thesis, University of Cambridge. UK.

Lambrughi, A, Medina Rodríguez, L & Castellanza, R 2012, 'Development and validation of a 3D numerical model for TBM–EPB mechanised excavations', Computers and Geotechnics, Vol. 40, pp. 97-113.

Rowe, RK, Lo, KY & Kack GJ 1983, 'A method of estimating surface settlement above tunnels constructed in soft ground', Canadian Geotechnical Journal, Vol. 20, No. 1, pp. 11-22.

Kasper, T & Meschke, G 2004, 'A 3D finite element simulation model for TBM tunnelling in soft ground', Int. J. Numer. Anal. Meth. Geomech., Vol. 28, pp. 1441-1460.

Lee, KM & Rowe, RK 1990, 'Finite Element modelling of the three dimensional ground deformations due to tunnelling in soft cohesive soils: Part I - Method of analysis', Computers and Geotechnics, Vol. 10, pp. 87-109.

Lee, KM & Rowe, RK 1990, 'Finite Element modelling of the three dimensional ground deformations due to tunnelling in soft cohesive soils: Part 2 – Results', Computers and Geotechnics, Vol. 10, pp. 111-138.

Lee, KM & Rowe, RK 1991, 'An analysis of 3-dimensional ground movements: The Thunder Bay Tunnel', Canadian Geotechnical Journal, Vol. 28, No. 1, pp. 25-45.

Lee, KM, Rowe, RK & Lo, KY 1992, 'Subsidence owing to tunnelling. I. Estimating the gap parameter', Canadian Geotechnical Journal, Vol. 29, No. 6, pp. 929-940.

Swoboda, G & Abu-Krisha, A 1999, 'Three-dimensional numerical modelling for TBM tunnelling in consolidated clay', Tunnelling and Underground Space Technology, Vol. 14, Issue 3, pp. 327-333.

Komiya, K, Soga, K, Akagi, H, Hagiwara, T & Bolton, MD 1999, 'Finite element modelling of excavation and advancement processes of a shield tunnelling machine', Soils and Foundations, Vol. 39, No. 3, pp. 37 -52.

Kasper, T & Meschke, G 2004, 'A 3D finite element simulation model for TBM tunnelling in soft ground', International Journal for Numerical and Analytical Methods in Geomechanics, Vol. 28, pp. 1441-1460.

Maynar, MM & Rodriguez, LM 2005, 'Predicted versus measured soil movements induced by shield tunnelling in the Madrid Metro extension', Canadian Geotechnical Journal, Vol. 42, No. 4, pp. 1160-1172.

Hassanpour, J, Rostami, J, Tarigh Azali, S, Zhao, J 2014, 'Introduction of an empirical TBM cutter wear prediction model for pyroclastic and mafic igneous rocks; a case history of Karaj water conveyance tunnel, Iran', Tunnelling and Underground Space Technology, Vol. 43, pp. 222-231.

Do, NA, Dias, D, Oreste, PP & Djeran-Maigre, I 2013, '2D numerical investigation of segmental tunnel lining behavior', Tunnell. Underground Space Technol., Vol. 37, pp. 115-127.

Mollon, G, Dias, D & Soubra, A 2013, 'Probabilistic analyses of tunneling-induced ground movements', Acta Geotechn., Vol. 8, pp. 181-199.

Loganathan, N, Poulos, HG & Stewart, DP 2000, 'Centrifuge model testing of tunnelling-induced ground and pile deformations', Geotechnique, Vol. 50, No. 3, pp. 283-294.

Bezuijen, A & Schier, J 1994, 'The influence of a bored tunnel on pile foundations', Proc. Centrifuge 94. Balkkema, Rotterdam.

Selemetas, D 2005, The response of full-scale piles to tunnelling, Ph.D. thesis, University Cambridge, UK.

Pang, CH 2006, The effects of tunnel construction on nearby pile foundation, Ph.D. Thesis, National University of Singapore, Singapore.

Midas GTS NX 2015, Manual and software, South Korea.

Itasca Consulting Group Inc. 2012, Fast Lagrangian Analysis of Continua in 3 Dimensions User's Guide, Version 5.0. Itasca Consulting Group Inc., USA

Knight-Hassell, CK 2000, 'Tunnelling through challenging ground condition in Singapore', Proceedings of the international conference on tunnels and underground structures Singapore 26-29 November 2000: Tunnels and Underground structures, pp. 633-638. Balkema.

Unlu, T & Gercek, H 2003, 'Effect of Poisson's ratio on the normalized radial displacements occurring around the face of a circular tunnel', Tunnelling and Underground Space Technology, Vol. 18, pp. 547-553.

Panet, M & Guenot, A, 1982, 'Analysis of convergence behind the face of a tunnel', Proceedings International Symposium Tunnelling '82, IMM, London, pp. 197-204.

Chern, JC, Shiao, FY & Yu, CW 1998, 'An empirical safety criterion for tunnel construction', Proceedings of the Regional Symposium on Sedimentary Rock Engineering, Taipei, Taiwan, pp. 222-227.

Corbetta, F, Bernaud, D, Nguyen-Minh, D 1991, 'Contribution a` la me´thode convergerce–confinement par le principe de la similitude', Rev. Fr. Ge´otech. Vol. 54, pp. 5-11.

Panet, M 1995, 'Calcul desT unnels par la Me´thode de Convergence–Confinement', Presses de l'Ecole Nationale des Ponts et Chausse´es, pp.178. Paris.

Hoek, E 1999, 'Support for very weak rock associated with faults and shear zones', Distinguished lecture for the opening of the International symposium on Rock support and reinforcement practice in Mining, Kalgoorlie, Australia, 14-19 March, 1999.

Lee, CJ, Lee, JH & Jeong, SS 2006, 'The influence of negative skin friction on piles in groups connected to a cap ', Geotechnique, Vol. 56, No.1, pp. 53-56.

Mroueh, H & Shahrour, I 2002, 'Three-dimensional finite element analysis of the interaction between tuneling and pile foundations', International Journal for Numerical and Analytical Methods in Geomechanics, Vol. 26, pp. 217-230.

Potts, DM & Zdravkovic, L 2001, Finite element analysis in geotechnical engineering: application, London, Thomas Telford, UK.

Ottaviani, M 1975, 'Three-dimensional finite element analysis of vertically loaded pile groups,' Geotechnique, Vol. 25, Issue 2, pp. 159-174.

Emilios M. Comodromos, Mello C. Papadopoulou, Lyesse Laloui 2016, 'Contribution to the design methodologies of piled raft foundations under combined loadings', Canadian Geotechnical Journal, Vol. 53, pp. 559-577.

Wakai, A, Gose, S & Ugai, K 1999, '3-d elasto-plastic finite element analyses of pile foundations subjected to lateral loading', Soils and Found., Vol. 39, No. 1, pp. 97-111.

Yang, Z & Jeremić, B 2003, 'Numerical study of group effects for pile groups in sands', International Journal for Numerical and Analytical Methods in Geomechanics, Vol. 27, No. 15, pp. 1255-1276.

Jeong, SS, Seo, D, Lee J & Park, J 2004, 'Time-dependent behavior of pile group by staged construction of an adjacent embankment on soft clay', Canadian Geotechnical Journal, Vol. 41, pp. 644-656.

Zhu, H 2000, Evaluation of load transfer behaviour of bored piles in residual soil incorporating construction effect, M.S. thesis, Nanyang Technological University, Singapore.

Powrie, W & Li, ESF 1991, 'Finite element analyses of an in situ wall propped at formation level', Geotechnique, Vol. 41, No. 4, pp. 499-514.

APPENDIX

Short pile case 01-1-1

Δv : 1D
Δht : 0
Cover depth : 33 m

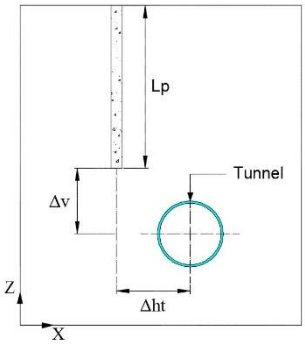

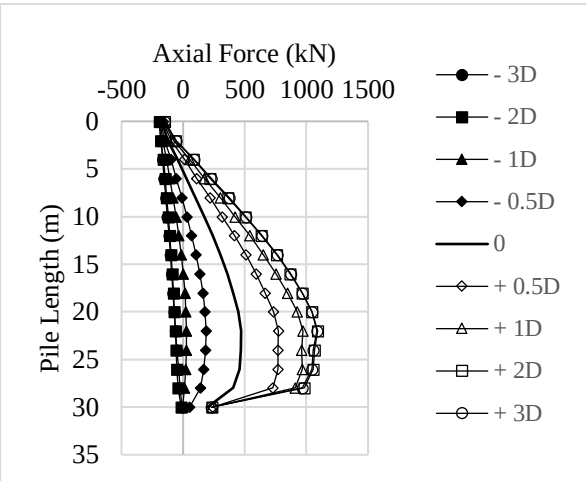

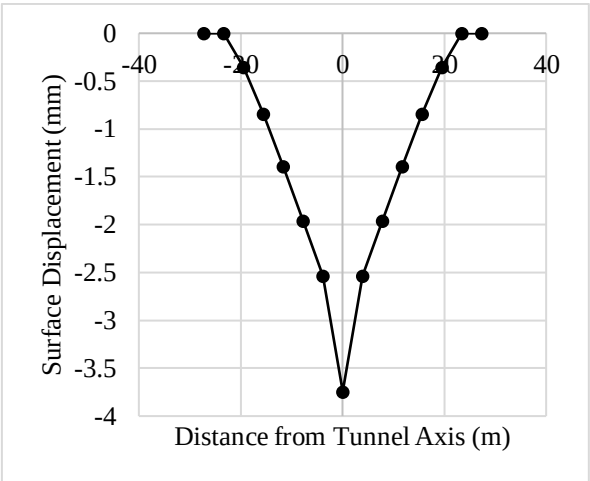

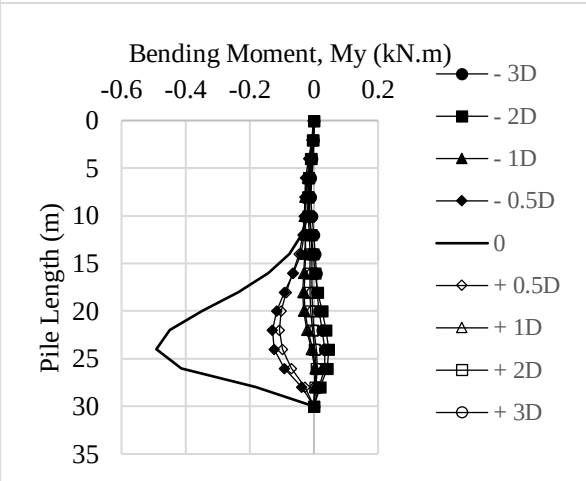

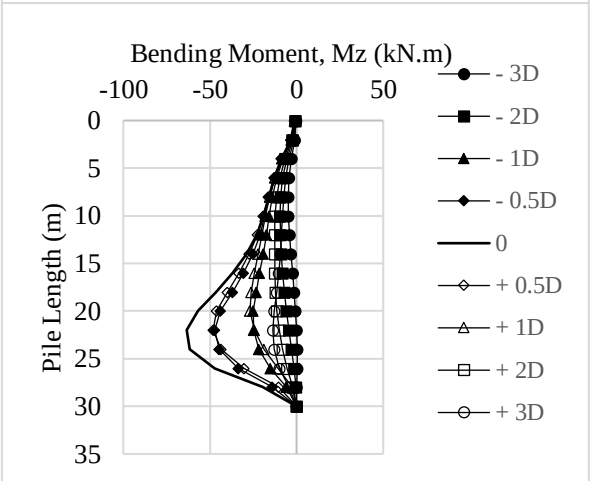

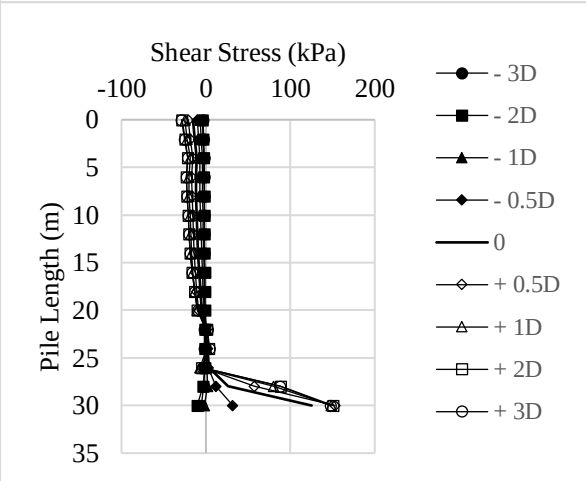

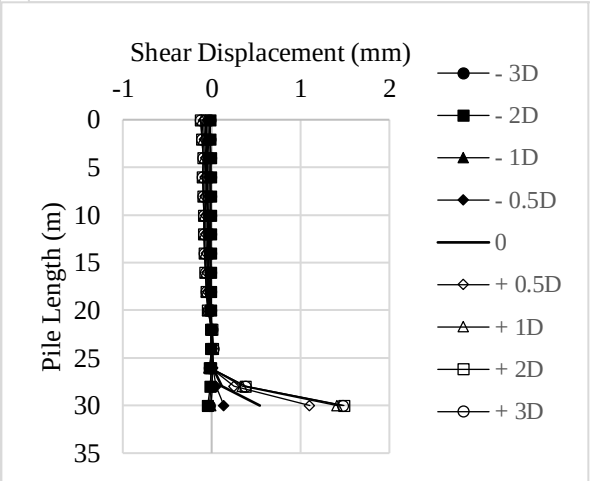

Short pile case 01-1-2

Δv : 1D
Δht : 0.5D
Cover depth : 33 m

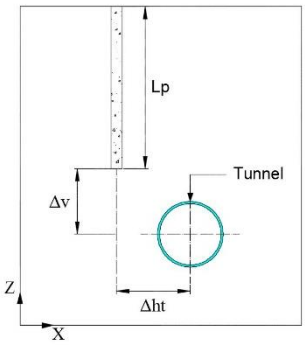

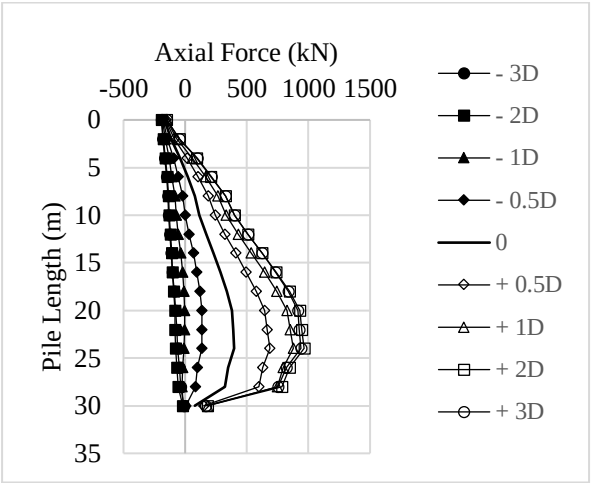

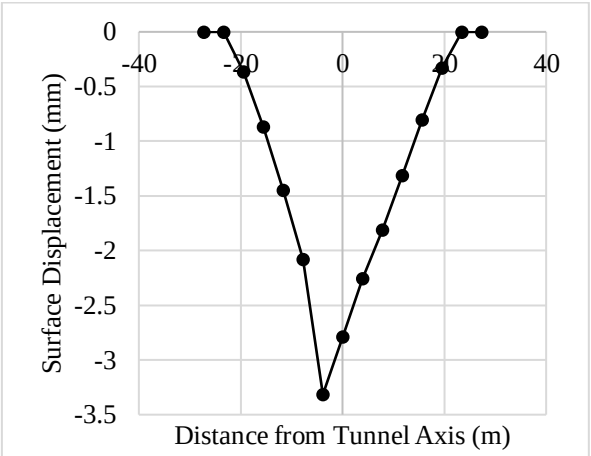

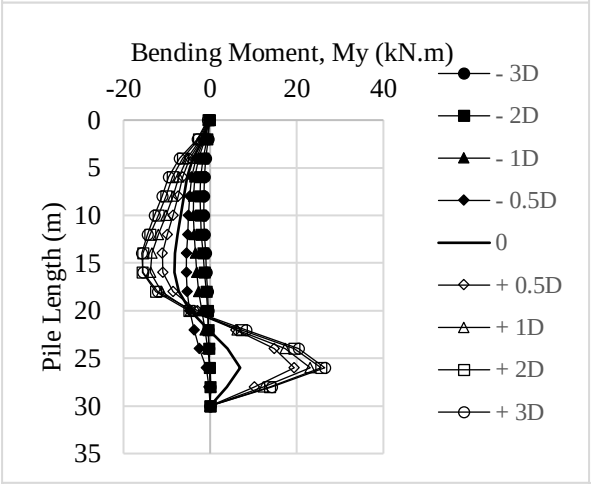

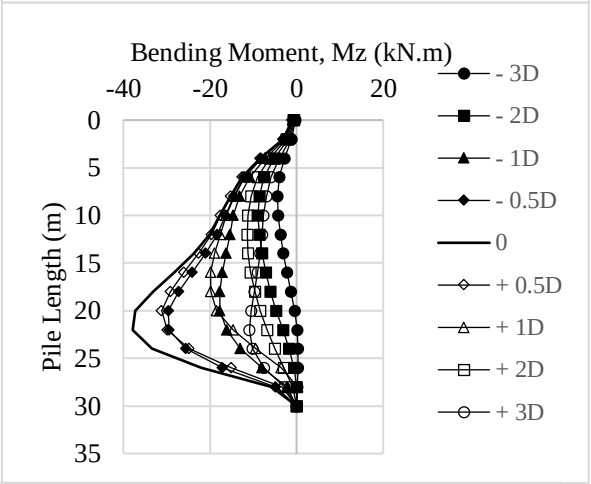

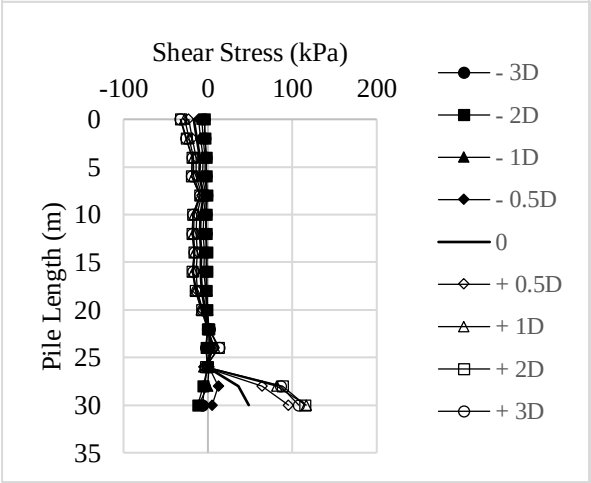

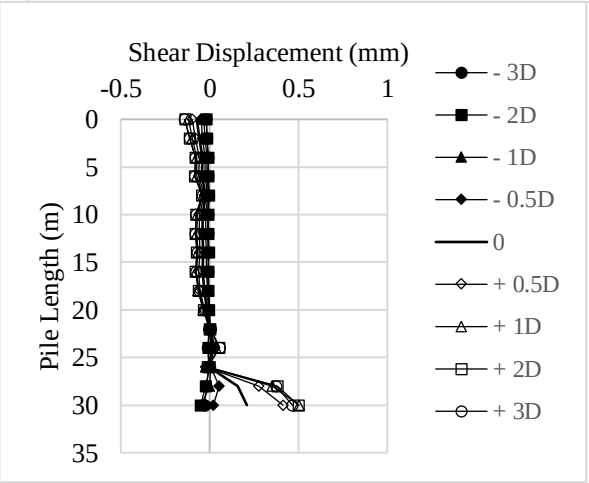

Short pile case 01-1-3

Δv : 1D
Δht : 1D
Cover depth : 33 m

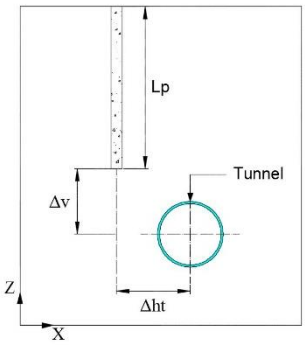

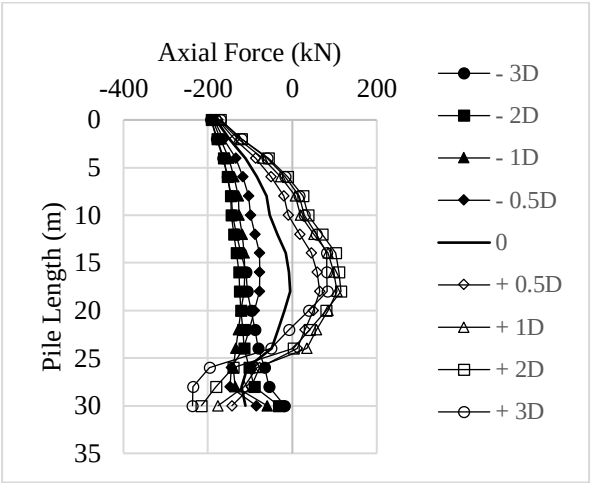

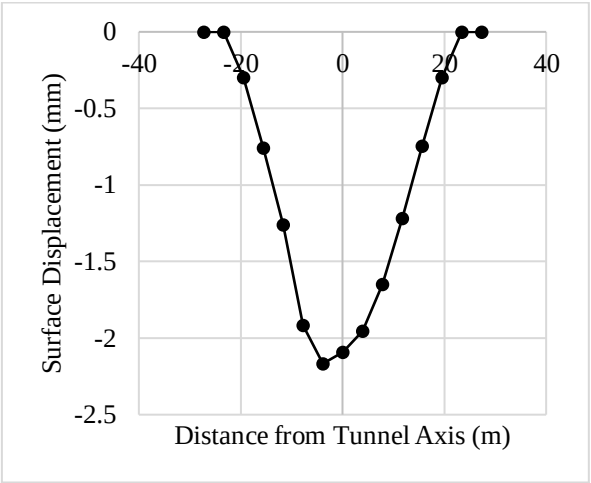

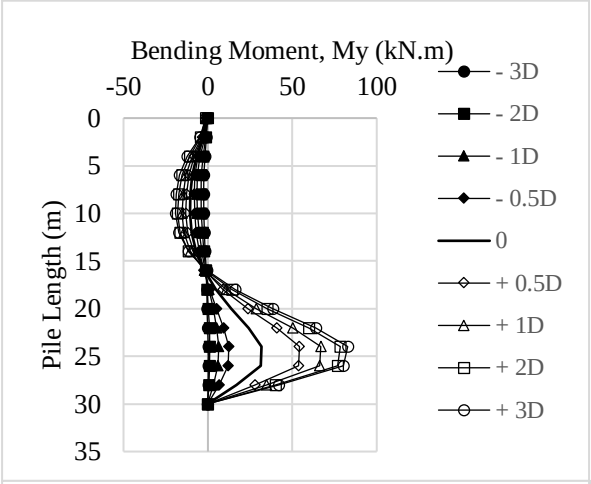

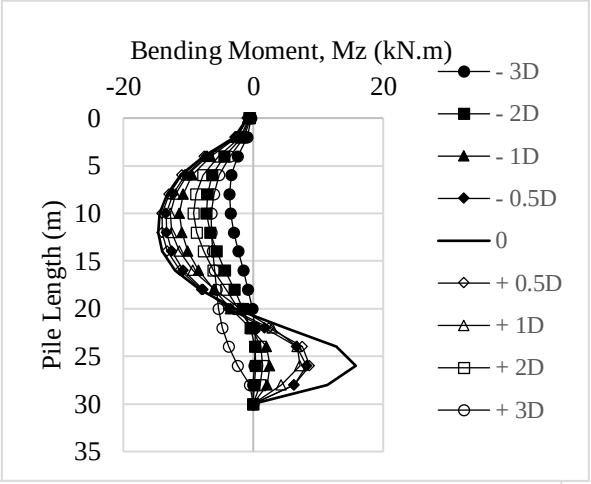

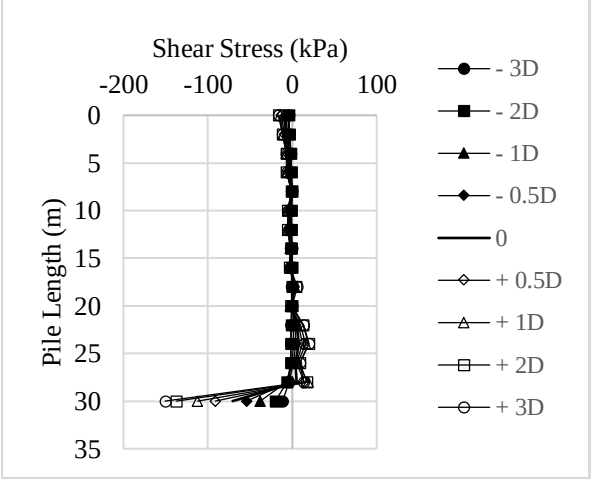

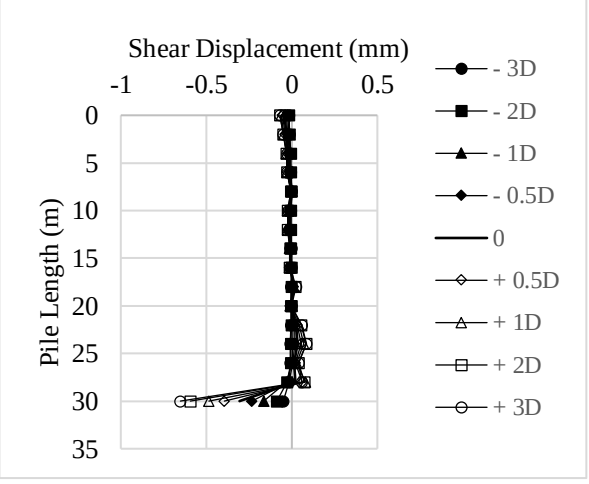

Short pile case 01-1-4

Δv : 1D
Δht : 1.5D
Cover depth : 33 m

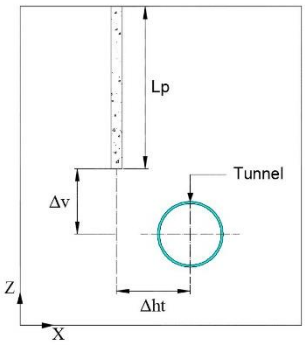

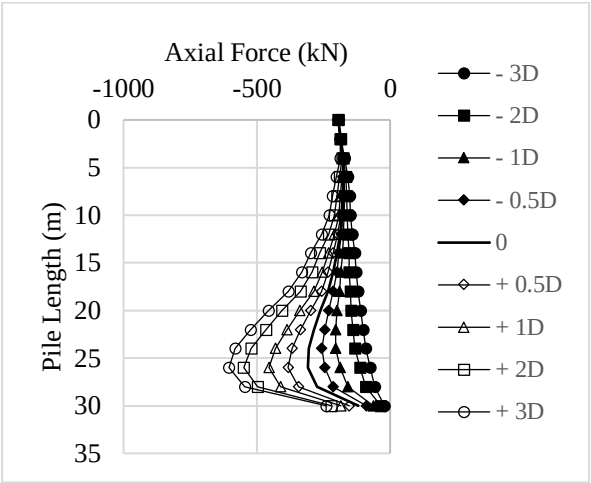

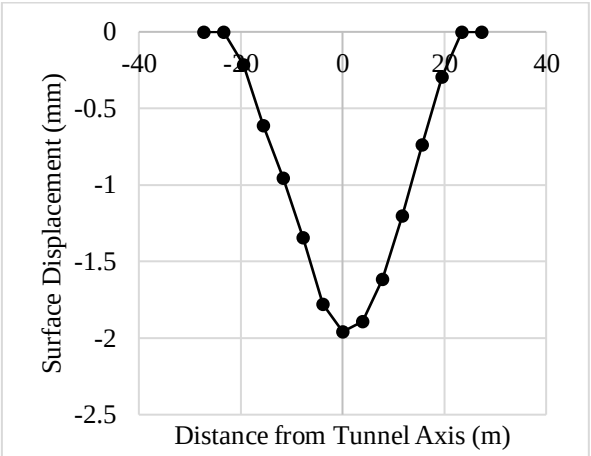

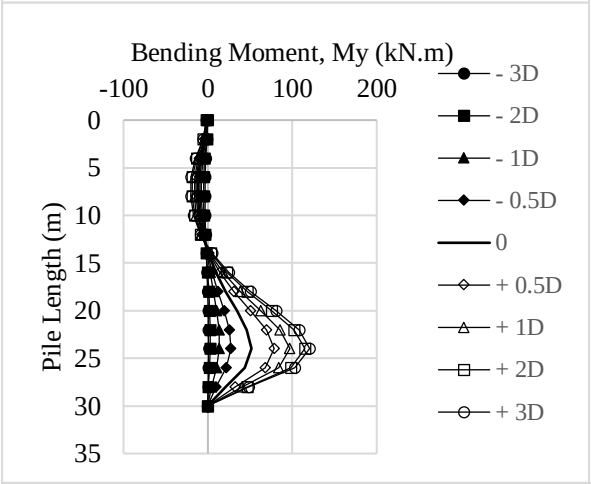

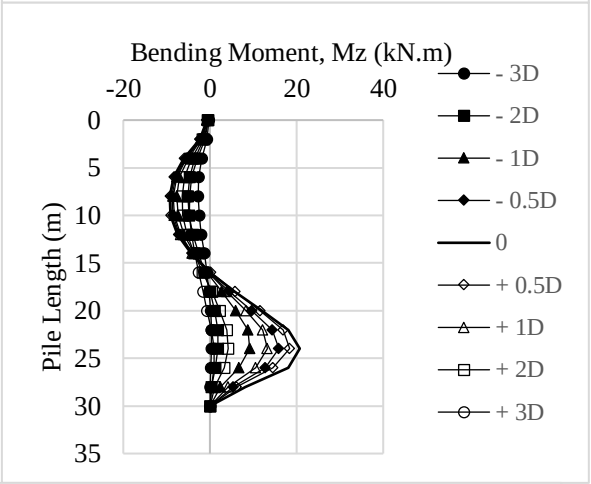

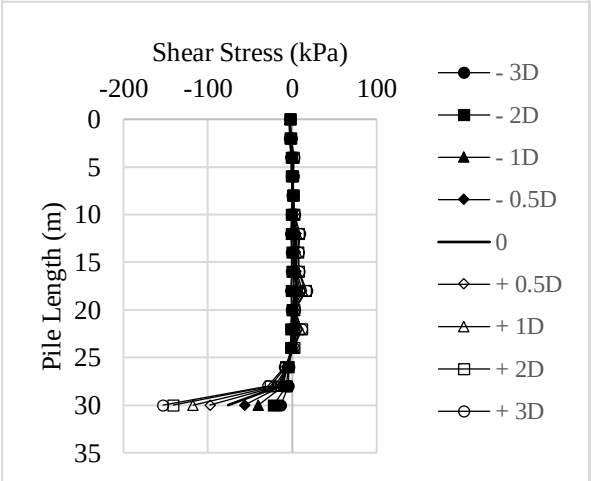

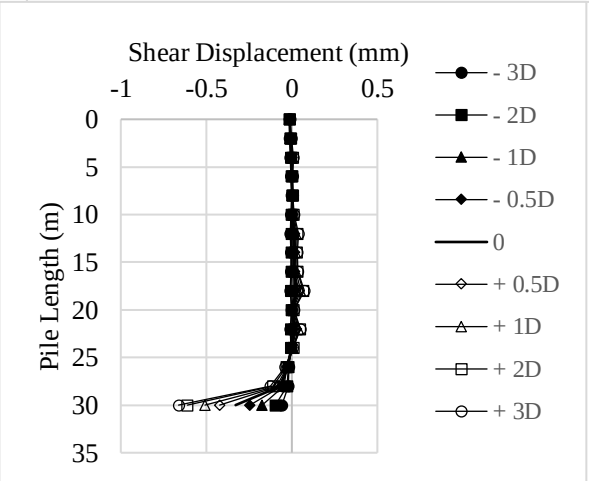

Short pile case 01-1-5

Δv : 1D
Δht : 2D
Cover depth : 33 m

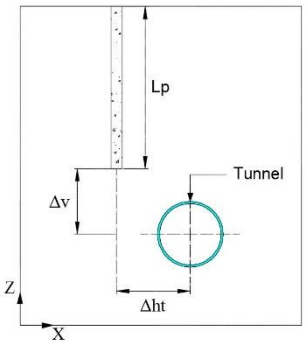

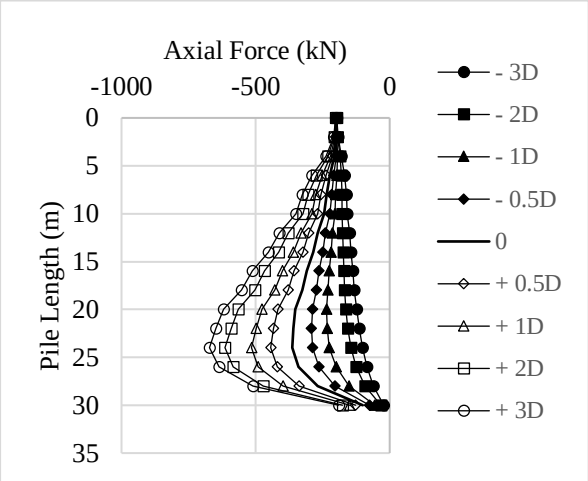

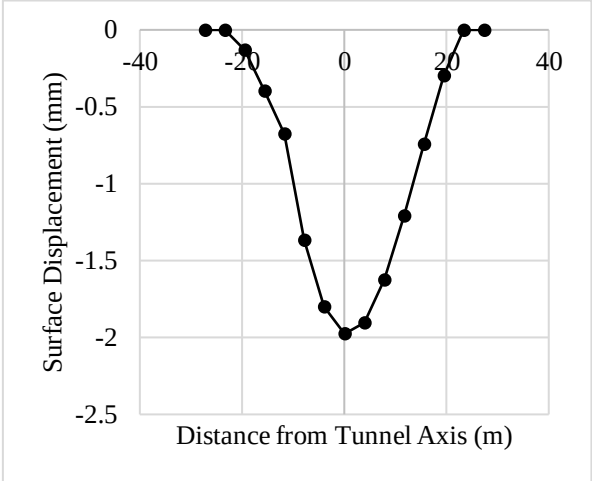

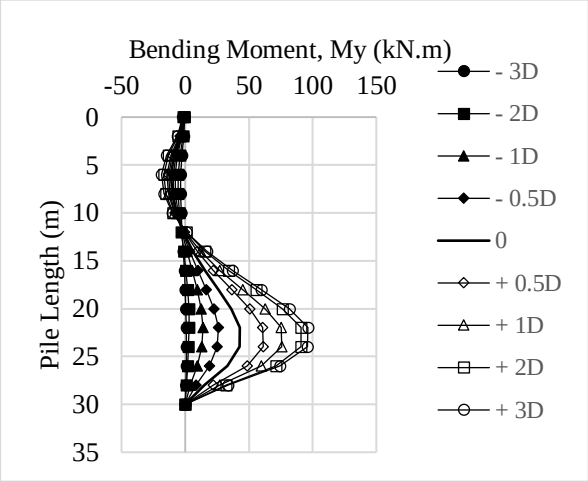

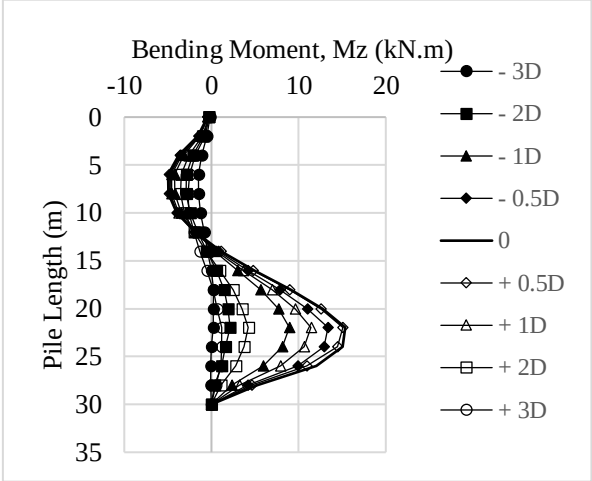

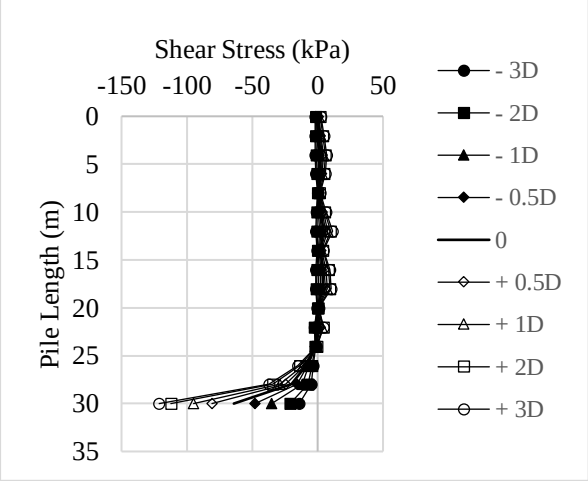

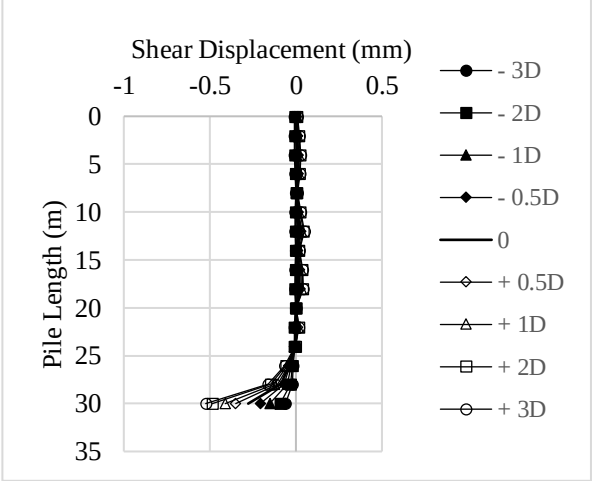

Short pile case 01-1-6

Δv : 1D
Δht : 2.5D
Cover depth : 33 m

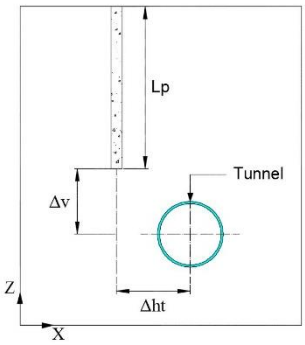

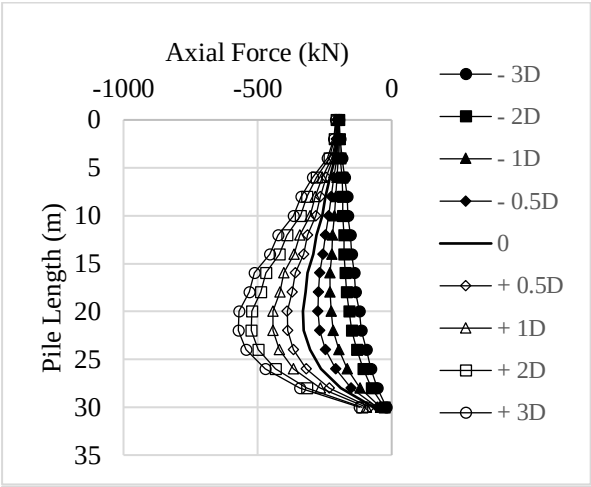

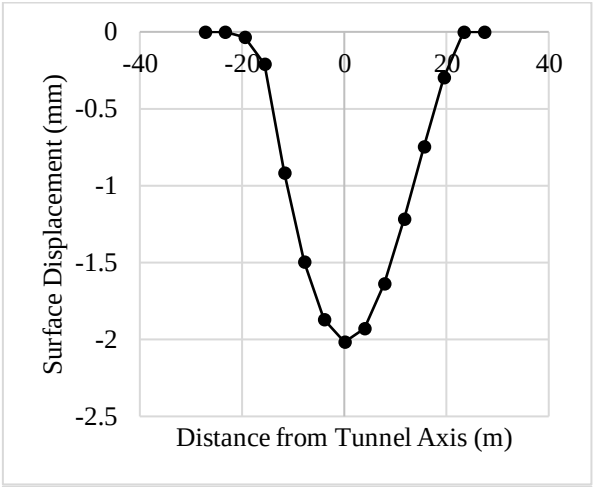

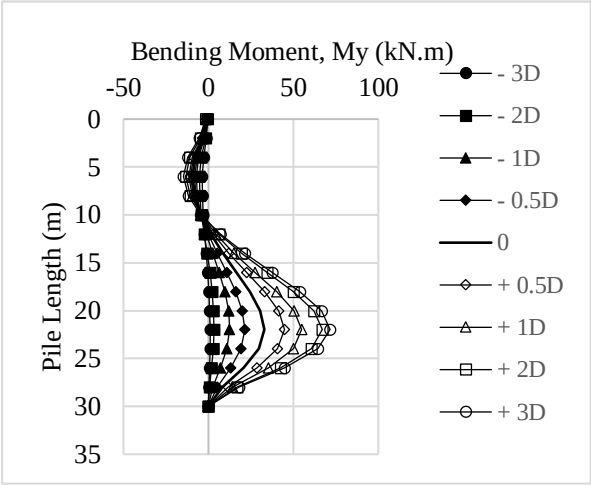

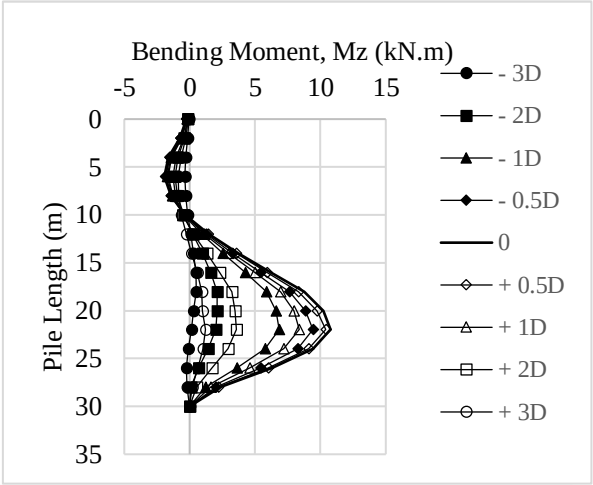

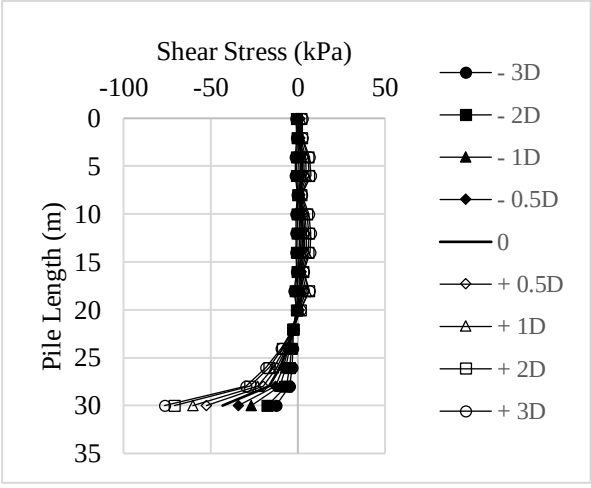

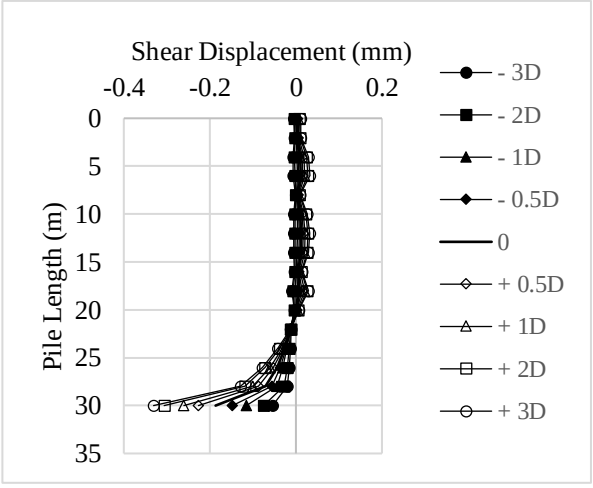

Short pile case 01-2-1

Δv : 1.5D
Δht : 0
Cover depth : 36 m

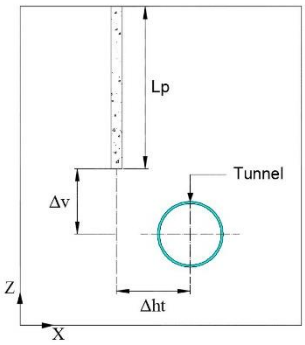

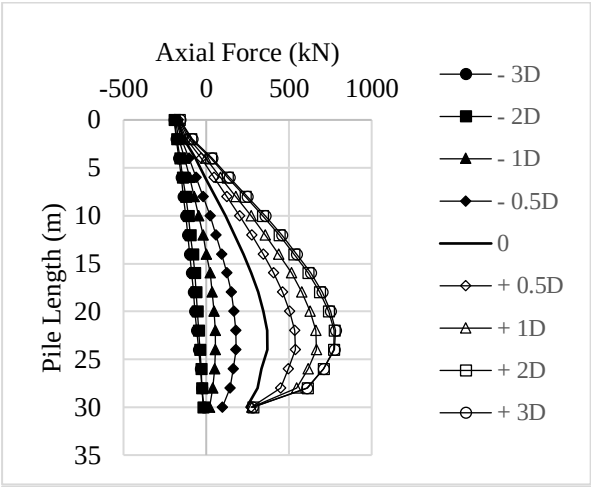

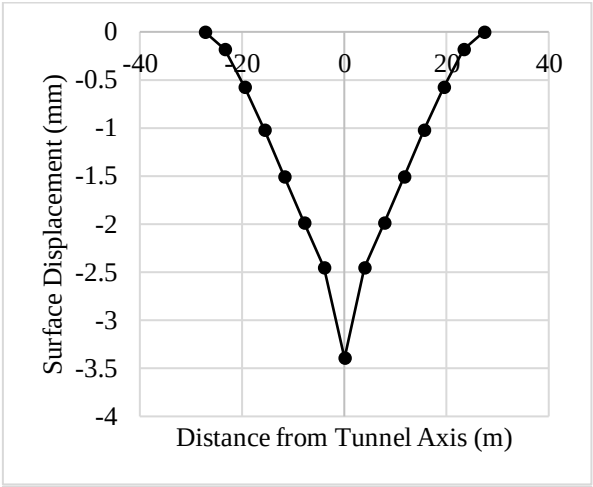

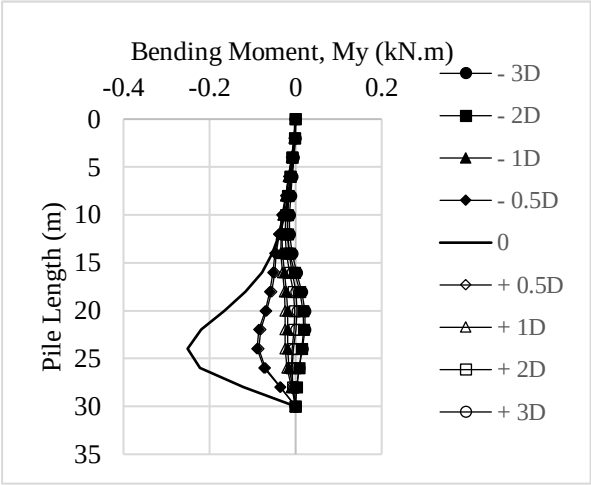

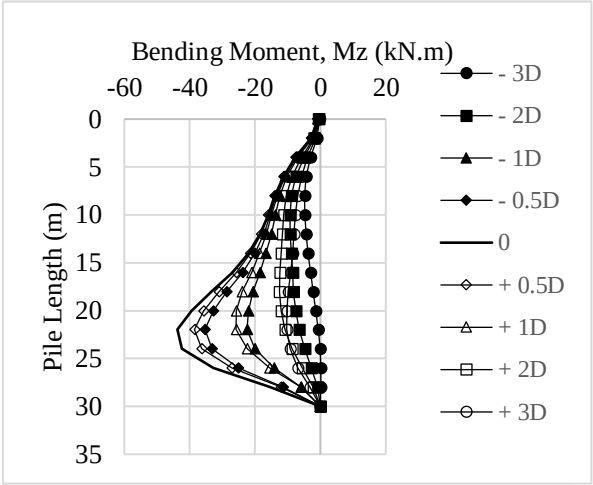

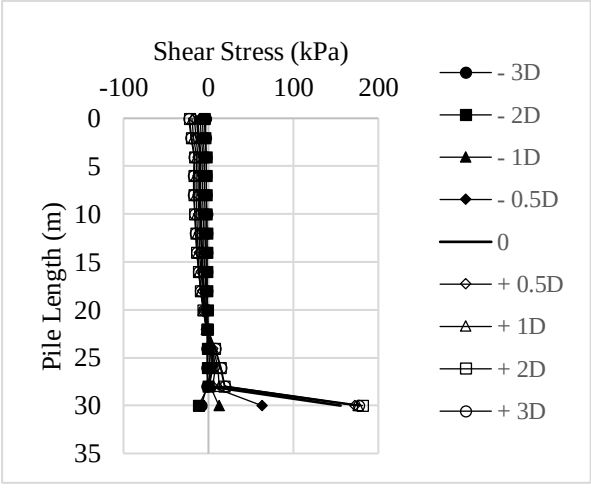

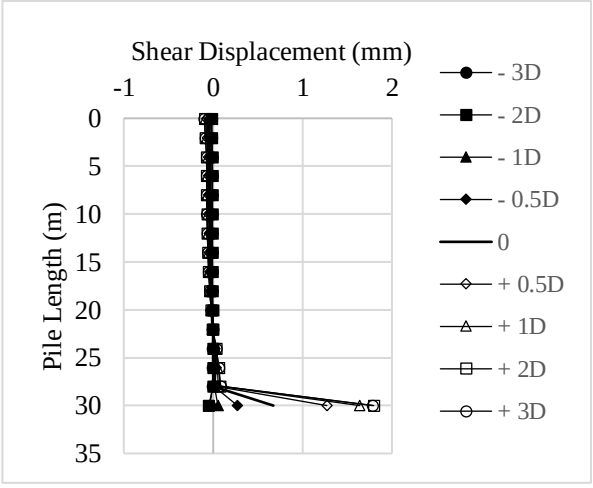

Short pile case 01-2-2

Δv : 1.5D
Δht : 0.5D
Cover depth : 36 m

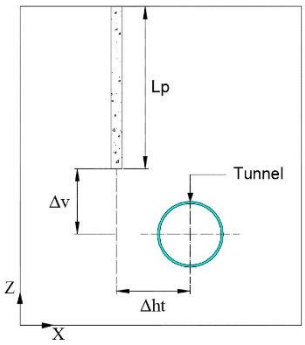

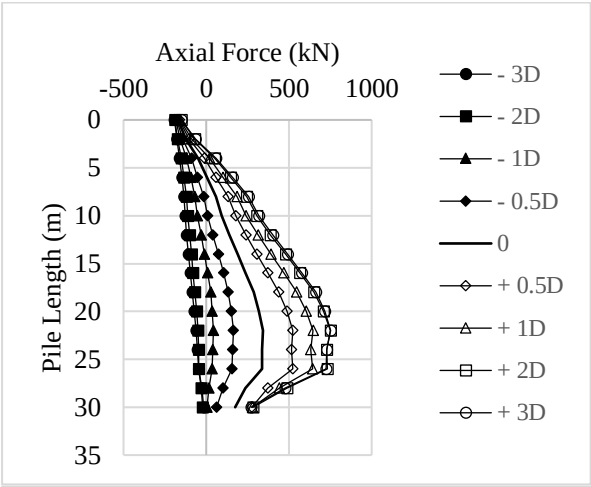

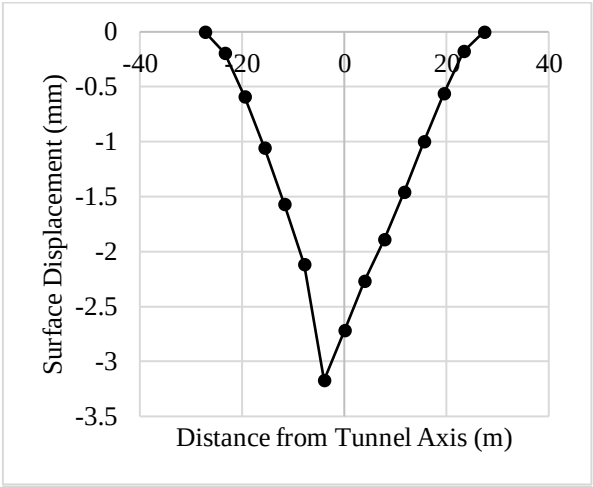

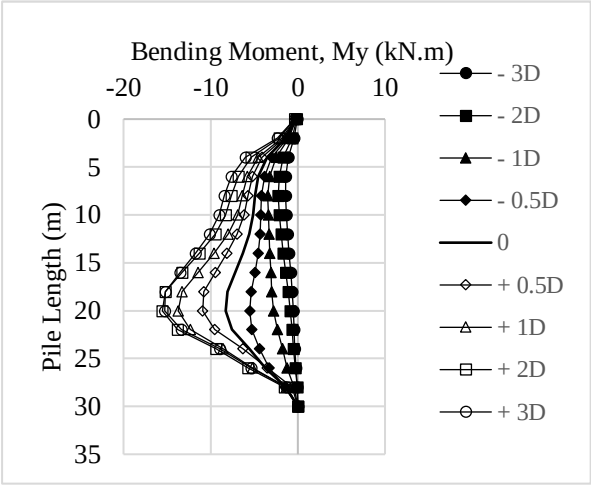

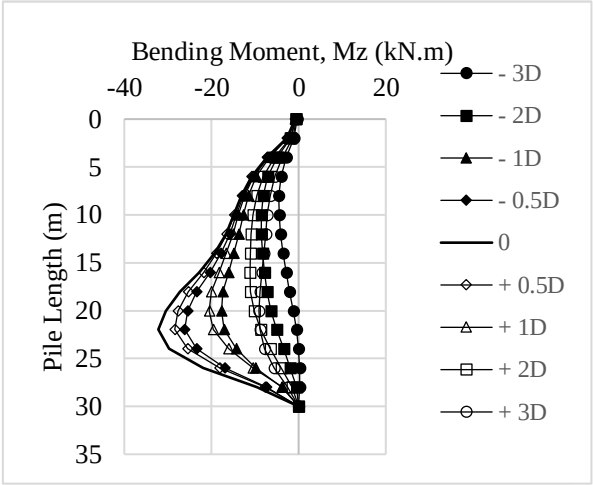

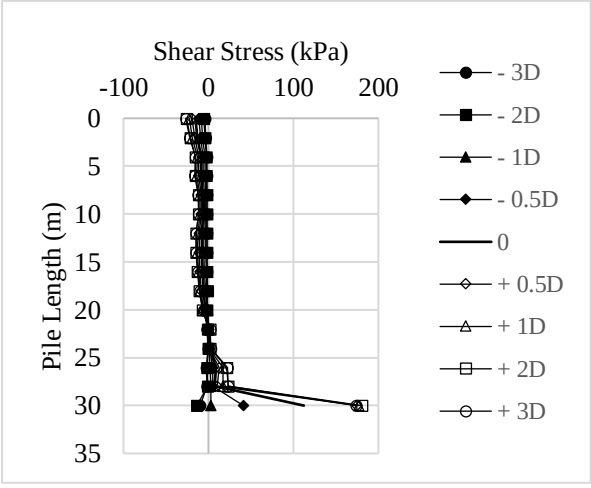

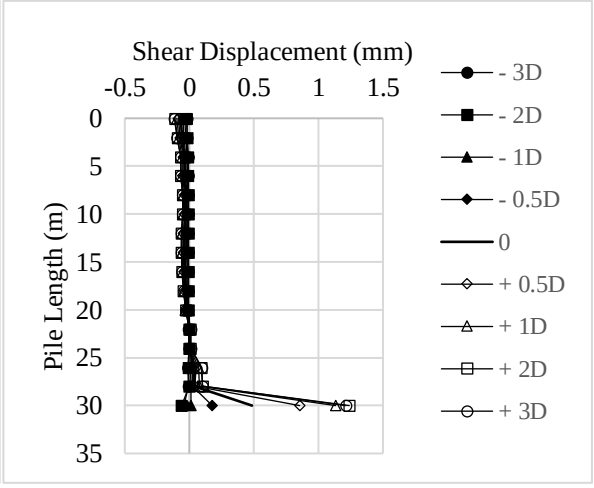

Short pile case 01-2-3

Δv : 1.5D
Δht : 1D
Cover depth : 36 m

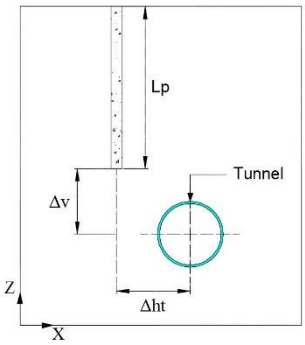

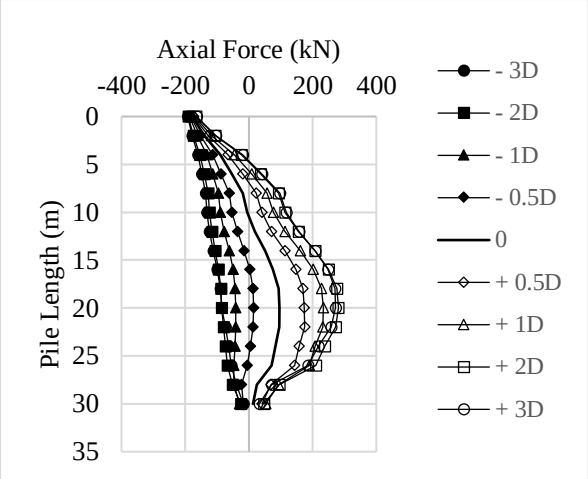

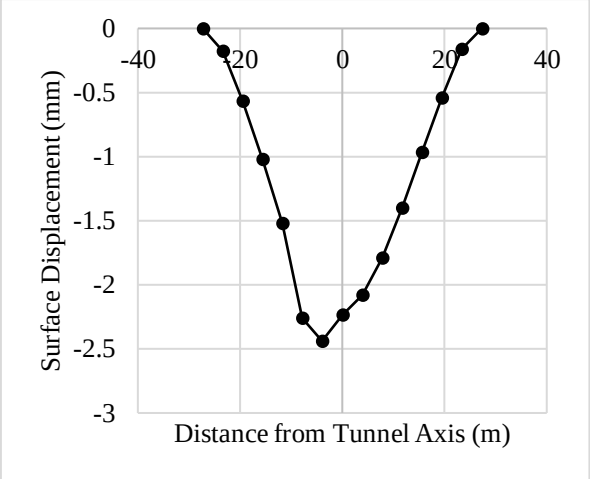

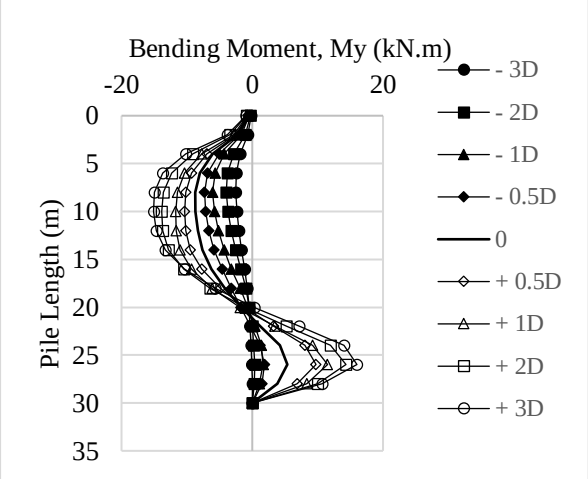

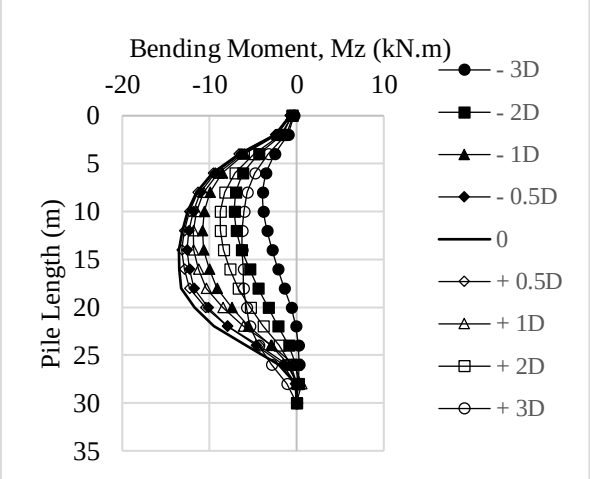

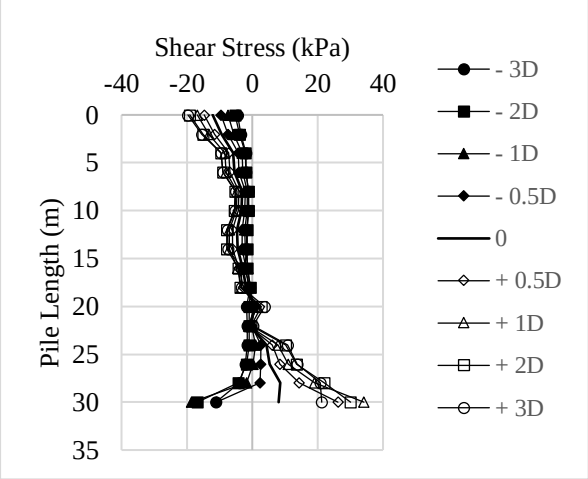

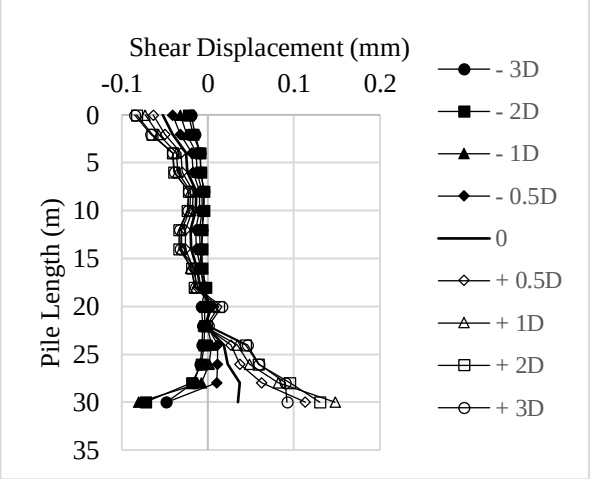

Short pile case 01-2-4

Δv : 1.5D
Δht : 1.5D
Cover depth : 36 m

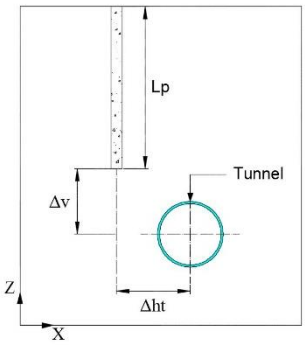

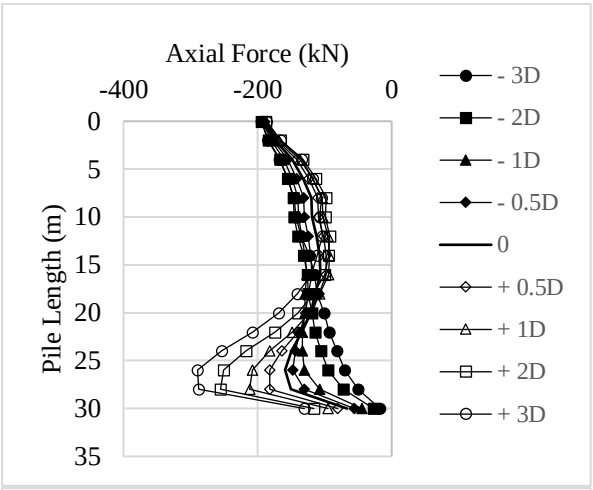

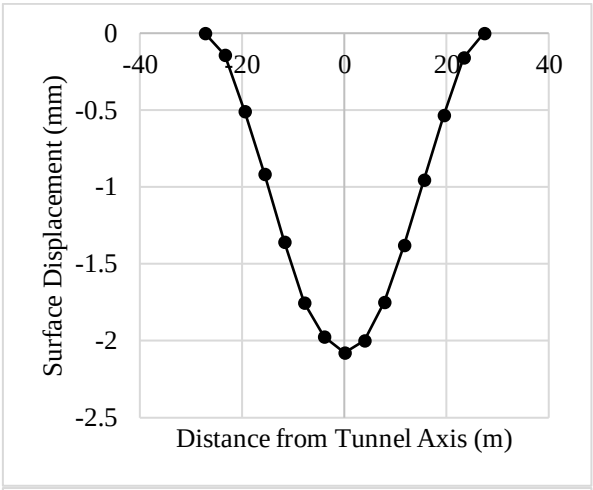

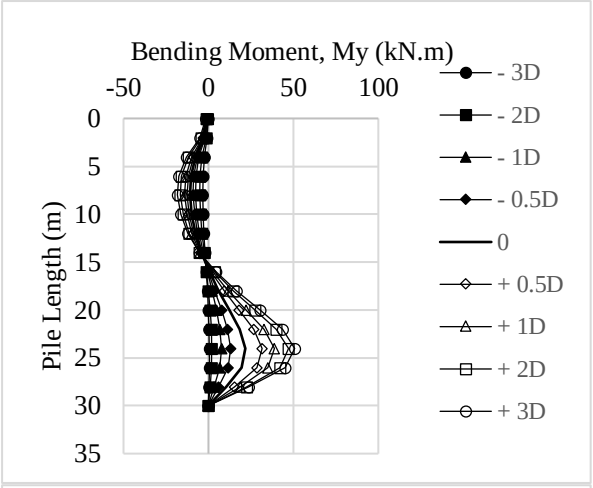

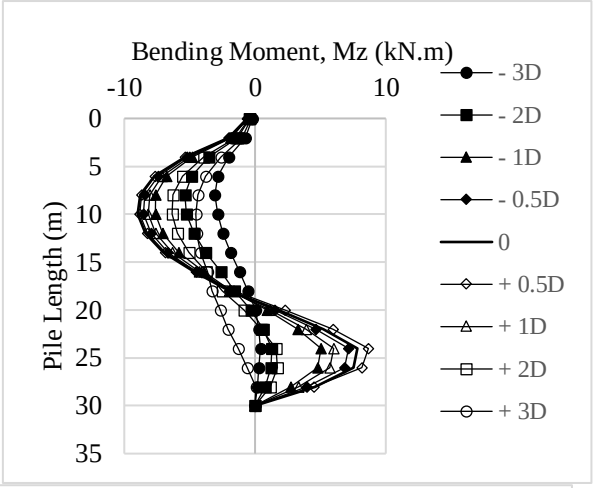

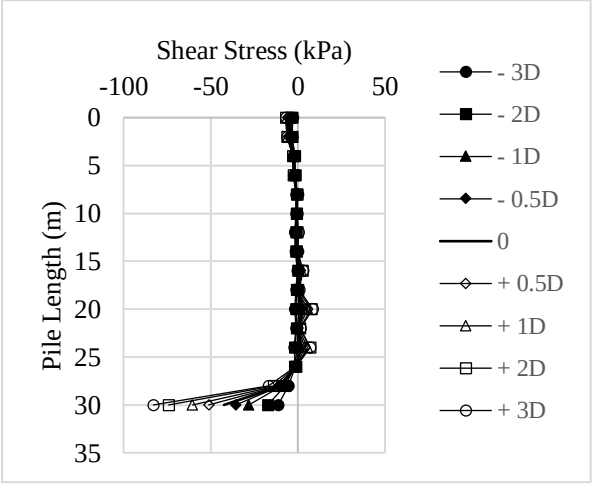

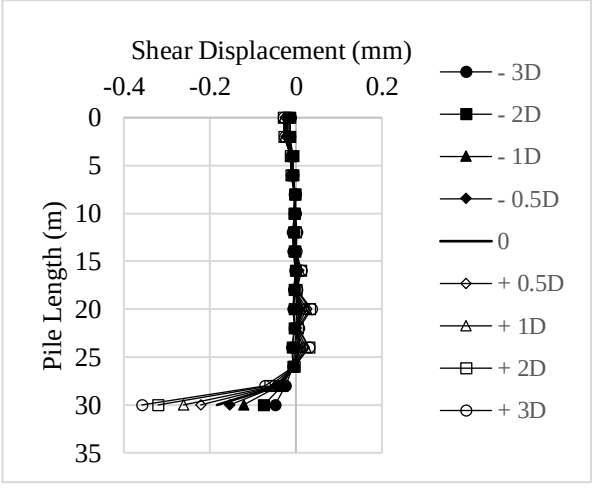

Short pile case 01-2-5

Δv : 1.5D
Δht : 2D
Cover depth : 36 m

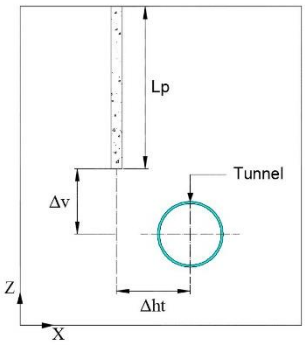

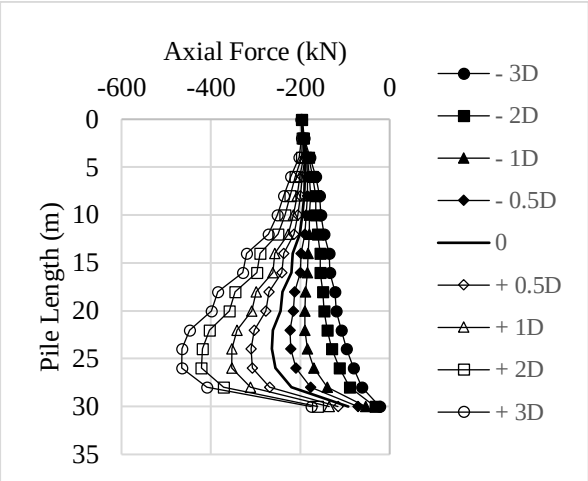

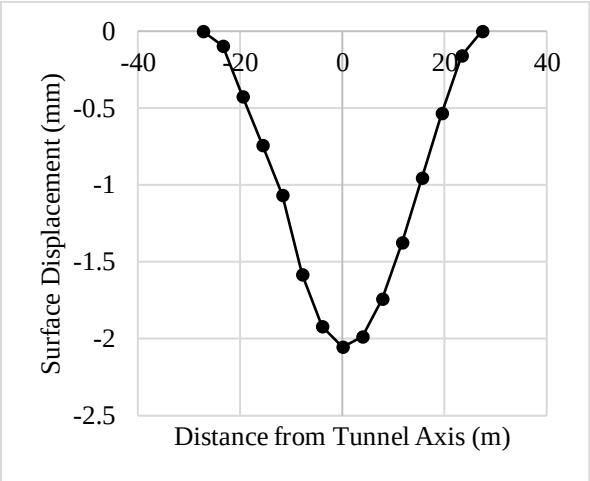

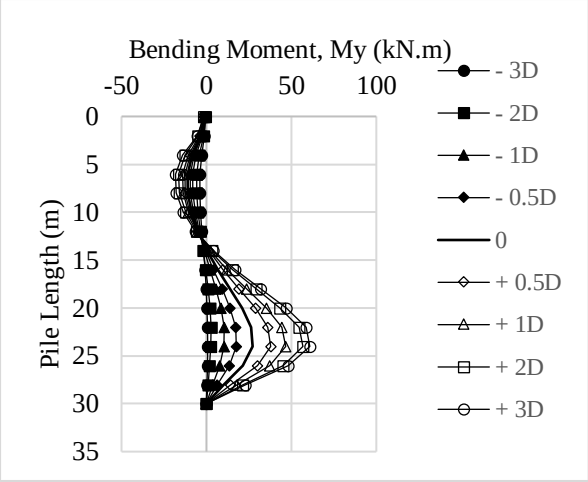

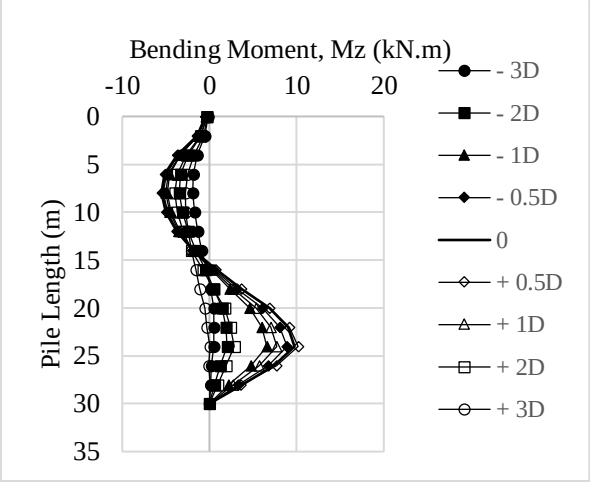

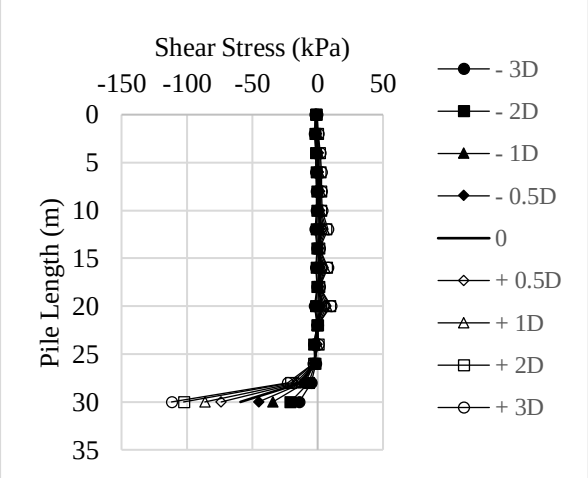

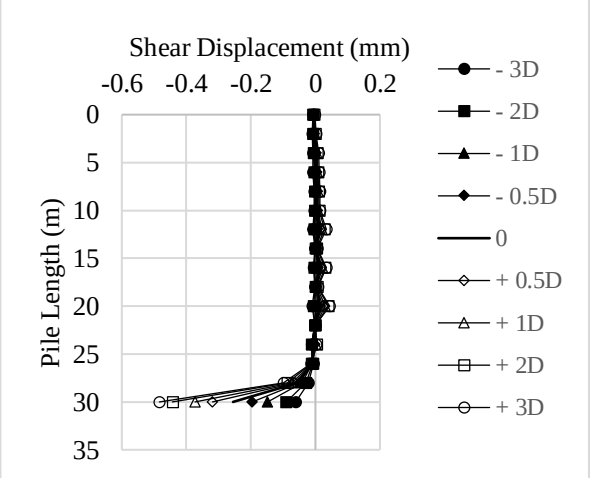

Short pile case 01-2-6

Δv	:	1.5D
Δht	:	2.5D
Cover depth	:	36 m

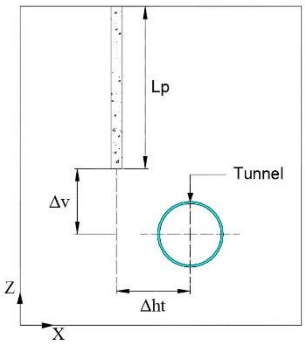

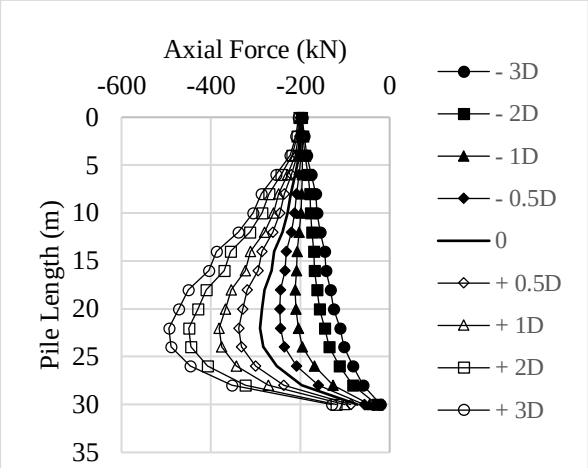

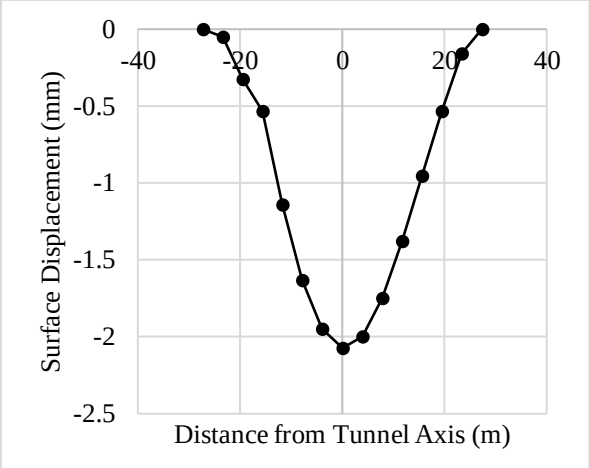

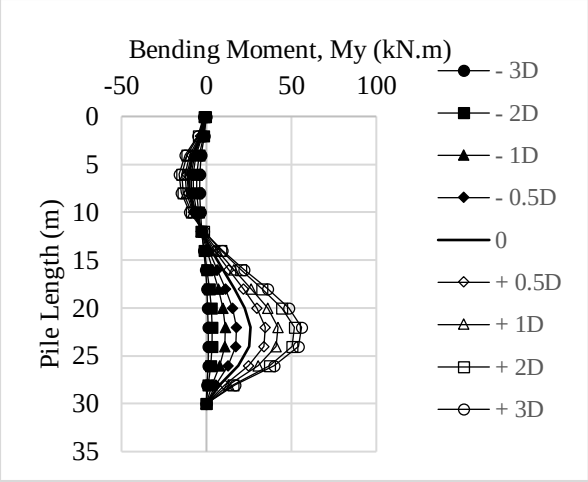

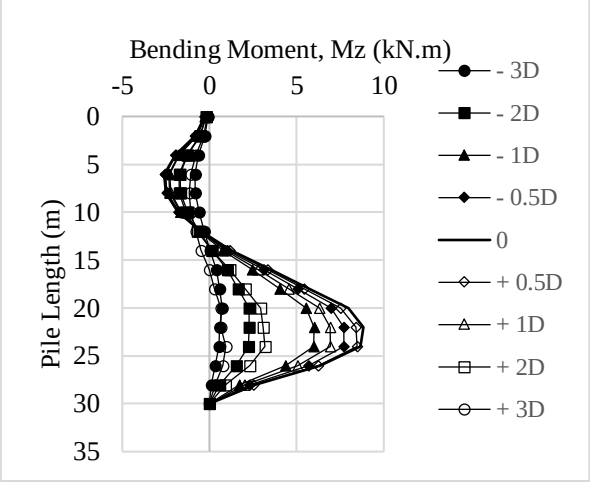

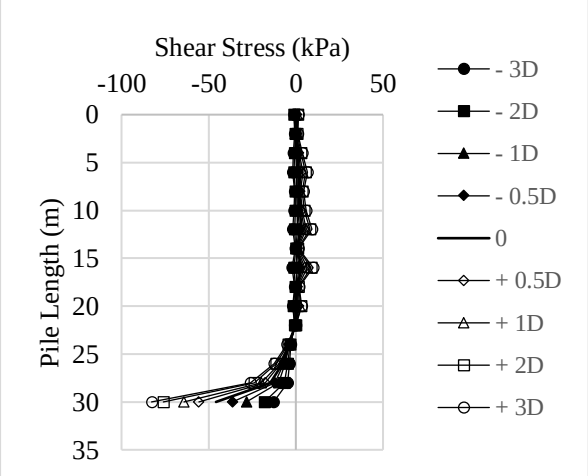

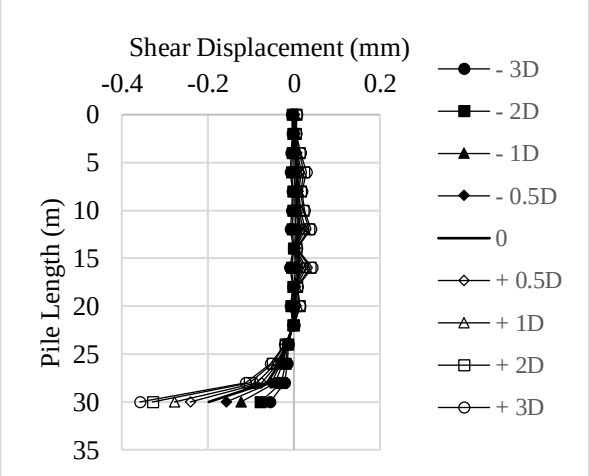

Short pile case 01-3-1

Δv : 2D
Δht : 0
Cover depth : 39 m

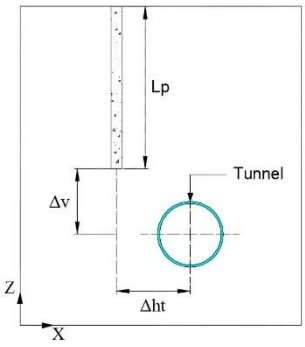

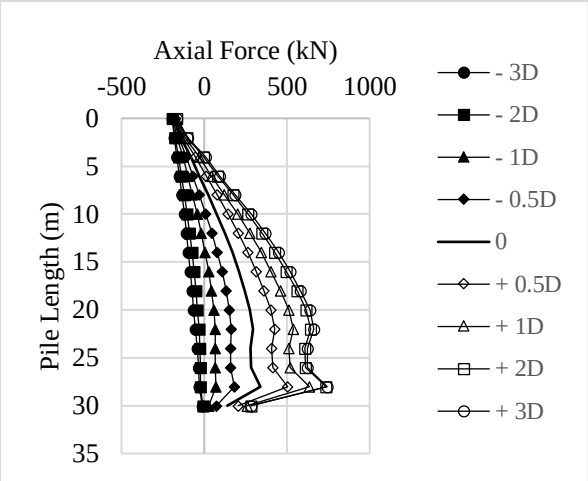

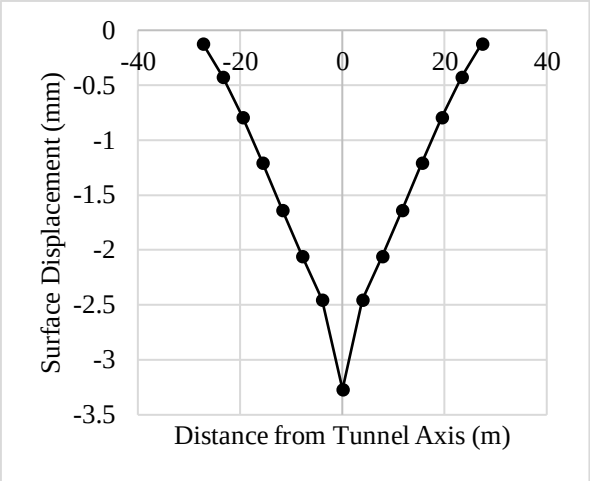

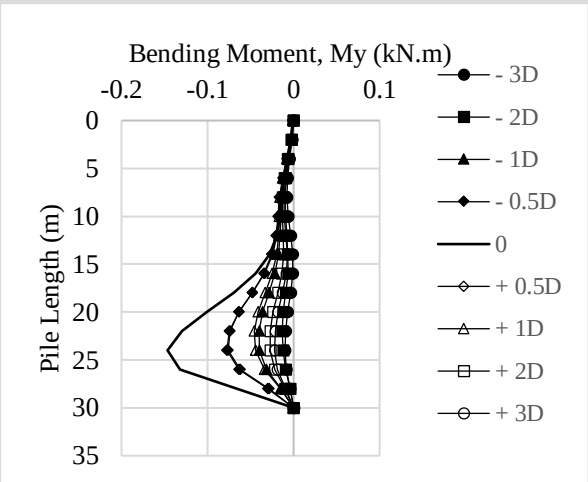

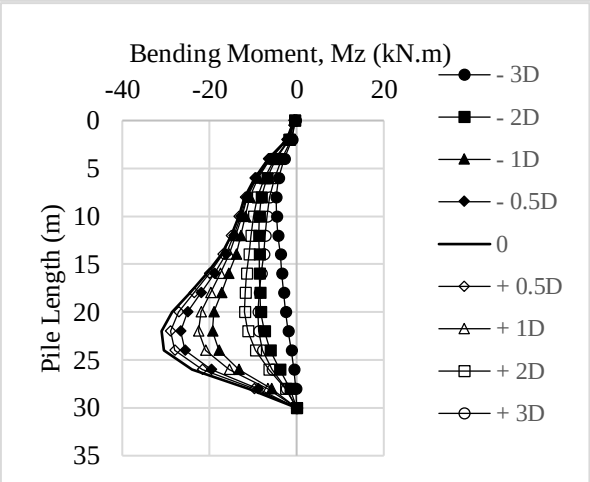

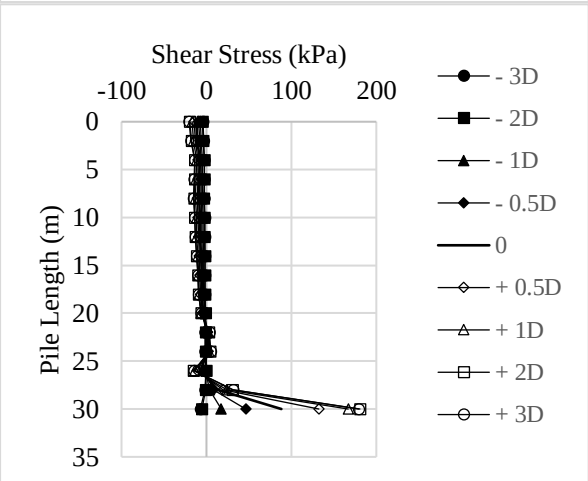

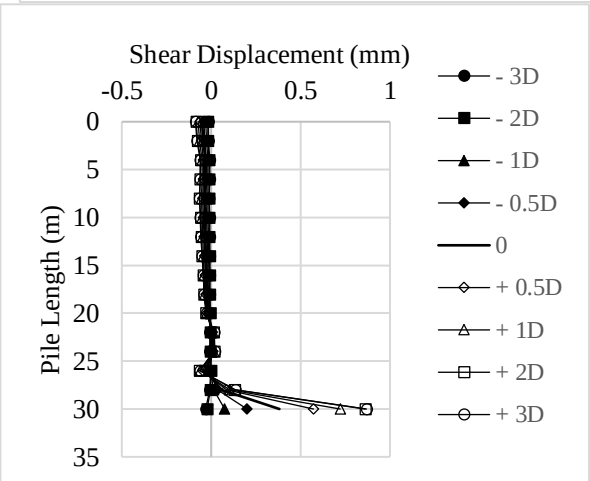

Short pile case 01-3-2

Δv : 2D
Δht : 0.5D
Cover depth : 39 m

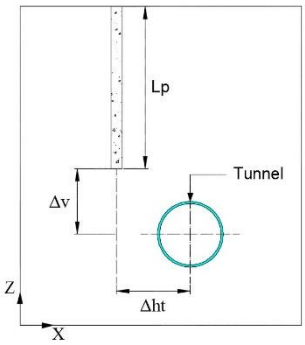

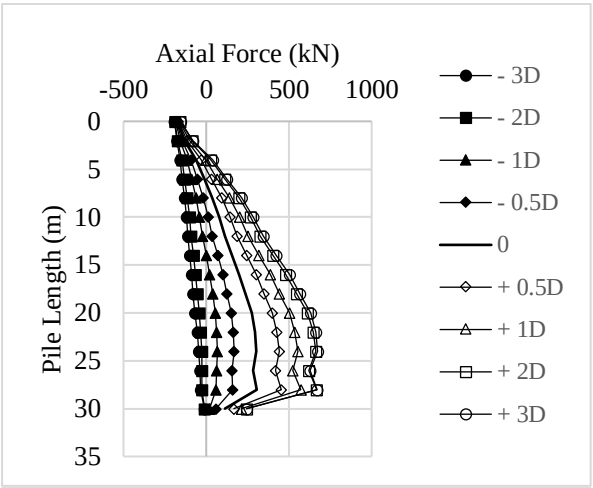

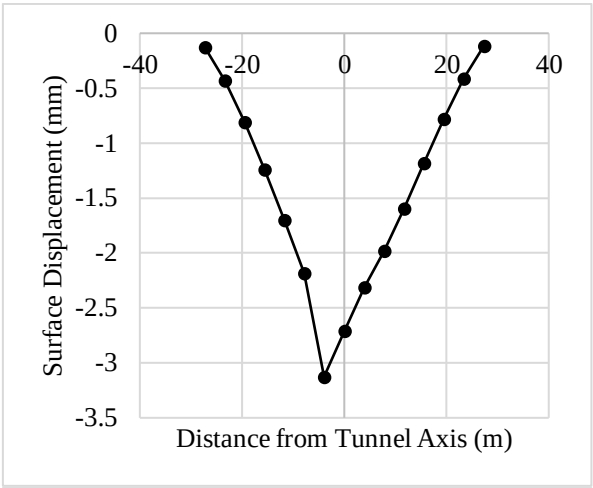

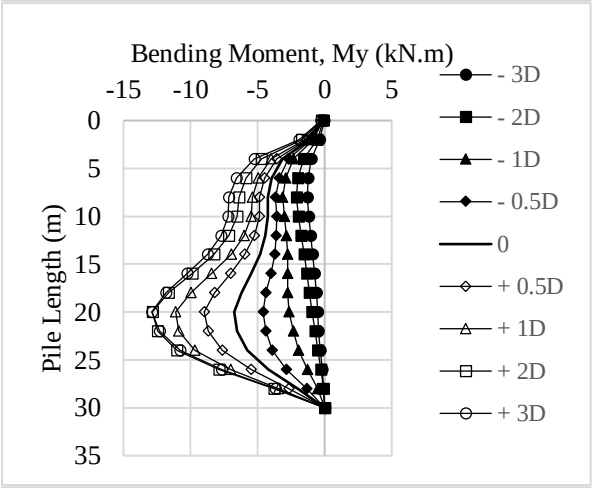

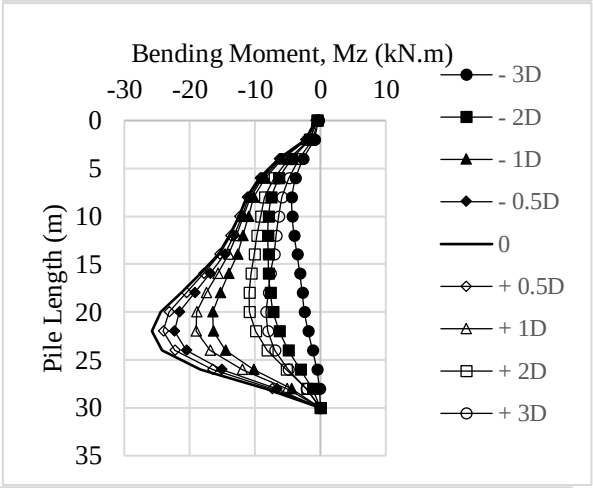

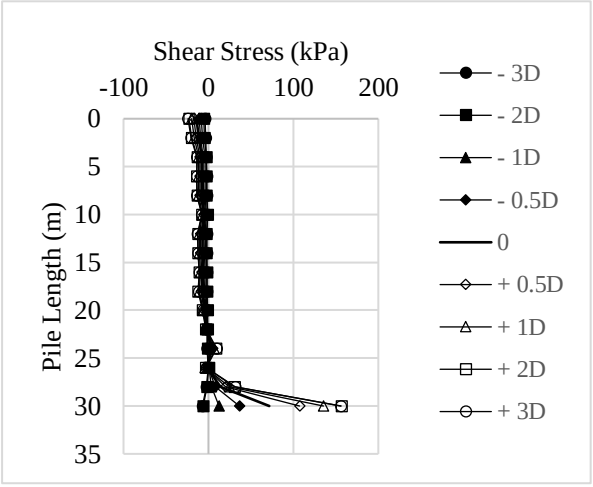

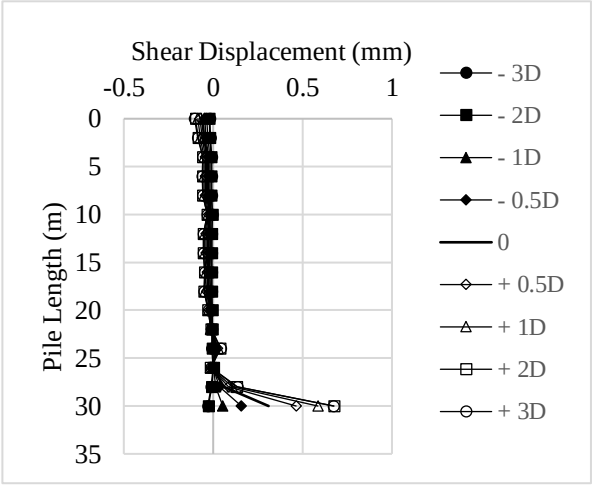

Short pile case 01-3-3

Δv : 2D
Δht : 1D
Cover depth : 39 m

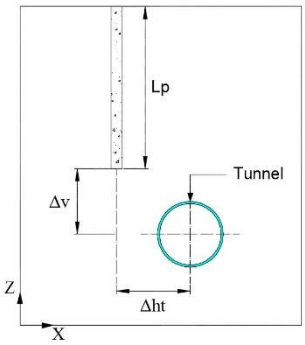

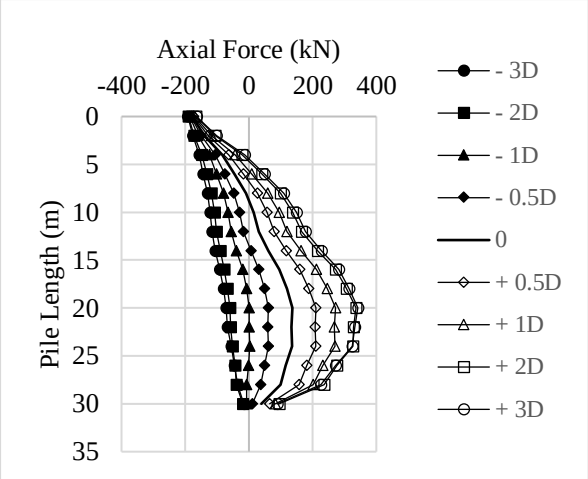

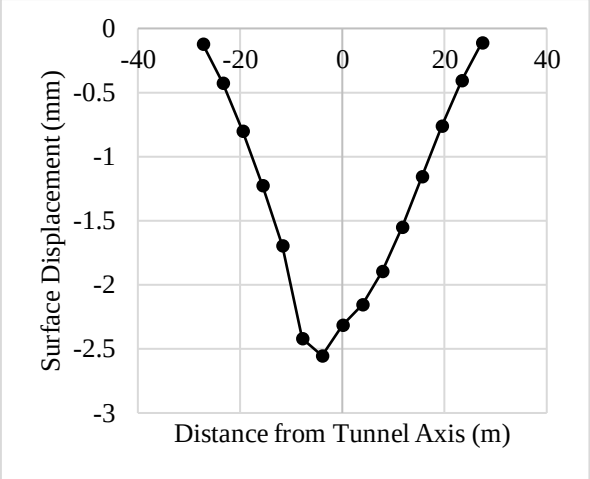

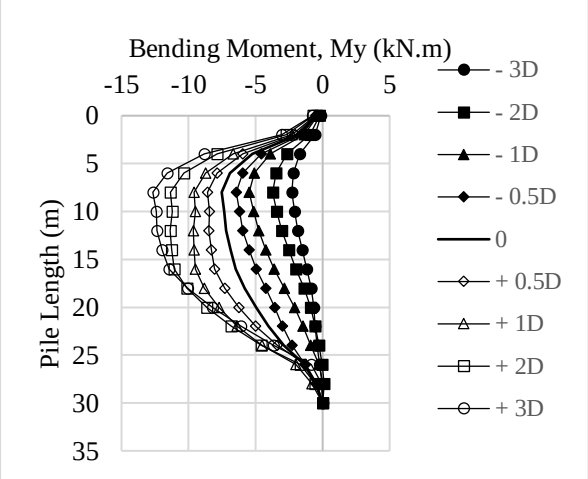

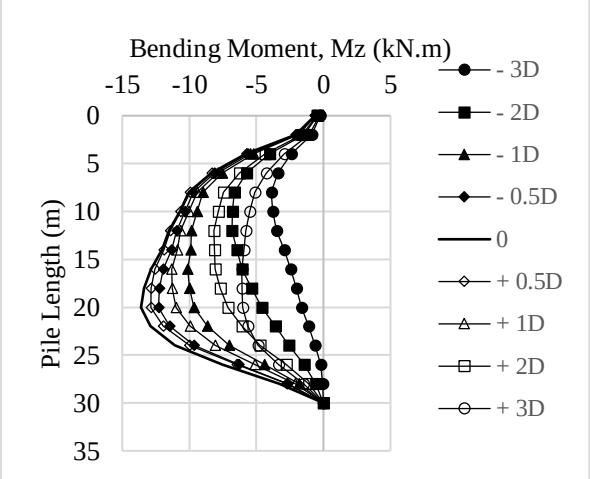

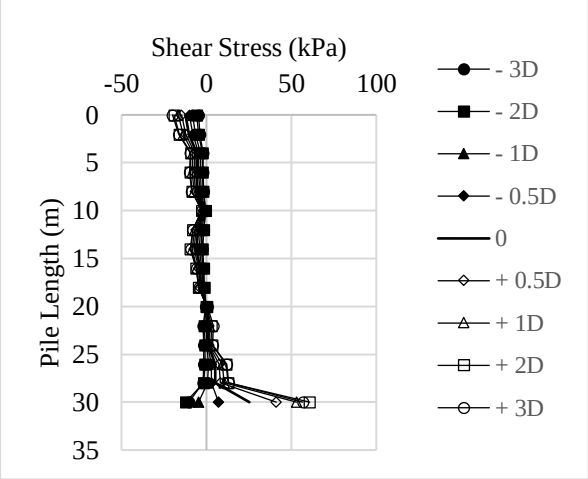

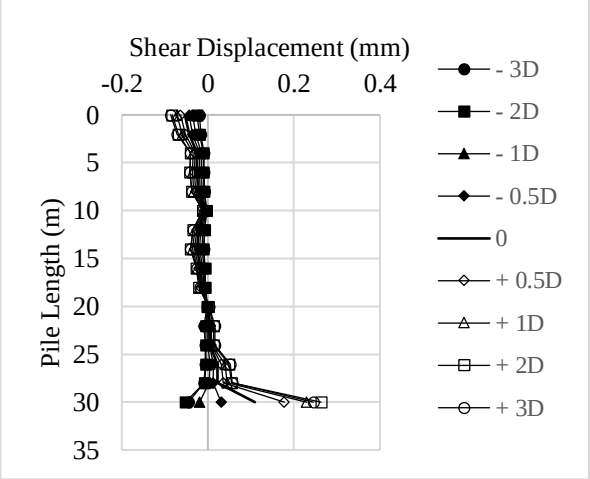

Short pile case 01-3-4

Δv : 2D
Δht : 1.5D
Cover depth : 39 m

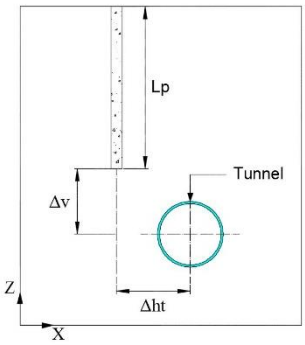

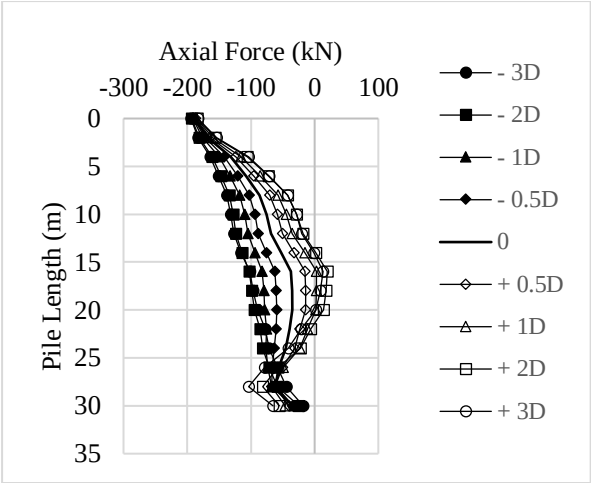

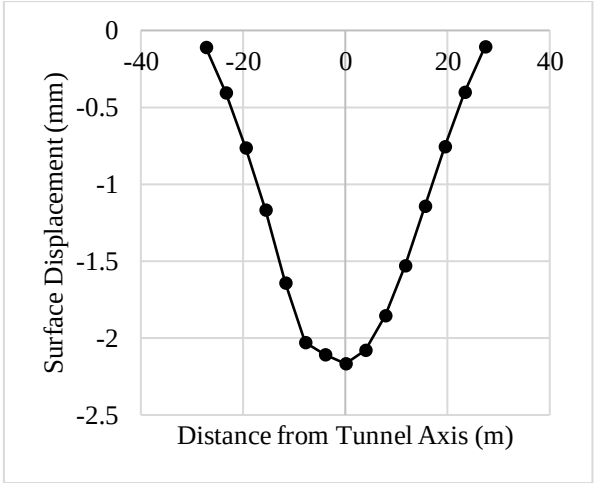

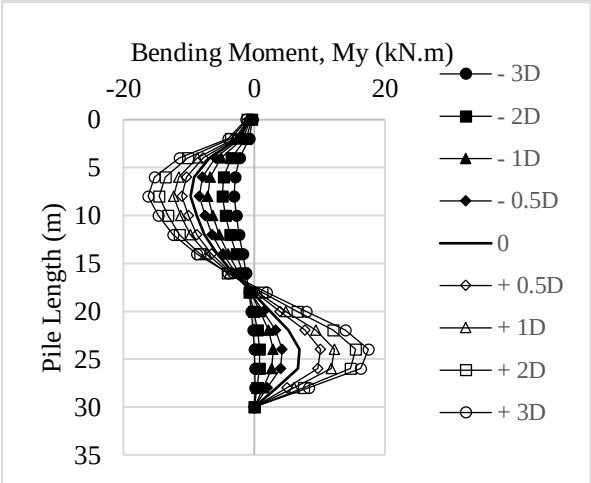

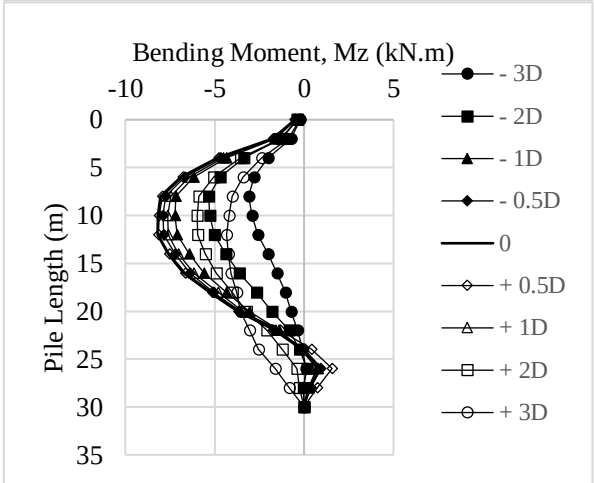

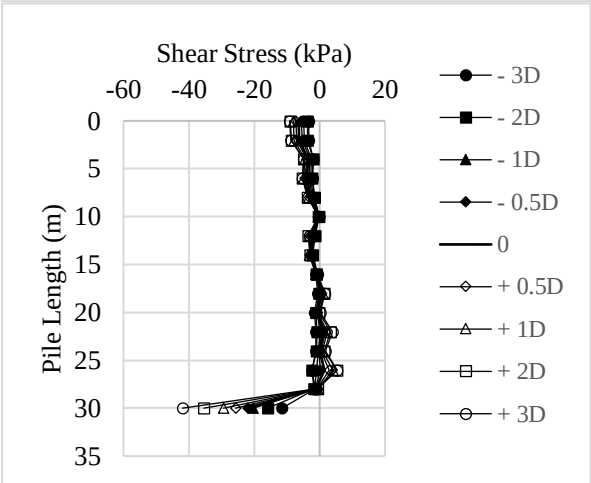

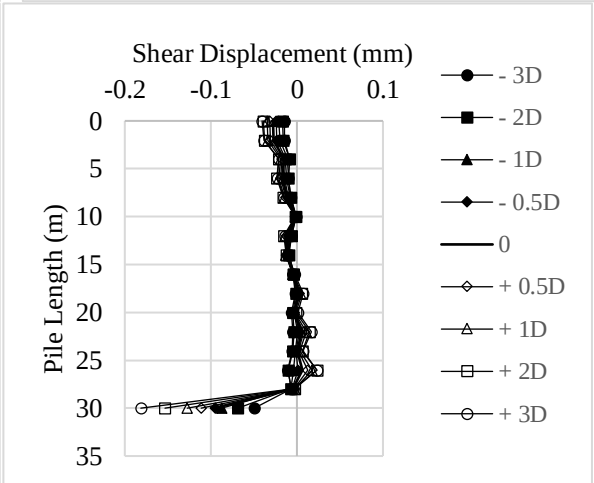

Short pile case 01-3-5

Δv : 2D
Δht : 2D
Cover depth : 39 m

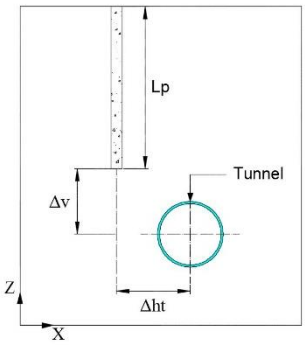

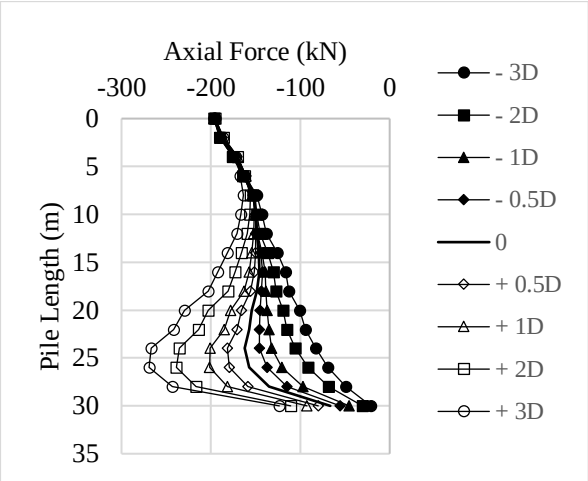

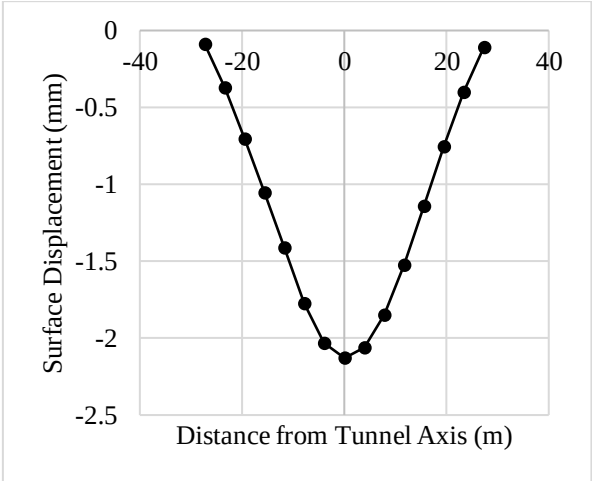

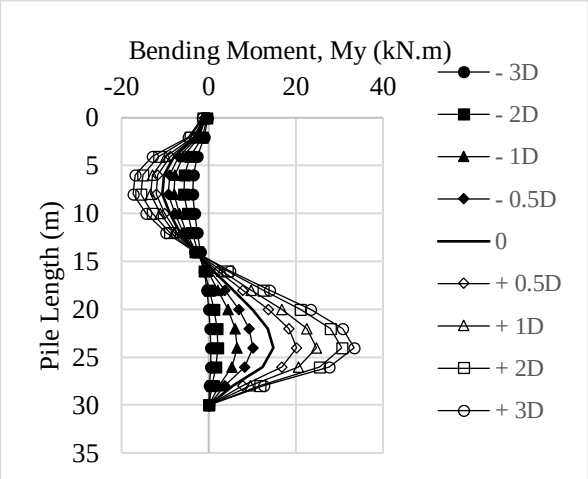

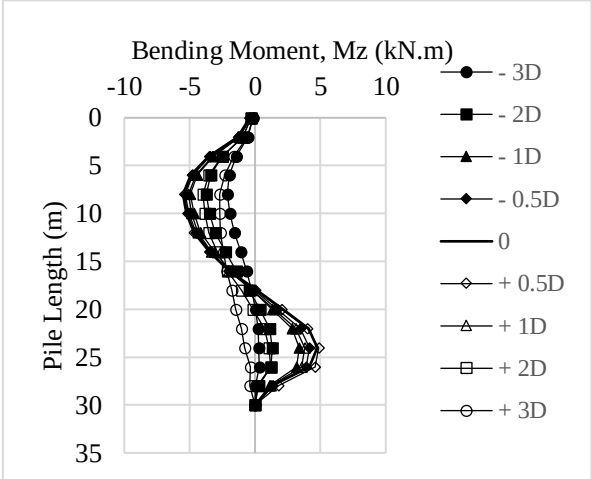

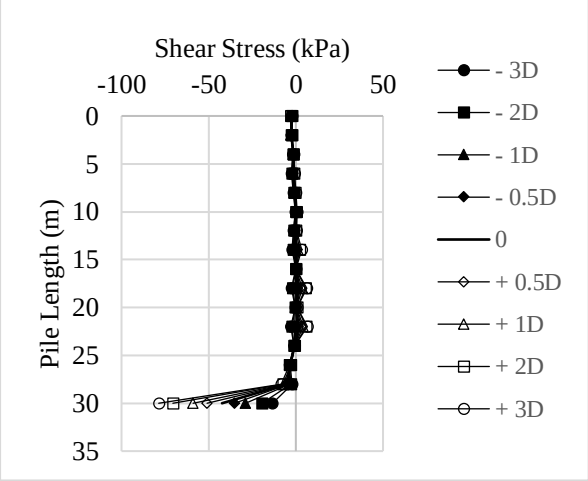

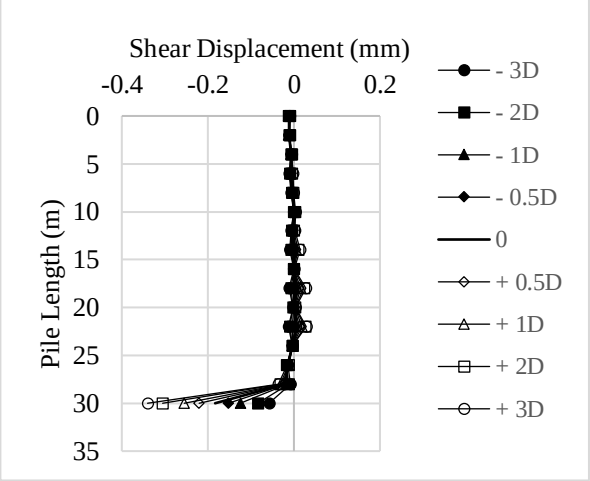

Short pile case 01-3-6

Δv	:	2D
Δht	:	2.5D
Cover depth	:	39 m

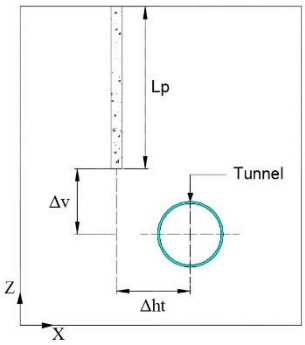

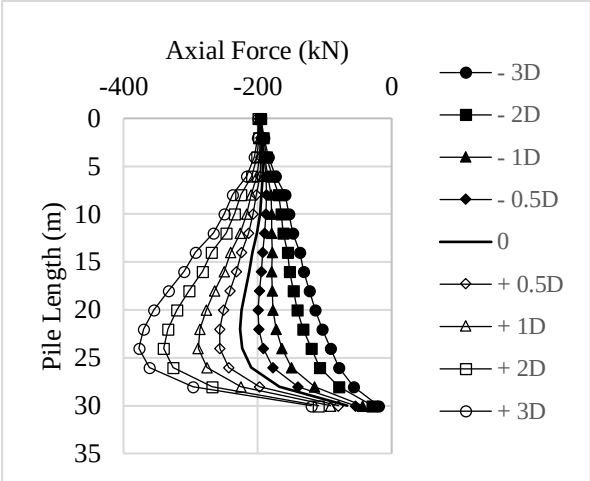

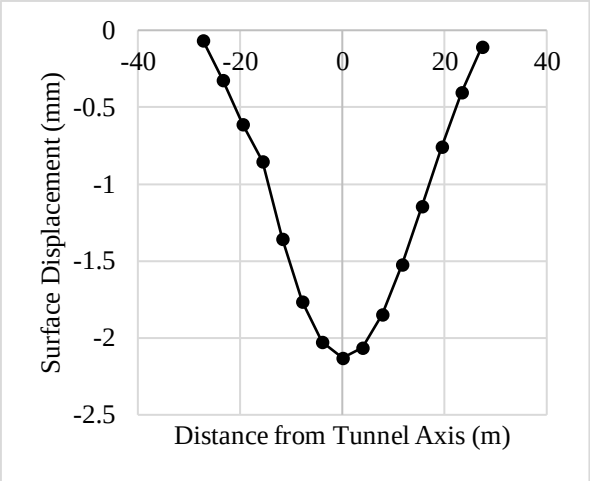

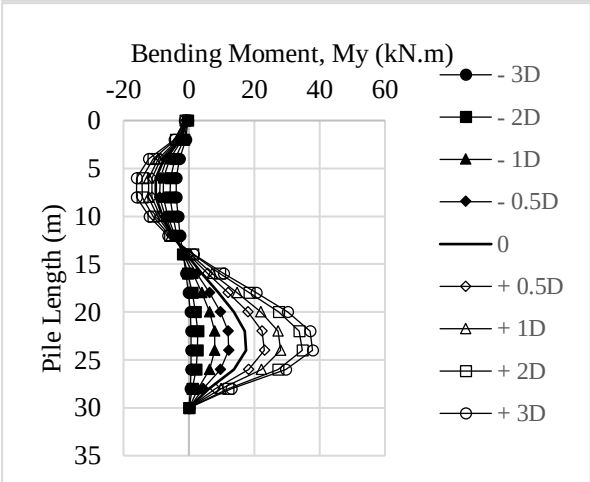

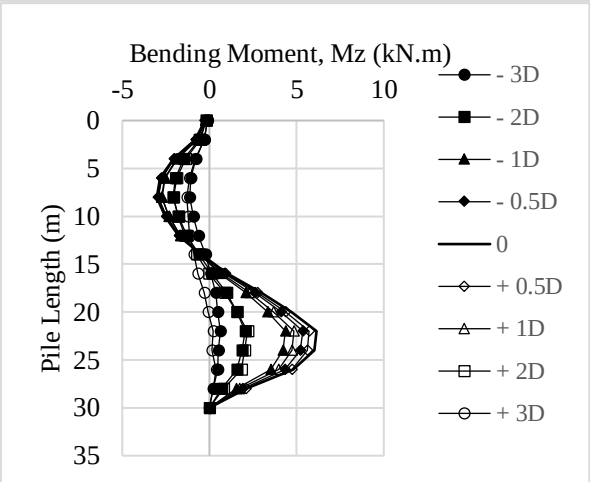

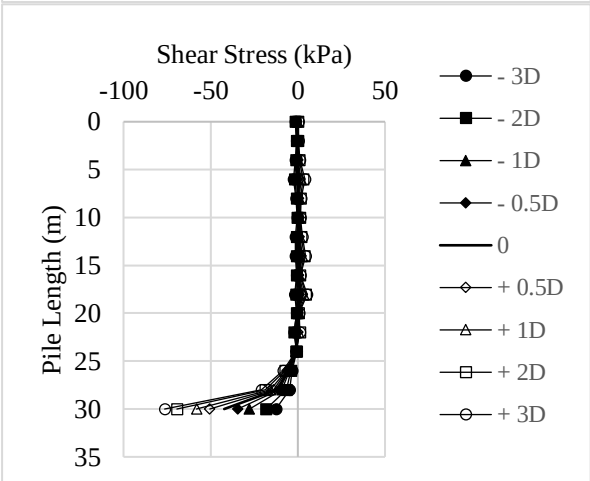

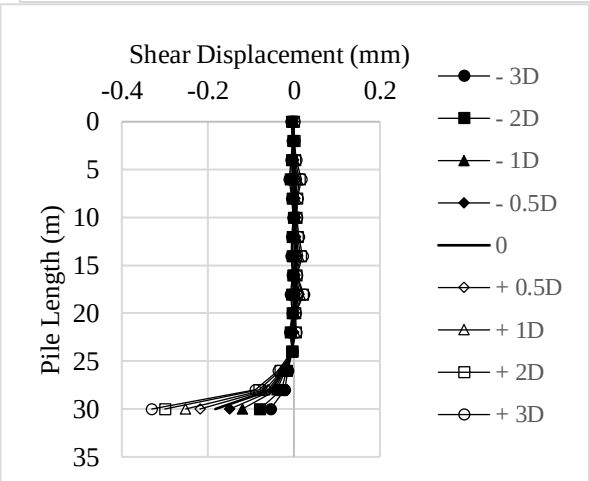

Short pile case 01-4-1

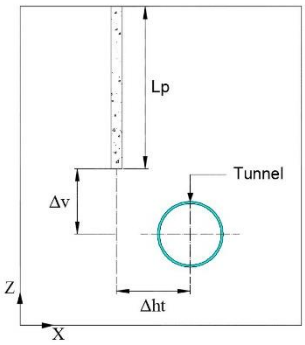

Δv : 2.5D
Δht : 0
Cover depth : 39 m

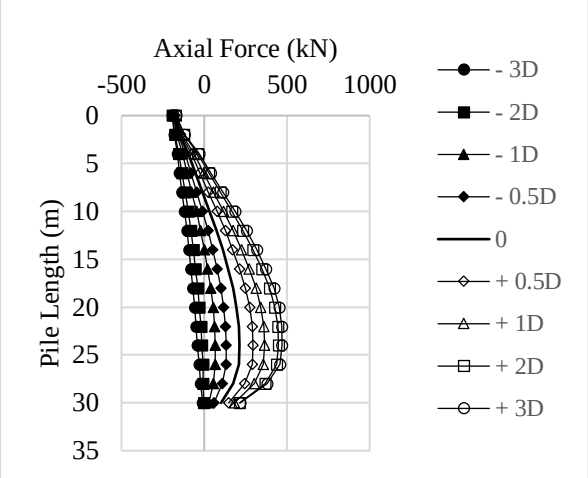

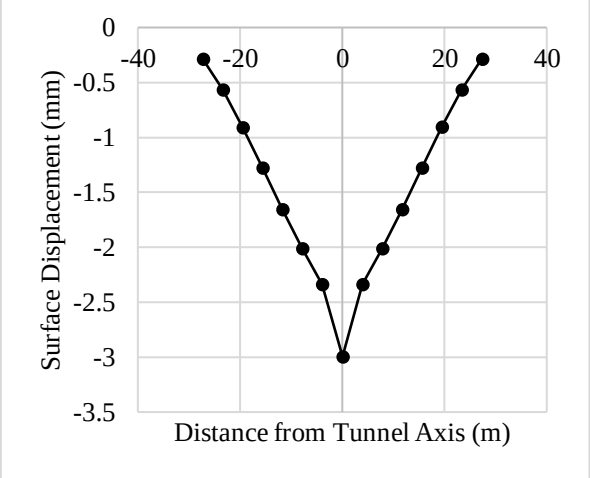

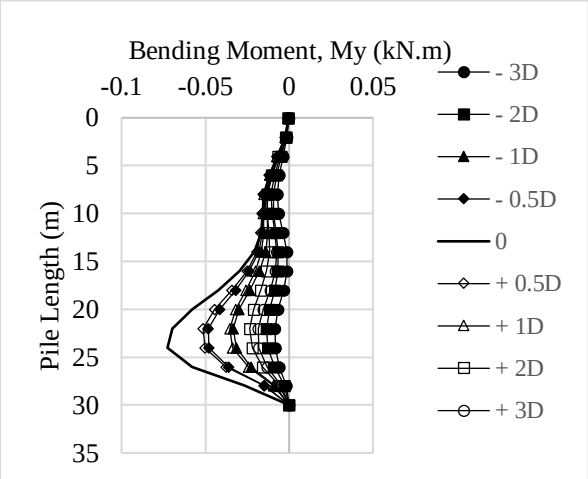

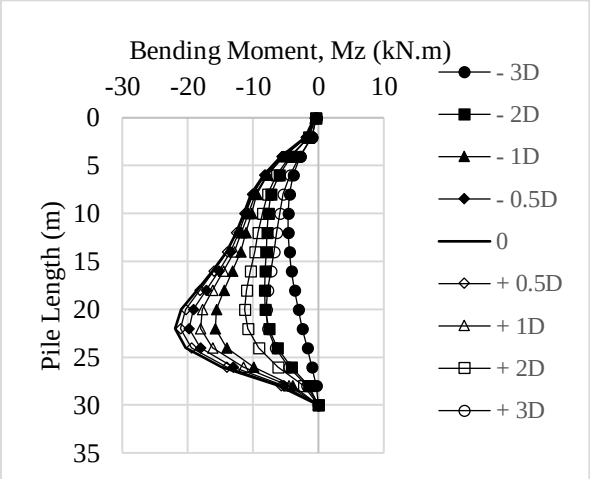

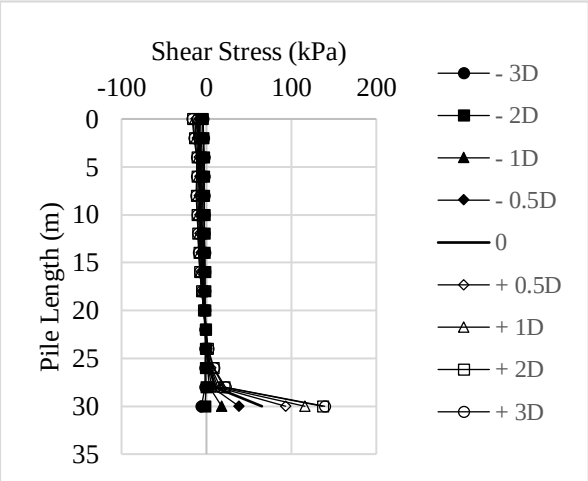

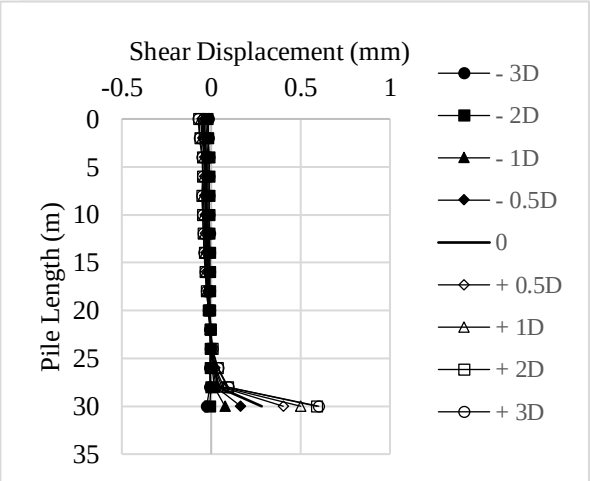

Short pile case 01-4-2

Δv : 2.5D
Δht : 0.5D
Cover depth : 39 m

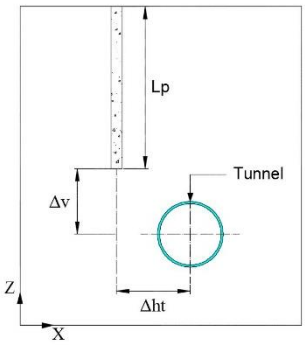

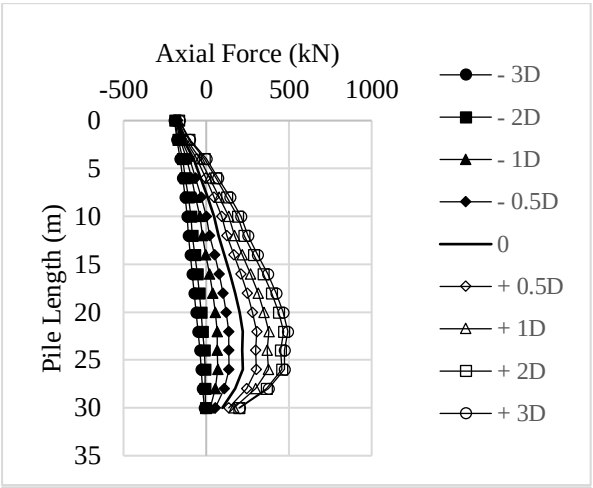

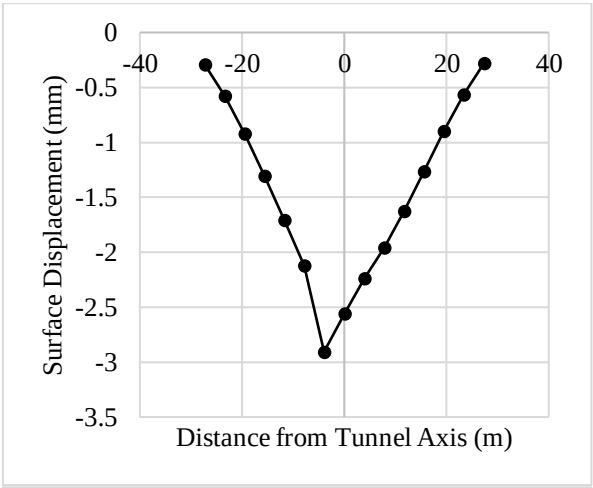

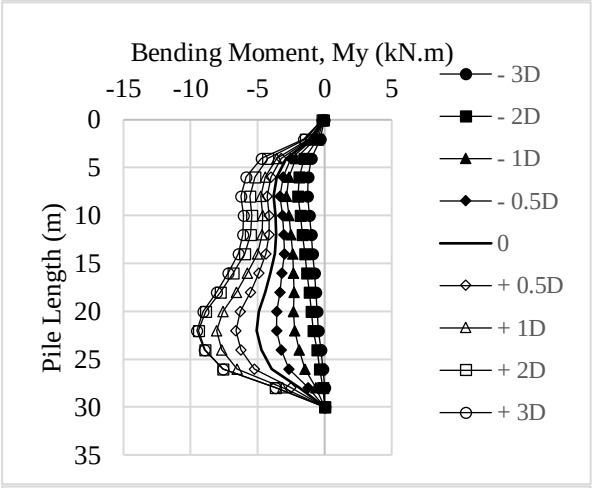

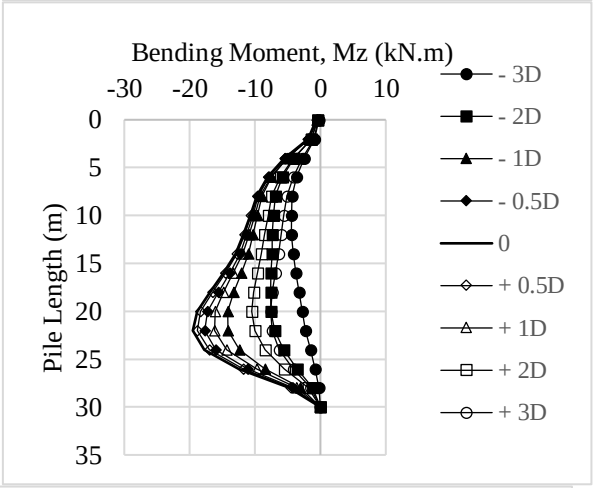

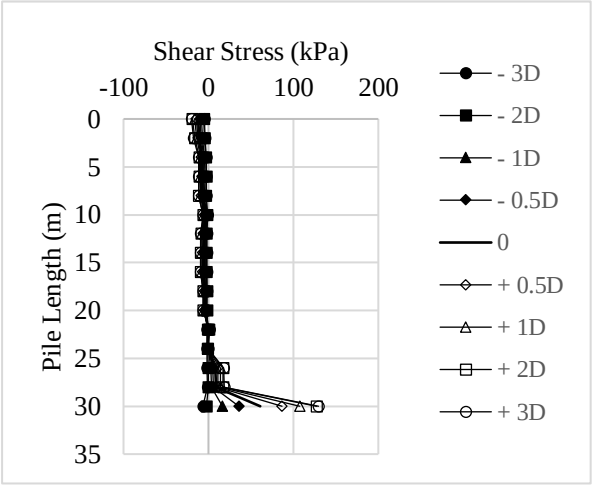

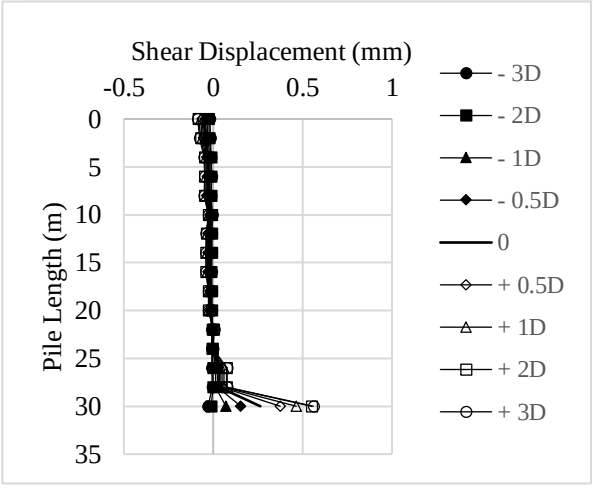

Short pile case 01-4-3

Δv : 2.5D
Δht : 1D
Cover depth : 39 m

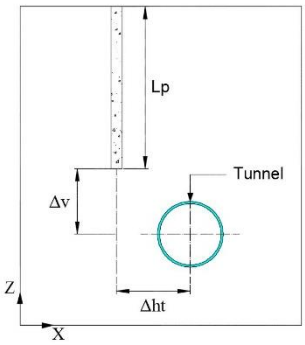

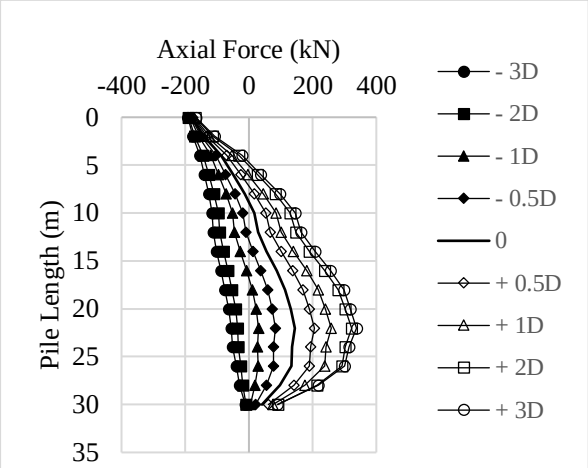

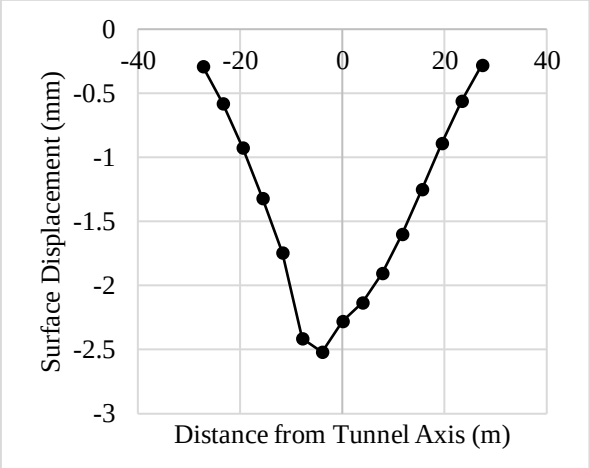

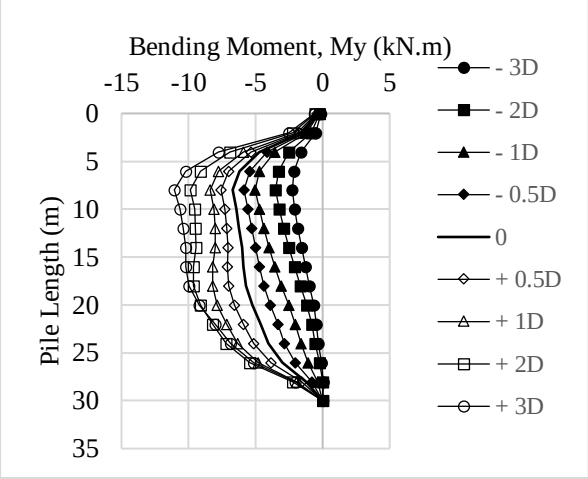

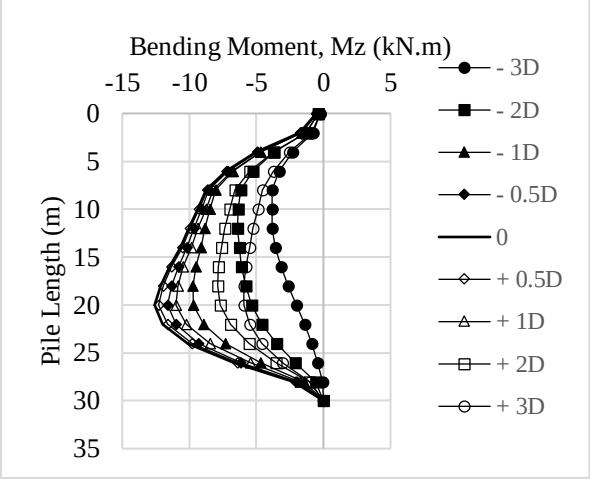

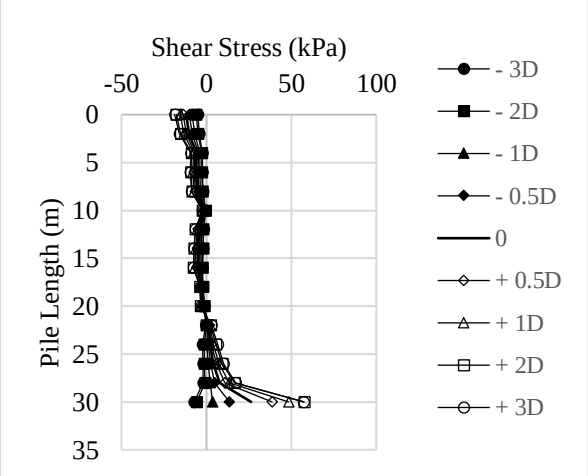

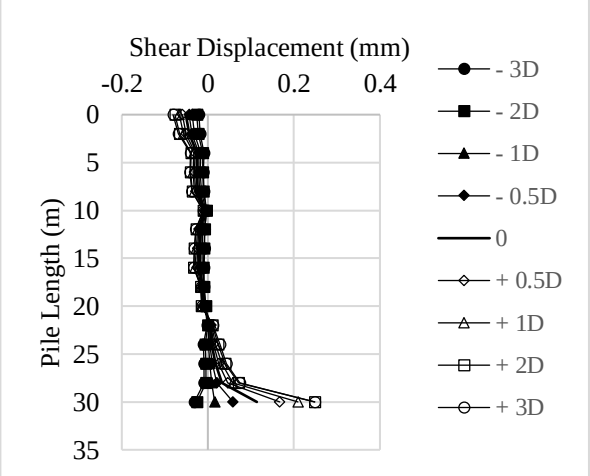

Short pile case 01-4-4

Δv : 2.5D
Δht : 1.5D
Cover depth : 39 m

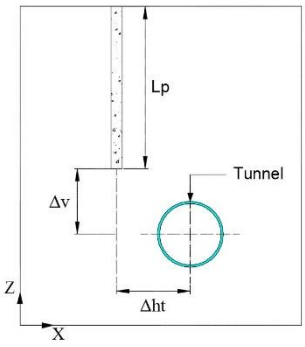

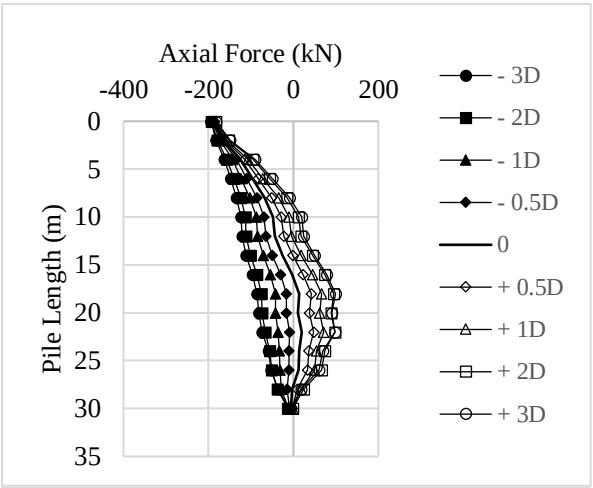

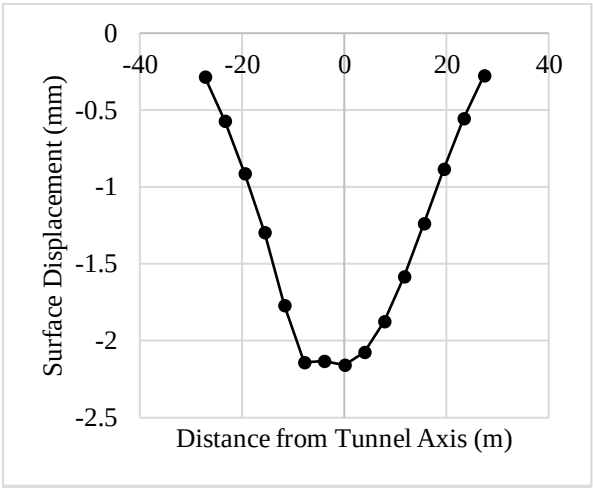

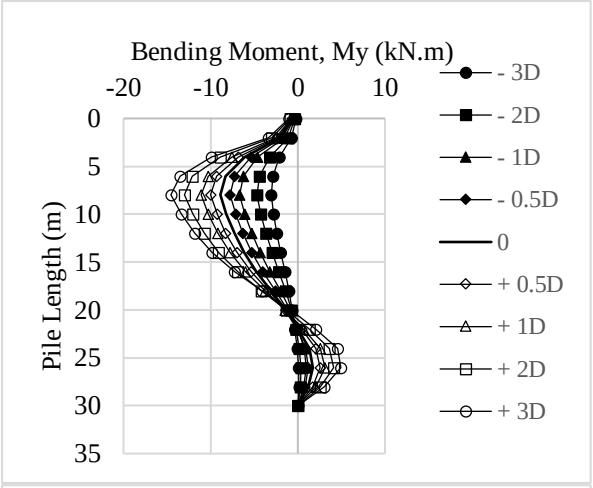

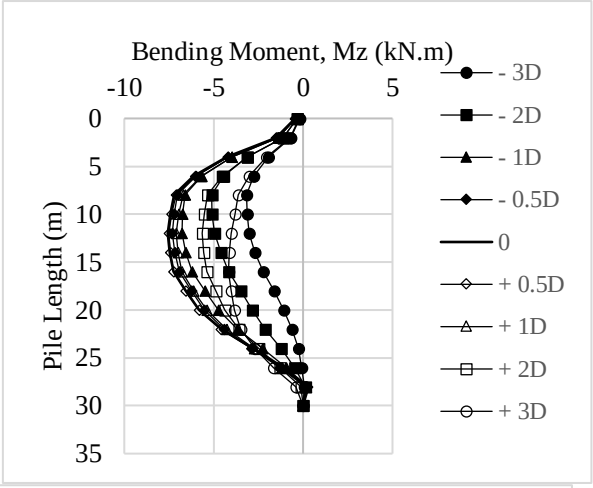

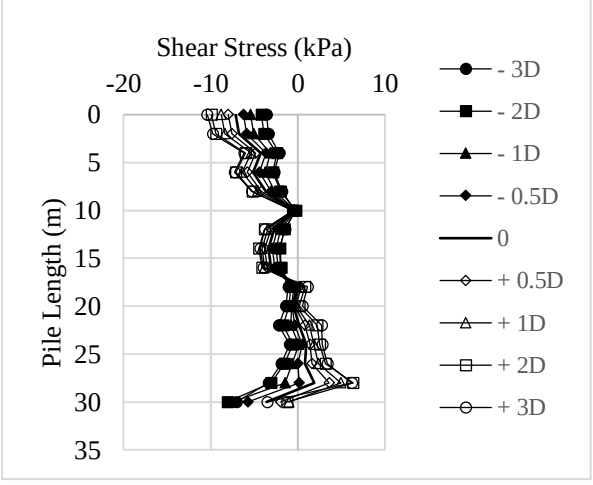

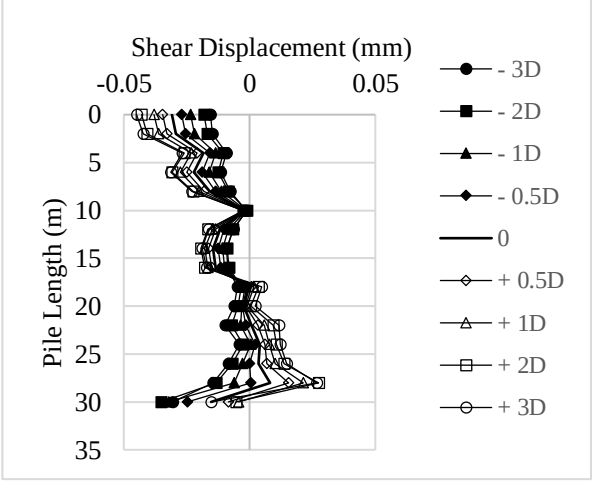

Short pile case 01-4-5

Δv : 2.5D
Δht : 2D
Cover depth : 39 m

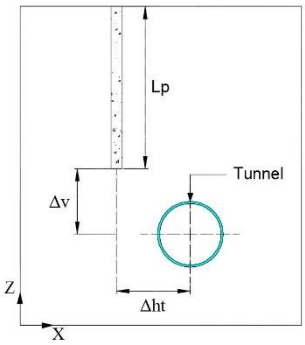

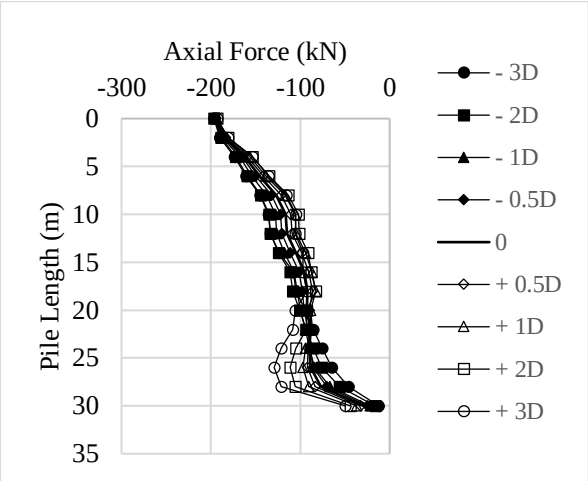

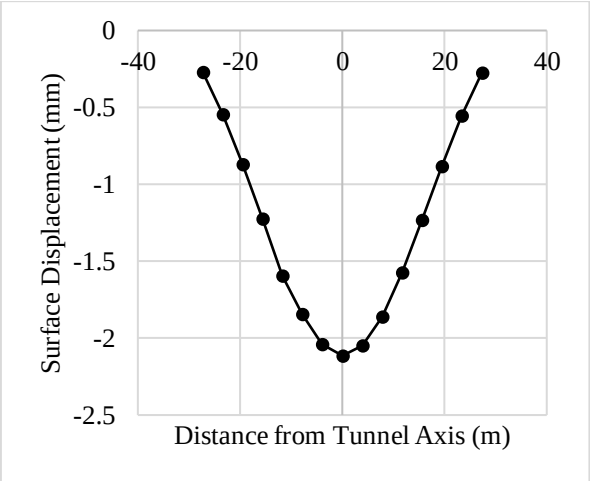

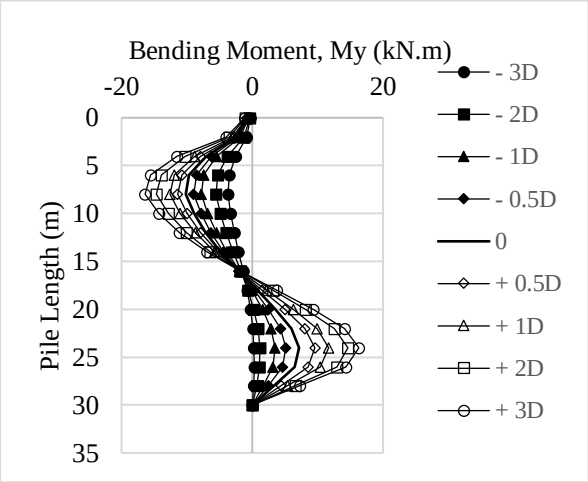

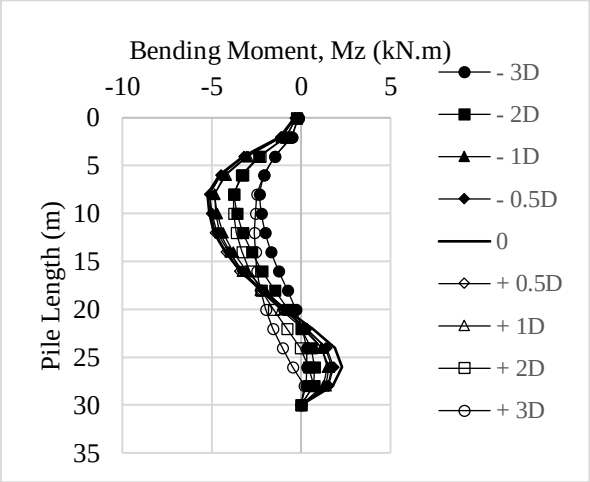

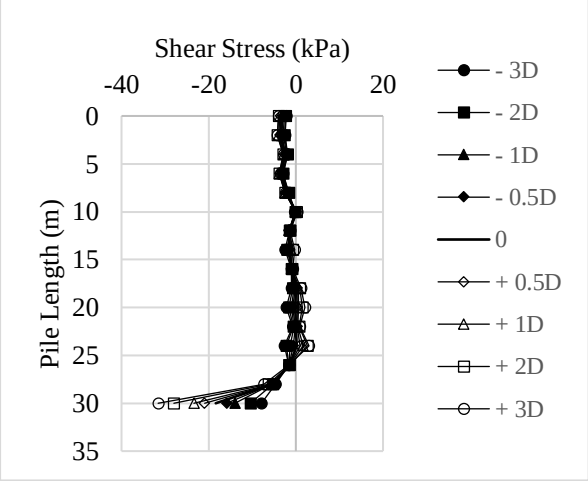

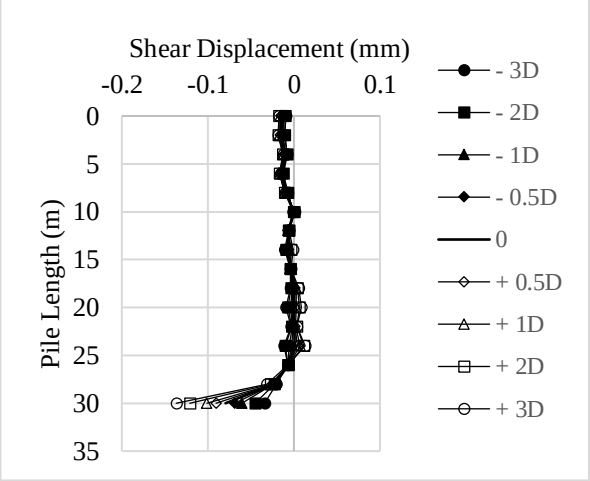

Short pile case 01-4-6

Δv : 2.5D
Δht : 2.5D
Cover depth : 39 m

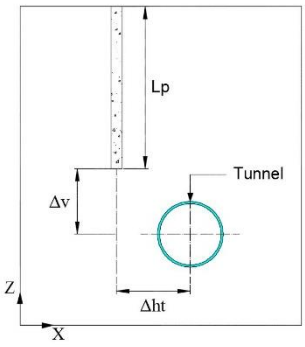

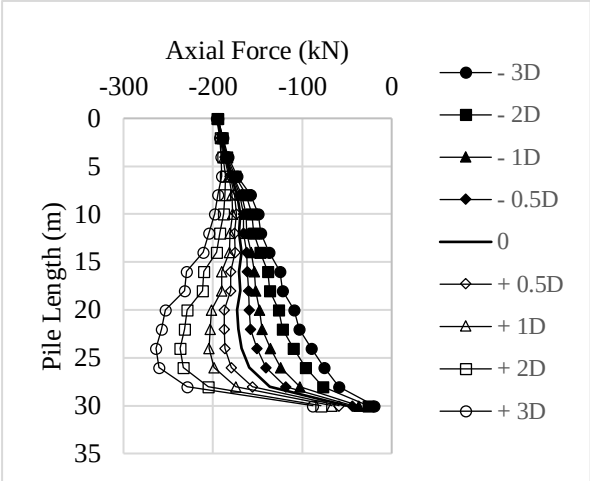

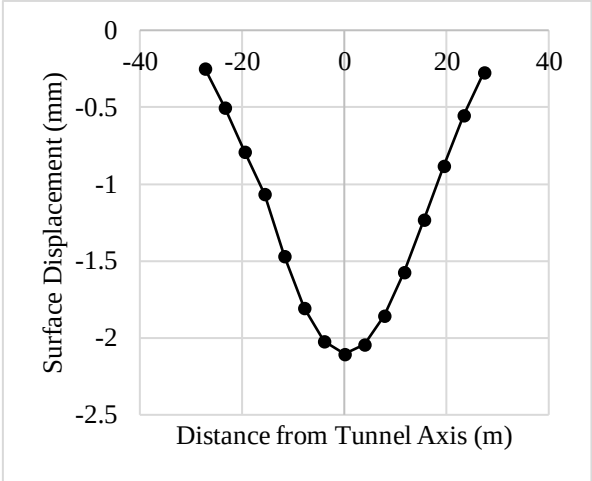

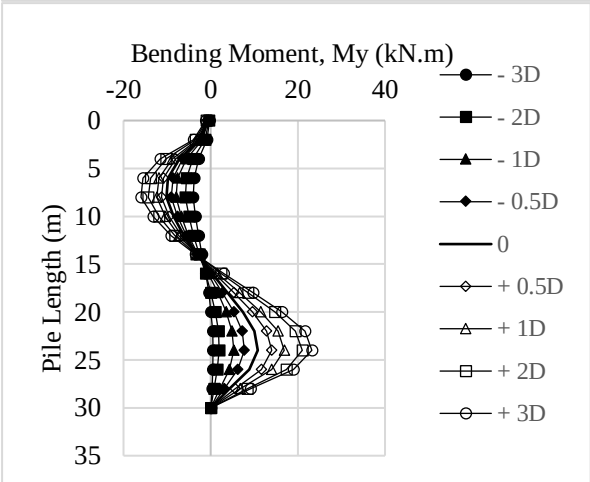

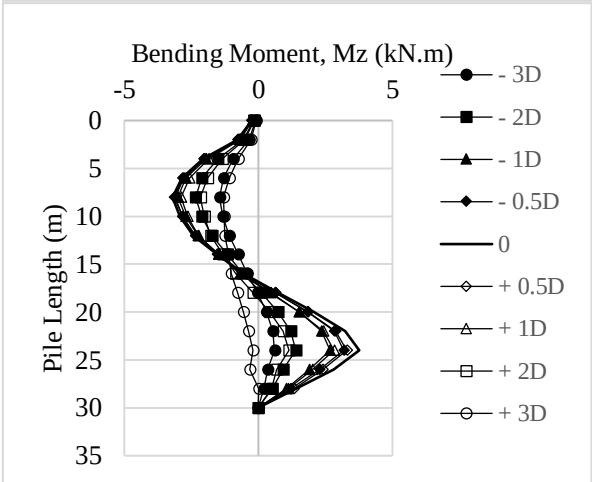

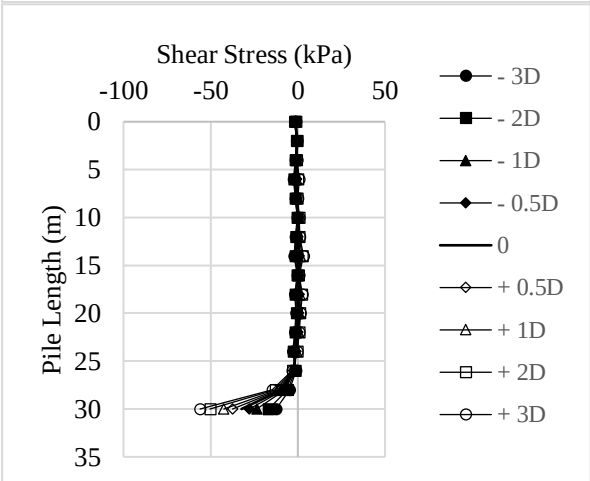

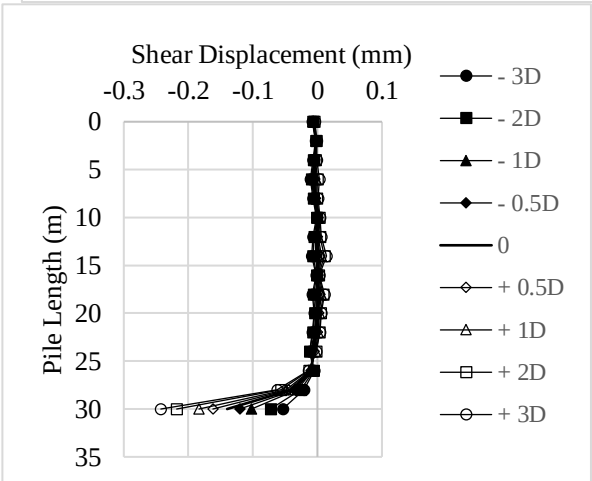

Short pile case 01-5-1

Δv : 3D
Δht : 0
Cover depth : 42 m

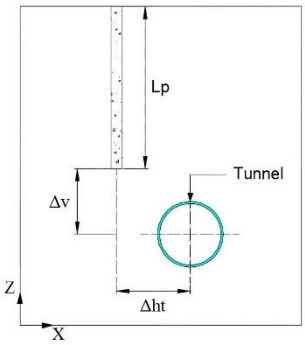

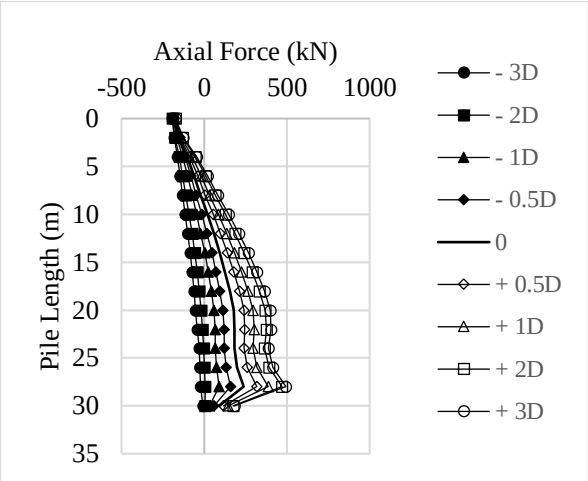

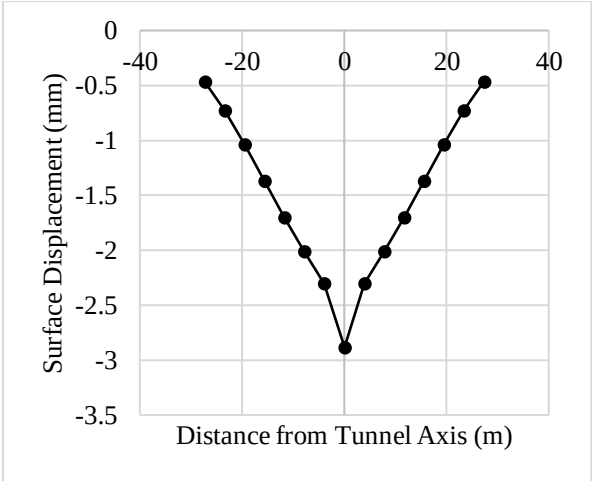

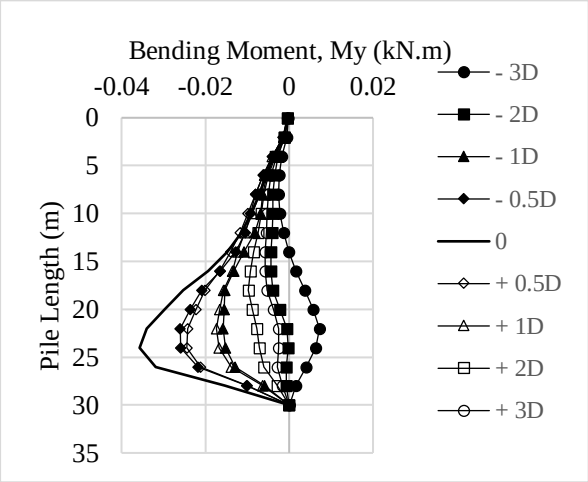

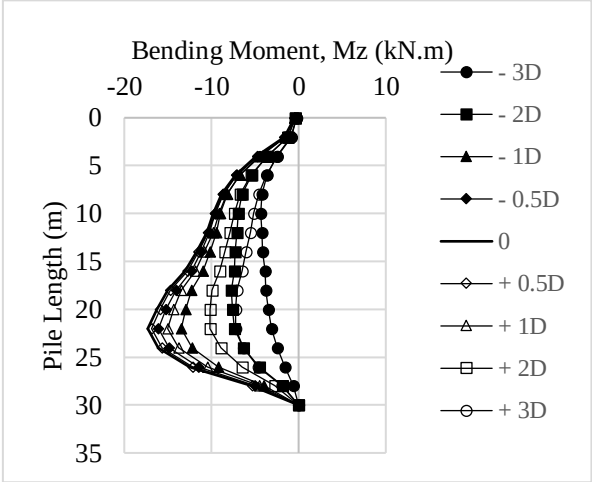

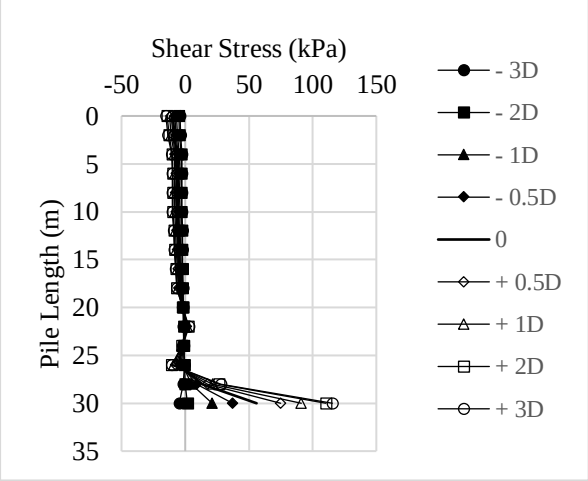

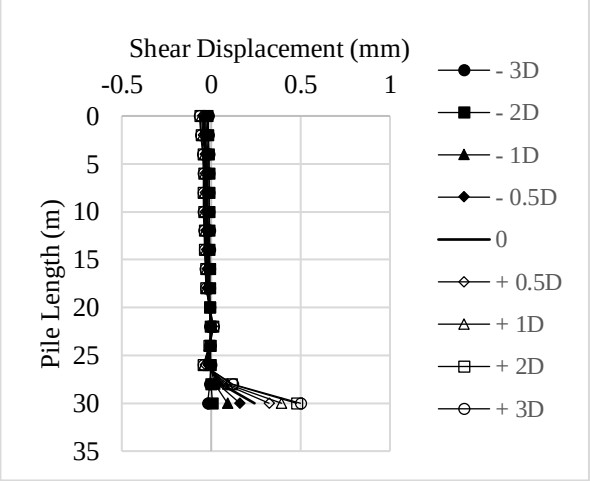

Short pile case 01-5-2

Δv	:	3D
Δht	:	0.5D
Cover depth	:	42 m

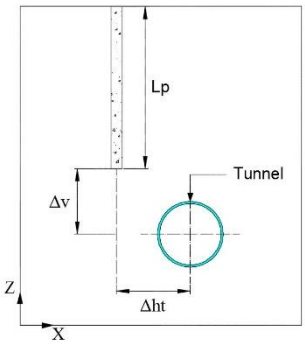

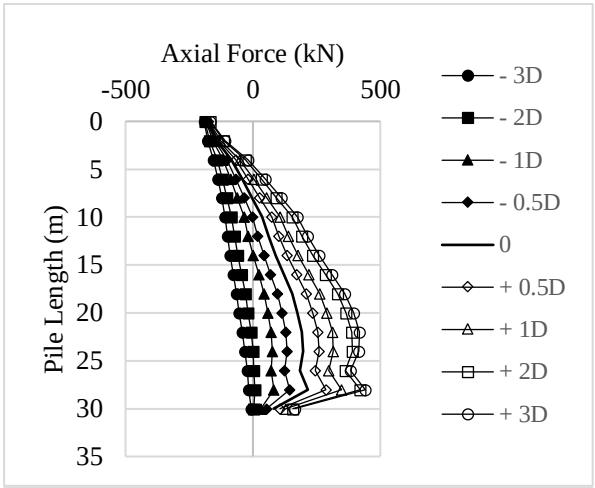

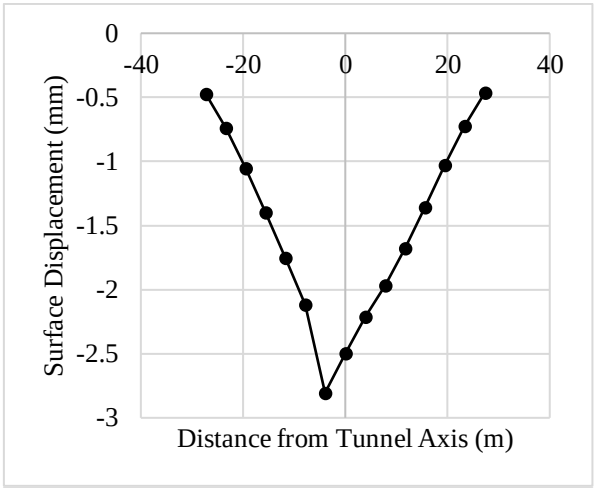

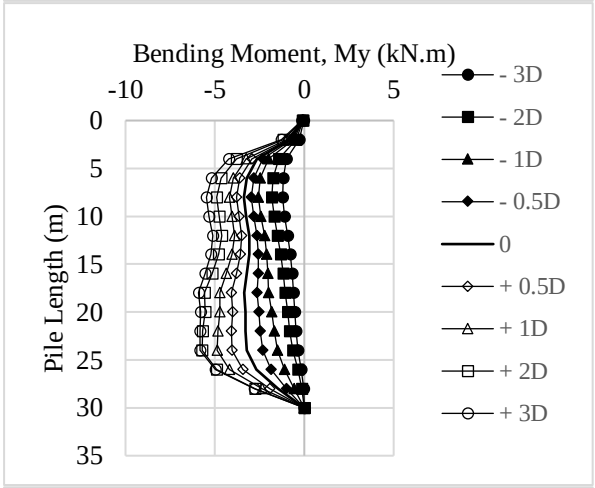

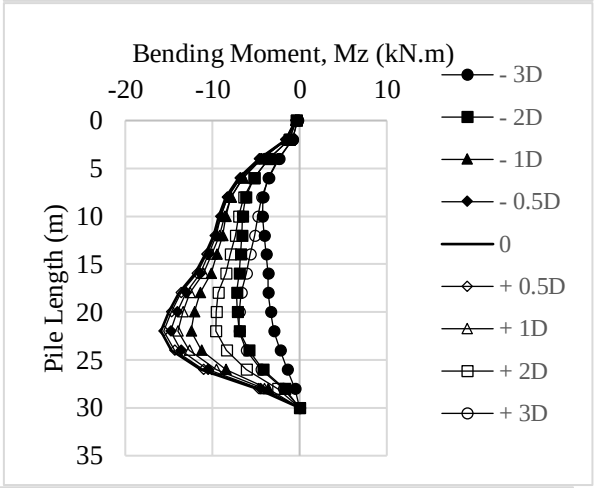

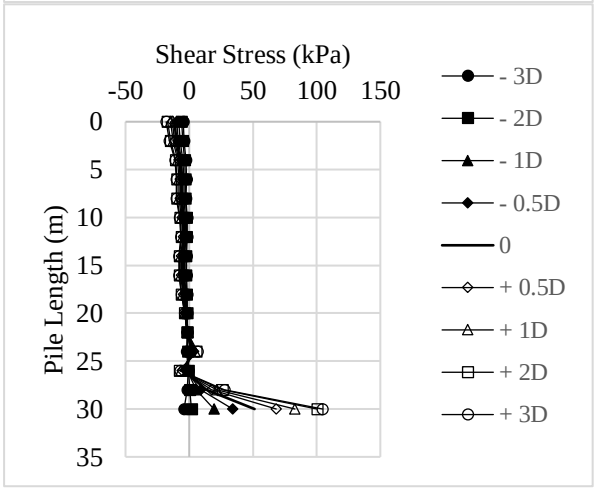

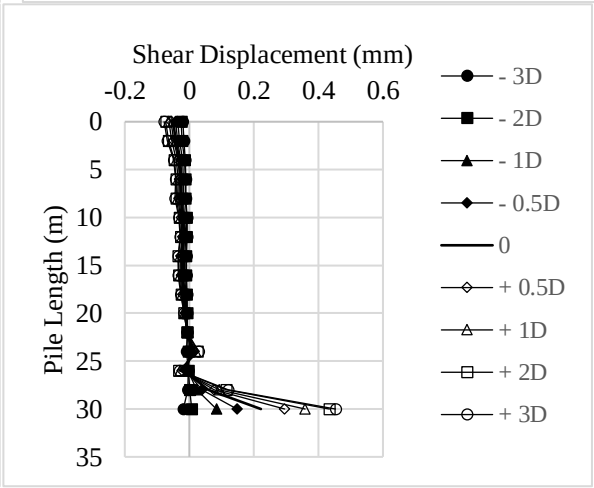

Short pile case 01-5-3

Δv : 3D
Δht : 1D
Cover depth : 42 m

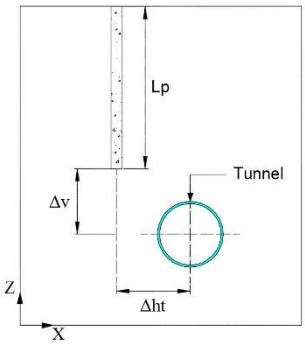

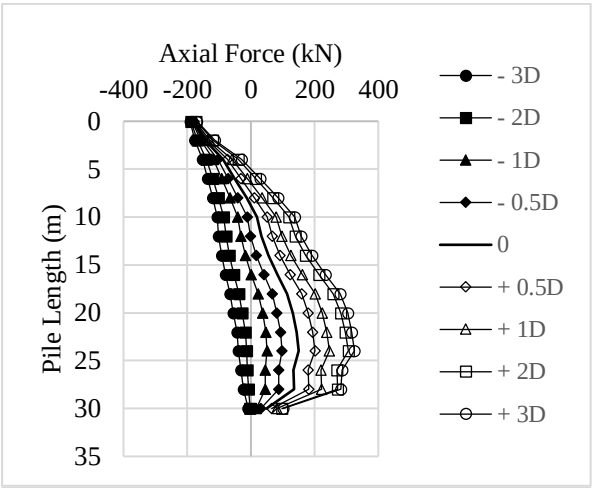

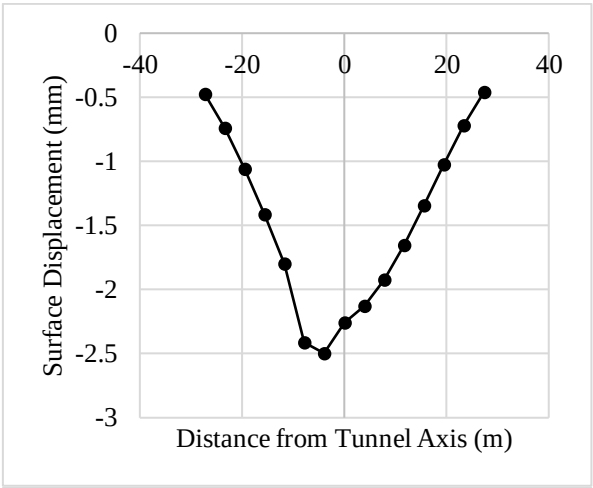

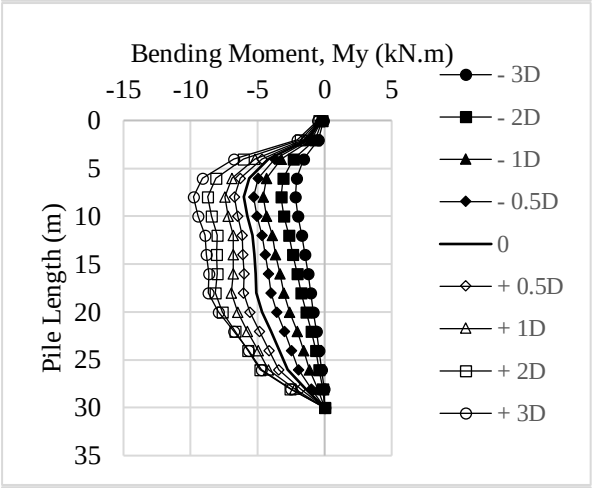

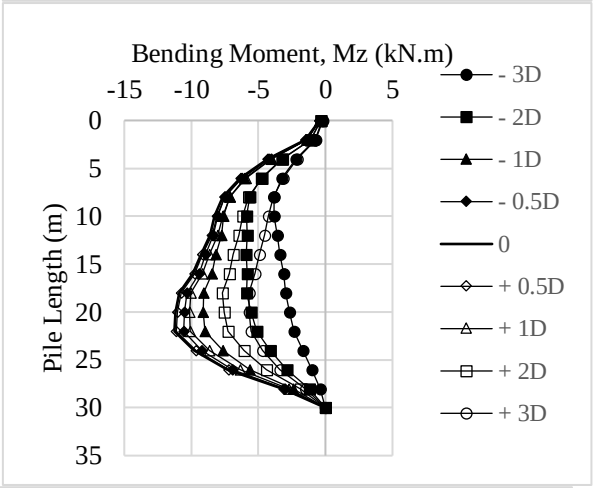

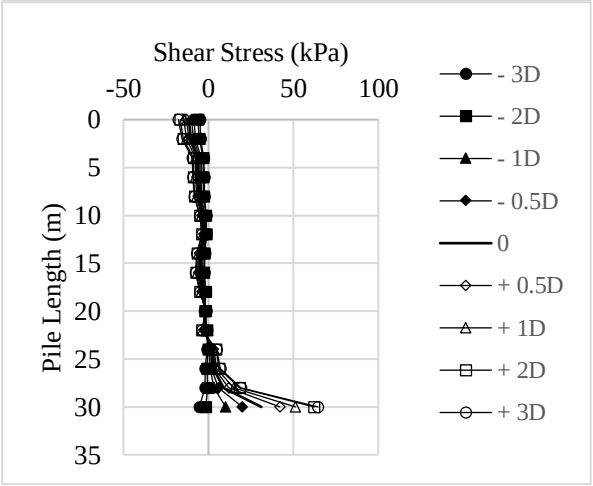

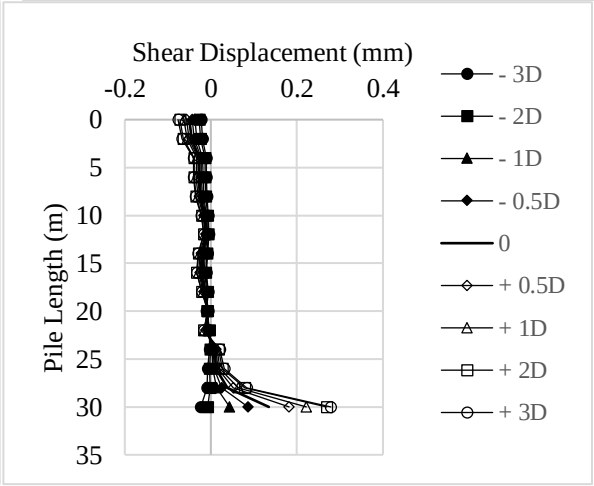

Short pile case 01-5-4

Δv : 3D
Δht : 1.5D
Cover depth : 42 m

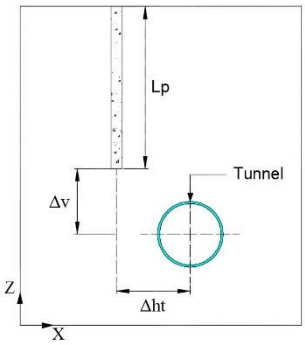

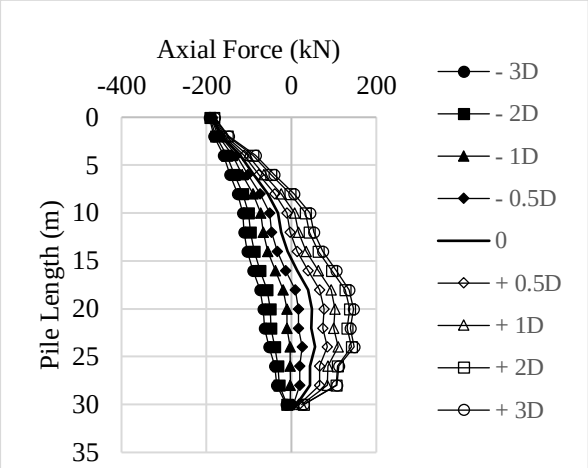

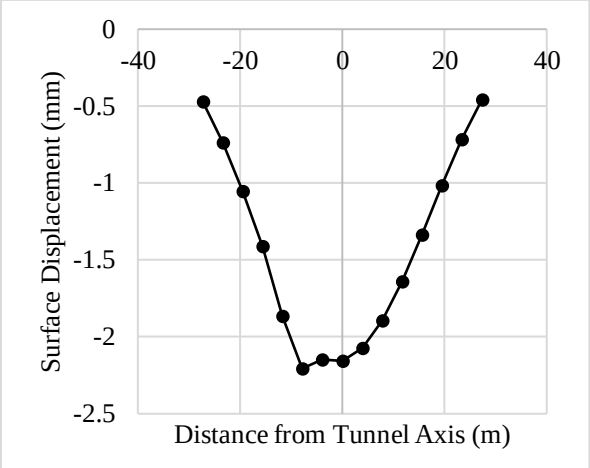

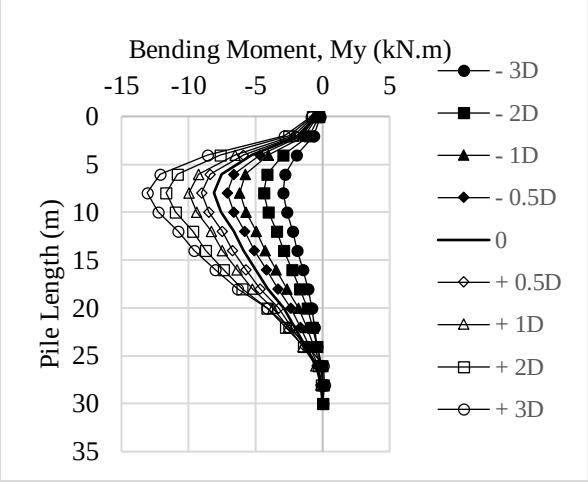

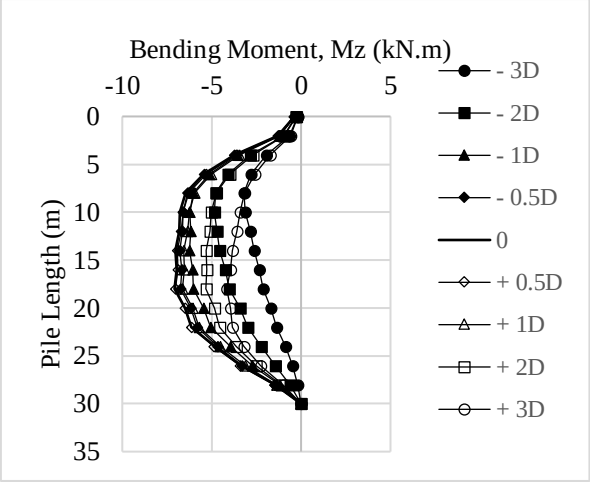

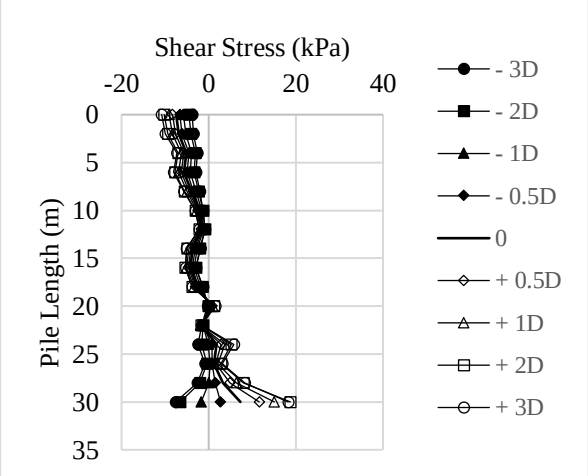

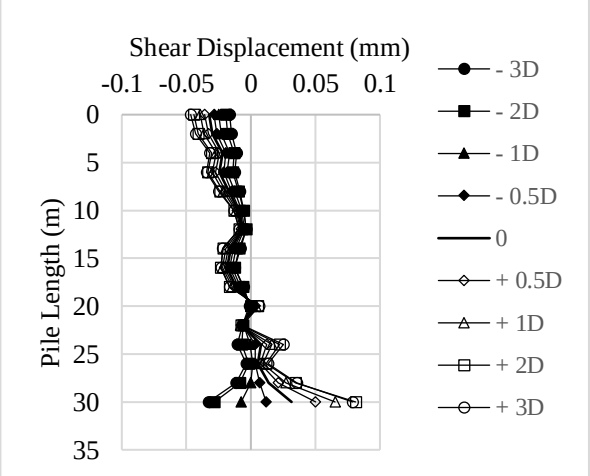

Short pile case 01-5-5

Δv : 3D
Δht : 2D
Cover depth : 42 m

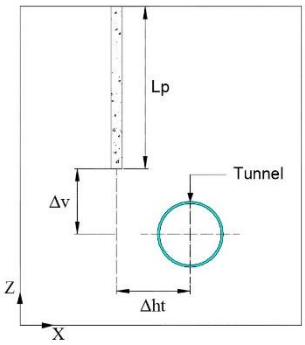

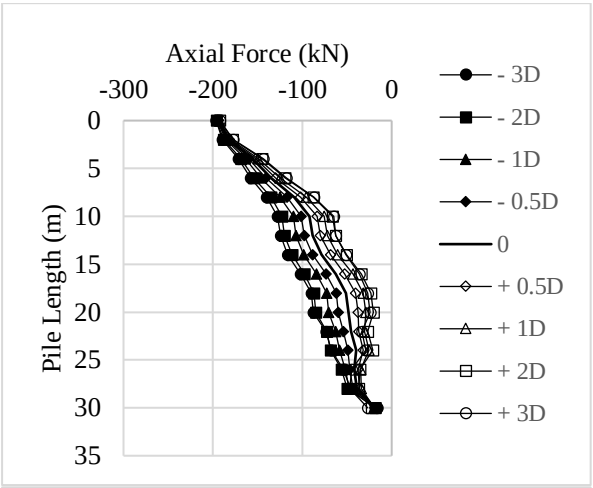

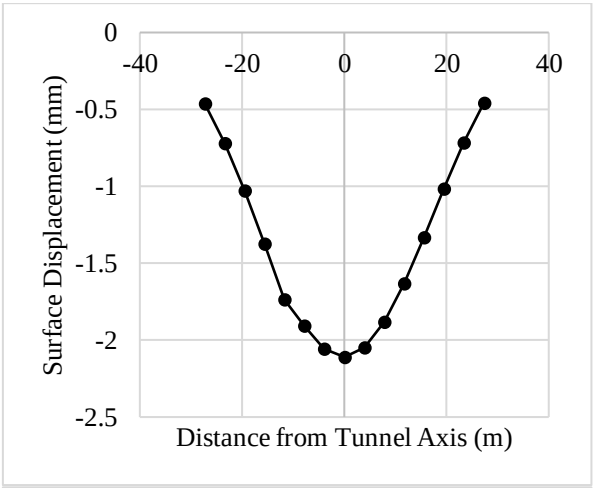

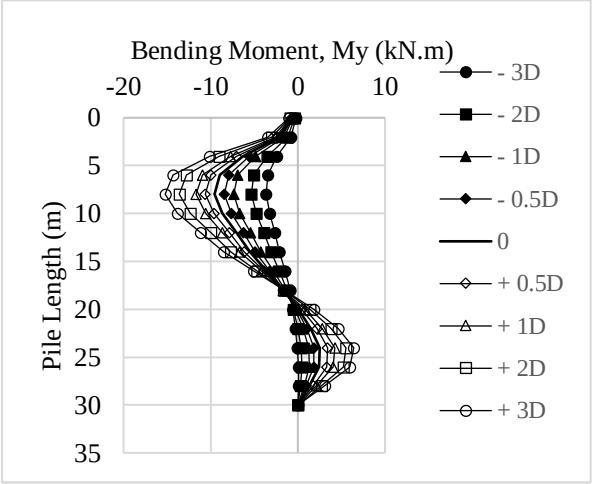

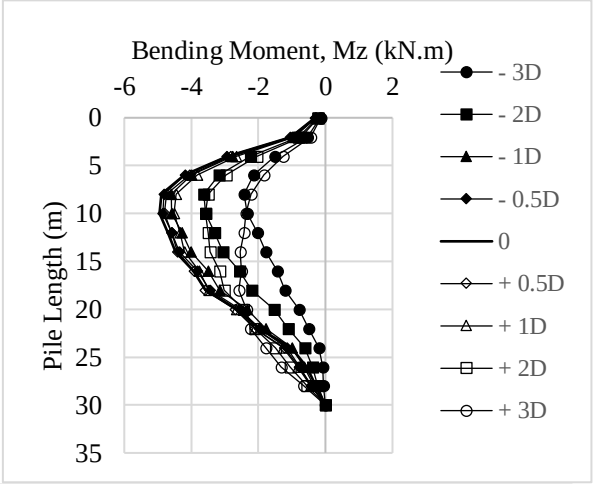

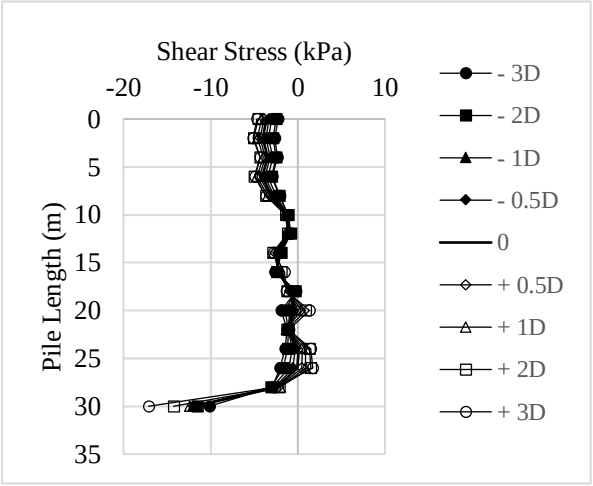

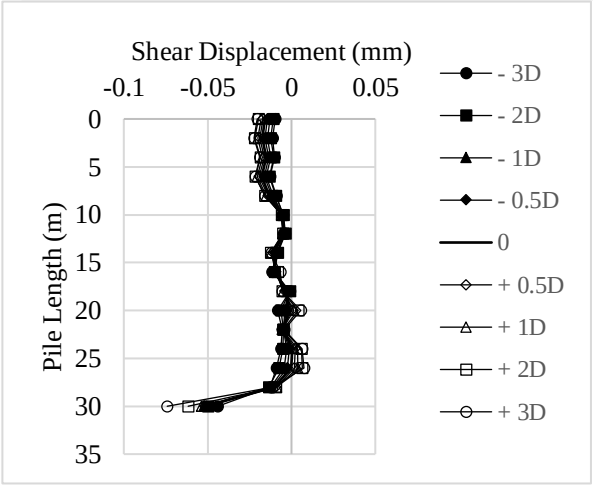

Short pile case 01-5-6

Δv : 3D
Δht : 2.5D
Cover depth : 42 m

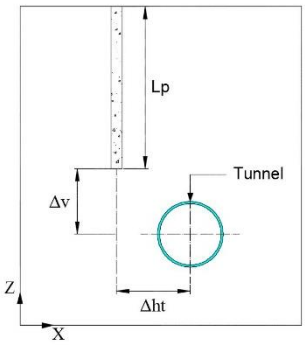

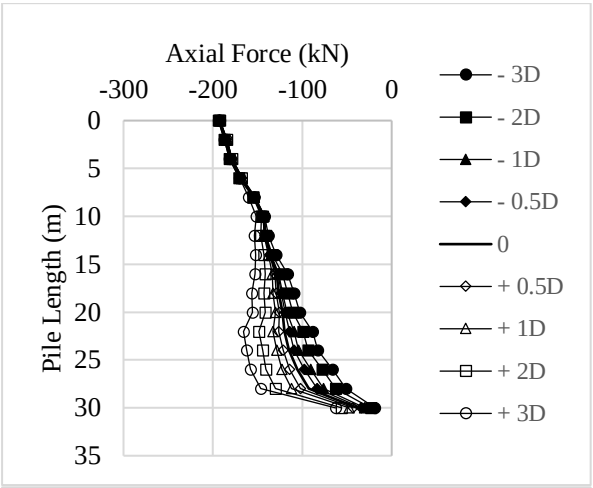

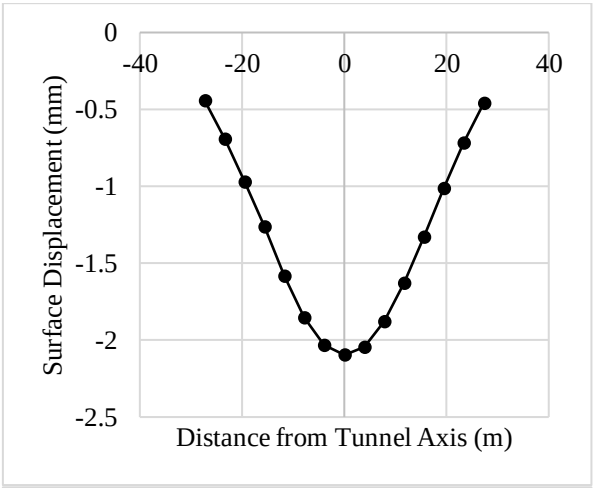

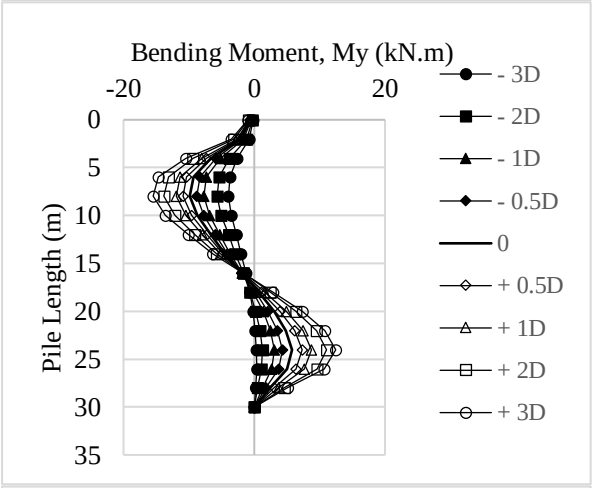

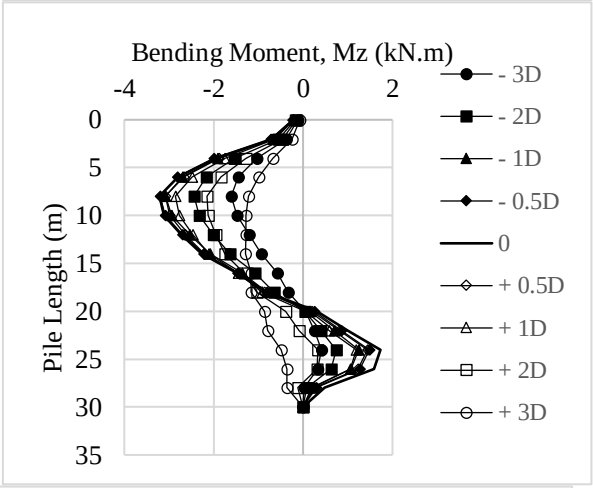

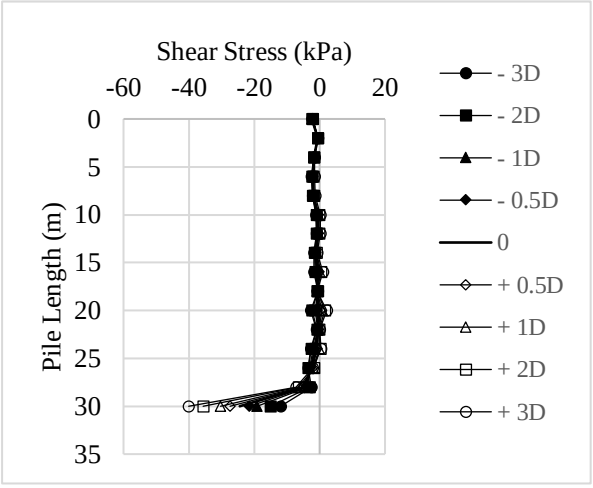

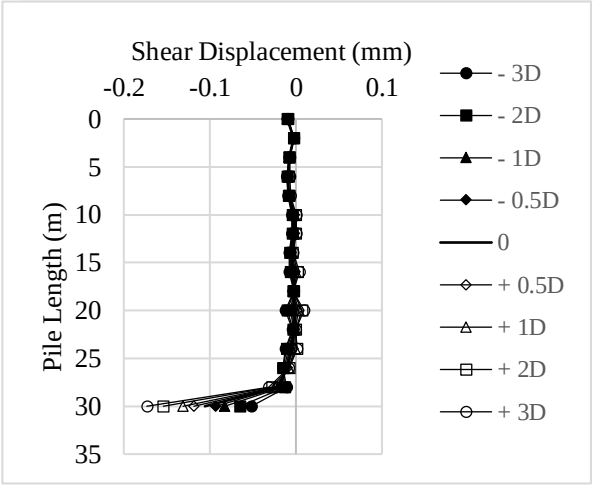

Short pile case 01-6-1

Δv : 3.5D
Δht : 0
Cover depth : 45 m

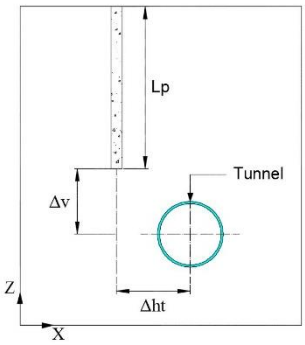

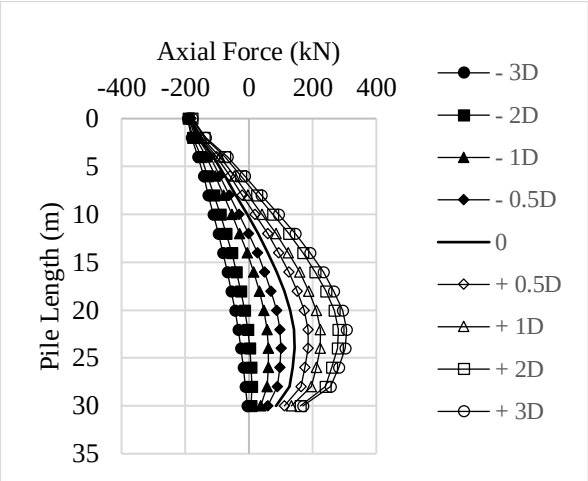

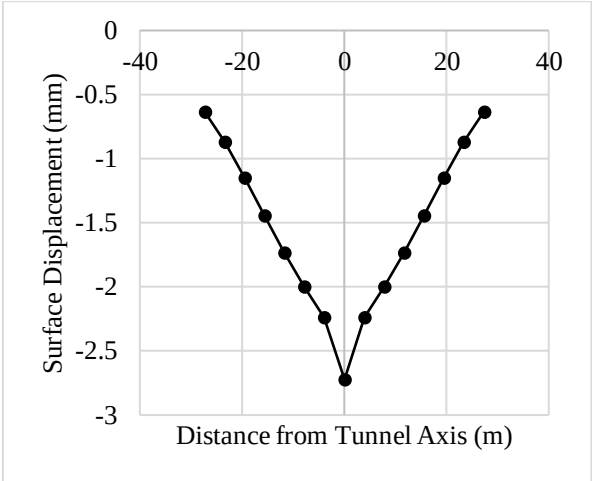

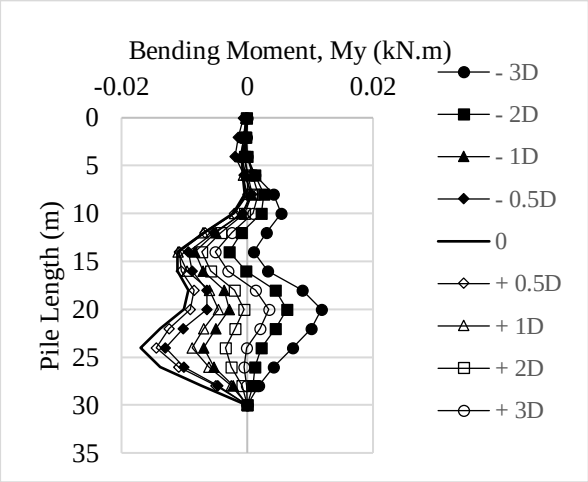

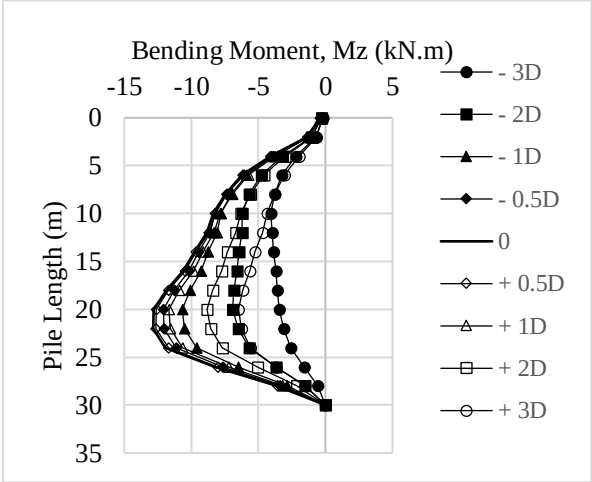

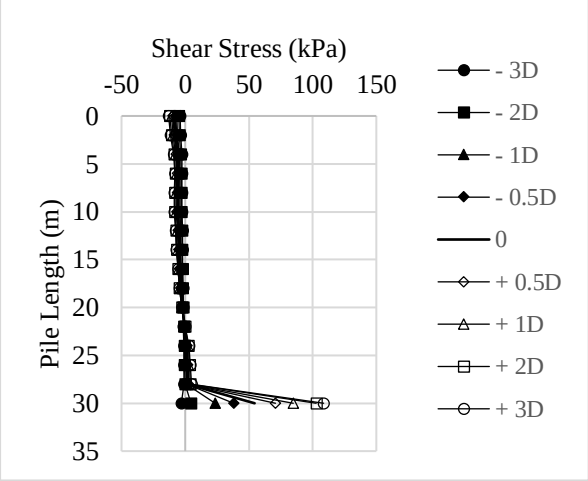

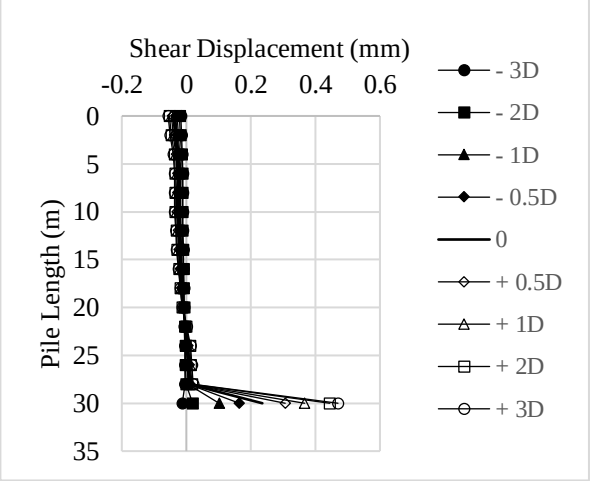

Short pile case 01-6-2

Δv : 3.5D
Δht : 0.5D
Cover depth : 45 m

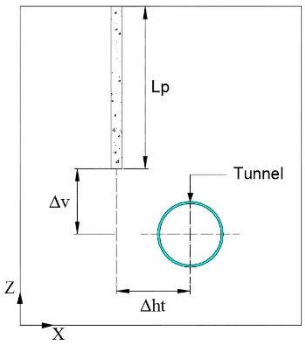

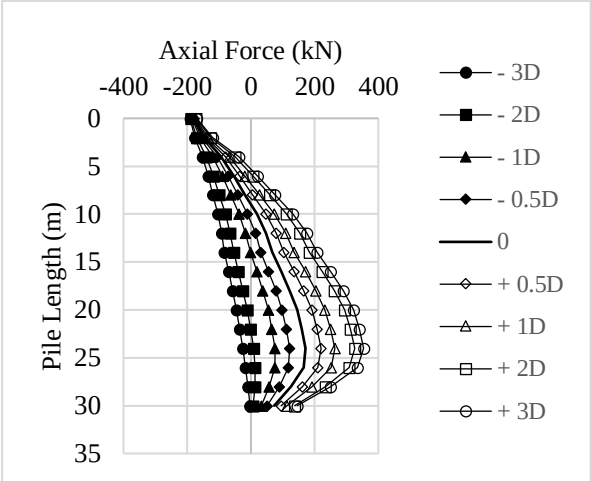

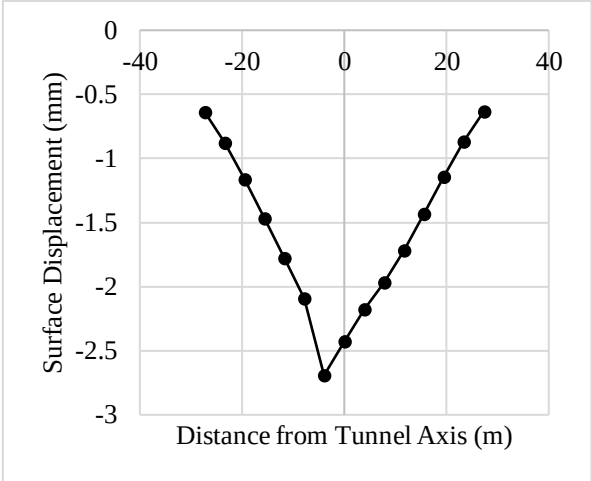

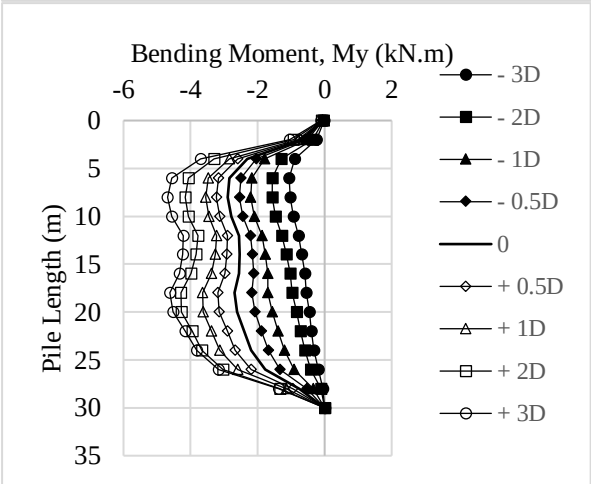

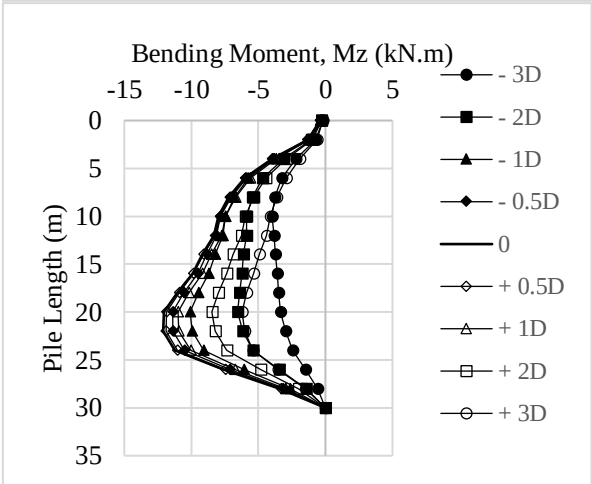

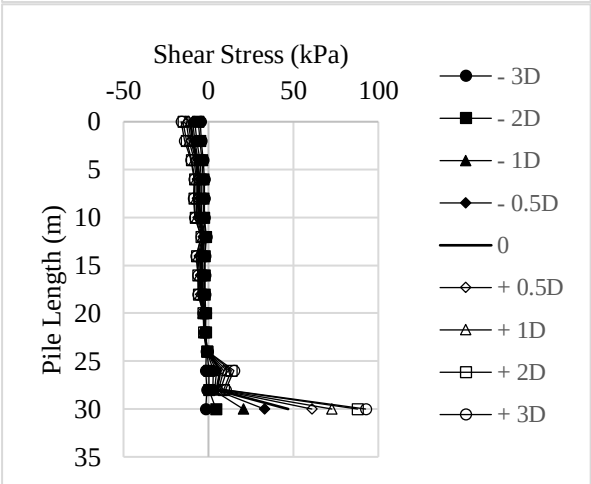

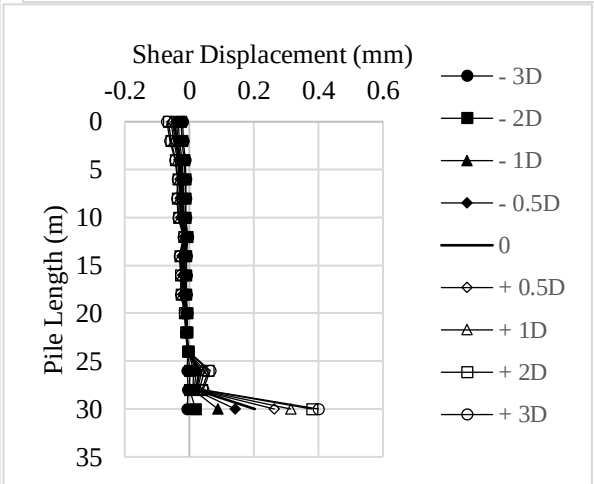

Short pile case 01-6-3

Δv : 3.5D
Δht : 1D
Cover depth : 45 m

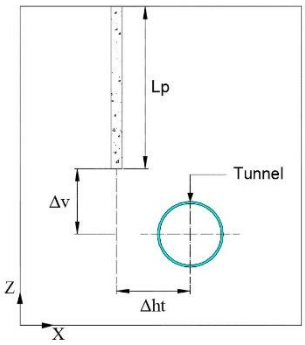

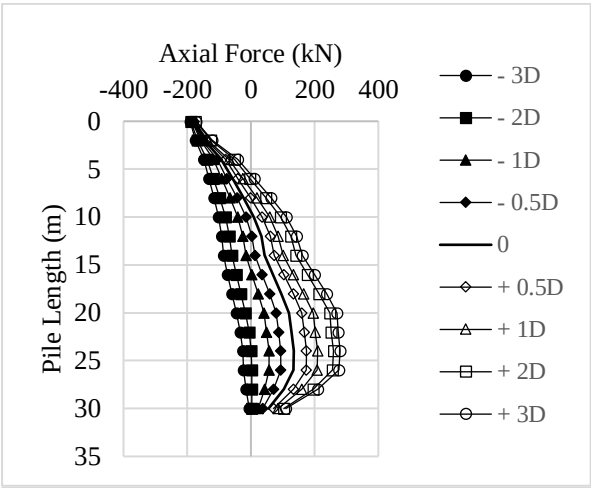

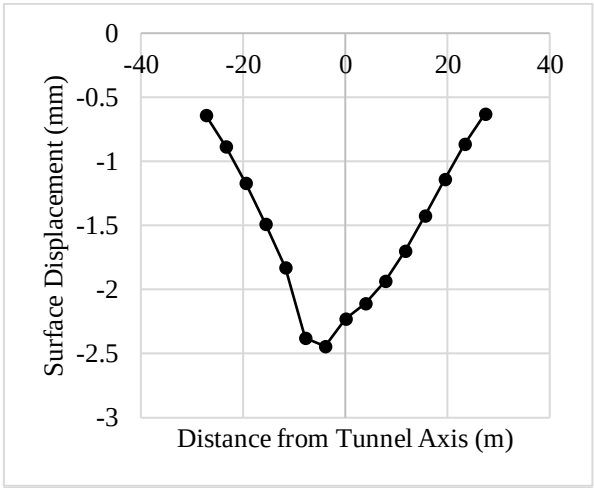

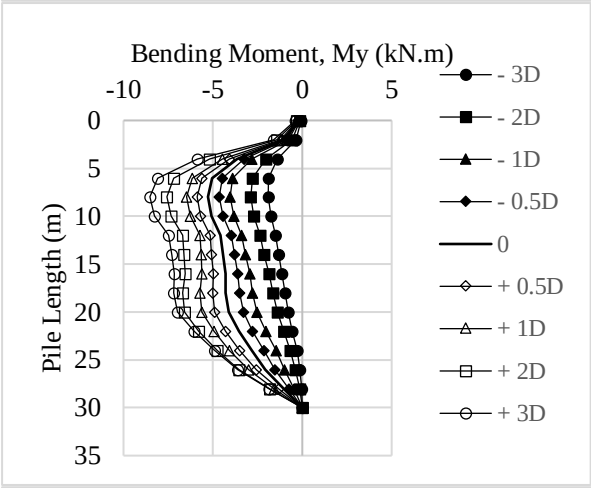

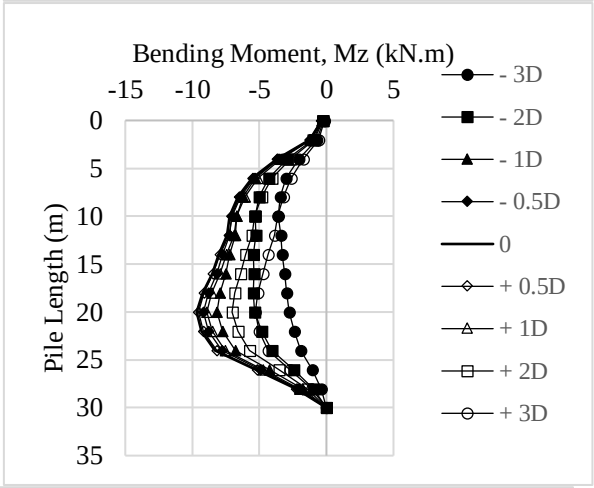

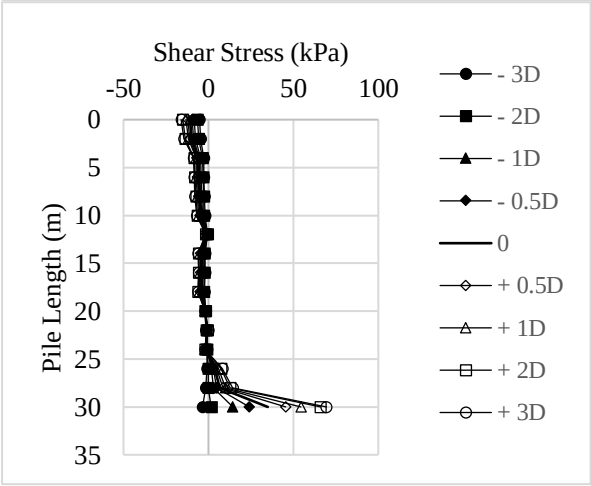

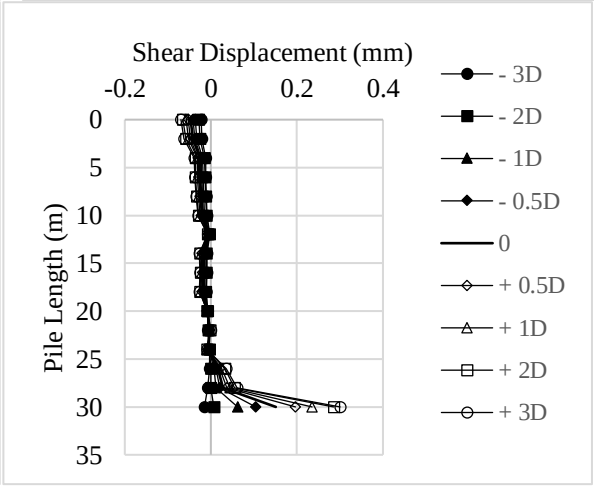

Short pile case 01-6-4

Δv : 3.5D
Δht : 1.5D
Cover depth : 45 m

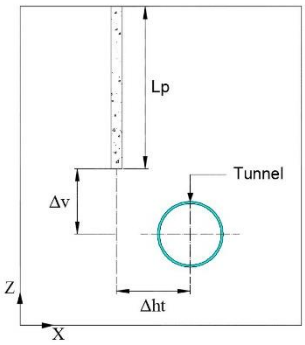

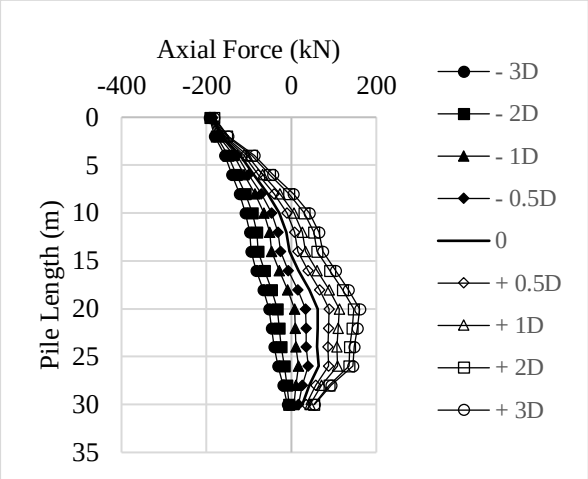

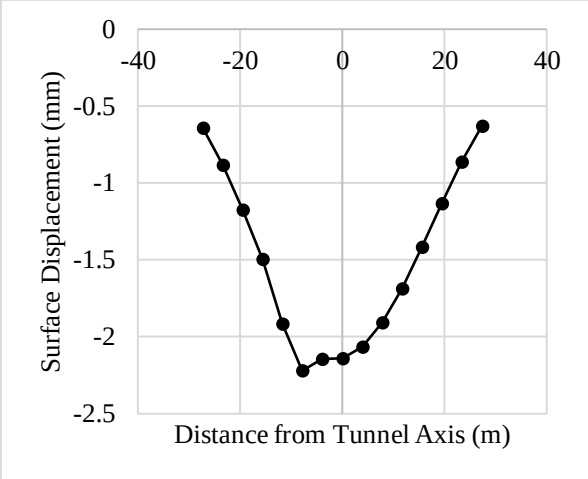

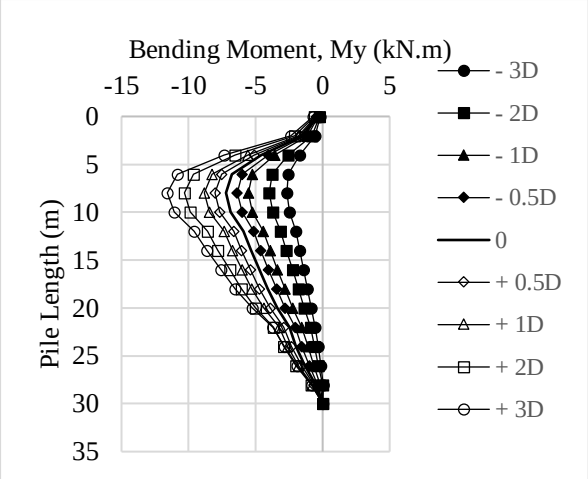

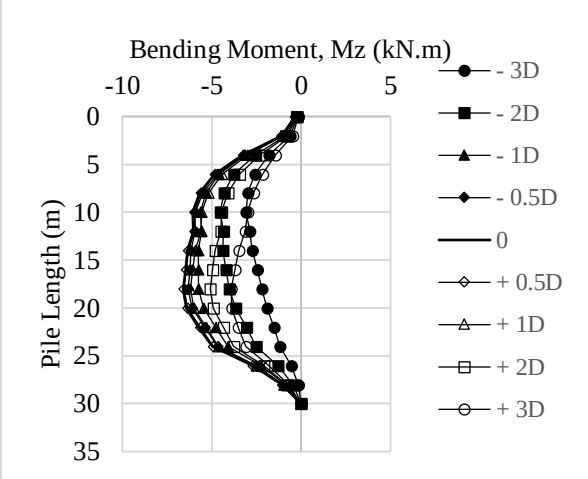

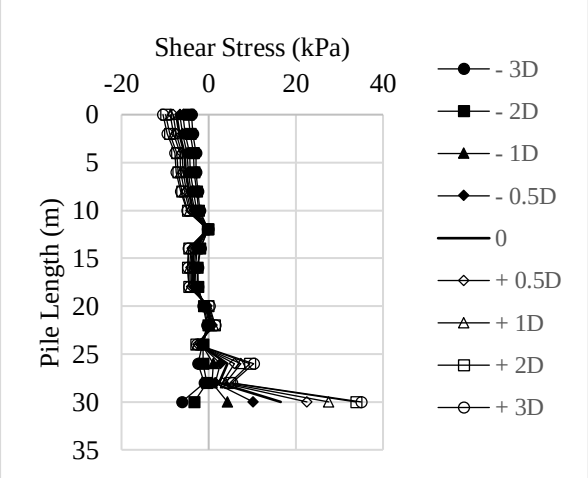

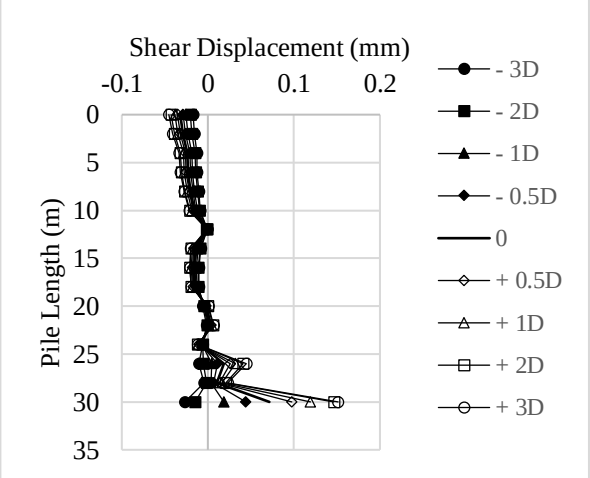

Short pile case 01-6-5

Δv : 3.5D
Δht : 2D
Cover depth : 45 m

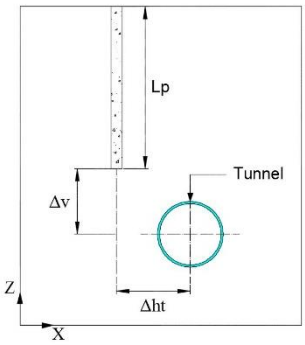

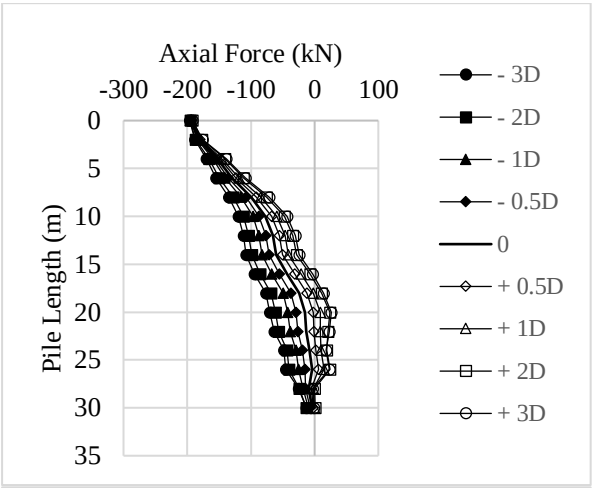

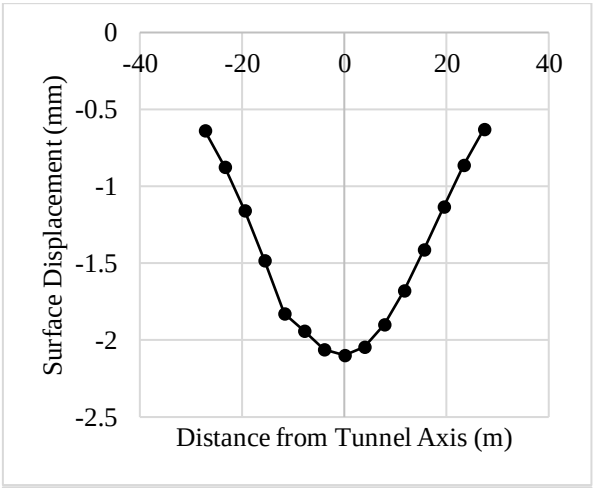

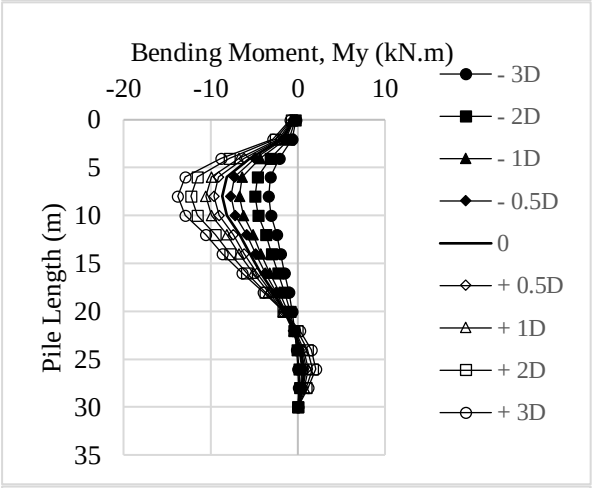

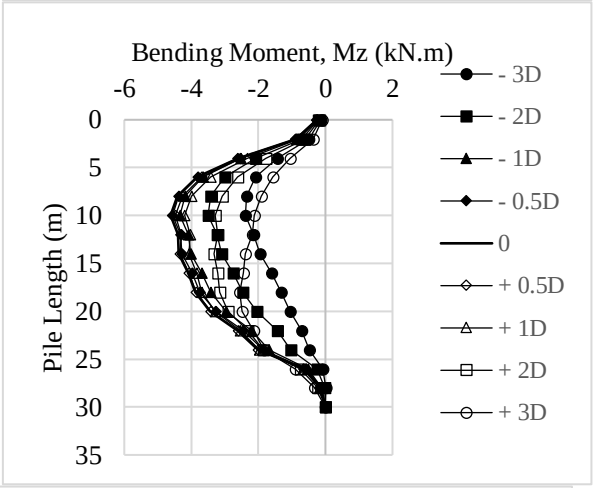

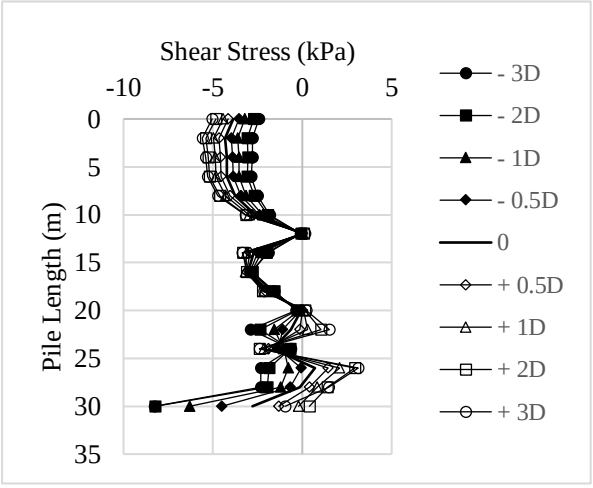

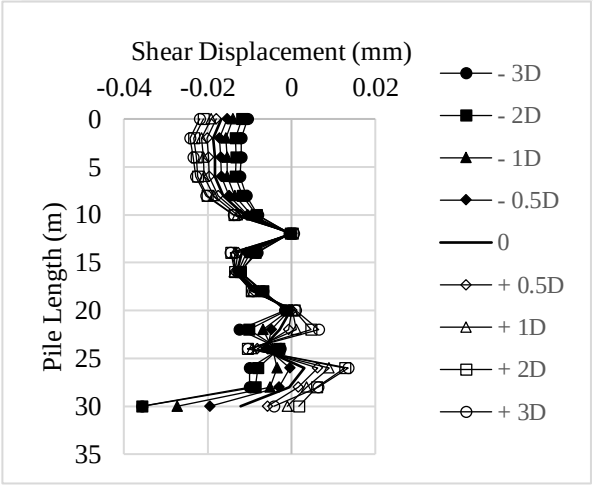

Short pile case 01-6-6

Δv	:	3.5D
Δht	:	2.5D
Cover depth	:	45 m

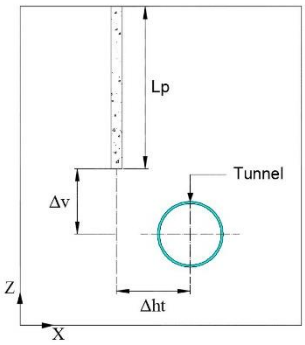

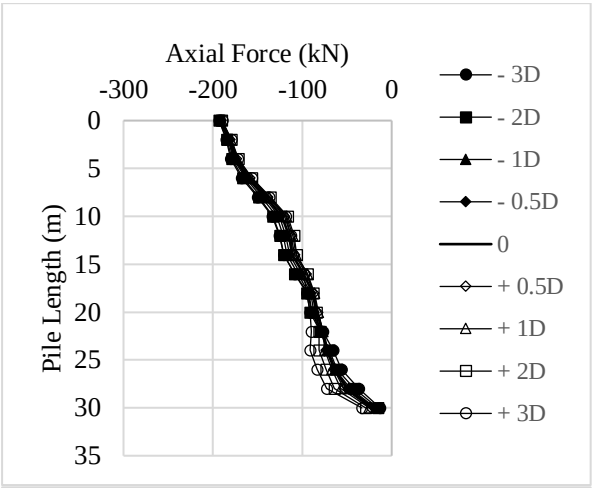

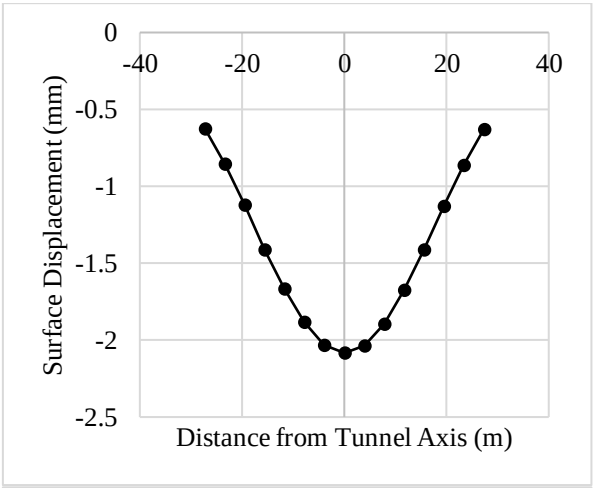

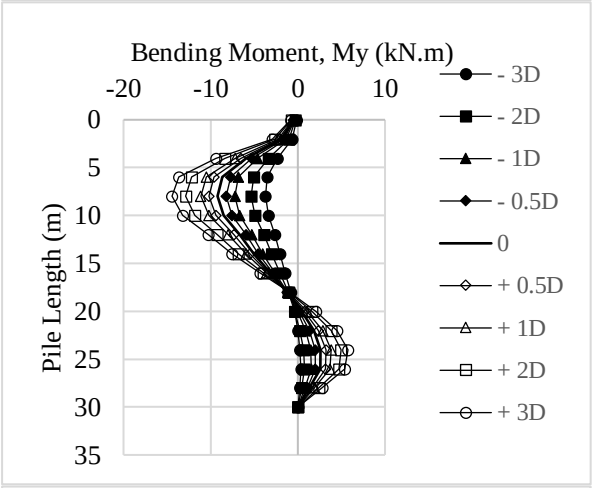

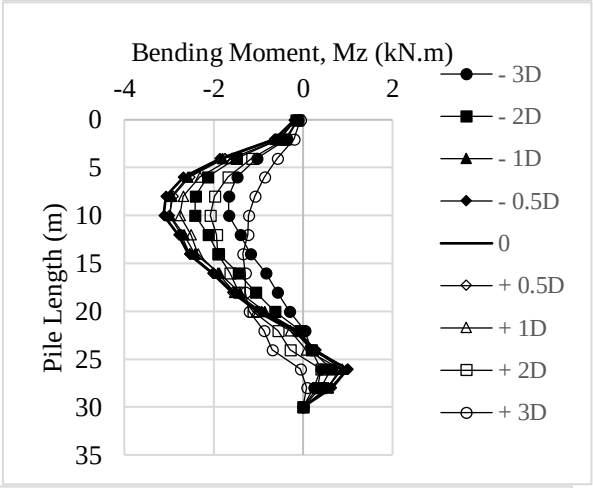

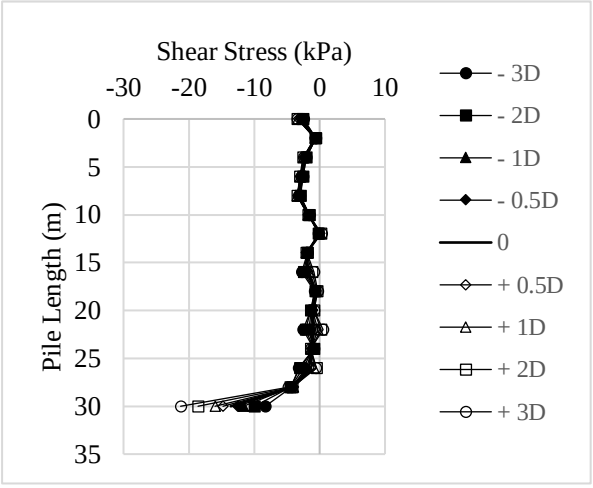

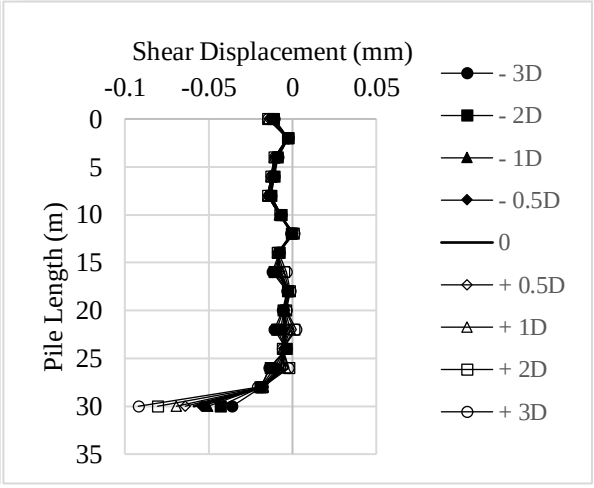

Long pile case 02-1-1

Δv : 0
Δht : 1D
Cover depth : 27 m

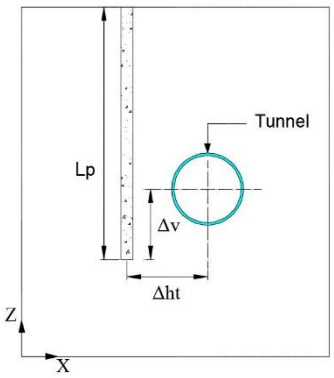

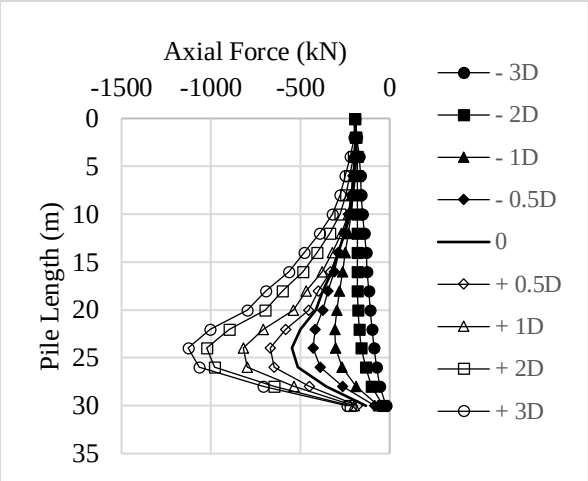

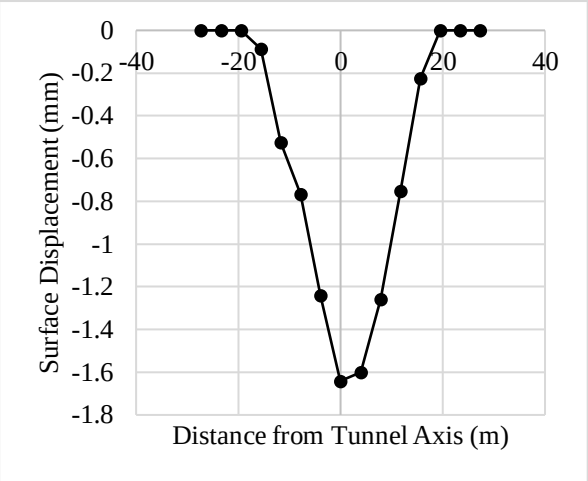

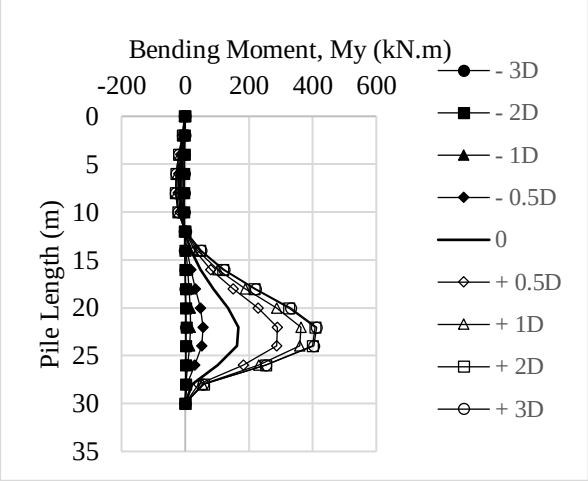

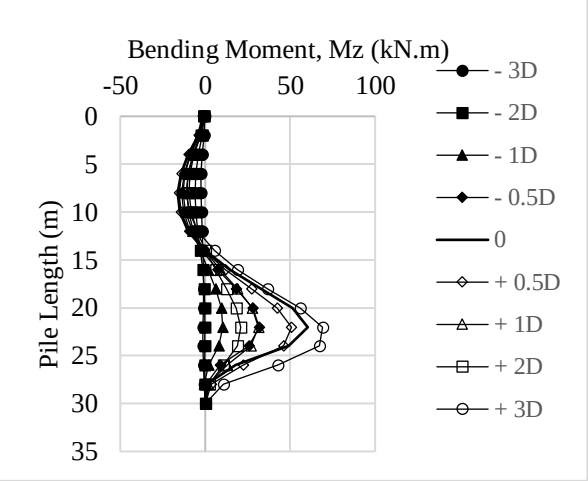

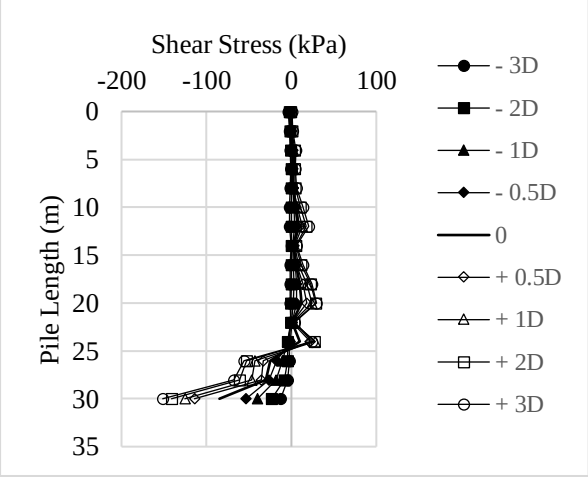

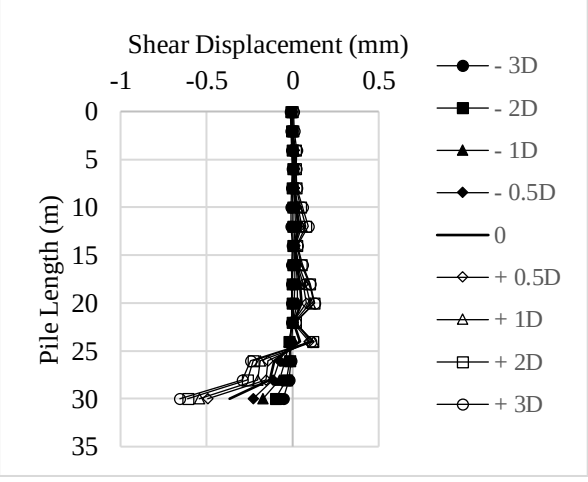

Long pile case 02-1-2

Δv : 0
Δht : 1.5D
Cover depth : 27 m

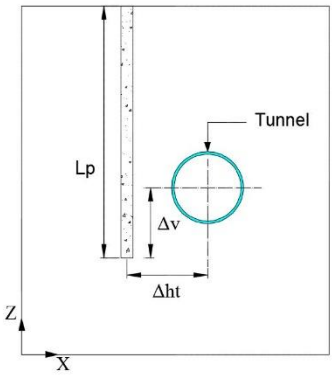

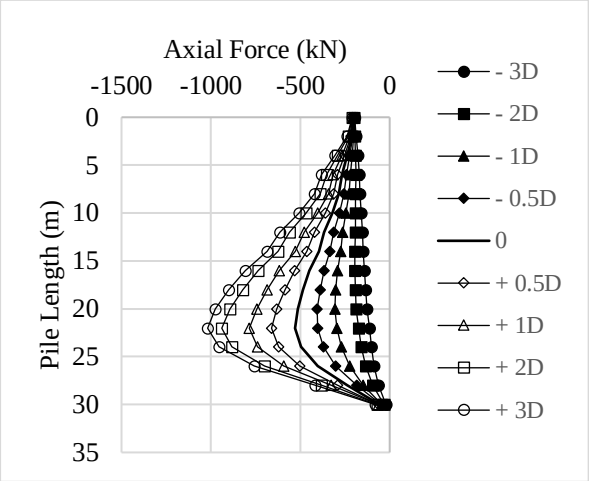

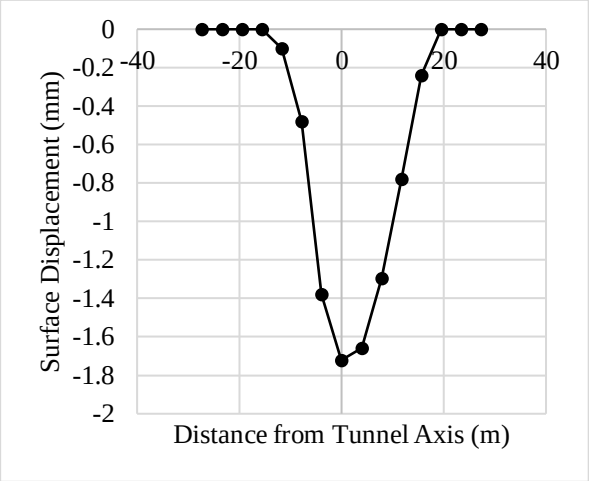

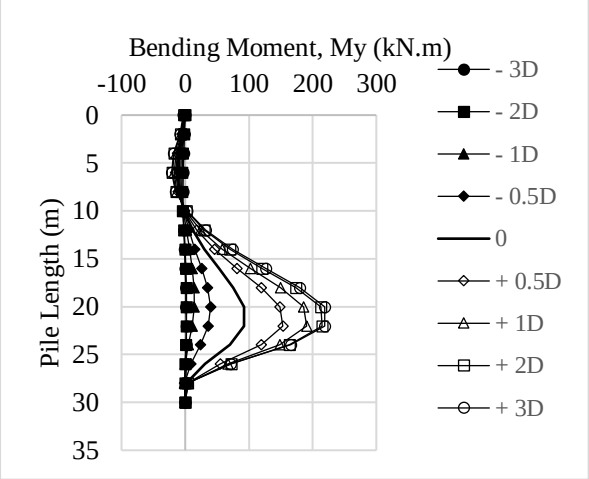

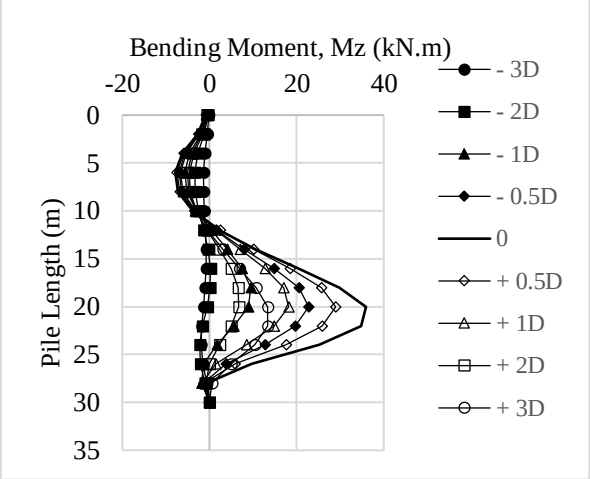

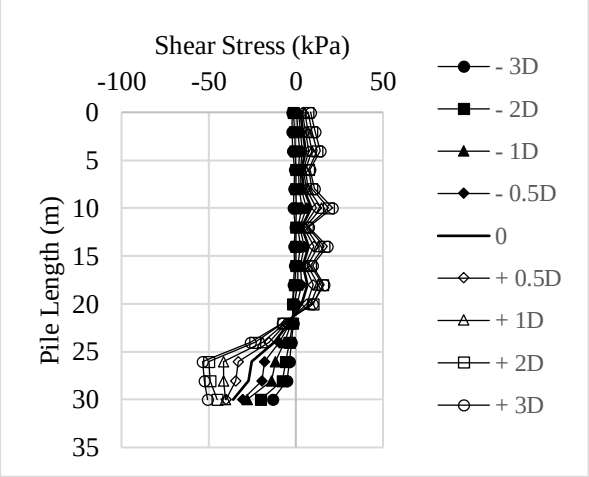

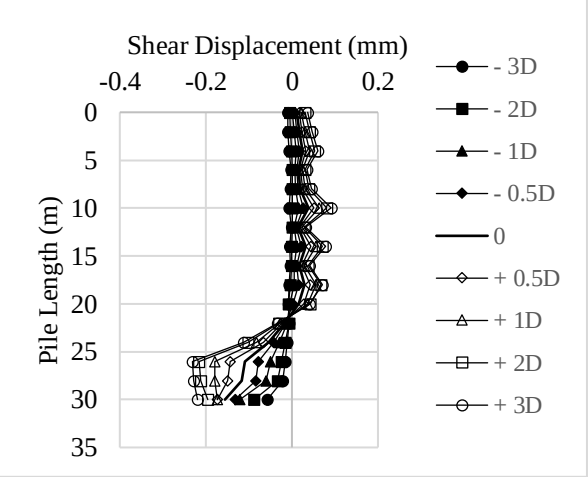

Long pile case 02-1-3

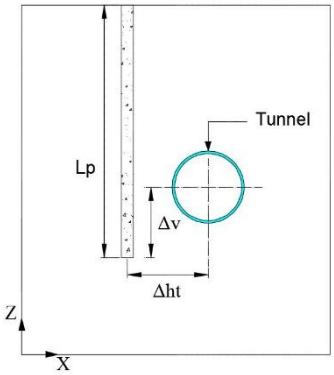

Δv : 0
Δht : 2D
Cover depth : 27 m

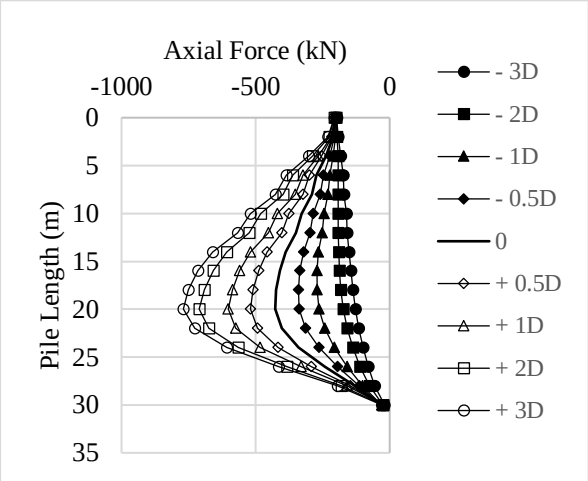

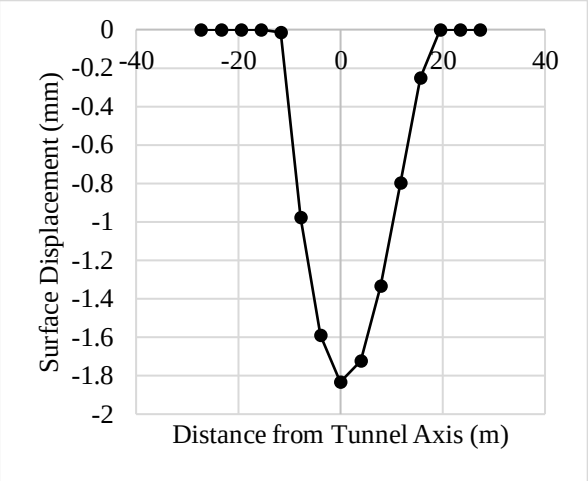

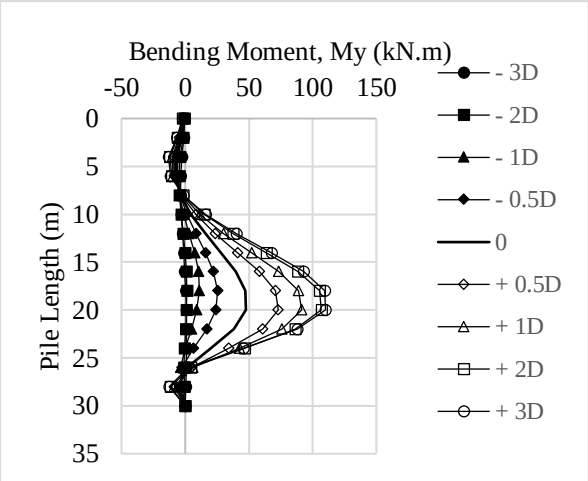

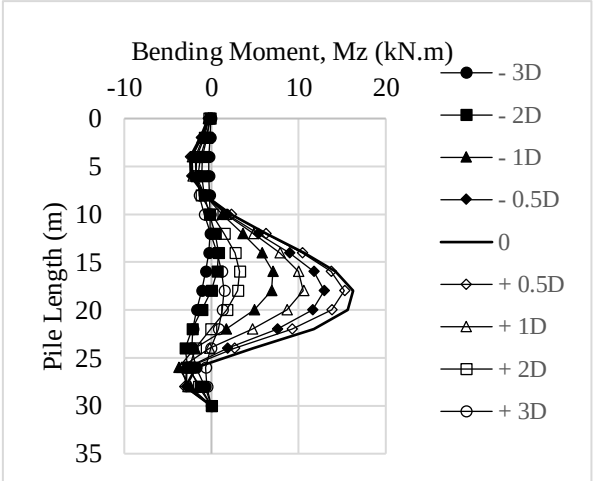

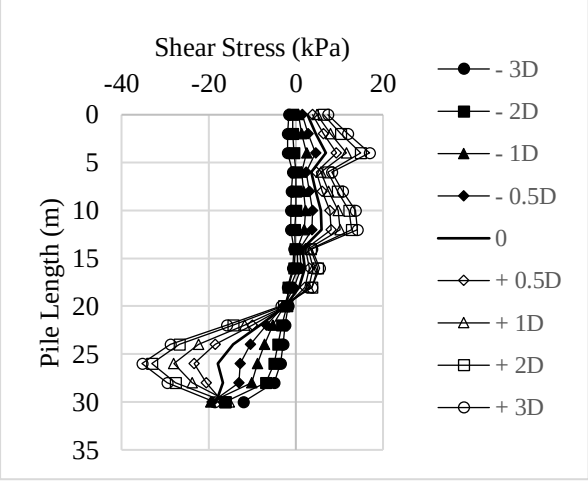

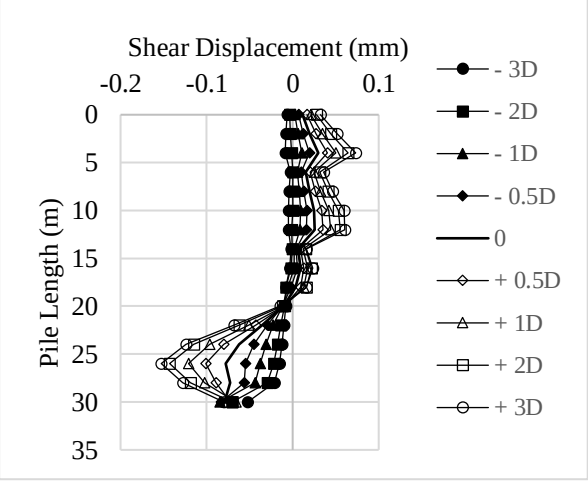

Long pile case 02-1-4

Δv	:	0
Δht	:	2.5D
Cover depth	:	27 m

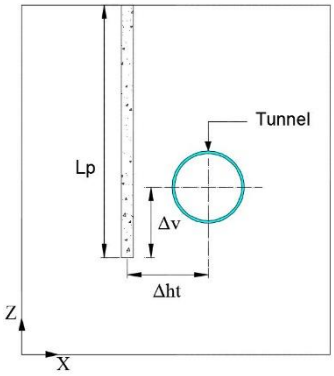

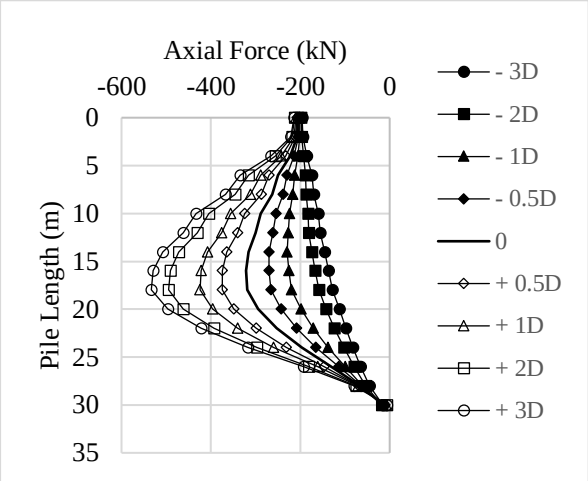

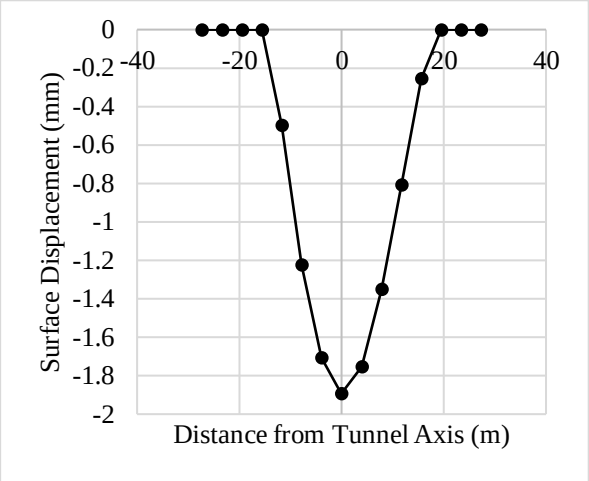

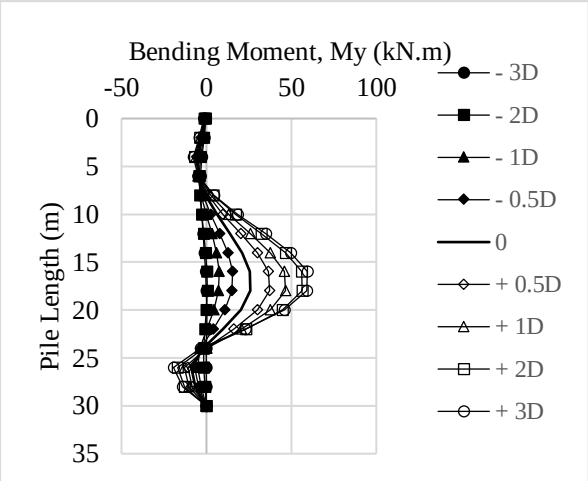

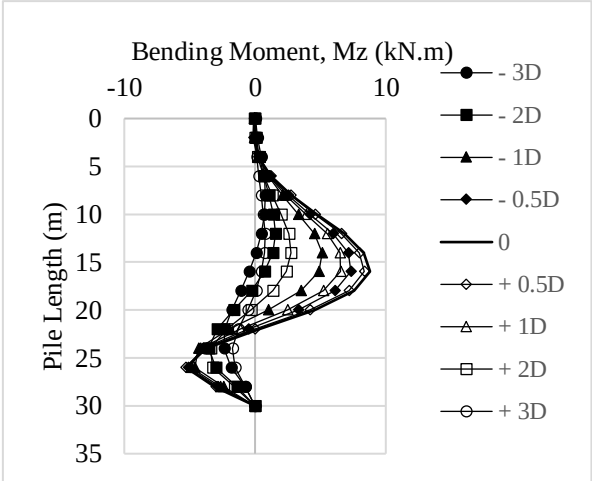

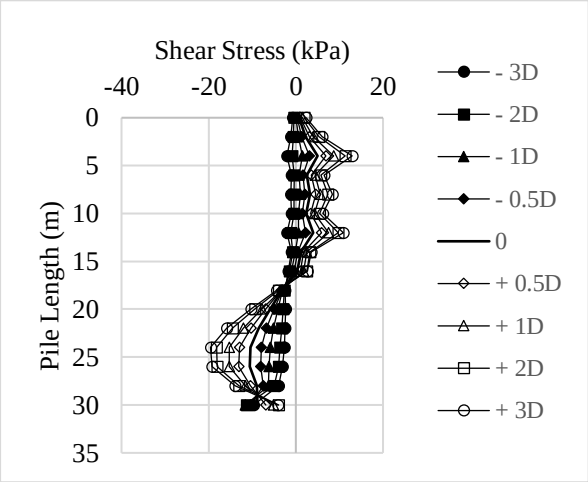

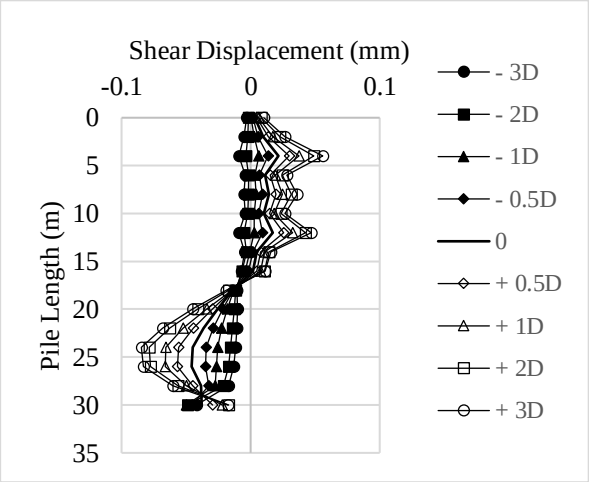

Long pile case 02-1-5

Δv : 0
Δht : 3D
Cover depth : 27 m

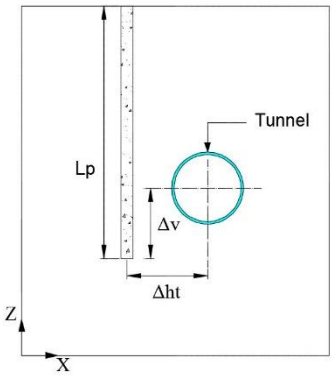

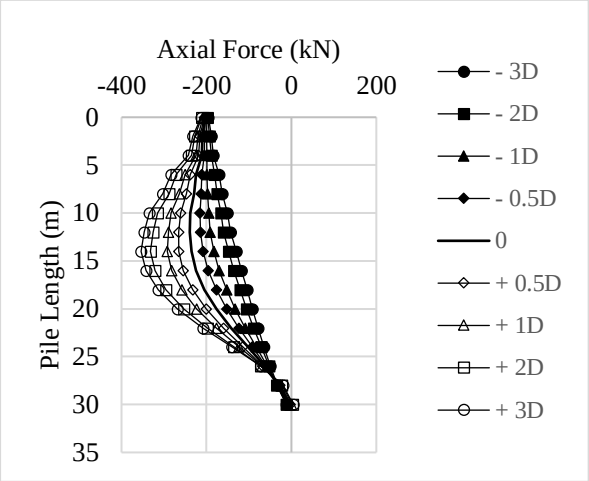

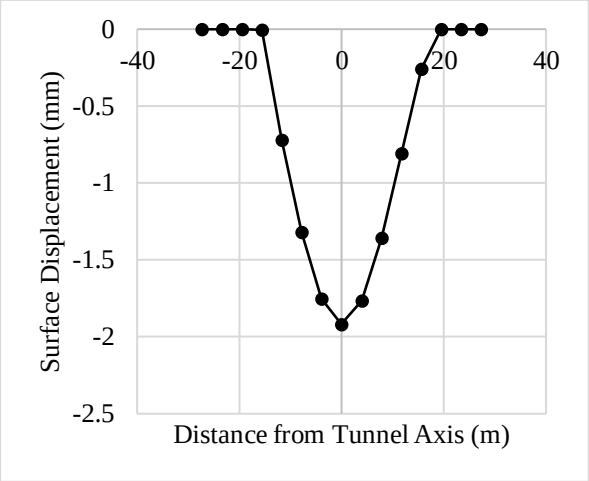

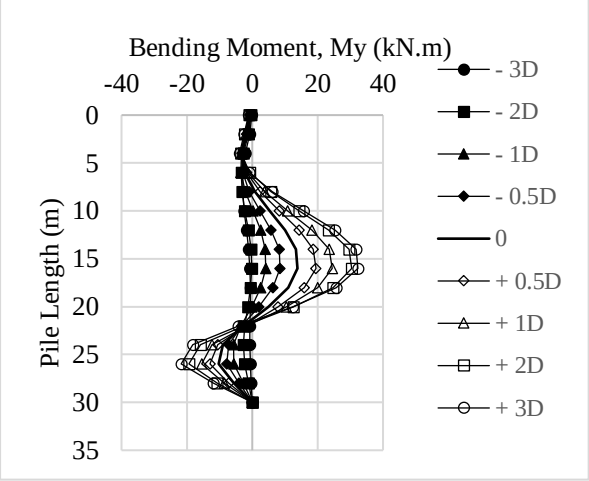

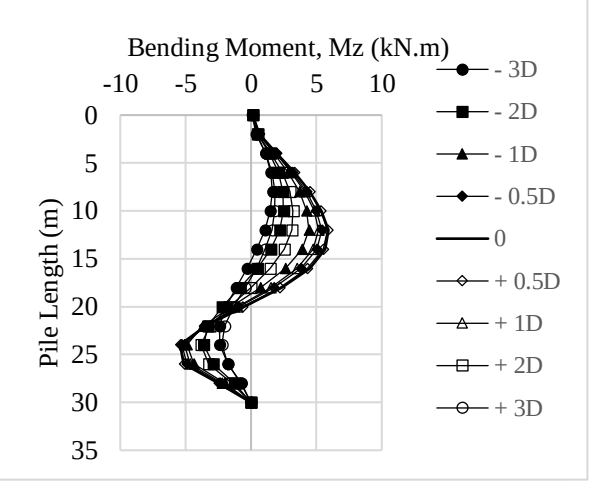

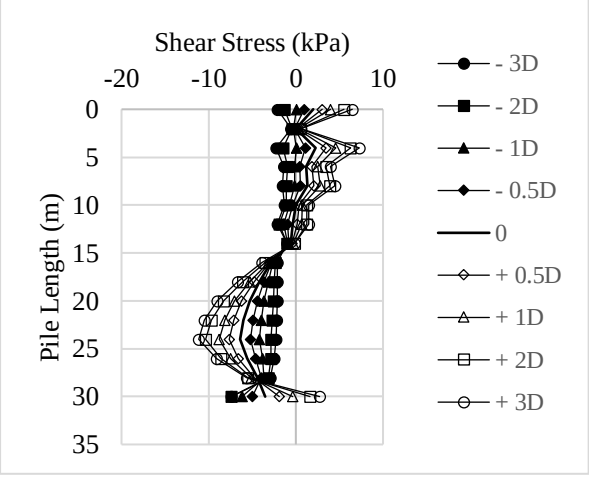

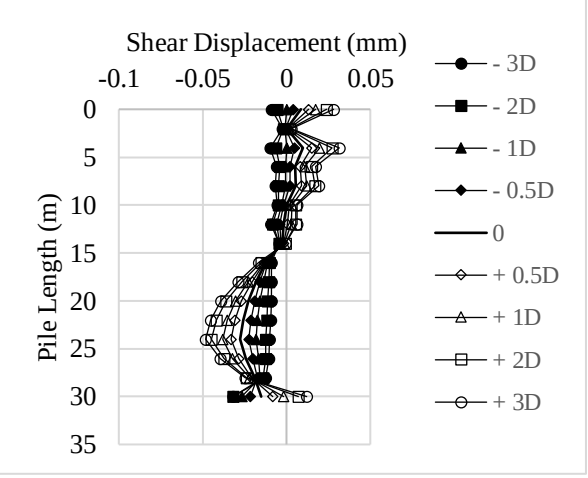

Long pile case 02-1-6

Δv	:	0
Δht	:	3.5D
Cover depth	:	27 m

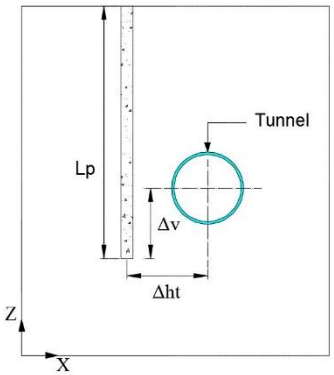

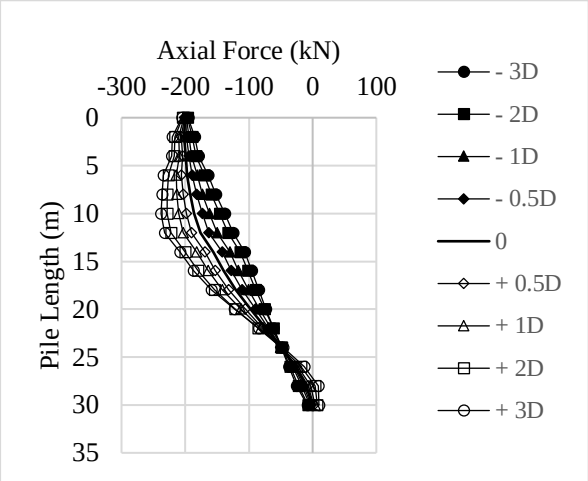

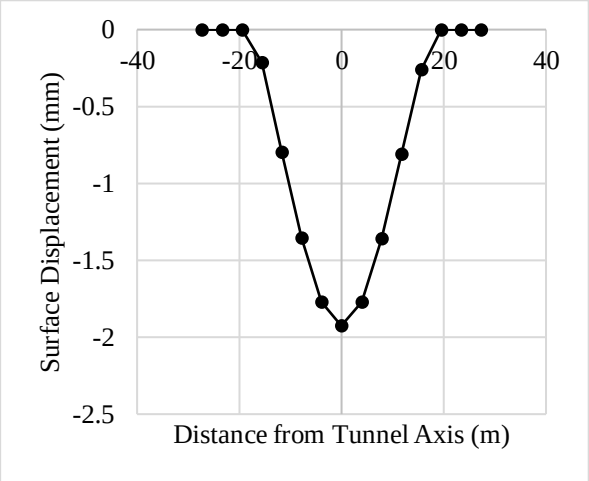

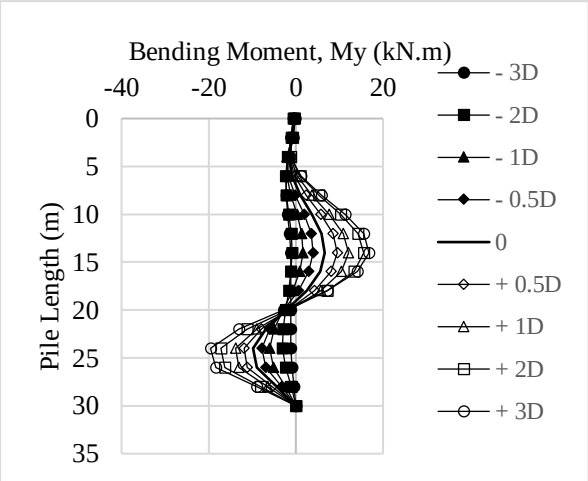

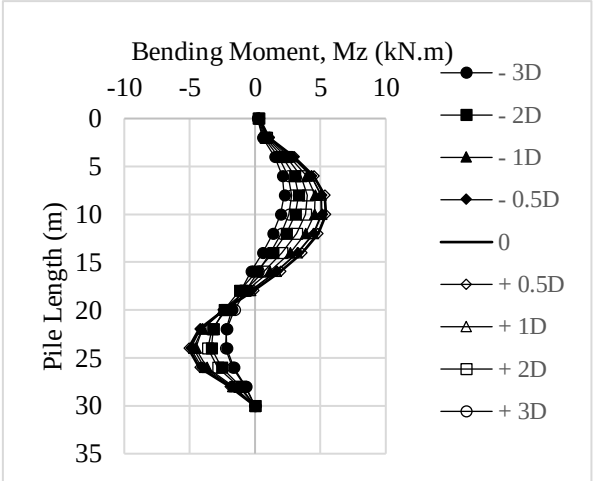

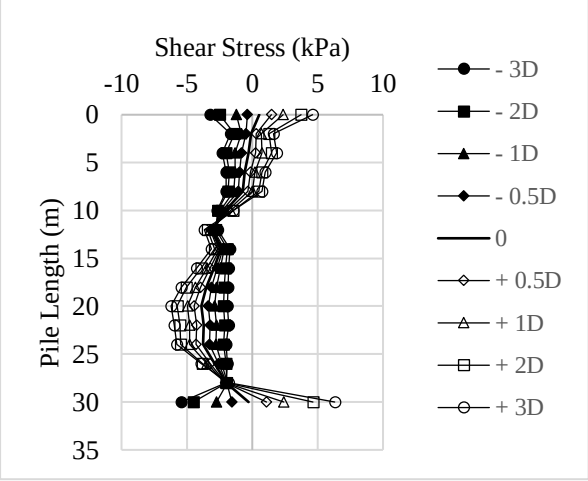

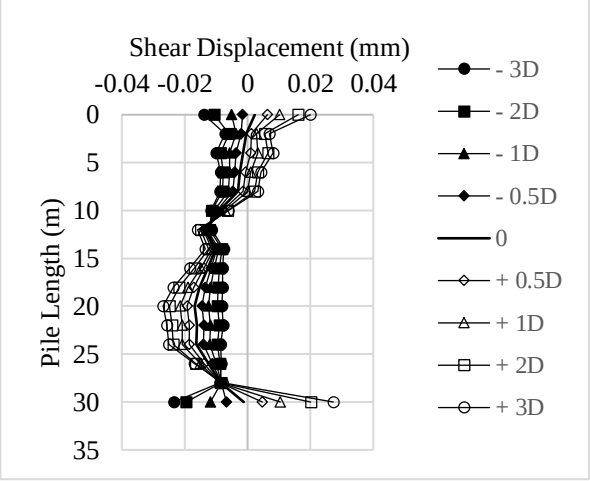

Long pile case 02-2-1

Δv	:	0.5D
Δht	:	1D
Cover depth	:	24 m

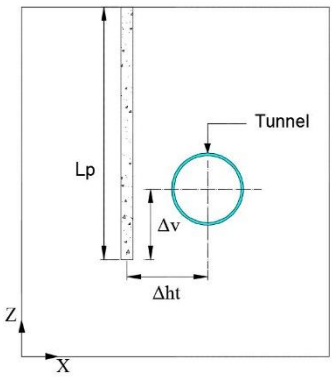

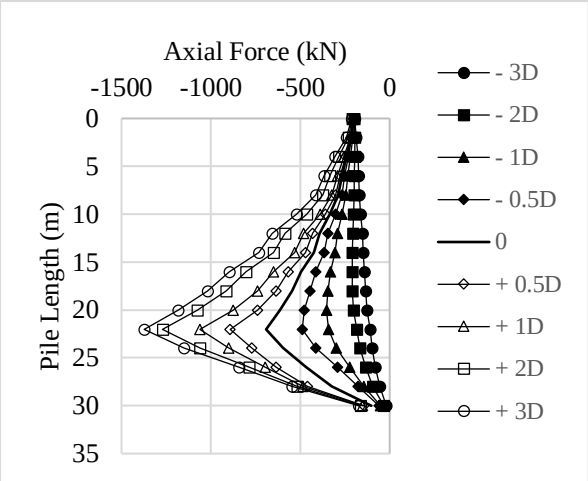

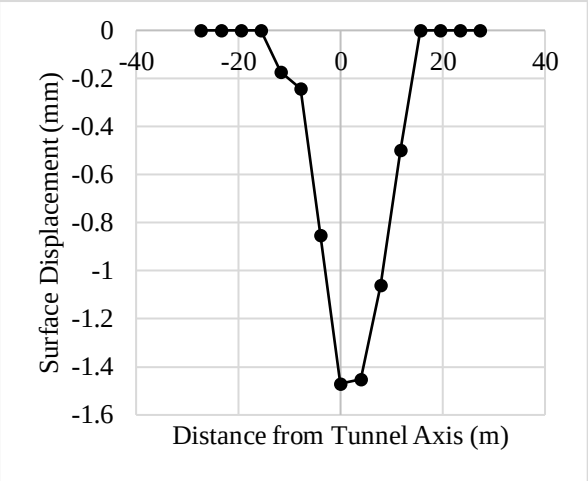

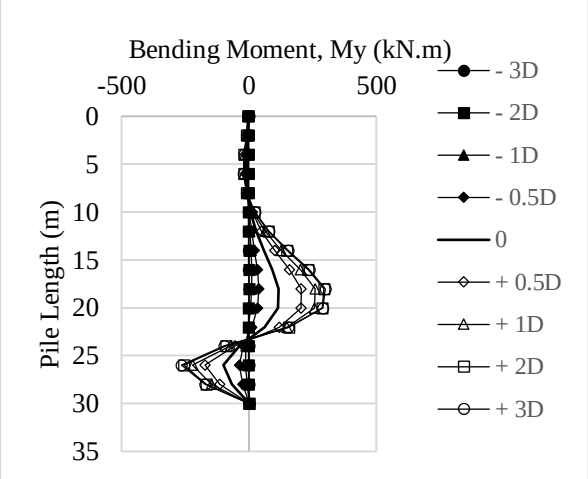

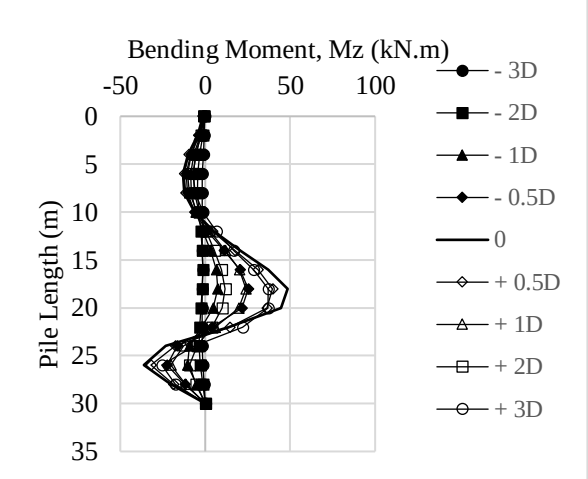

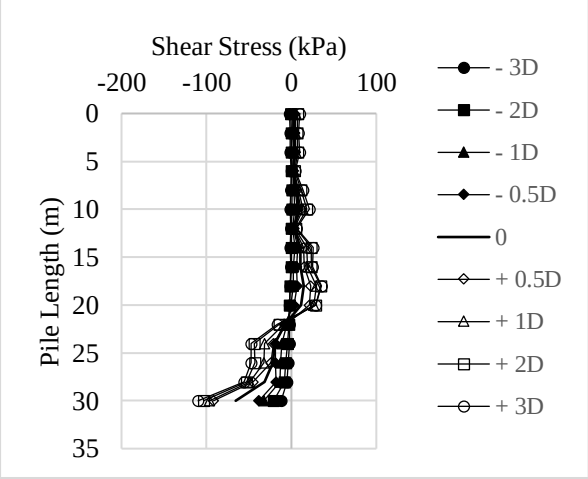

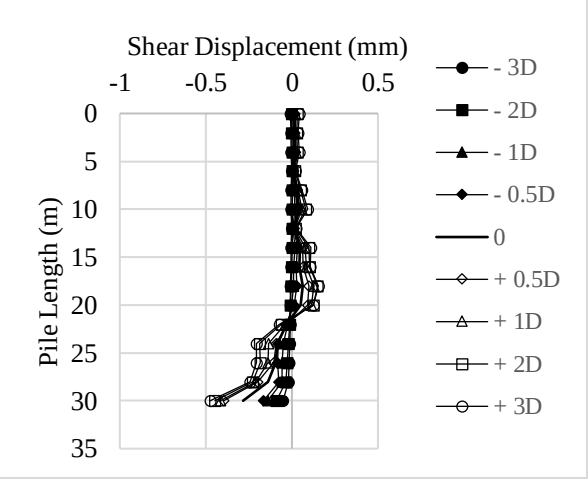

Long pile case 02-2-2

Δv	:	0.5D
Δht	:	1.5D
Cover depth	:	24 m

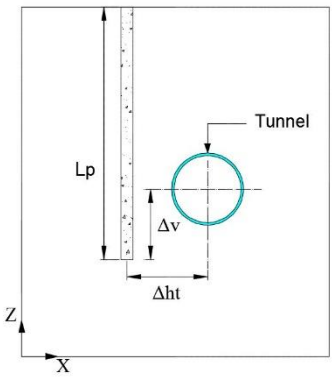

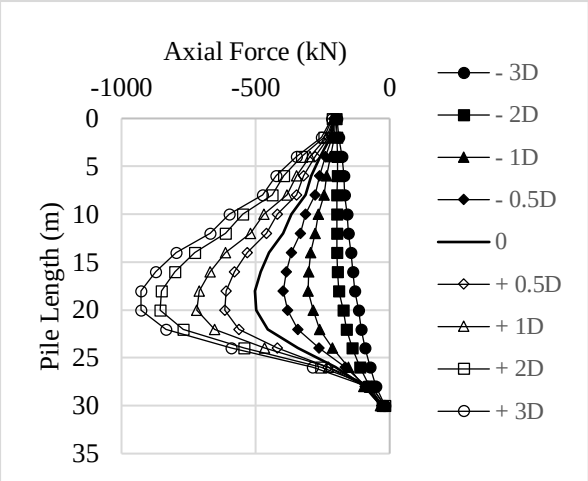

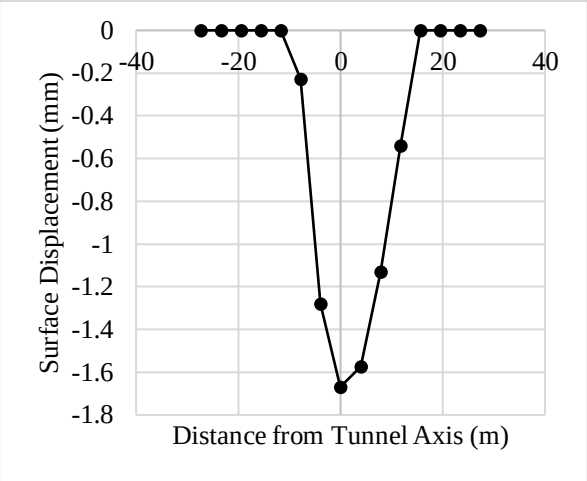

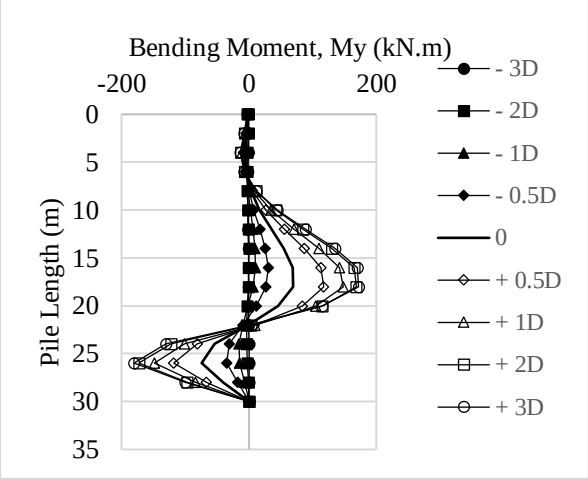

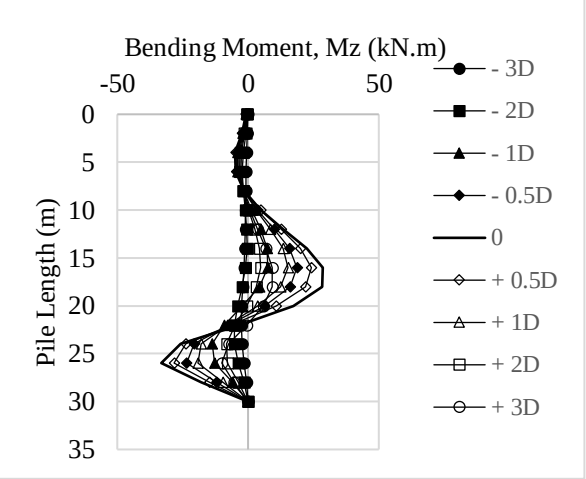

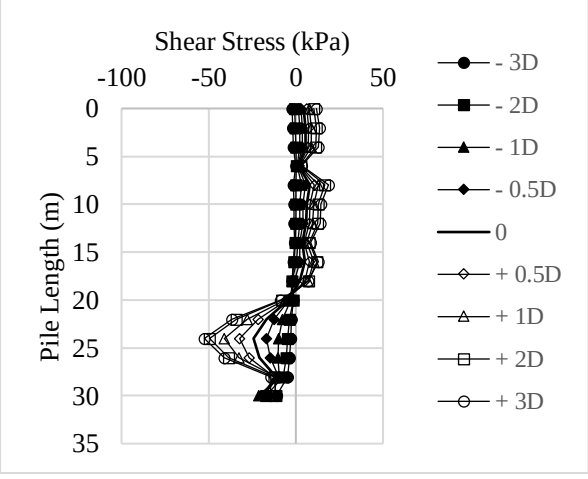

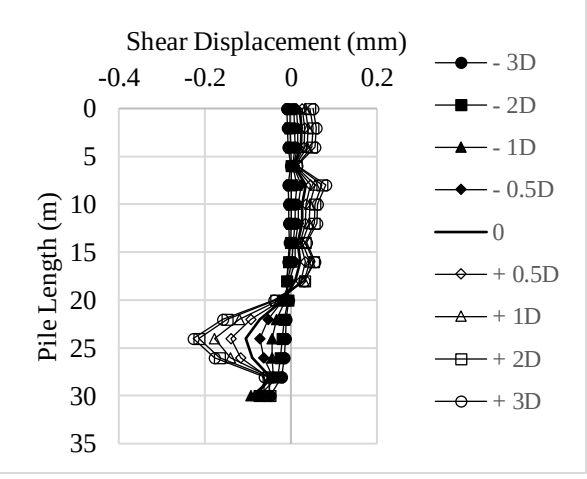

Long pile case 02-2-3

Δv	:	0.5D
Δht	:	2D
Cover depth	:	24 m

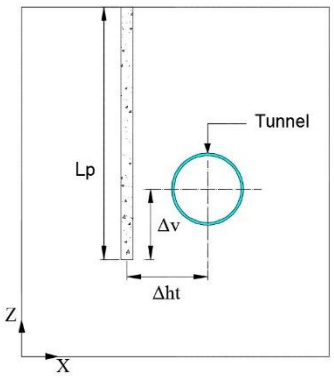

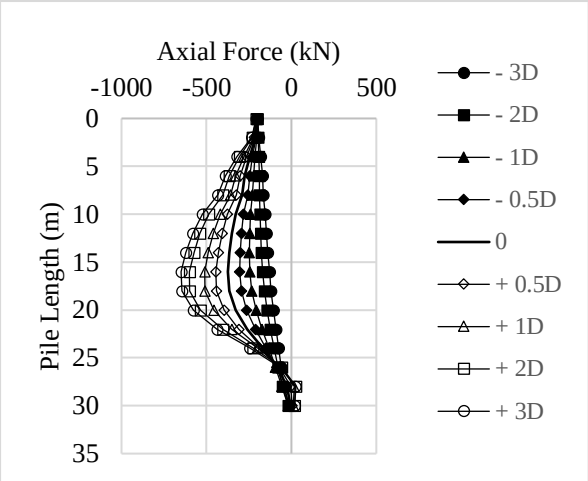

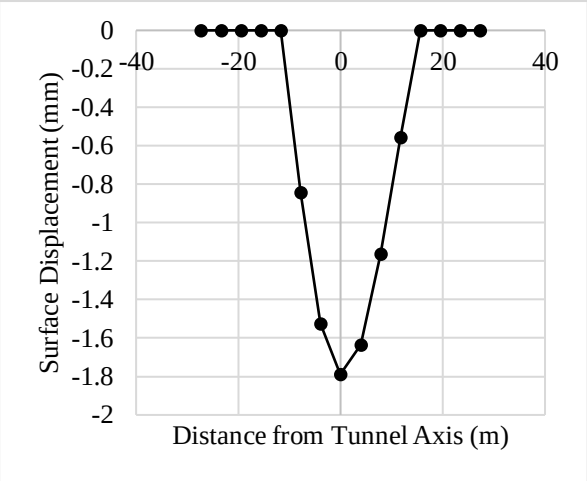

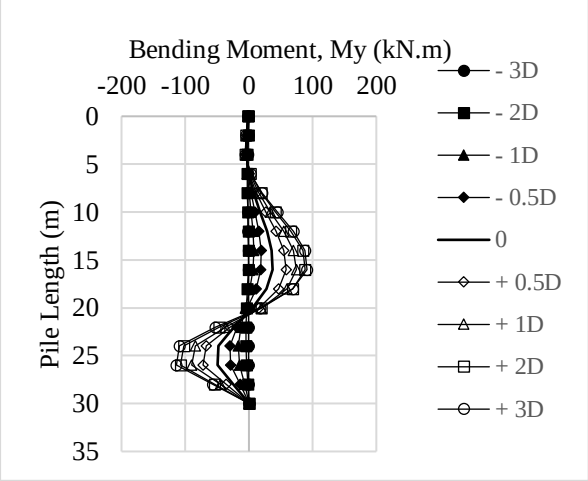

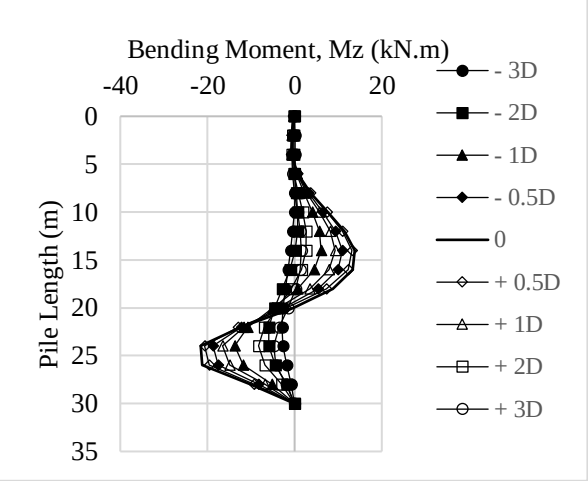

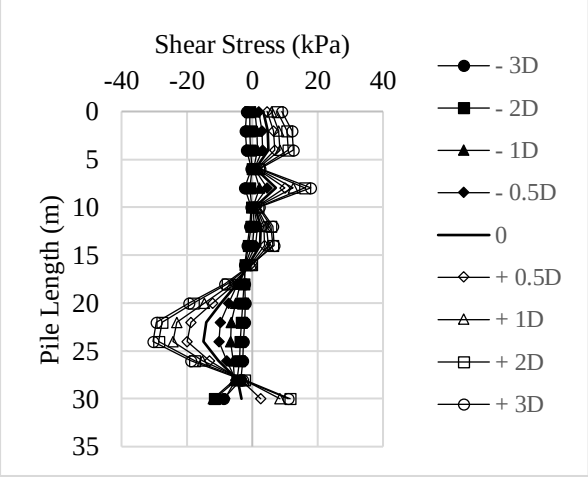

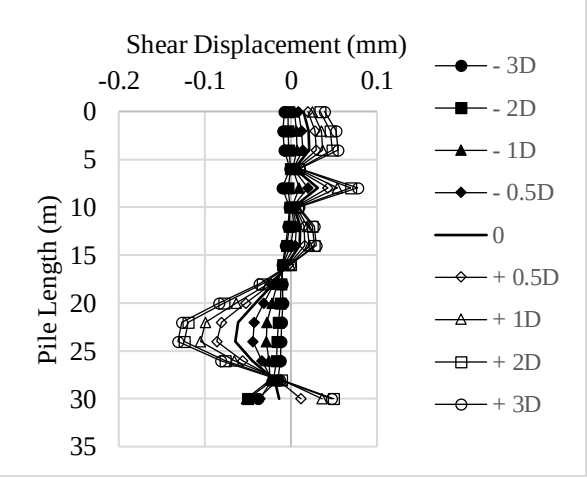

Long pile case 02-2-4

Δv	:	0.5D
Δht	:	2.5D
Cover depth	:	24 m

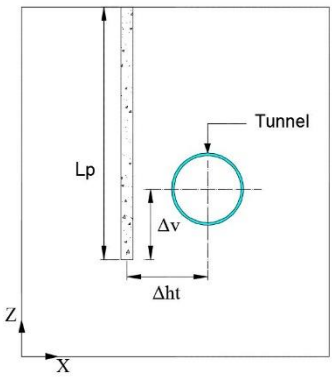

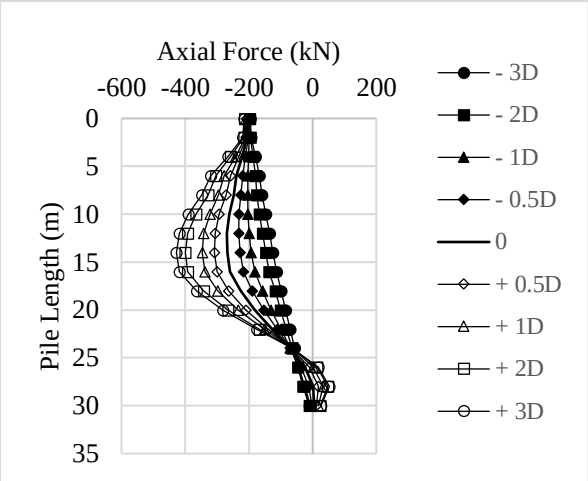

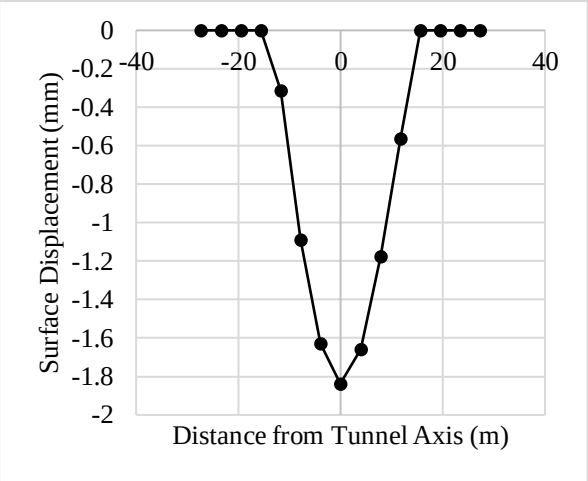

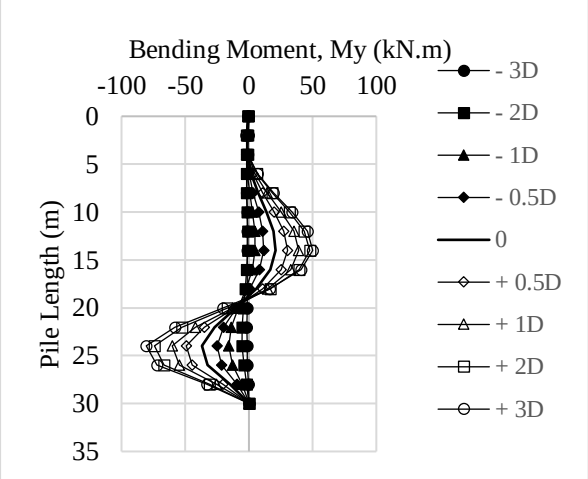

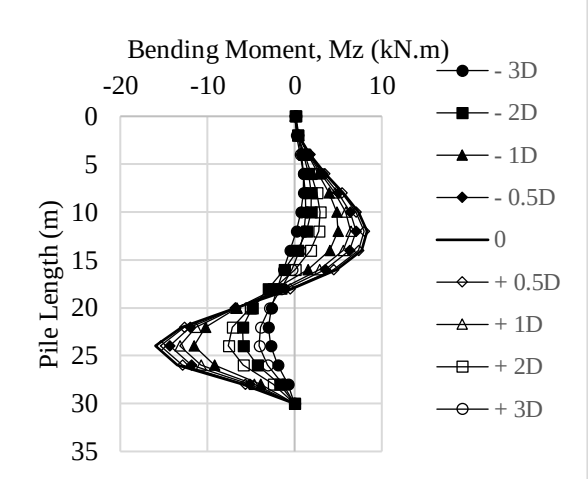

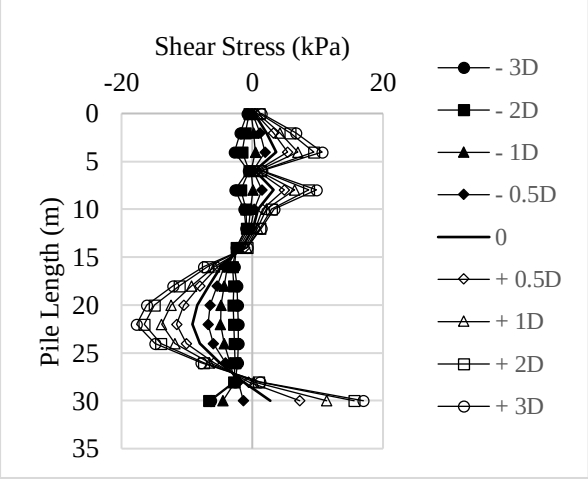

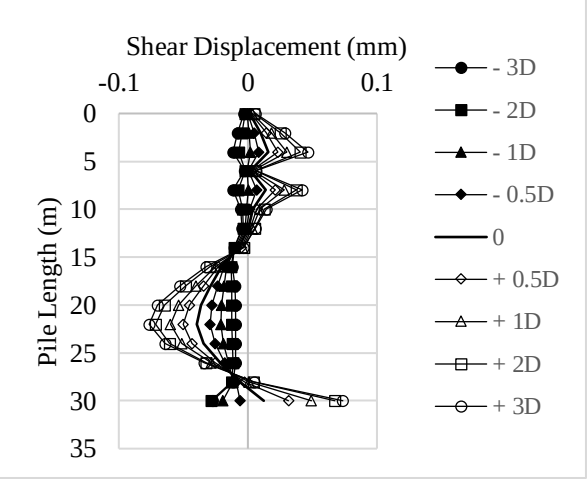

Long pile case 02-2-5

Δv	:	0.5D
Δht	:	3D
Cover depth	:	24 m

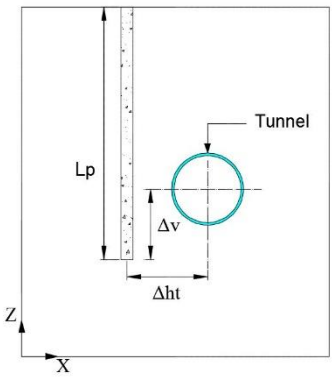

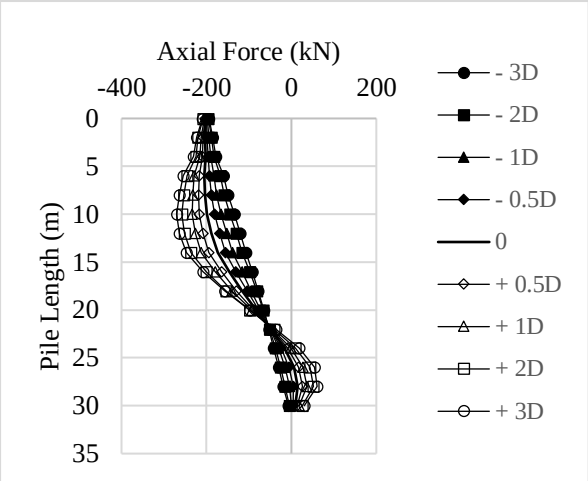

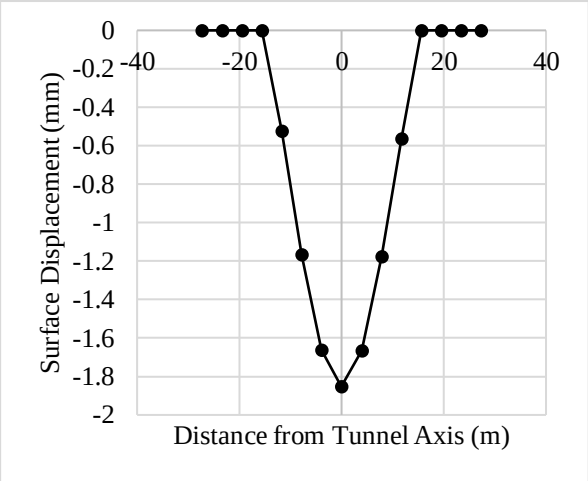

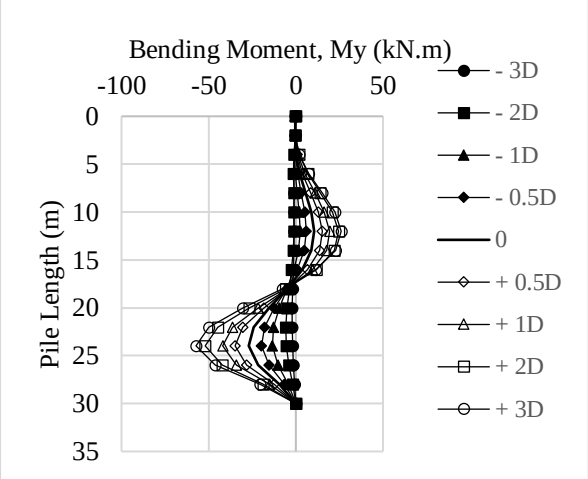

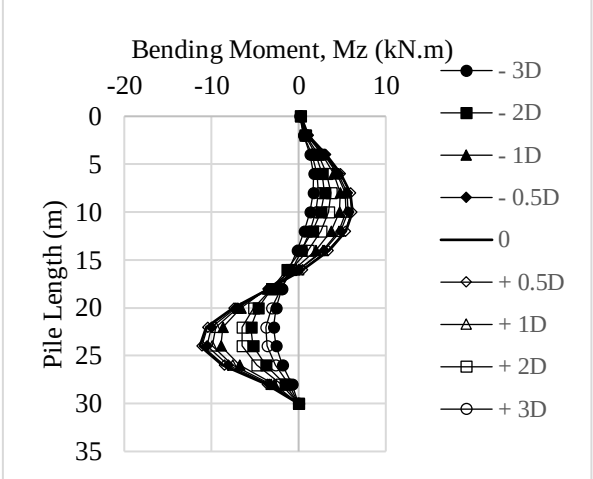

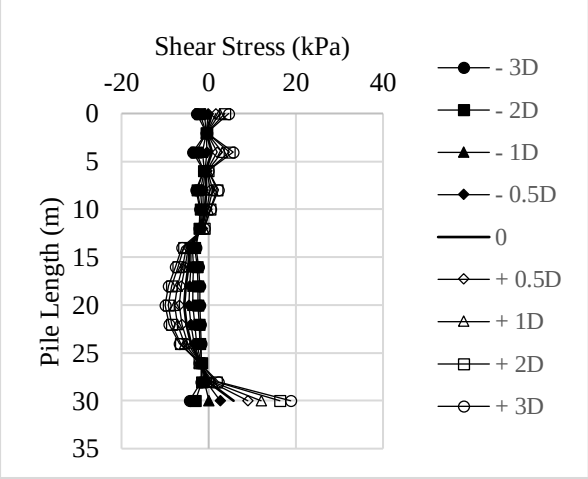

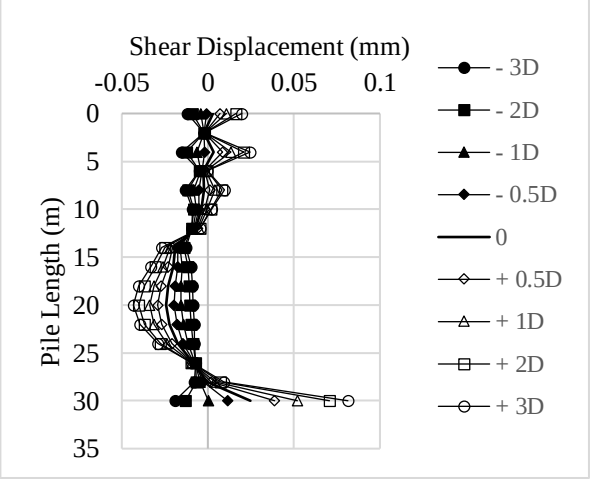

Long pile case 02-2-6

Δv	:	0.5D
Δht	:	3.5D
Cover depth	:	24 m

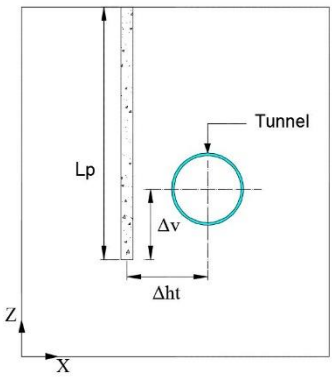

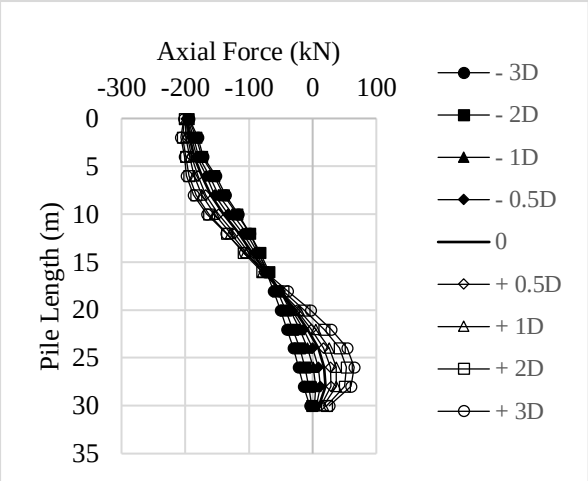

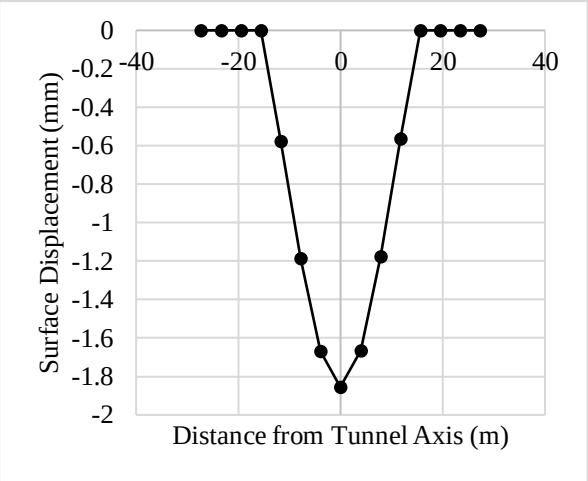

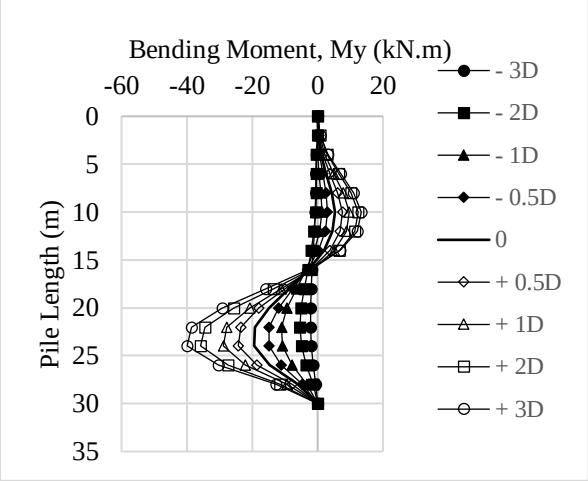

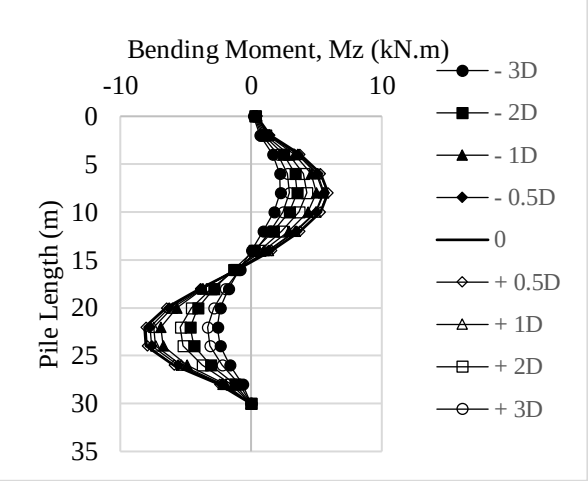

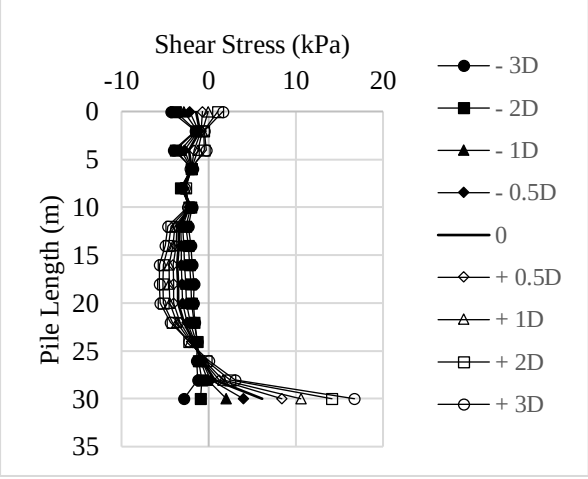

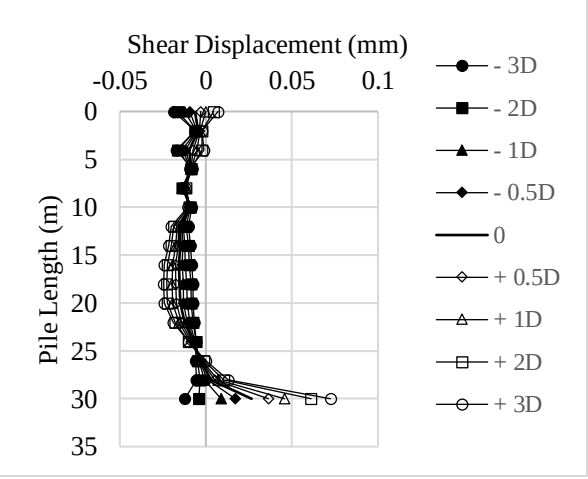

Long pile case 02-3-1

Δv : 1D
Δht : 1D
Cover depth : 21 m

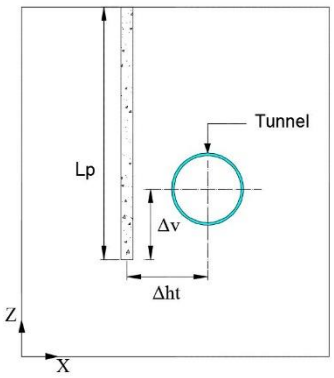

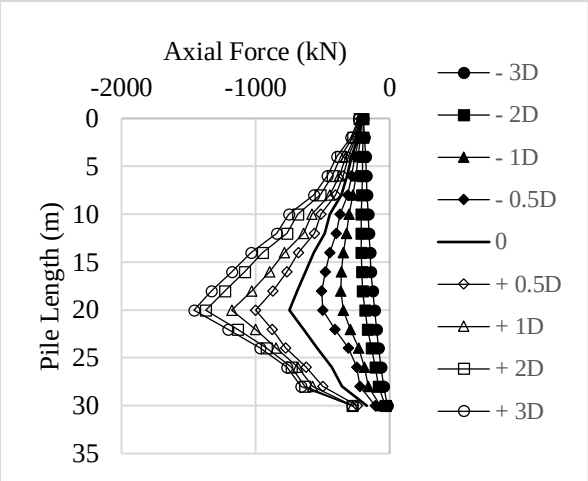

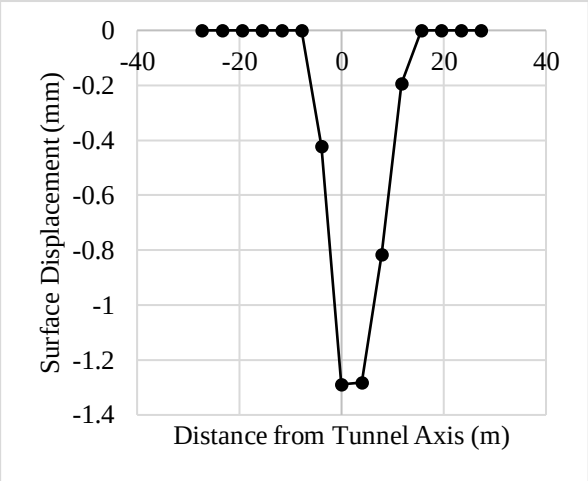

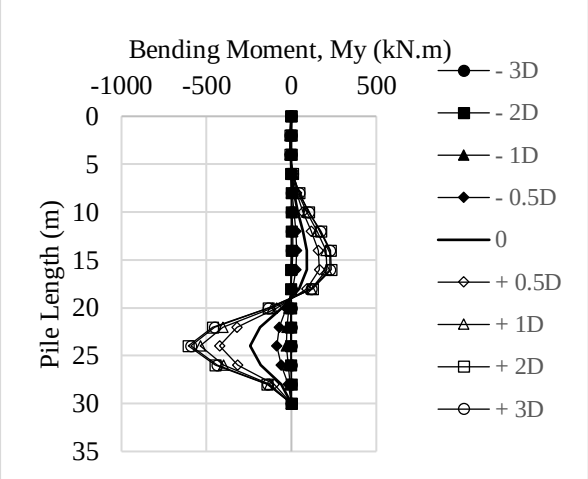

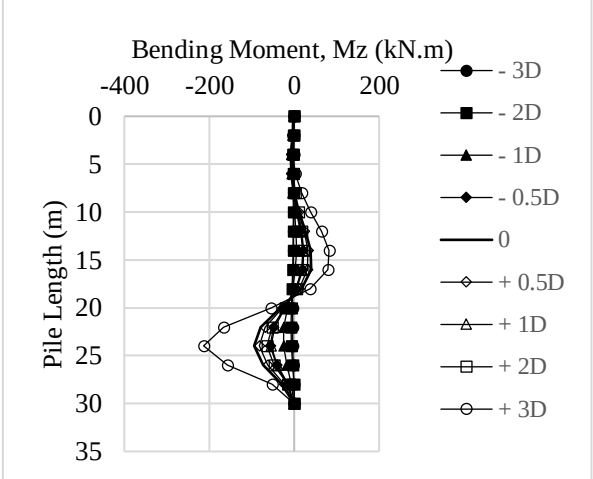

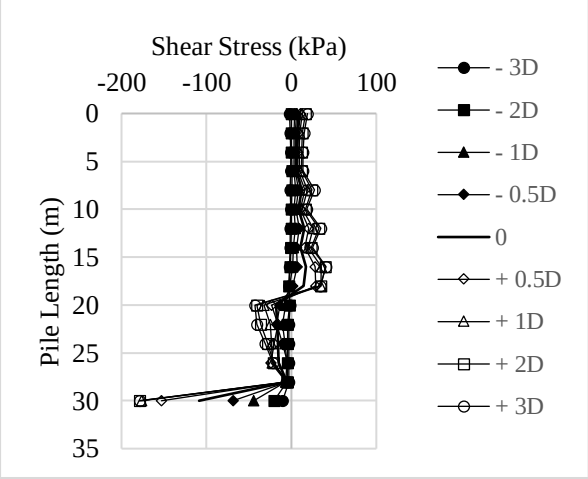

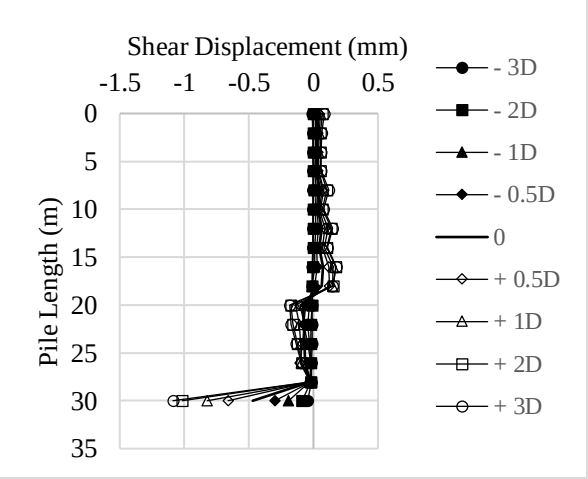

Long pile case 02-3-2

Δv	:	1D
Δht	:	1.5D
Cover depth	:	21 m

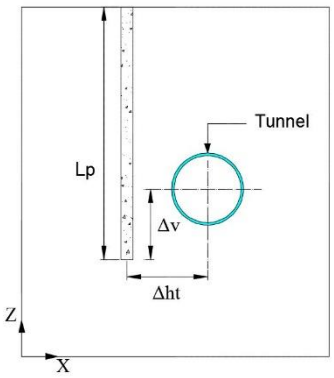

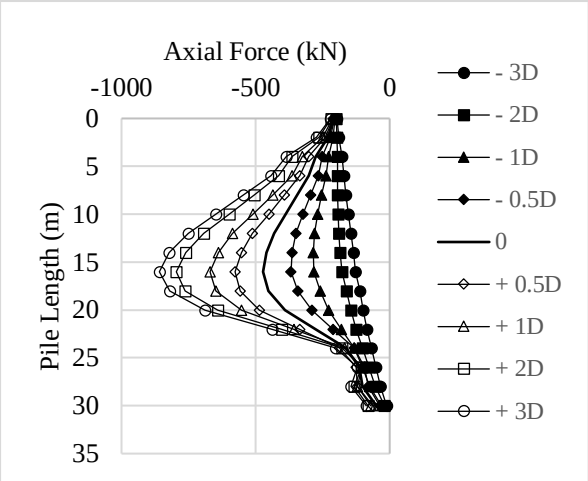

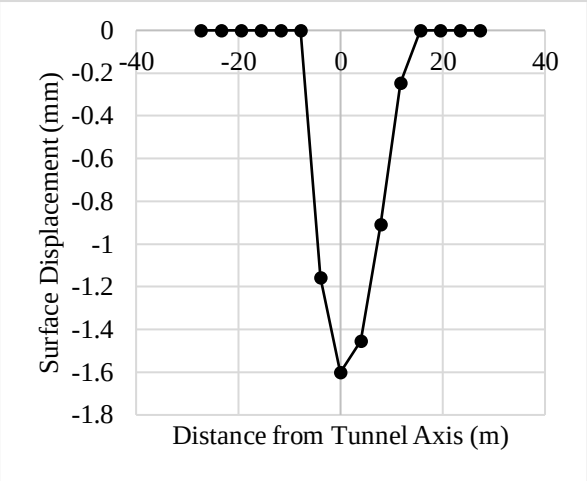

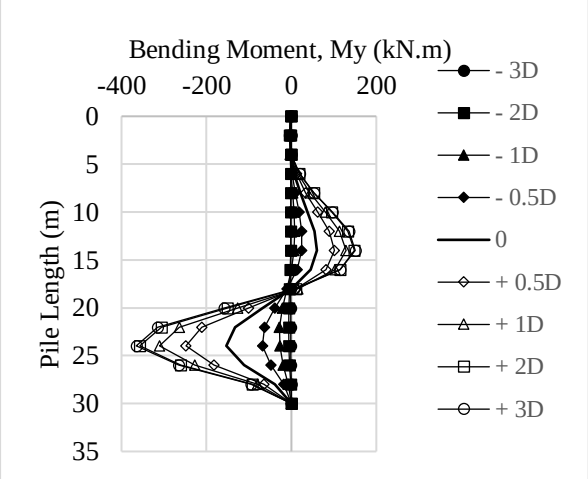

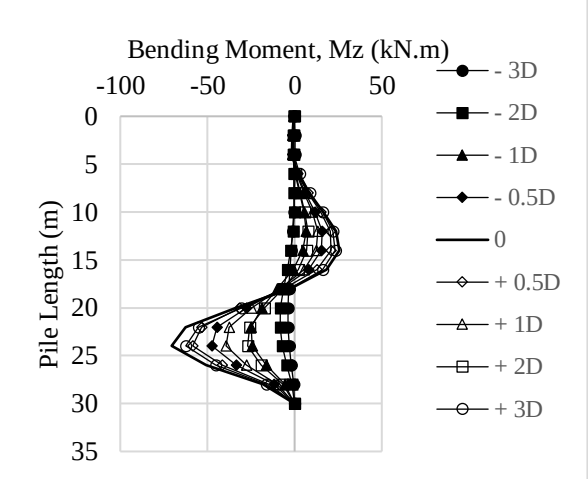

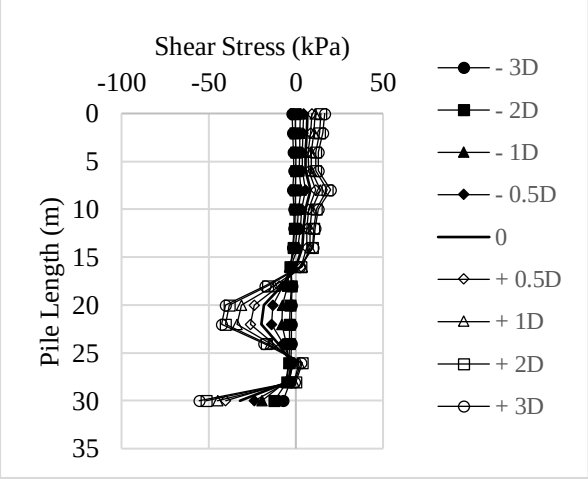

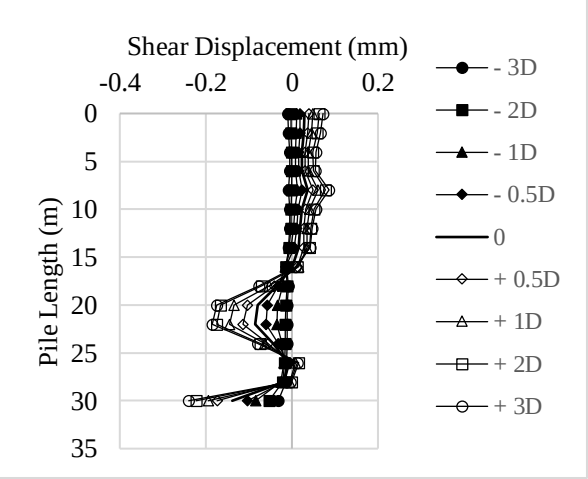

Long pile case 02-3-3

Δv	:	1D
Δht	:	2D
Cover depth	:	21 m

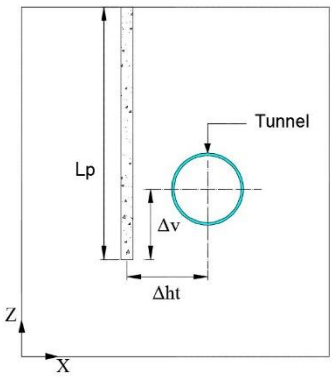

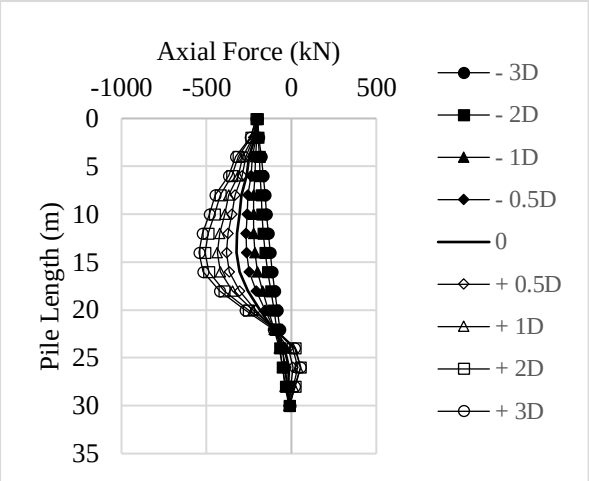

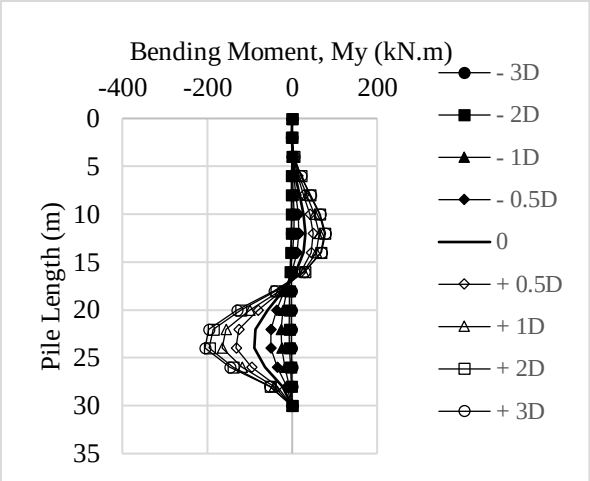

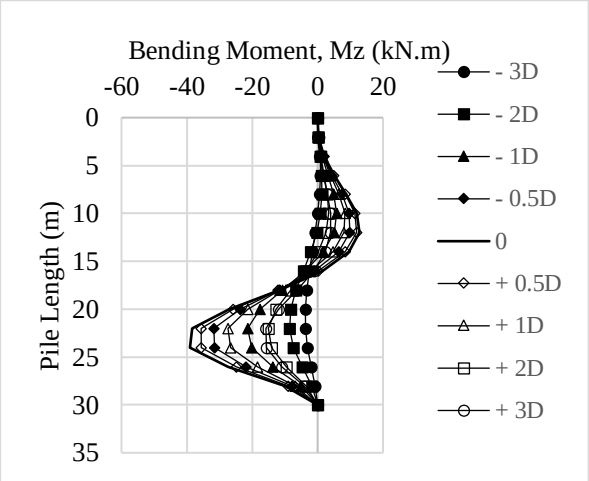

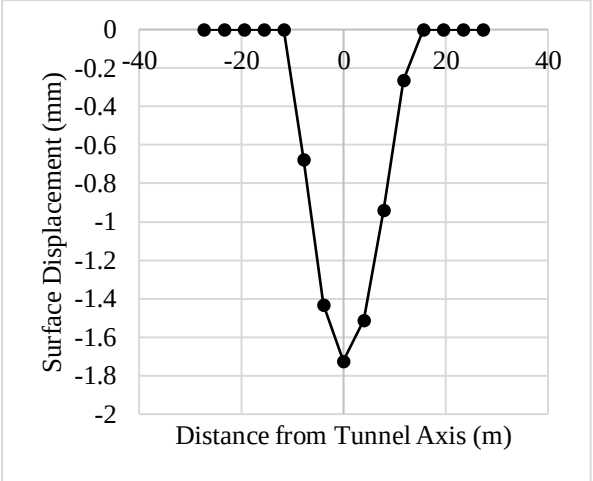

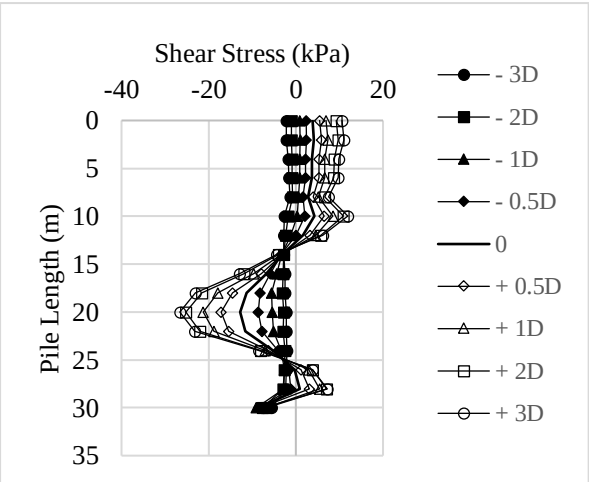

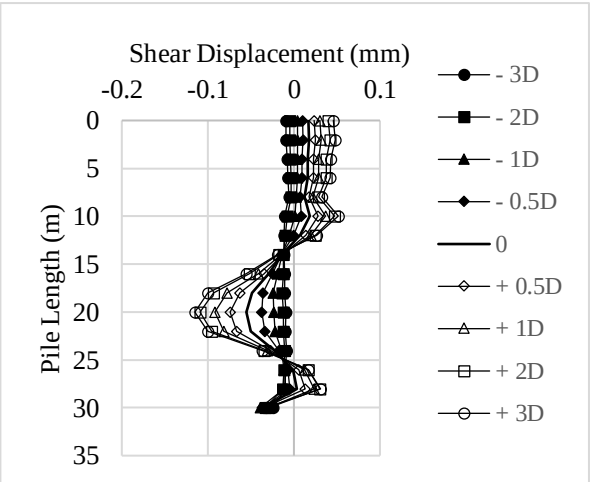

Long pile case 02-3-4

Δv	:	1D
Δht	:	2.5D
Cover depth	:	21 m

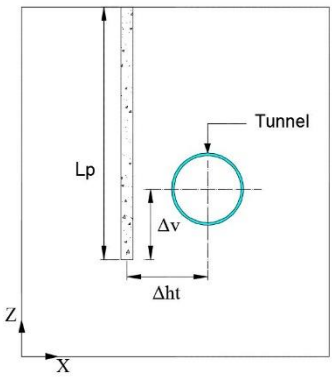

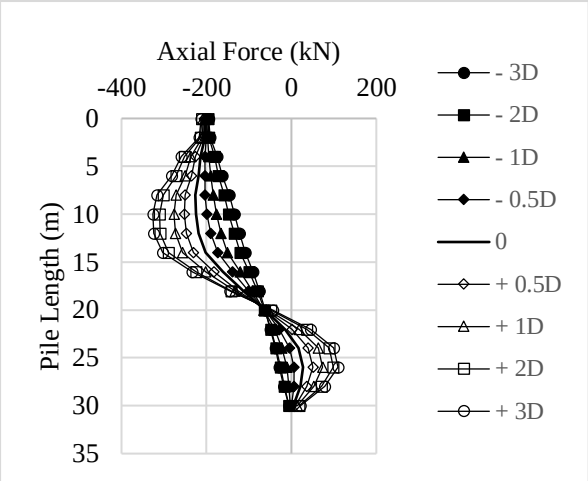

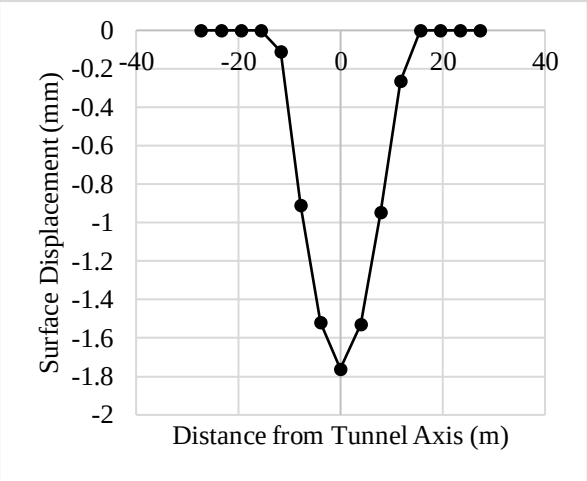

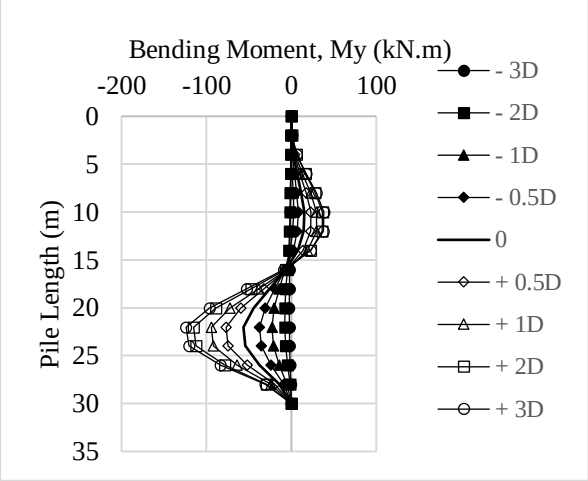

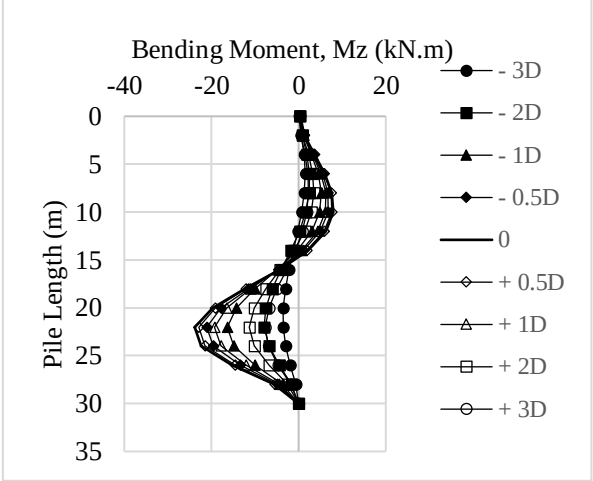

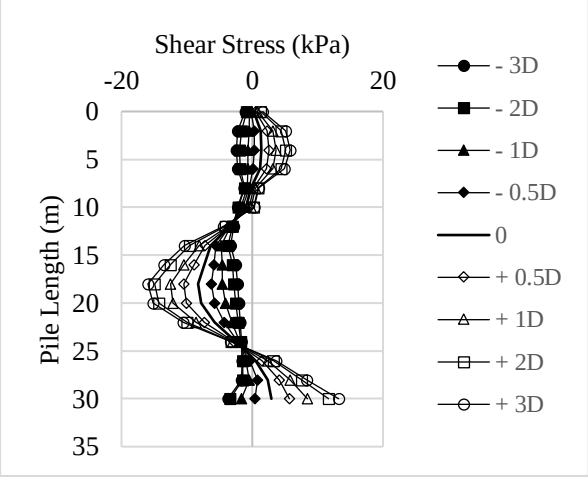

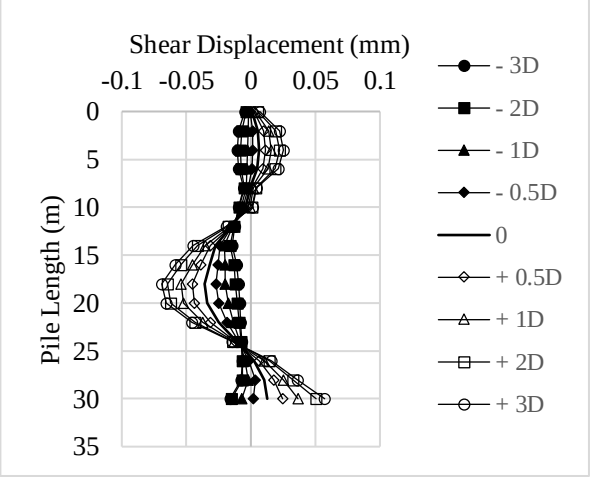

Long pile case 02-3-5

Δv : 1D
Δht : 3D
Cover depth : 21 m

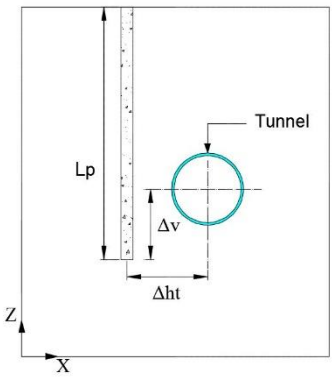

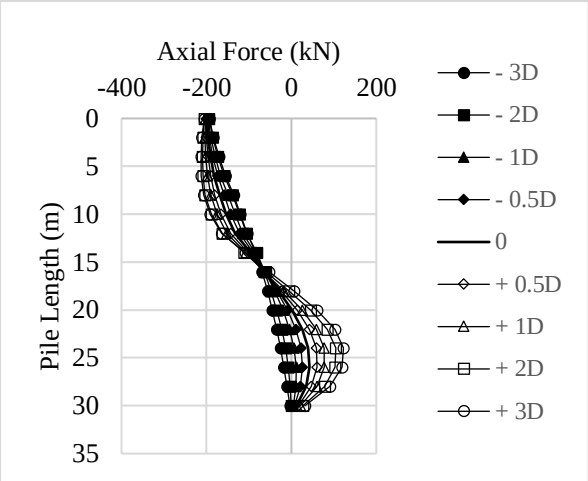

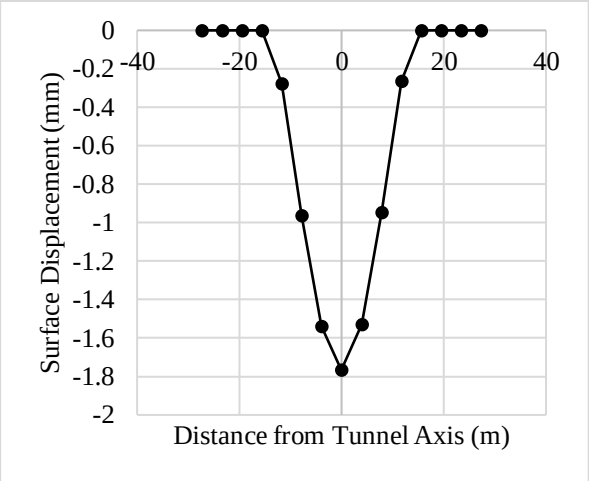

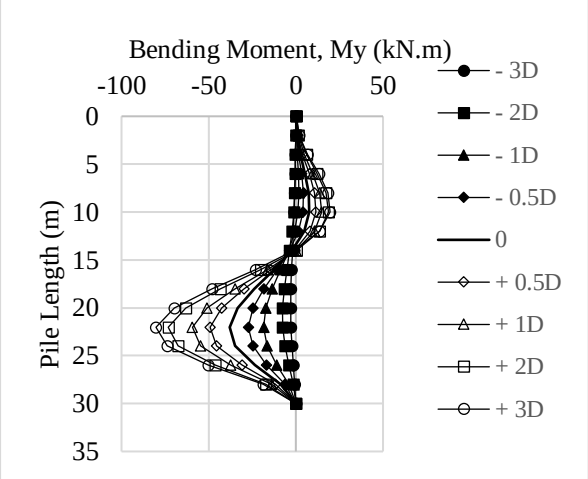

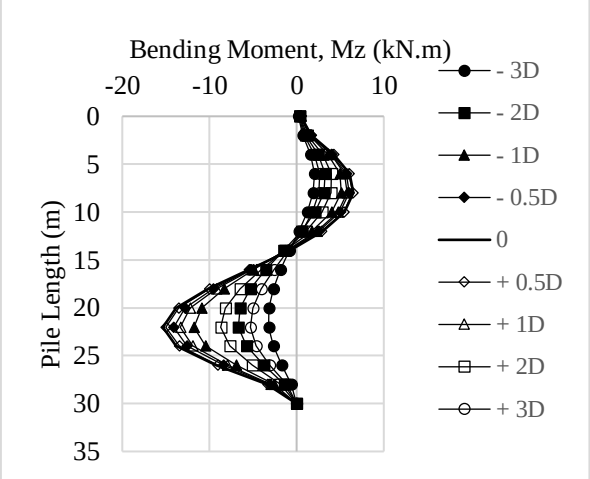

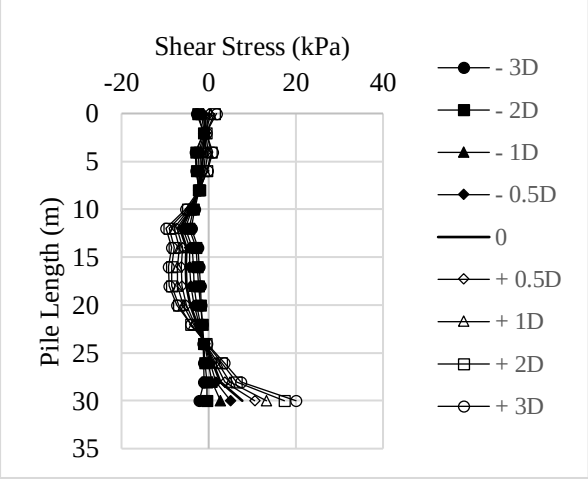

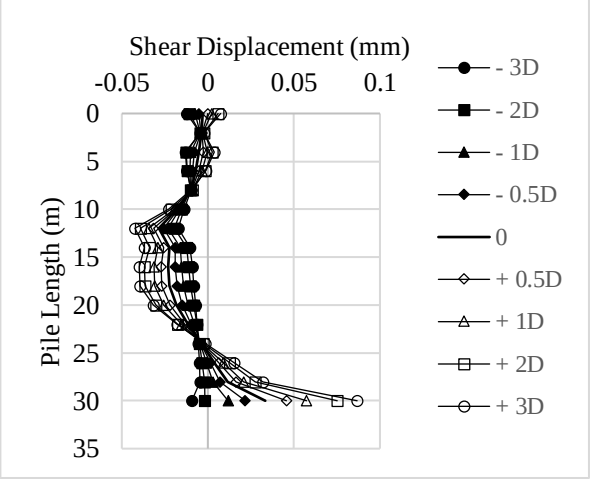

Long pile case 02-3-6

Δv	:	1D
Δht	:	3.5D
Cover depth	:	21 m

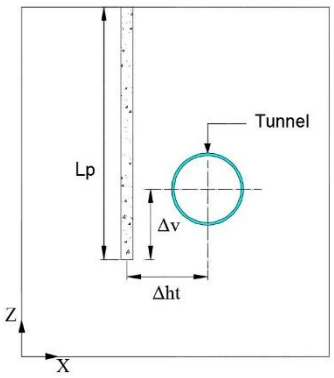

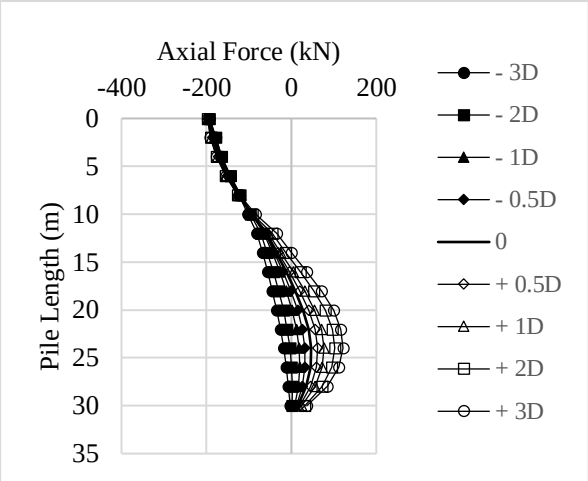

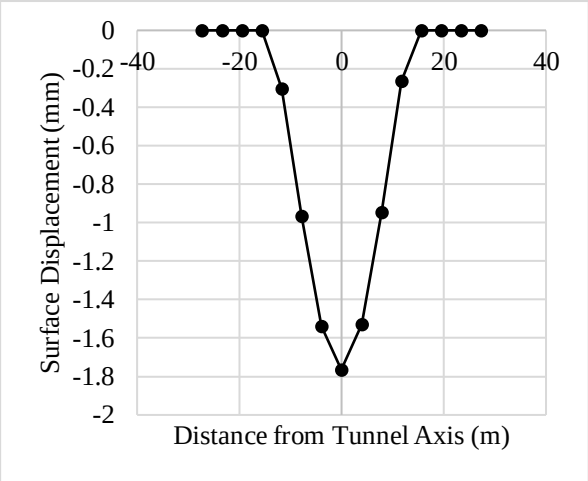

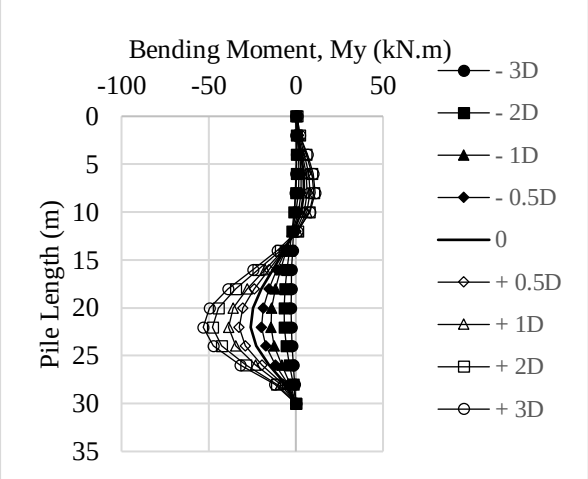

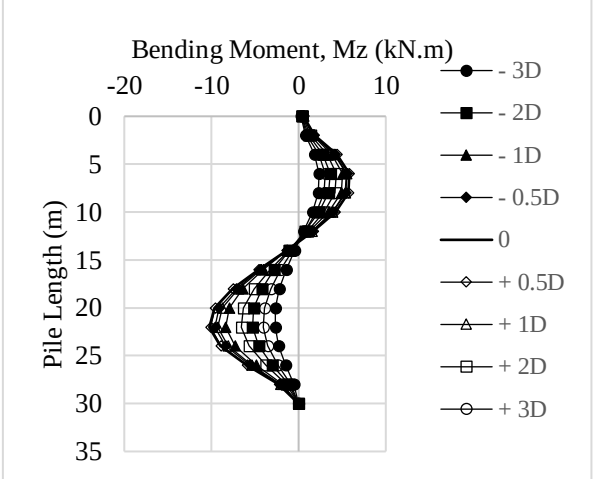

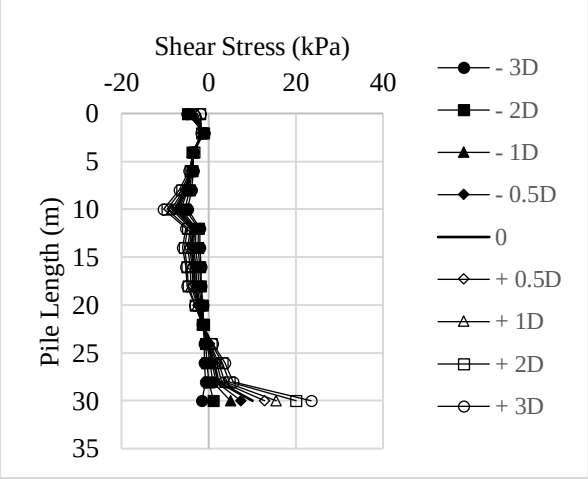

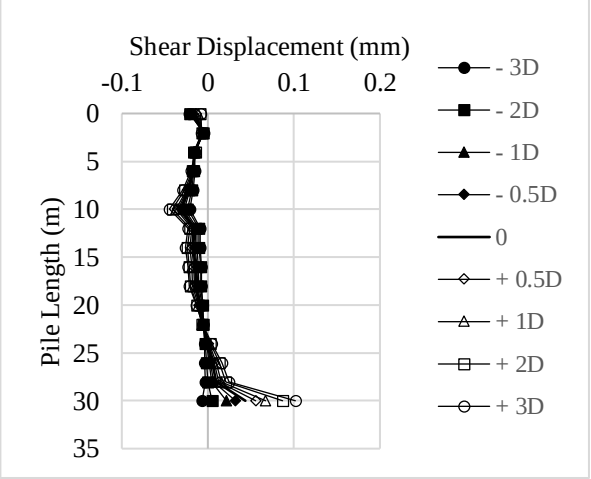

Long pile case 02-4-1

Δv : 1.5D
Δht : 1D
Cover depth : 18 m

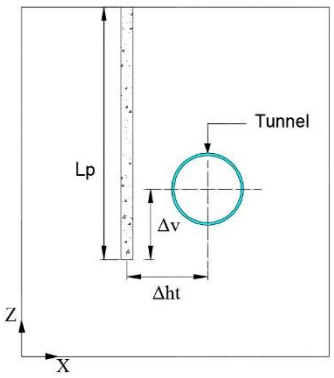

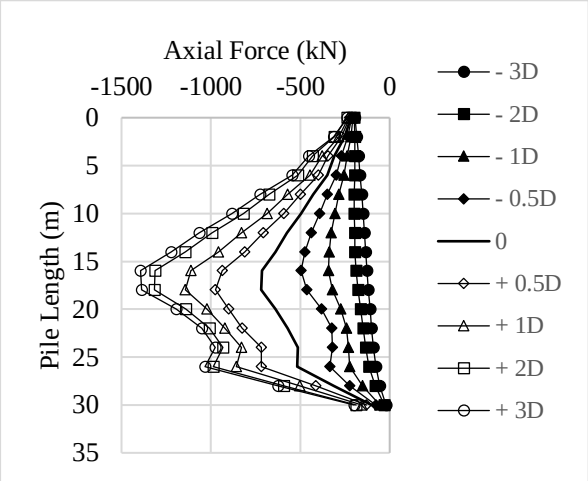

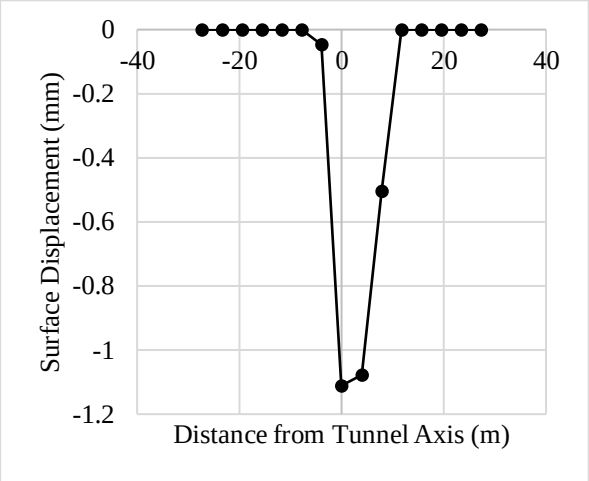

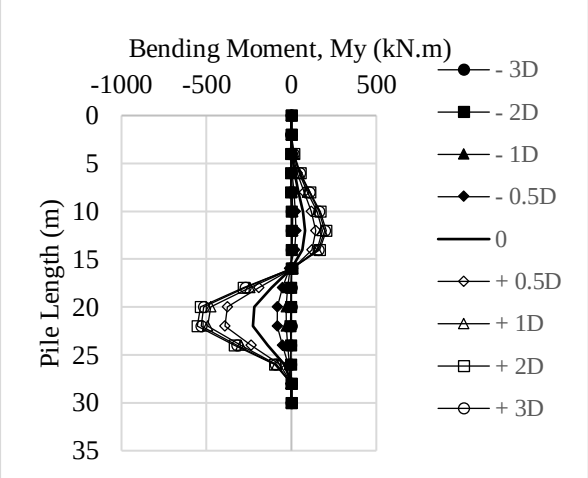

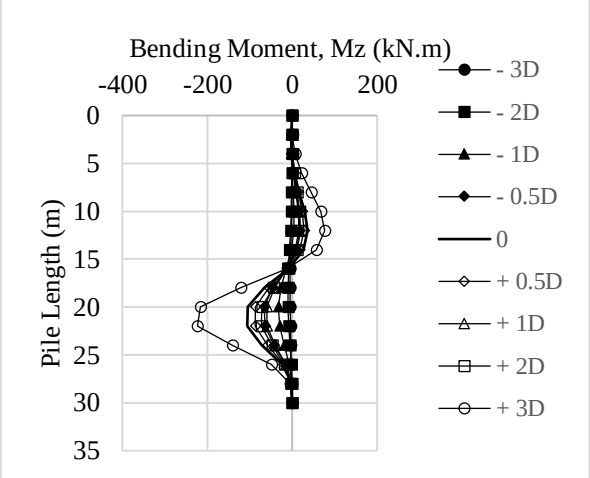

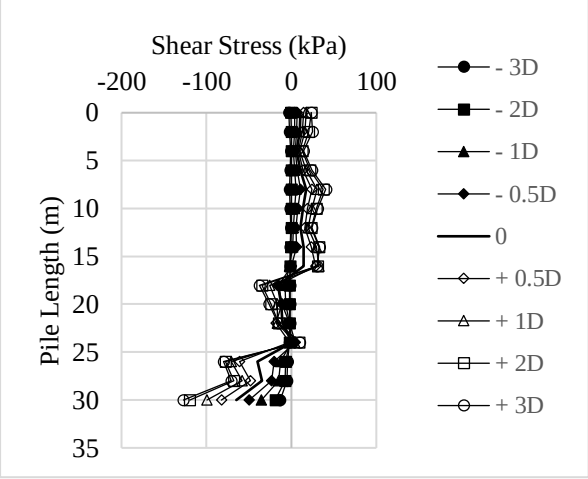

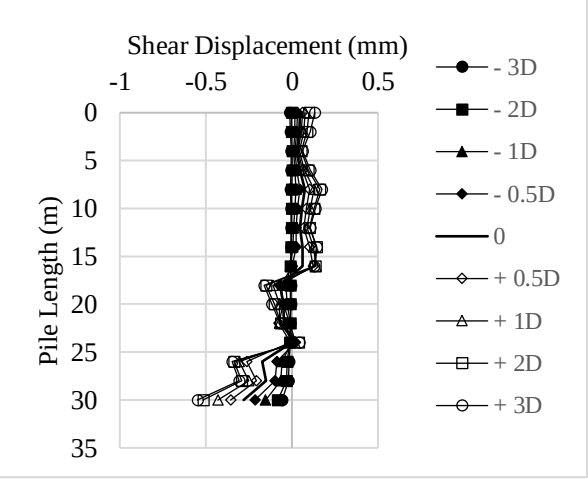

Long pile case 02-4-2

Δv	:	1.5D
Δht	:	1.5D
Cover depth	:	18 m

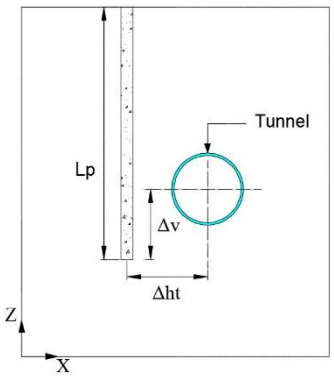

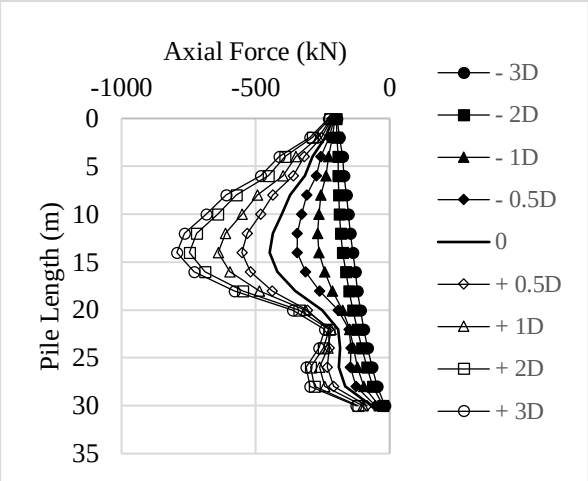

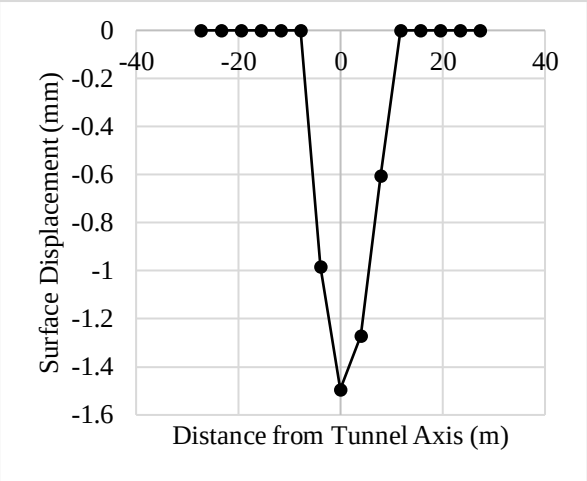

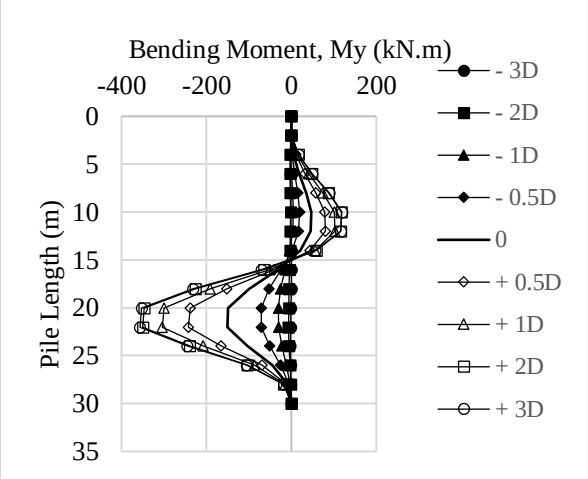

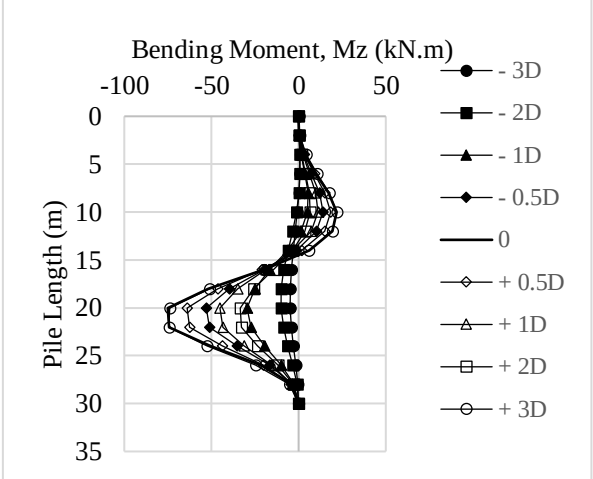

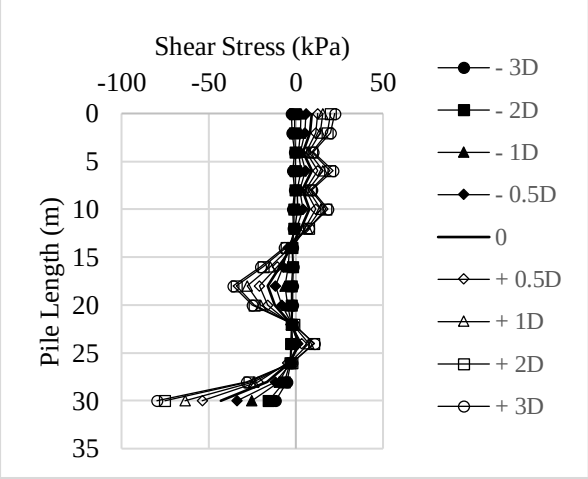

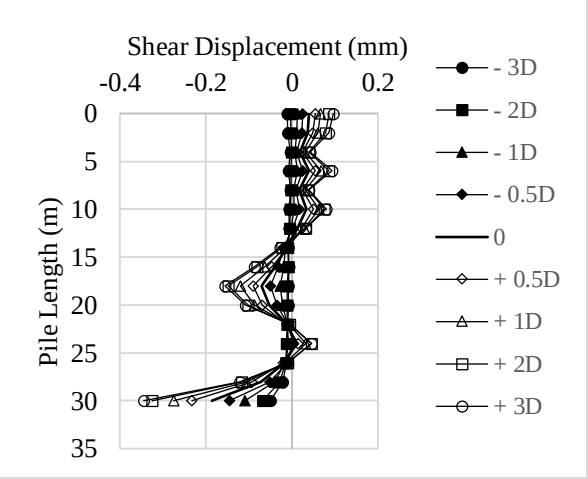

Long pile case 02-4-3

Δv : 1.5D
Δht : 2D
Cover depth : 18 m

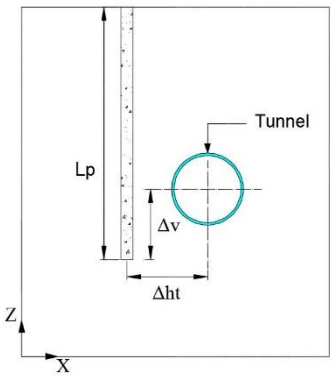

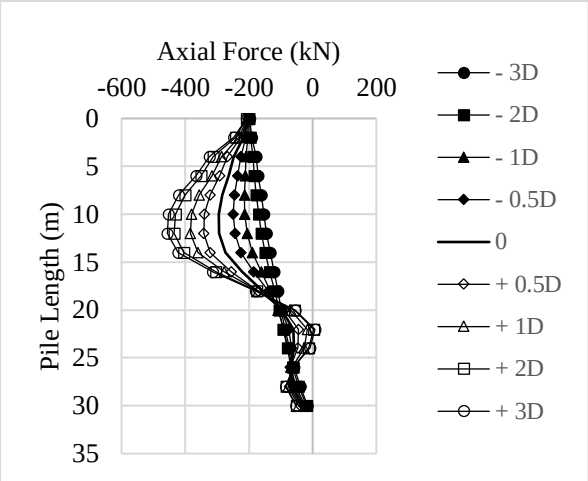

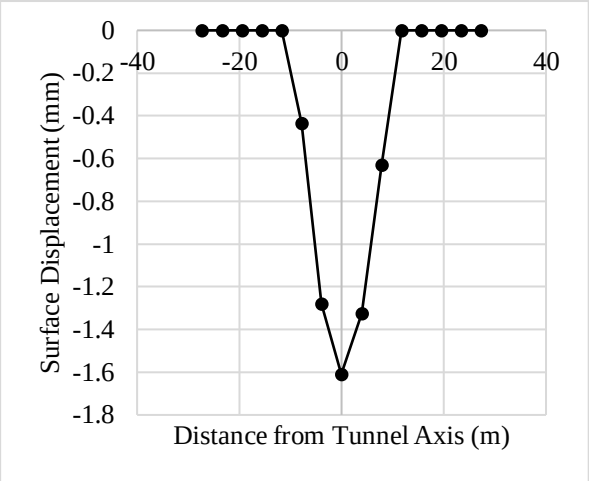

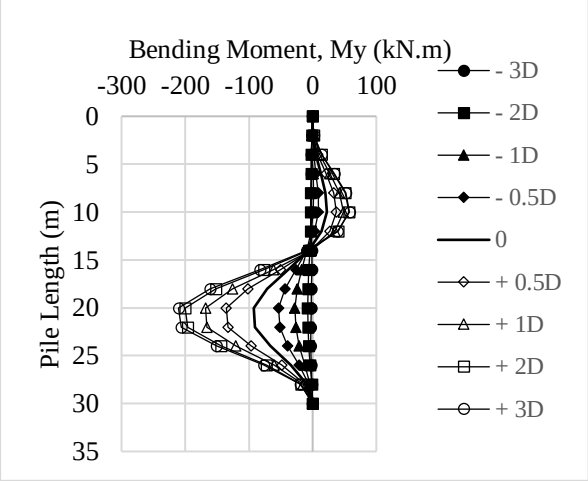

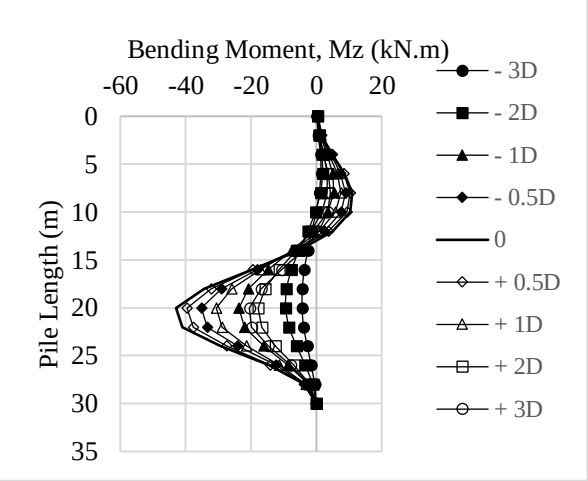

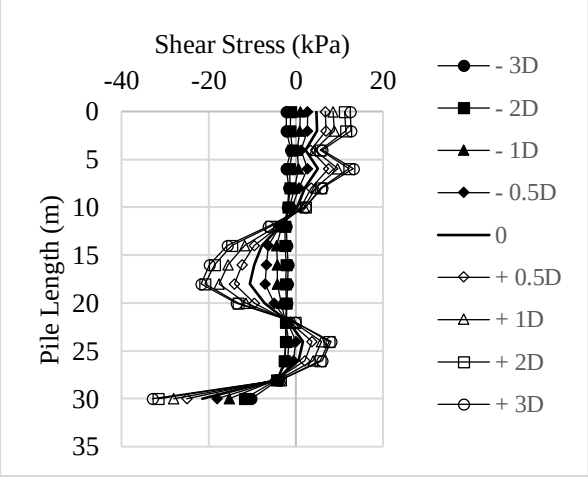

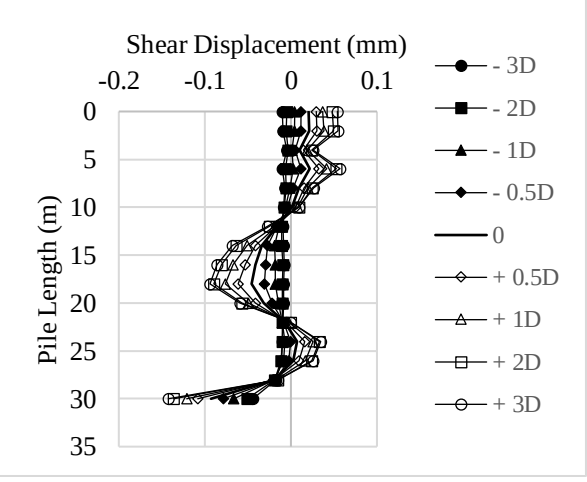

Long pile case 02-4-4

Δv : 1.5D
Δht : 2.5D
Cover depth : 18 m

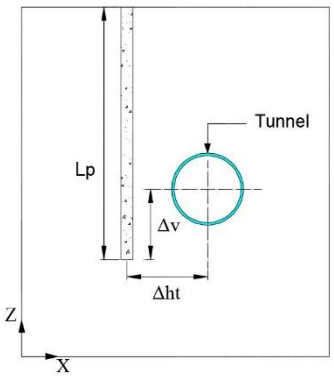

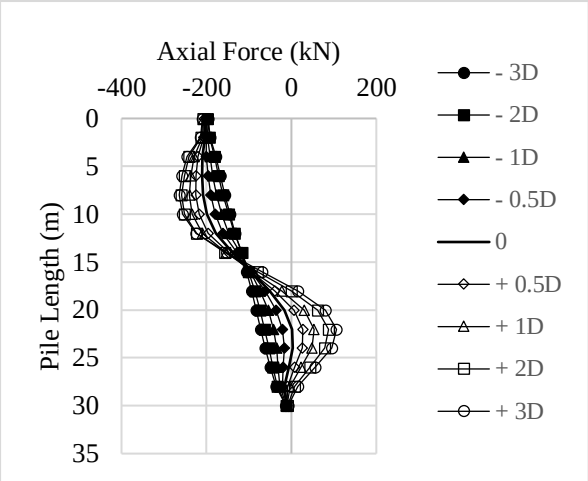

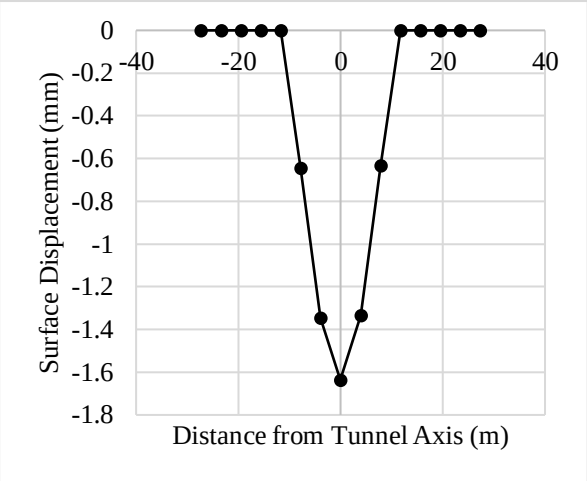

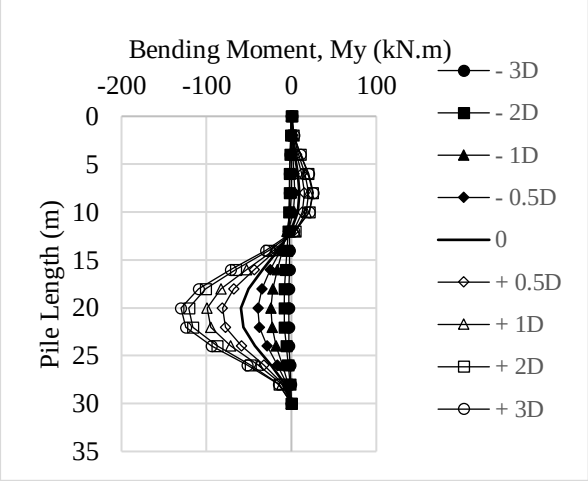

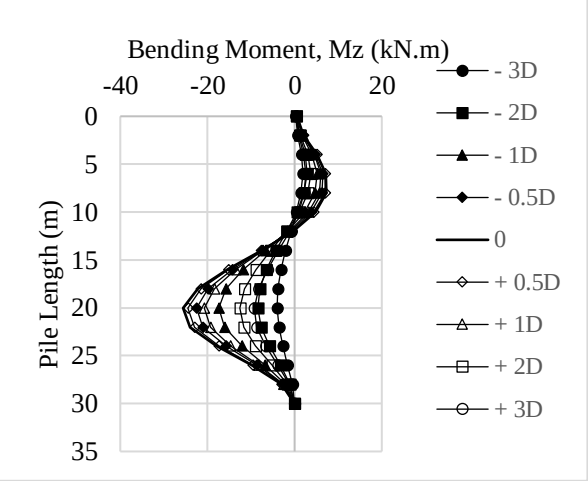

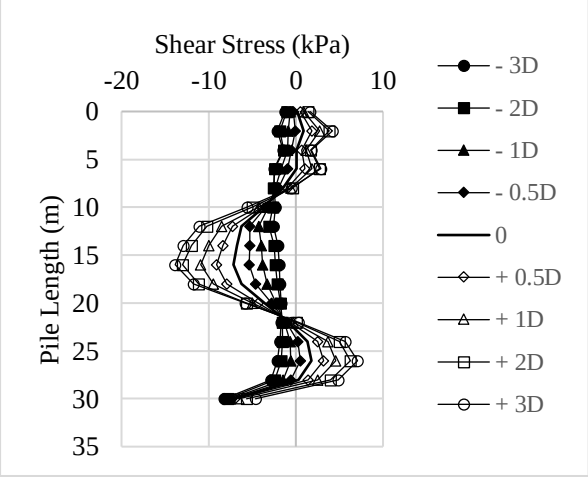

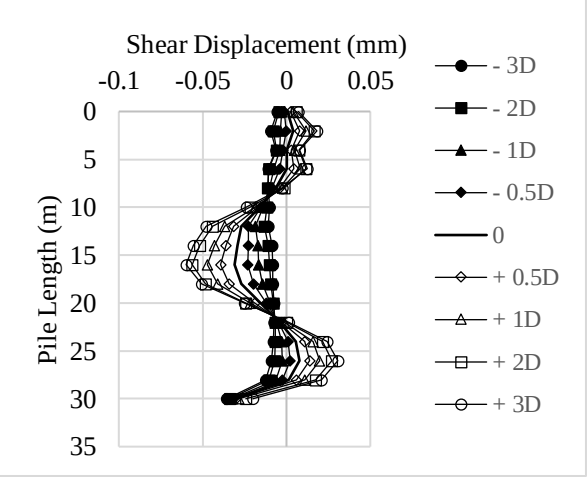

Long pile case 02-4-5

Δv : 1.5D
Δht : 3D
Cover depth : 18 m

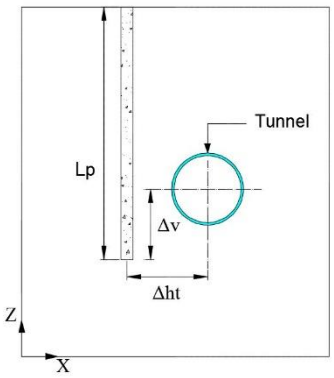

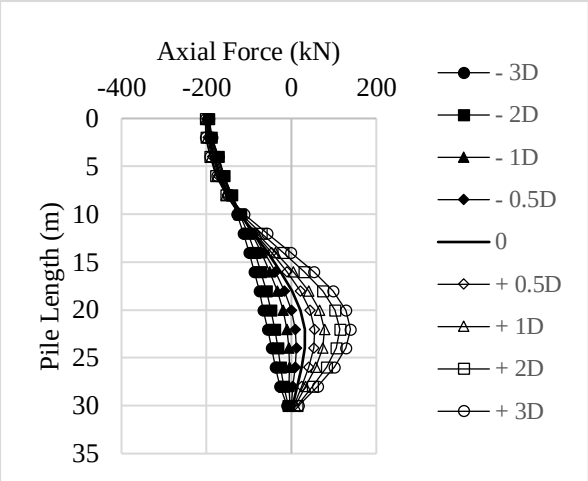

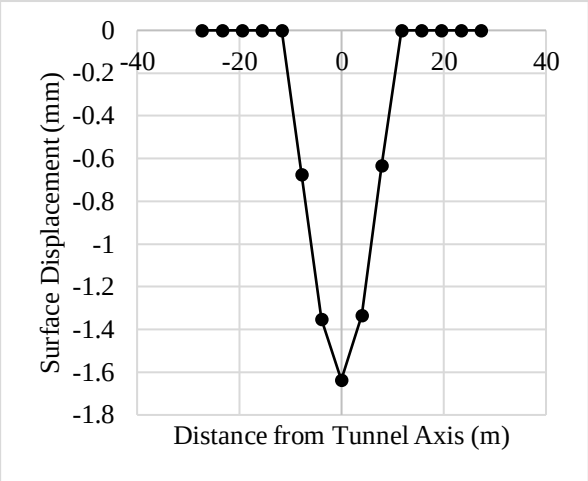

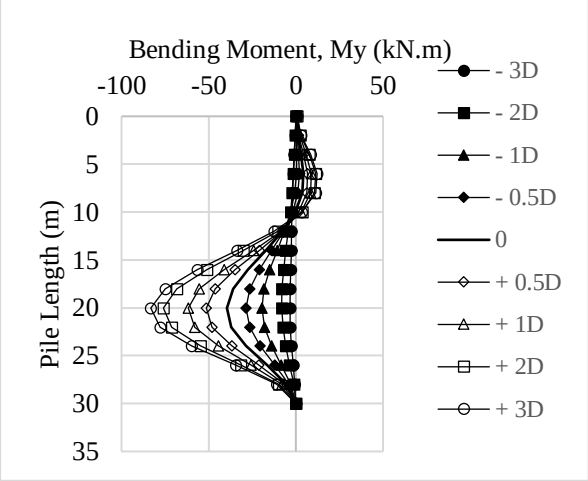

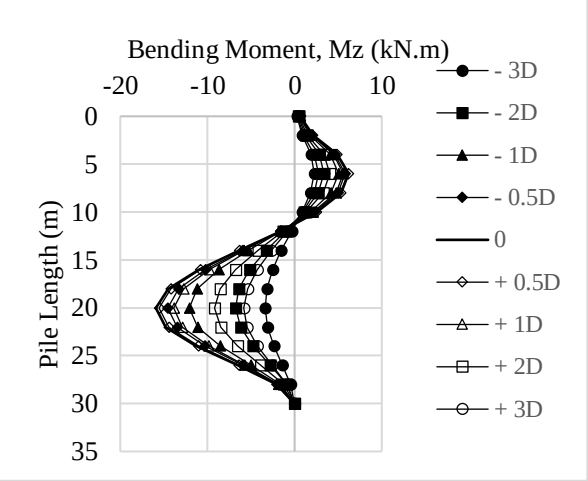

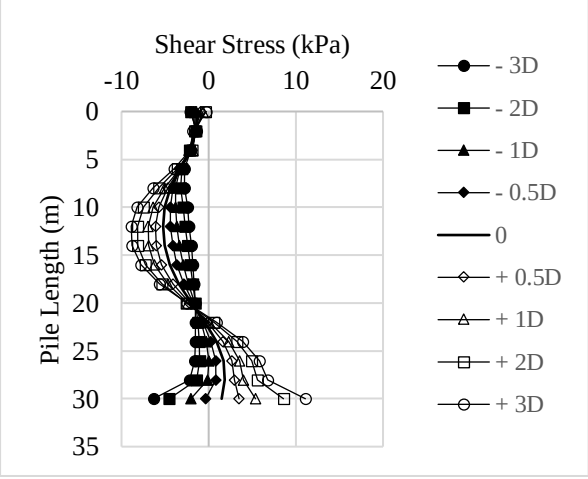

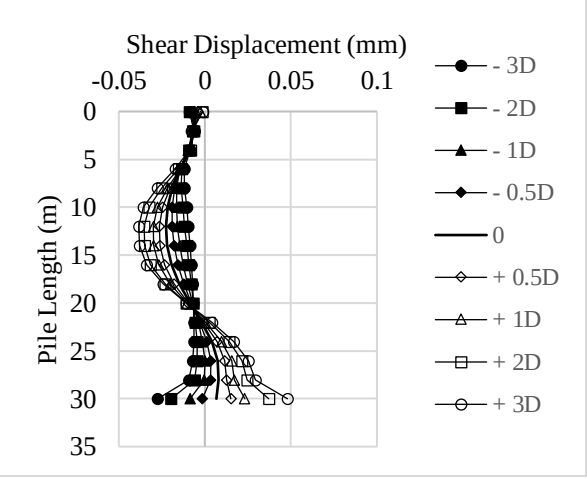

Long pile case 02-4-6

Δv	:	1.5D
Δht	:	3.5D
Cover depth	:	18 m

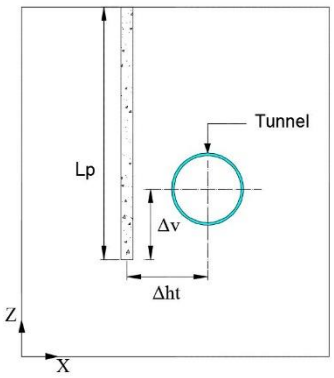

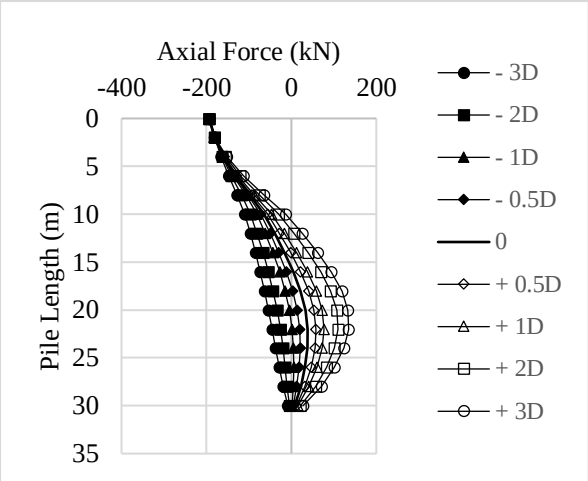

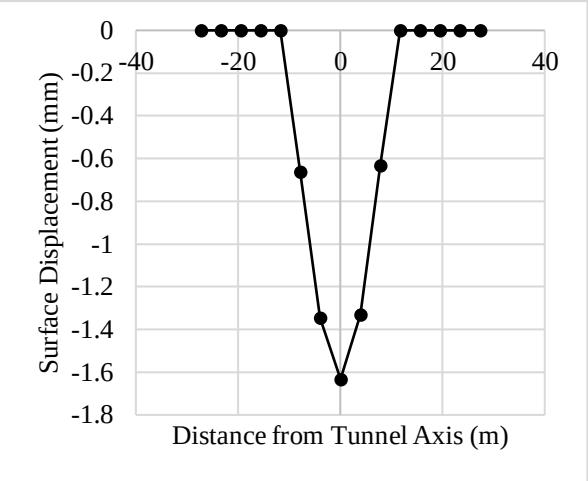

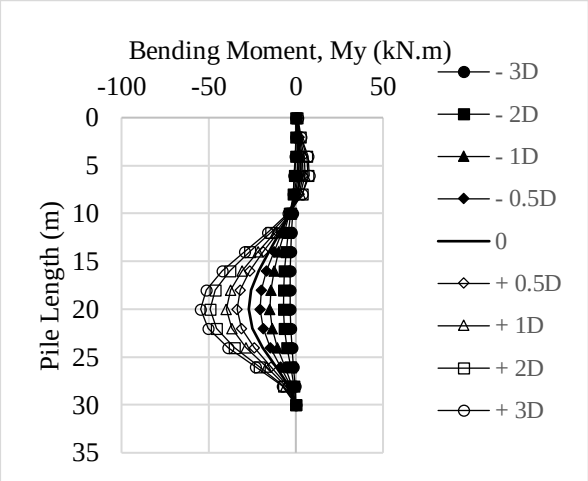

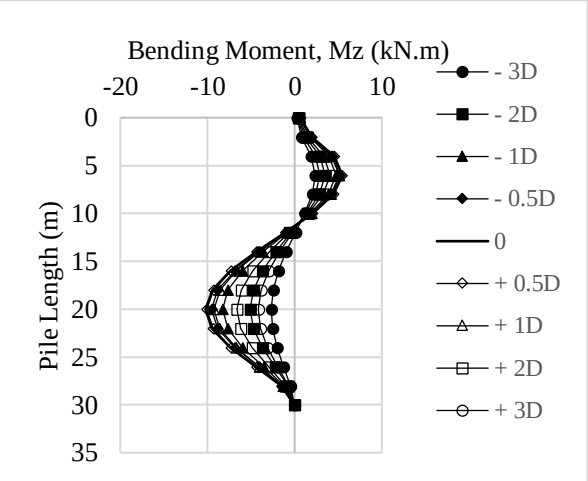

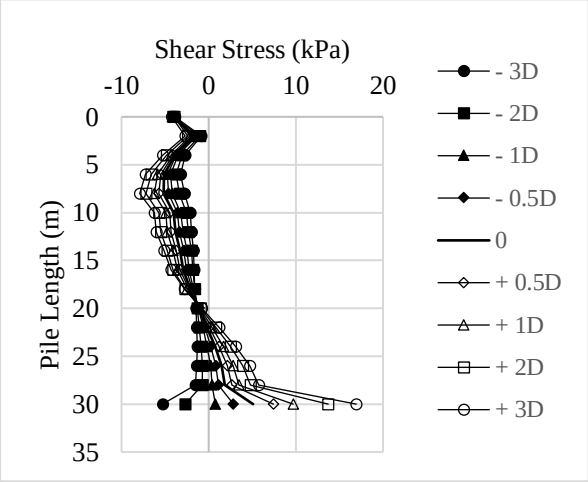

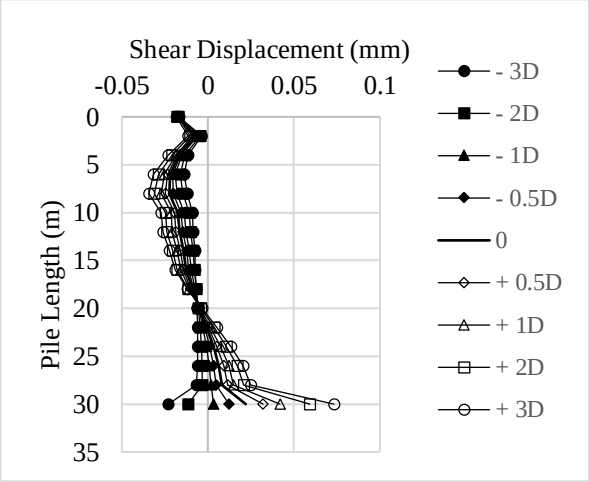

Long pile case 02-5-1

Δv : 2D
Δht : 1D
Cover depth : 15 m

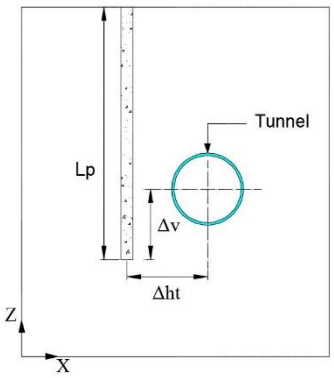

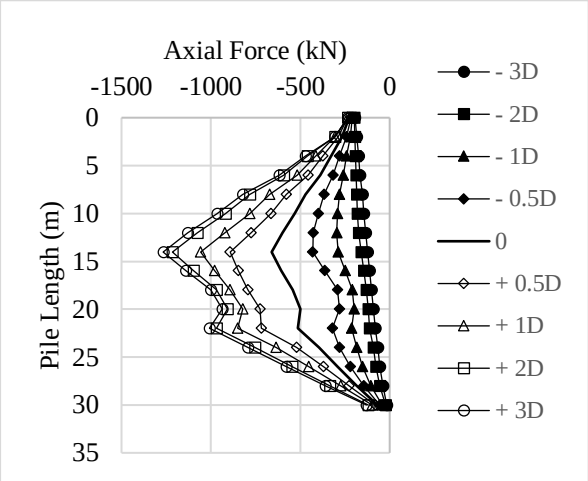

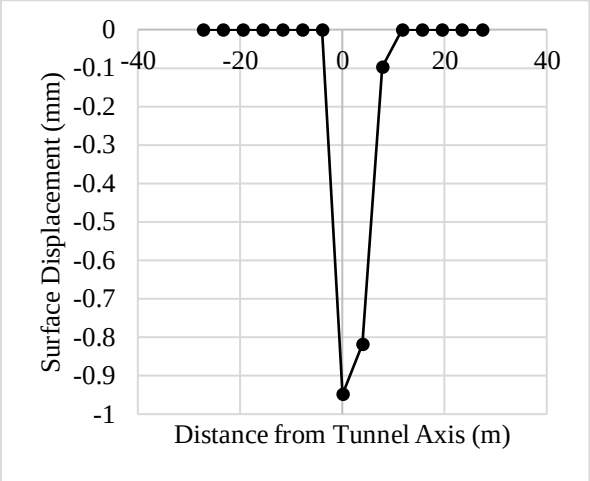

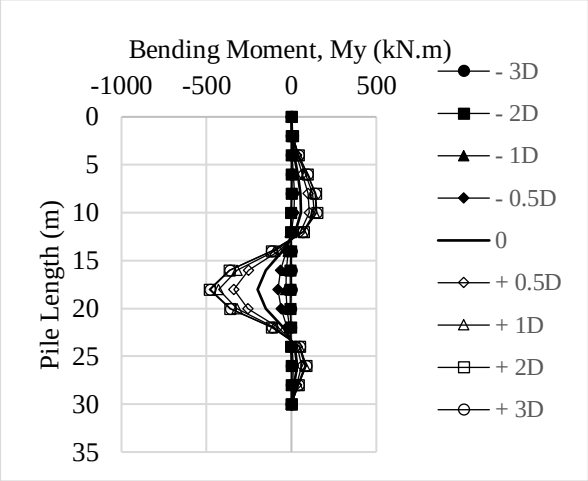

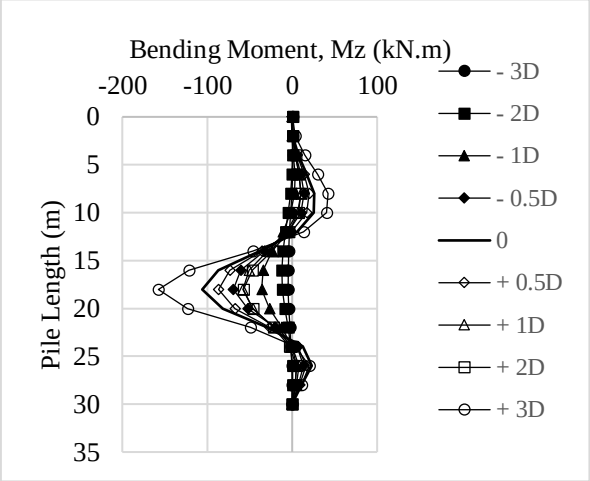

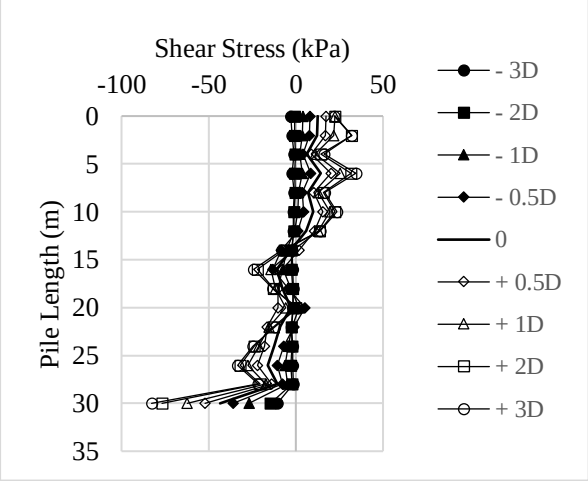

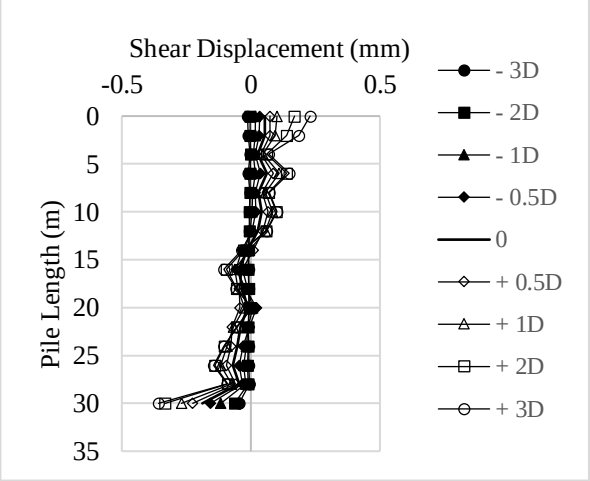

Long pile case 02-5-2

Δv : 2D
Δht : 1.5D
Cover depth : 15 m

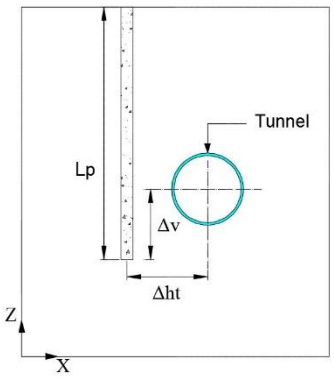

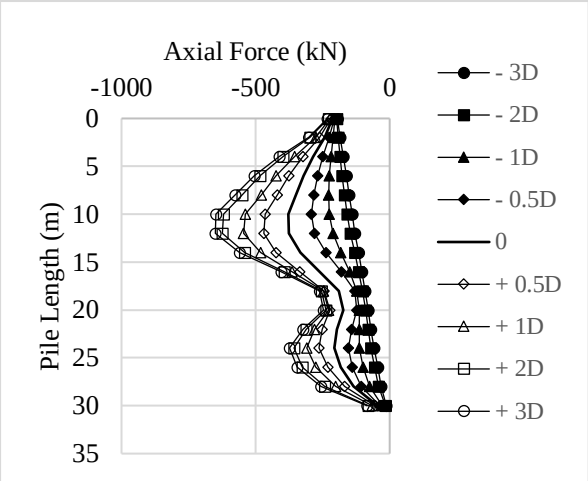

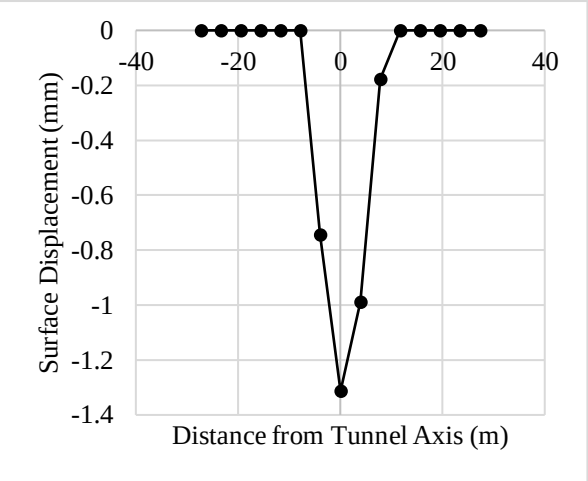

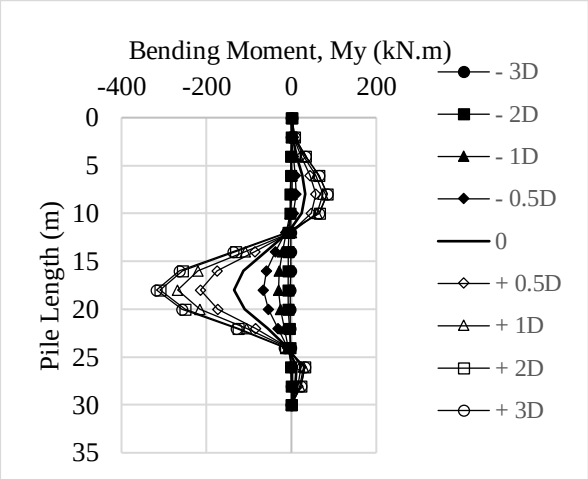

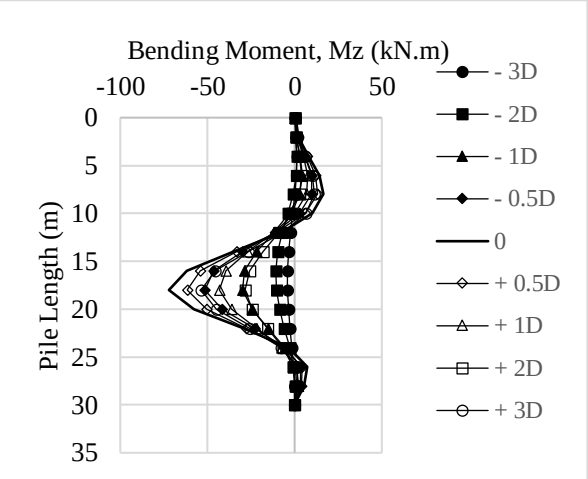

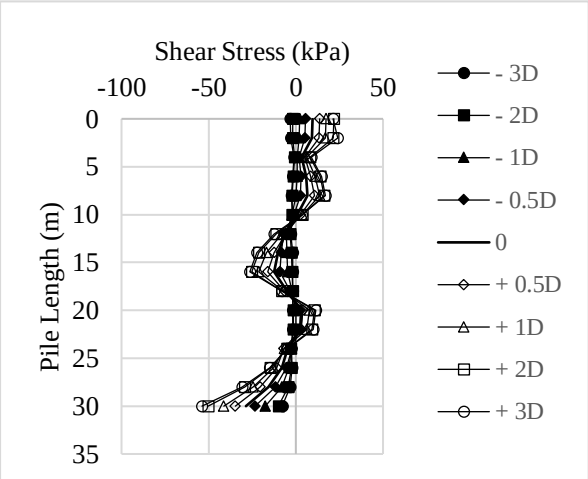

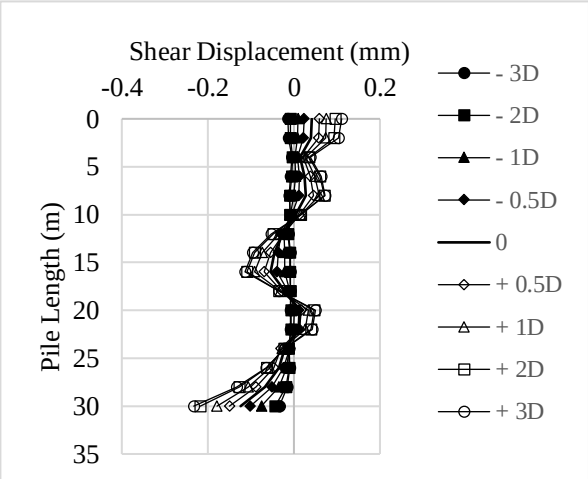

Long pile case 02-5-3

Δv : 2D
Δht : 2D
Cover depth : 15 m

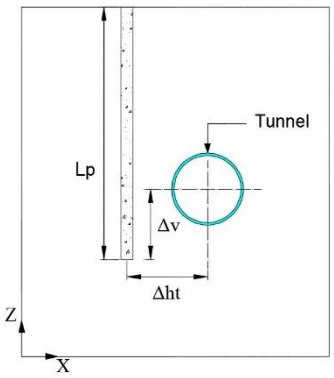

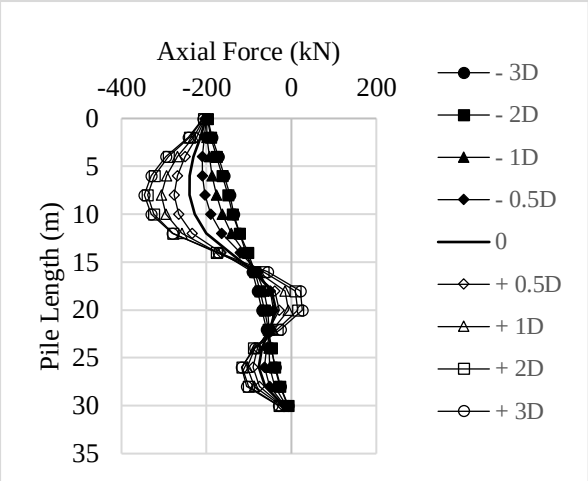

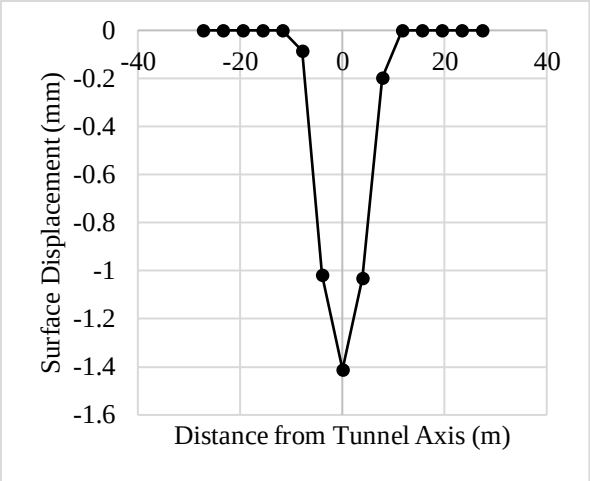

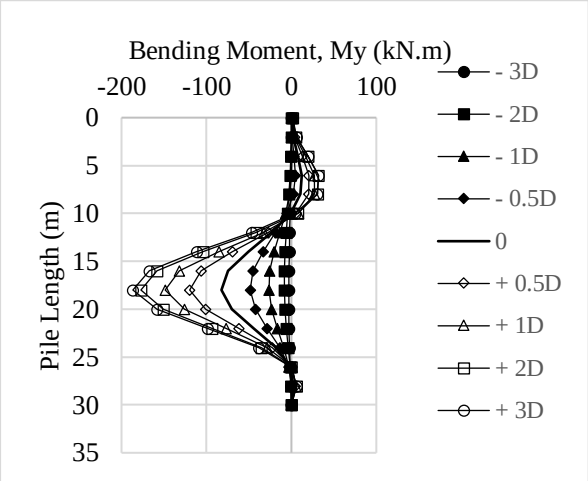

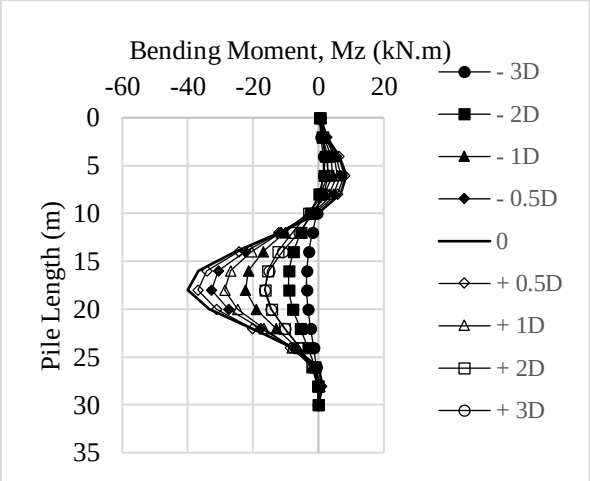

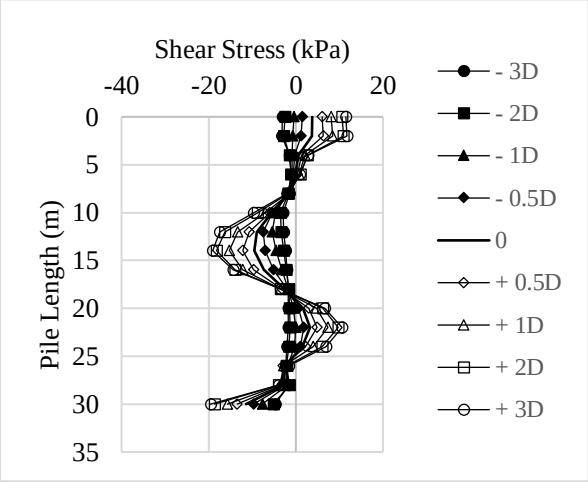

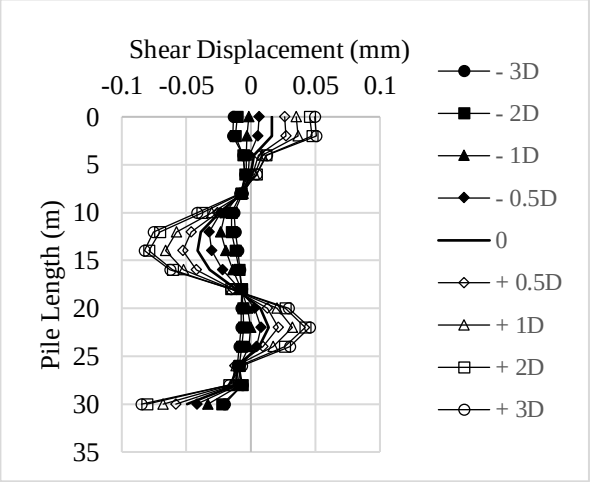

Long pile case 02-5-4

Δv	:	2D
Δht	:	2.5D
Cover depth	:	15 m

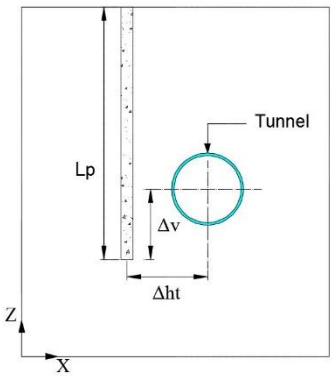

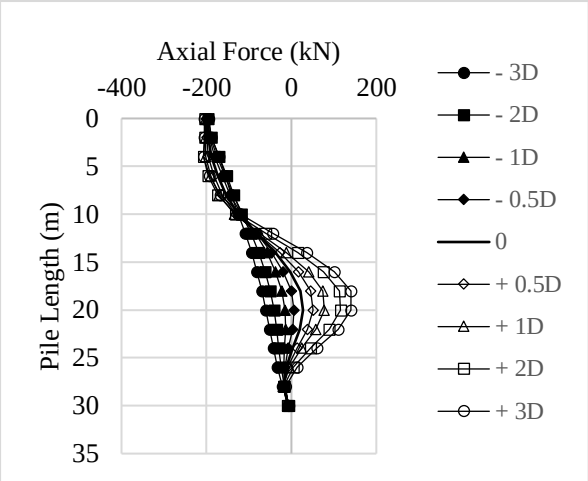

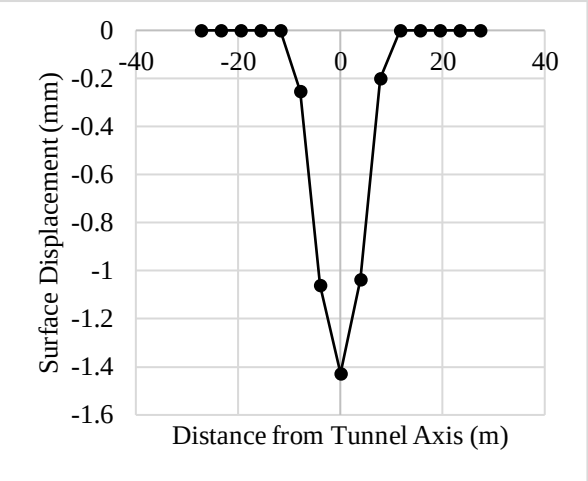

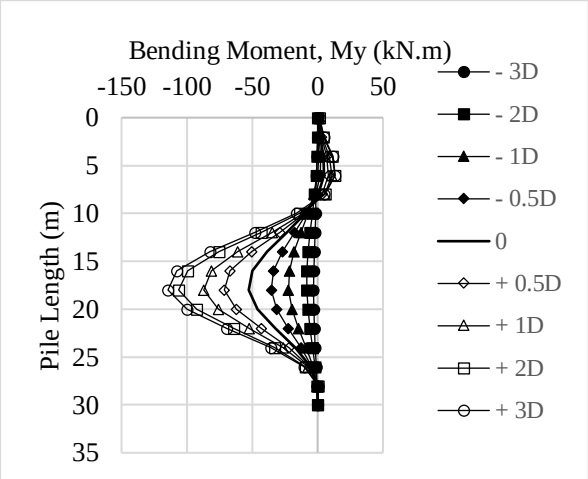

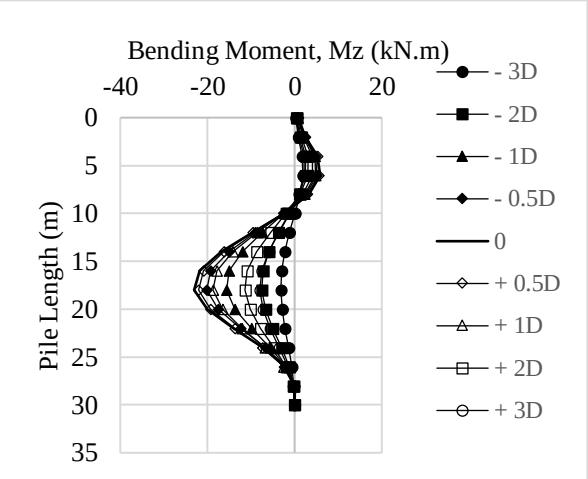

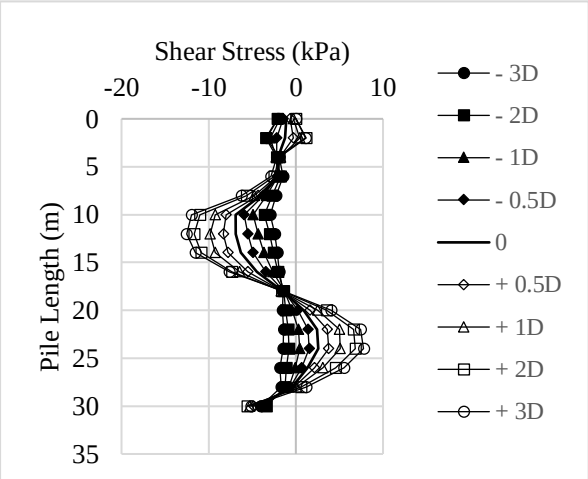

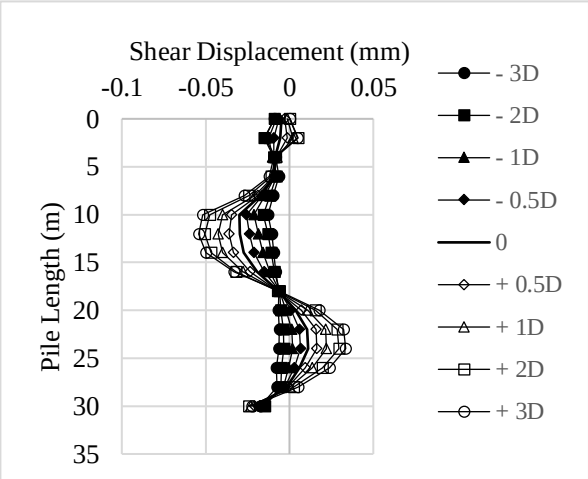

Long pile case 02-5-5

Δv : 2D
Δht : 3D
Cover depth : 15 m

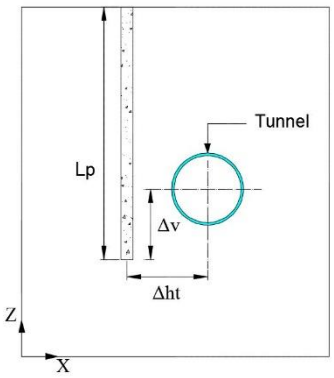

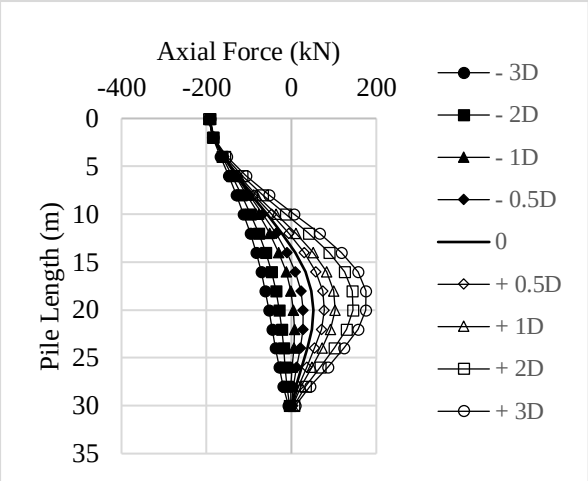

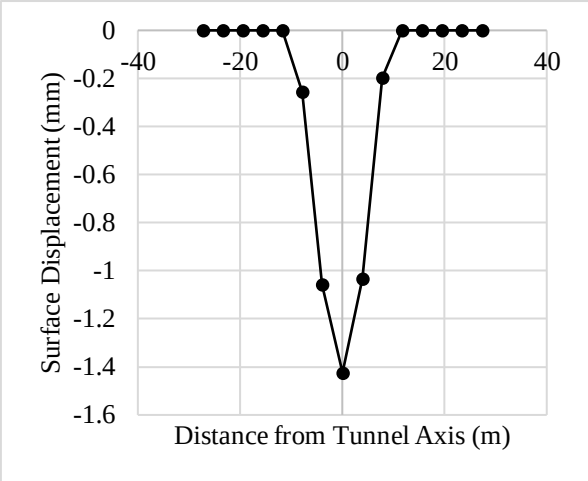

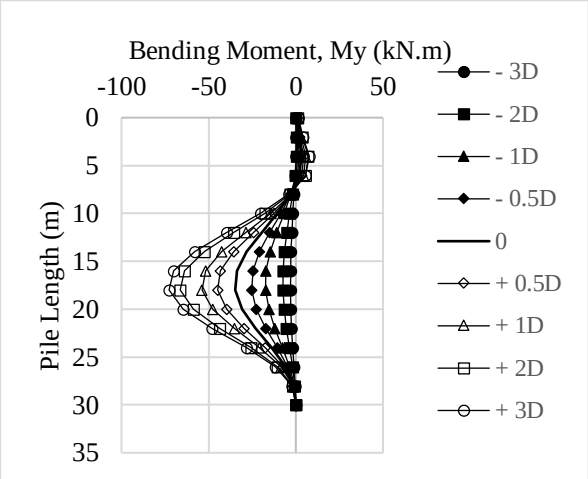

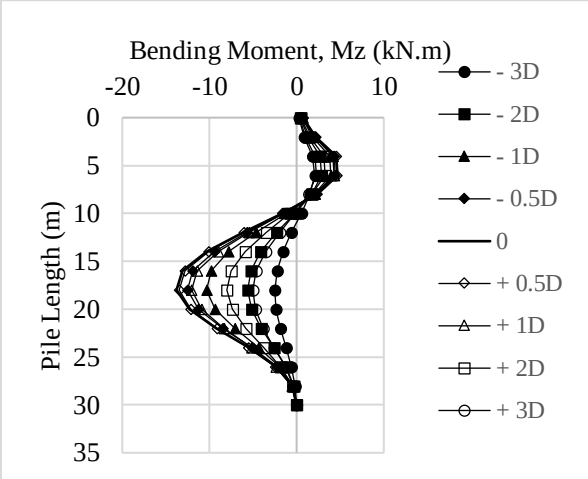

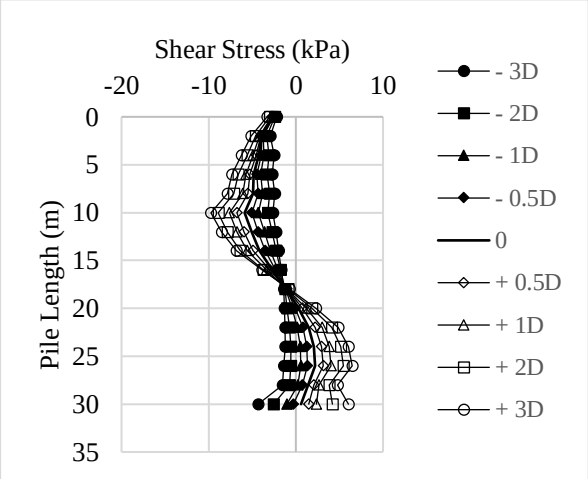

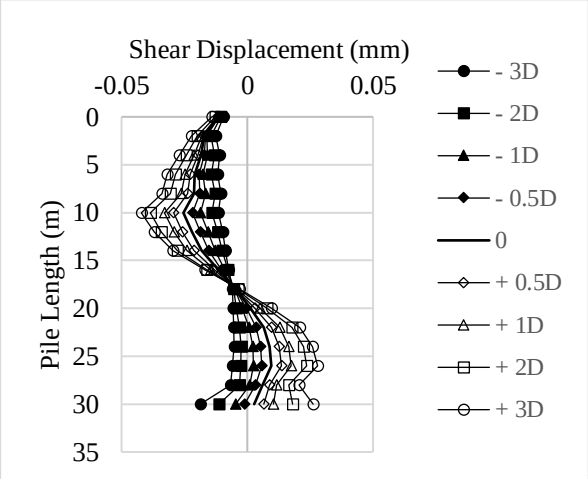

Long pile case 02-5-6

Δv	:	2D
Δht	:	3.5D
Cover depth	:	15 m

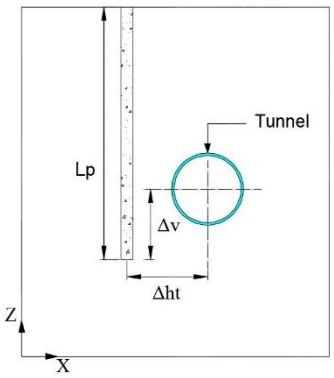

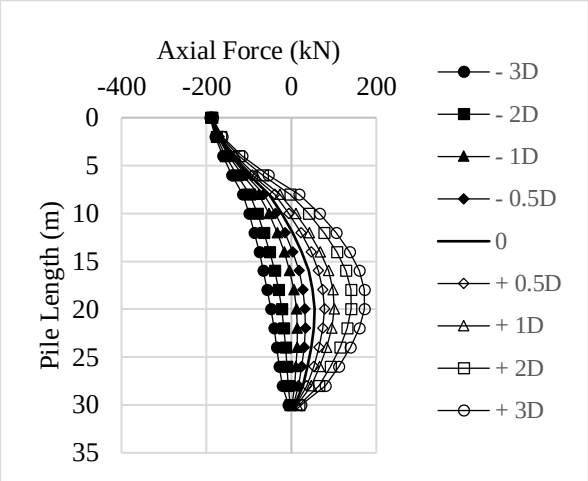

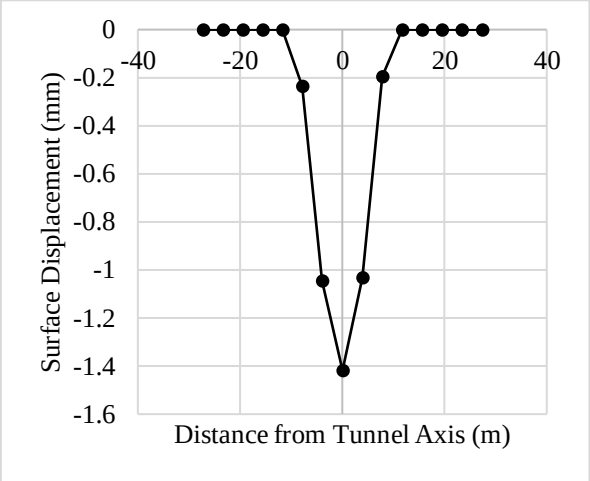

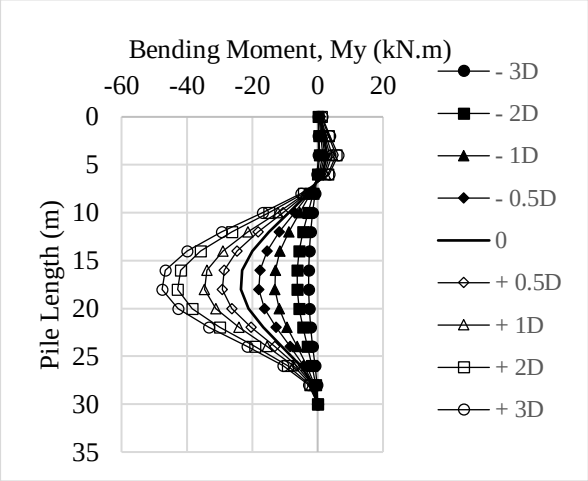

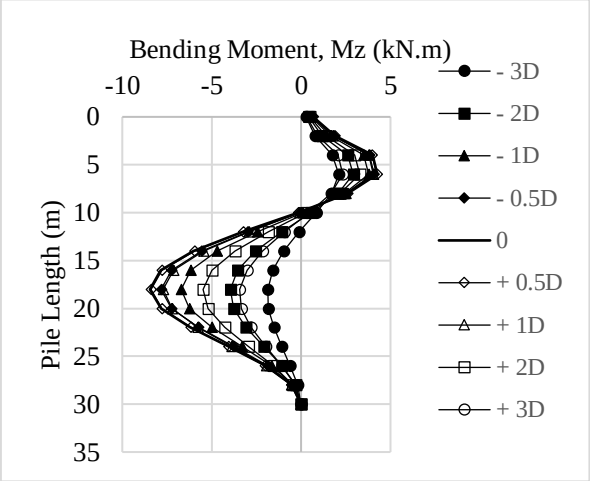

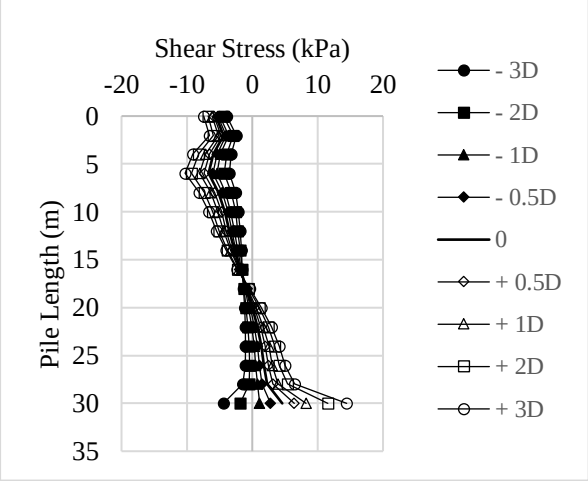

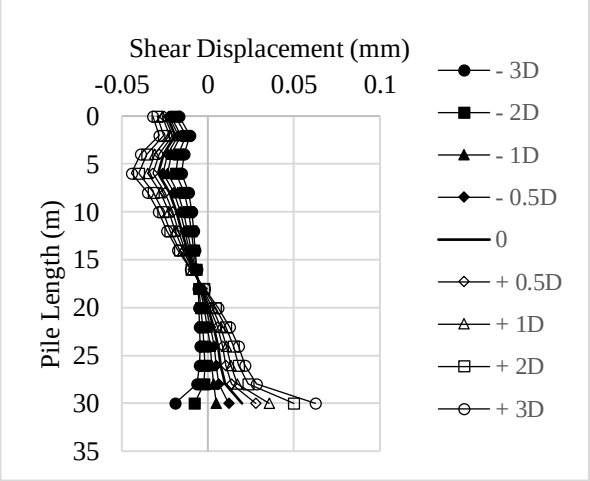

Long pile case 02-6-1

Δv : 2.5D
Δht : 1D
Cover depth : 12 m

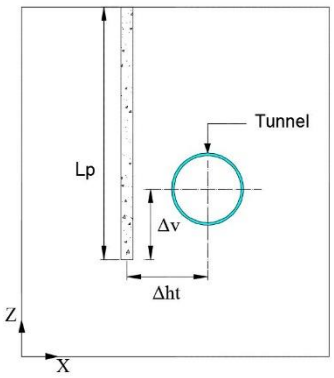

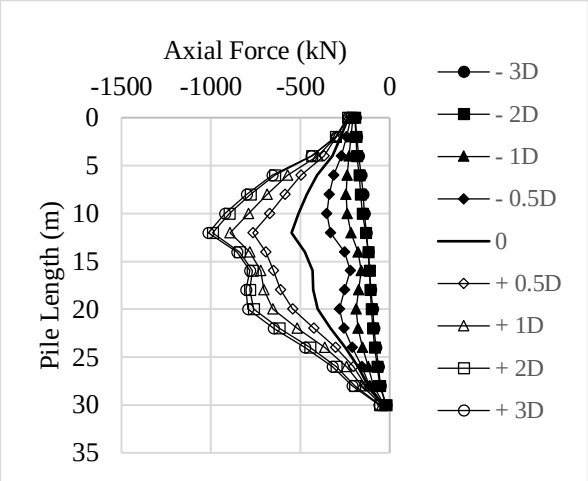

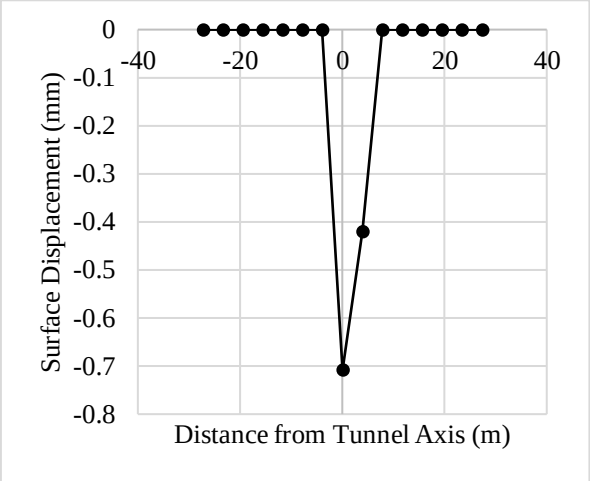

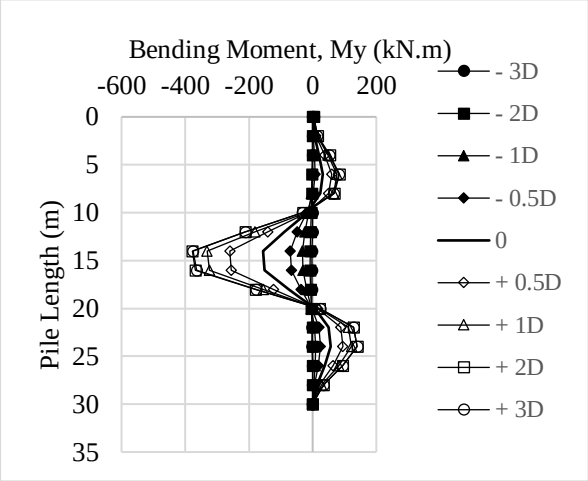

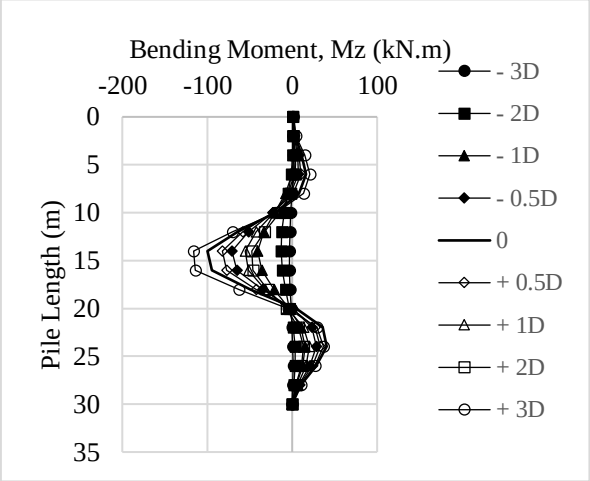

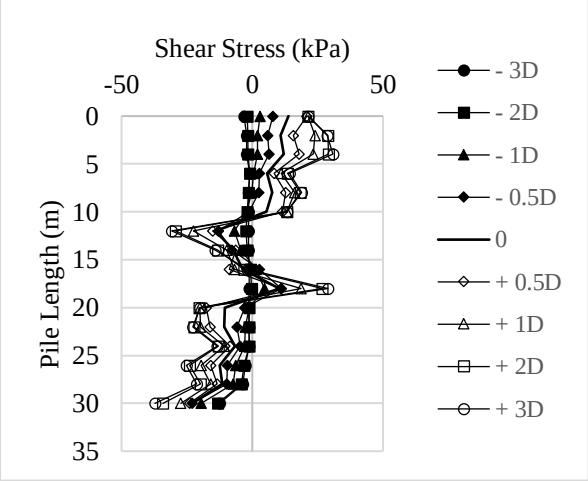

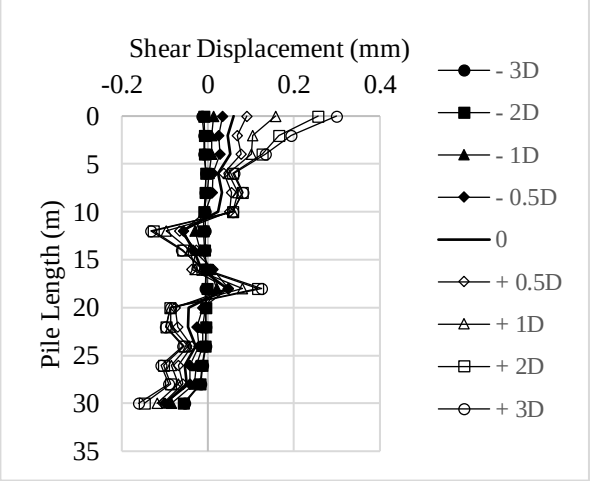

Long pile case 02-6-2

Δv : 2.5D
Δht : 1.5D
Cover depth : 12 m

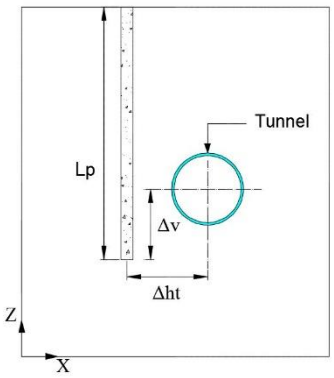

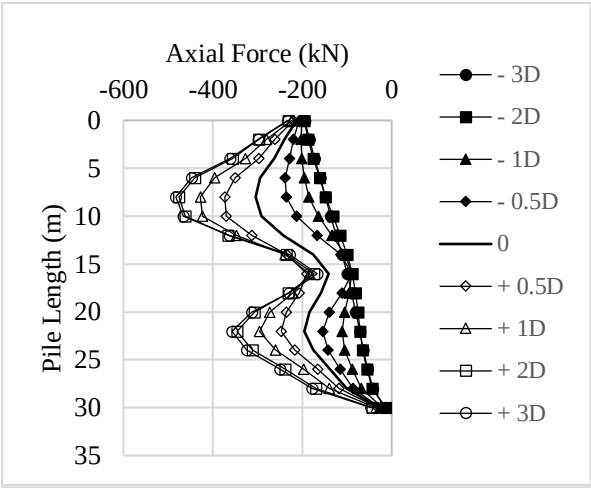

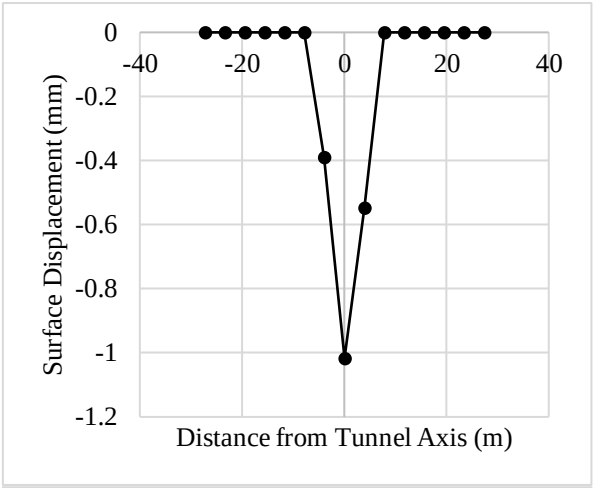

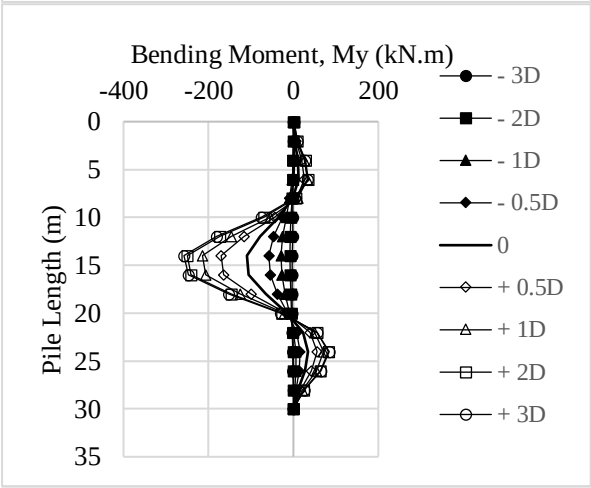

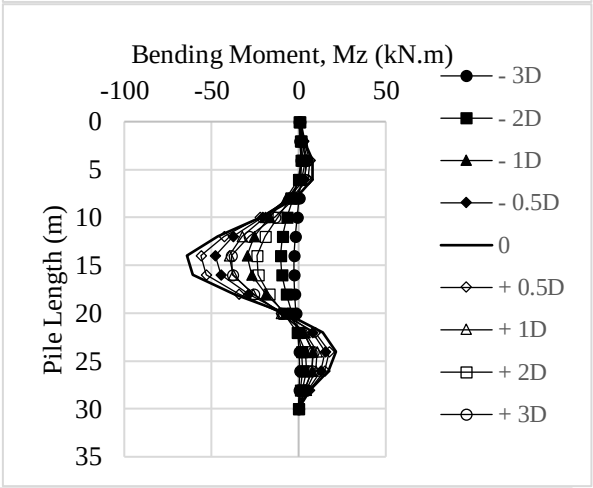

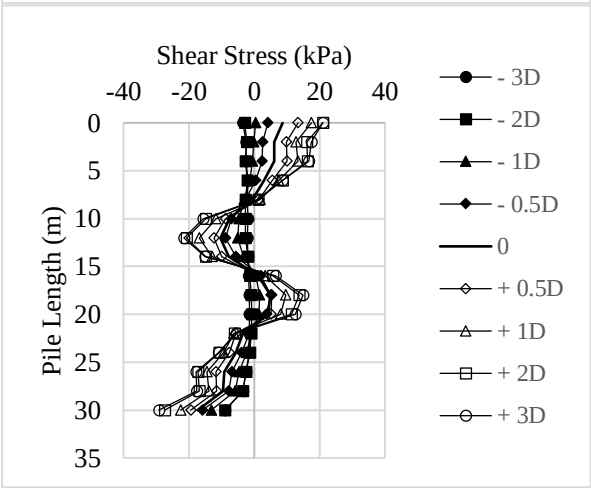

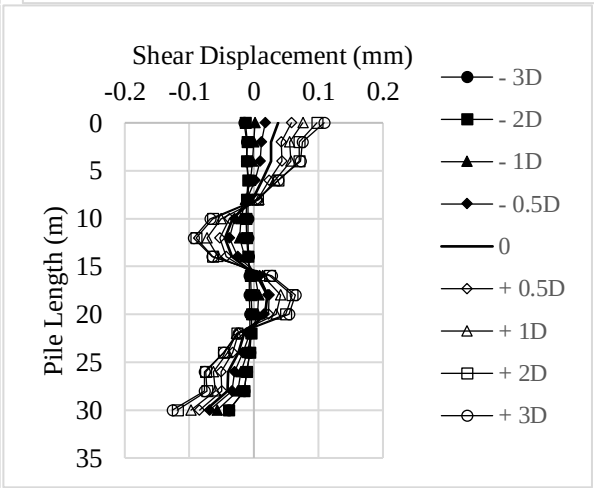

Long pile case 02-6-3

Δv	:	2.5D
Δht	:	2D
Cover depth	:	12 m

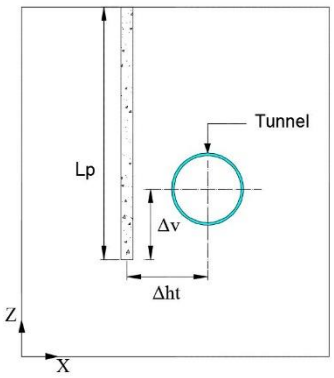

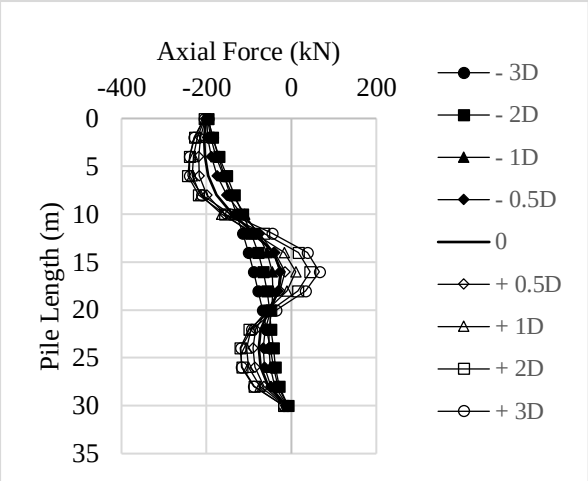

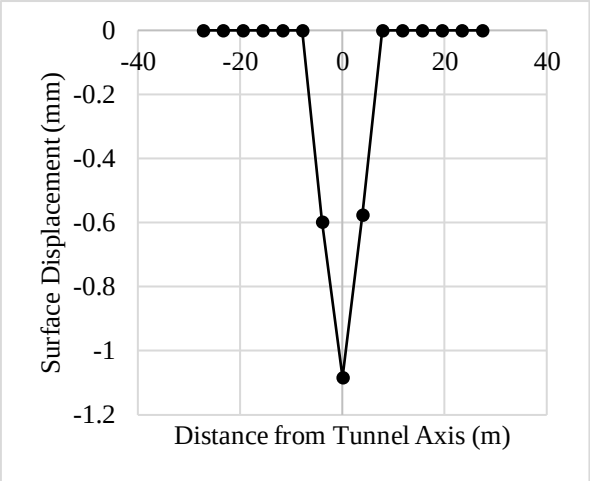

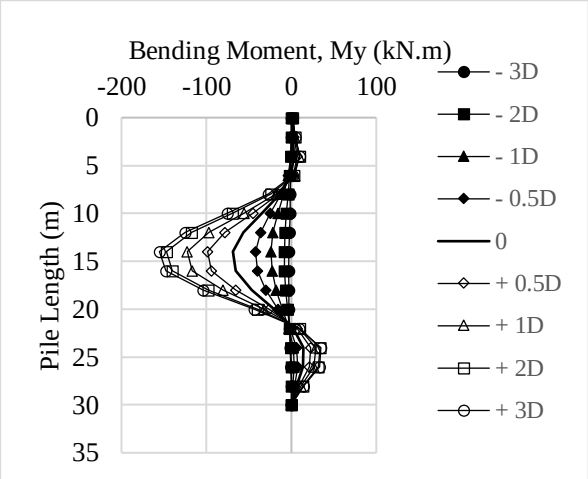

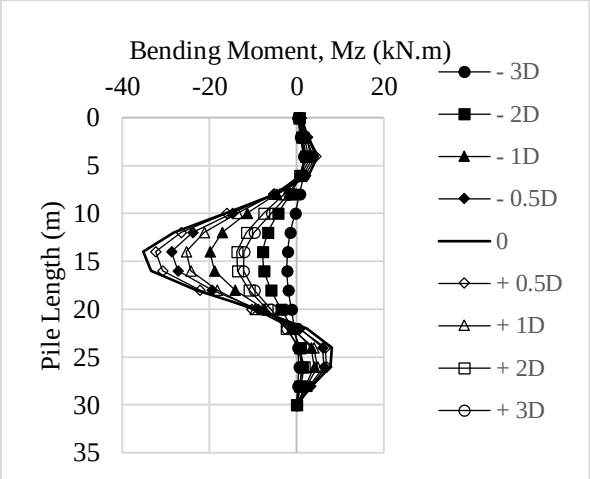

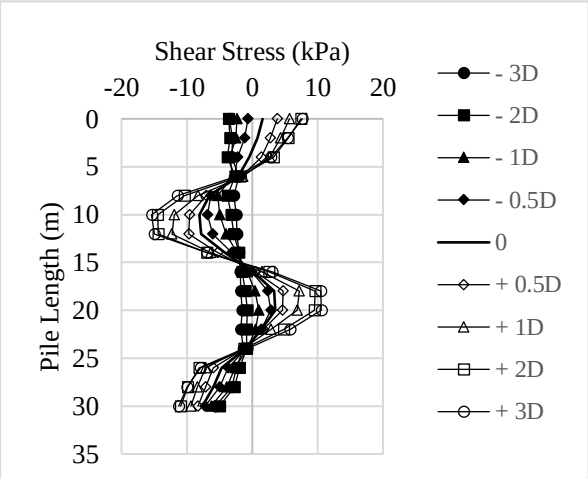

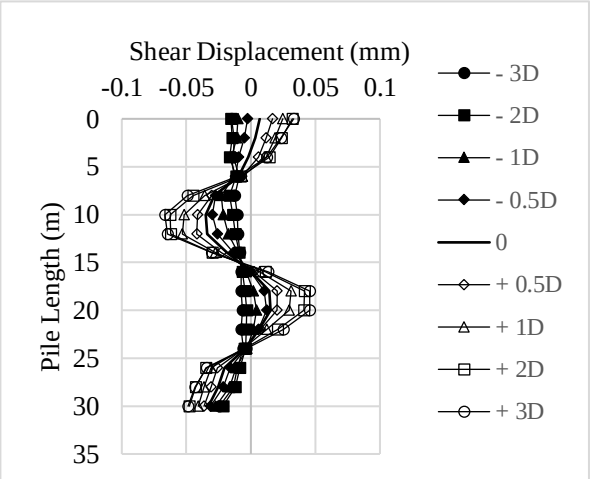

Long pile case 02-6-4

Δv : 2.5D
Δht : 2.5D
Cover depth : 12 m

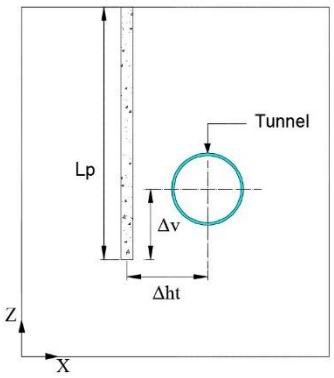

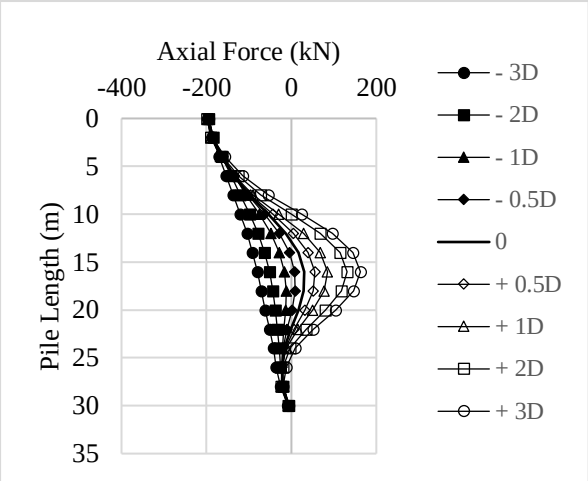

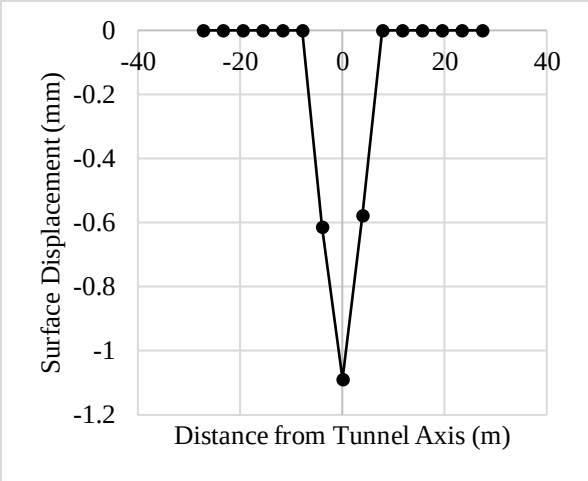

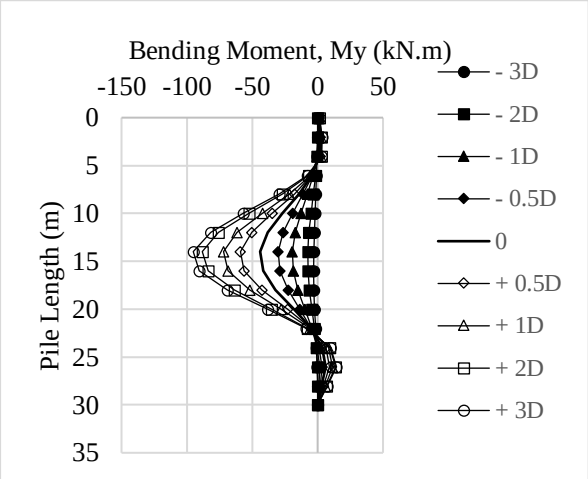

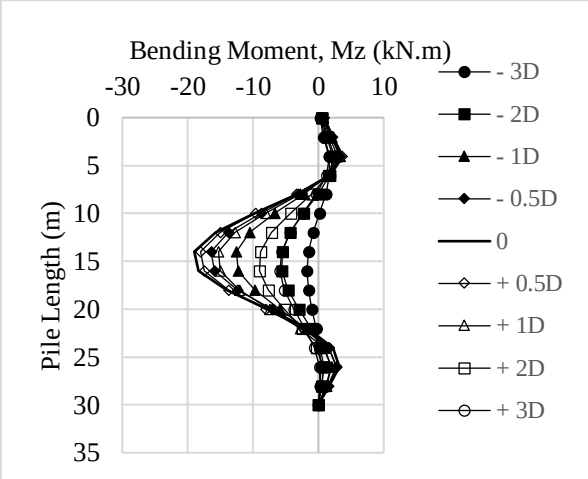

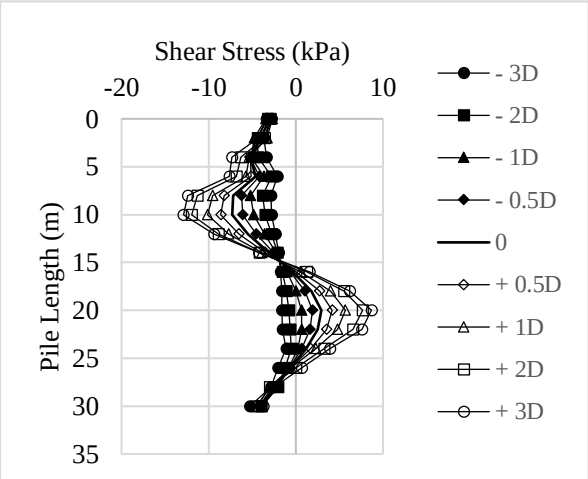

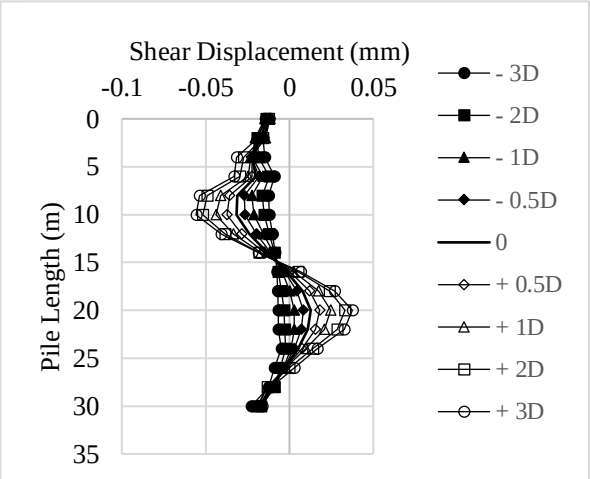

Long pile case 02-6-5

Δv	:	2.5D
Δht	:	3D
Cover depth	:	12 m

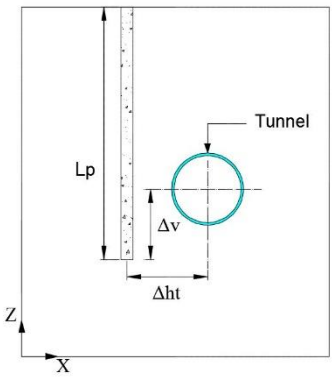

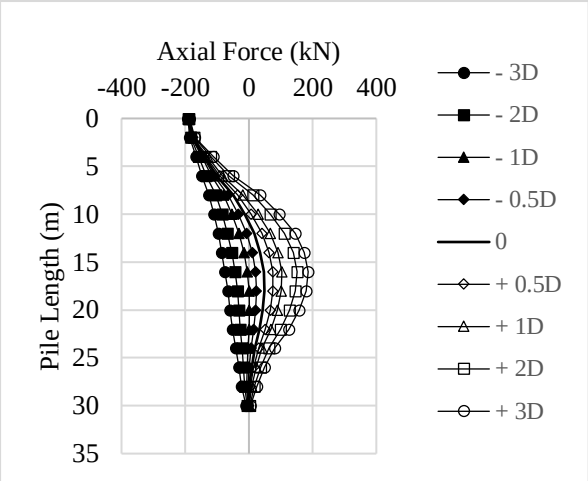

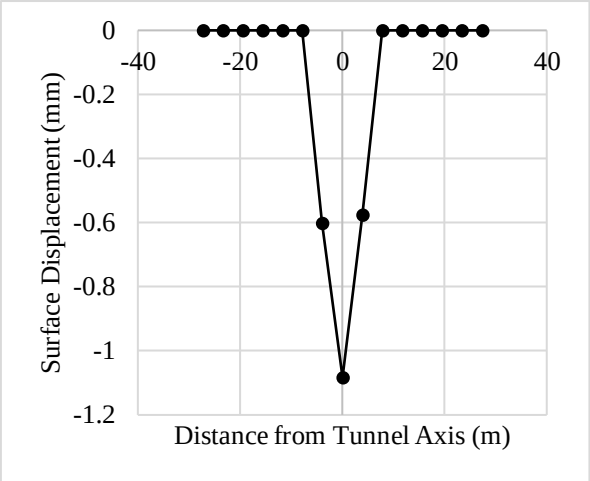

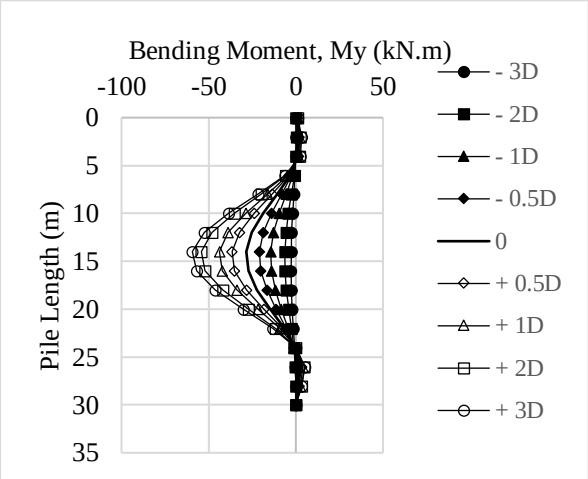

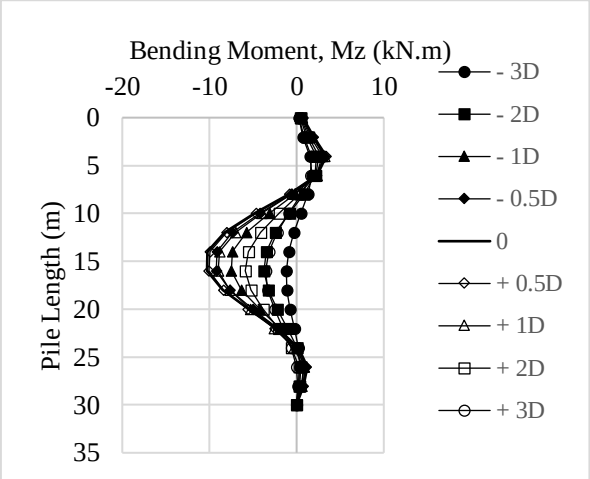

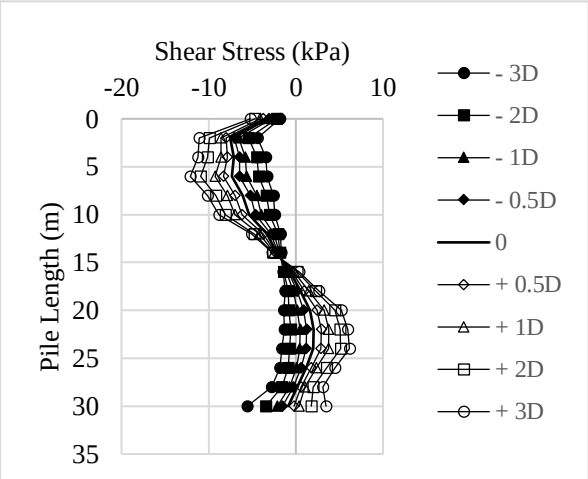

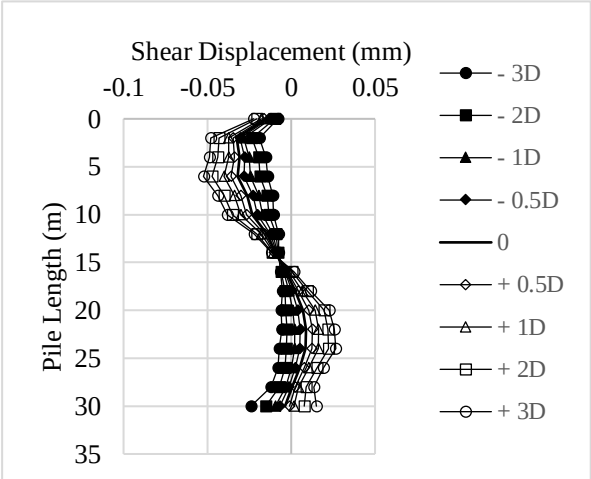

Long pile case 02-6-6

Δv : 2.5D
Δht : 3.5D
Cover depth : 12 m